The effects of biomass pretreatments on catalytic fast pyrolysis

A thesis submitted in full fulfilment of the

requirements for the Degree of Doctor of

Philosophy in Chemical and Process Engineering

at the University of Canterbury

Xing Xin

University of Canterbury

2018

Table of Contents

Acknowledgements

I would like to acknowledge Scion for the financial support to this project and my scholarship, it made this PhD study possible. When looking back the last four and half years, it is still hard to believe that I am achieving my PhD study. In November 2013 I took a single flight from Beijing to Christchurch with a light luggage, knowing nothing about my future but feeling extremely excited. Besides the difficulties in a new environment, the study was such a challenge. Initially I was working on a hydrotreating project as planned, unfortunately, I had to give it up two years later and restarted on a new one. I switched my research on catalytic fast pyrolysis, however the issues about the catalyst dust, the reactor and more seemed unsolvable at the beginning. But I made it eventually! Definitely this research cannot be accomplished without the support of many people, I wish I can deliver my gratitude to all of them.

Firstly I would like to thank my supervisory team, Prof. Shusheng Pang, Dr. Kirk Torr and Dr. Ferran De Miguel Mercader. Shusheng introduced me to a collaborative project with Scion, a great opportunity to do this PhD study. He always made time to discuss my research progress when I studying in Christchurch despite his busy schedule. His guidance, patience and help to me have been invaluable. My research work has largely been based at Scion under direct supervision of Kirk and Ferran. When I relocated to Rotorua, I had no friends and my English ability was very limited. I realized I was pretty far from my comfort zone. Thanks to their kindness and trust, let me feel that it was the right place for my study. Kirk is specialised in chemistry, and Ferran is in chemical engineering. They worked together on the supervision like “Yin” and “Yang” in Taoism, it was a perfect cooperation on this project. They offered me the freedom and laboratory conditions as much as possible to design and conduct my research.

Moreover, Kirk helped me a lot in the English and the writing skills, and he also taught me to think in a critical way. Ferran was always ready to solve the problems I met in the research. He set a high standard for my research work, I really appreciated that when I look back at it.

Secondly, I would like to thank the people who kindly helped me during my PhD study. At the University Tansy Wigley patiently showed me how to operate the biomass pretreating equipment and the fluidised bed reactor. Special thanks to my friends, Ben, Jack and David, I cherish our friendship and hope it can last forever. As to the people from Scion, I would like to thank Daniel van de Pas for his help on the chemical analysis. It was always a pleasure working with you, I do hope I can be that enthusiastic and professional like you. I also thank Martin Cooke-Willis for his support on the fluidised bed reactor operation and the maintenance. You contributed a lot to the pyrolysis experiments, it would be impossible to catch up the schedule without your hardwork and talent. I also express my gratitude to the technical team, George Estcourt, Ben McDonald and Ian McElroy, and the Clean Tech team leaders, Paul Bennett, Kim McGrouther and Ian Suckling. Huge thanks to the three internship students, Thimo te Molder, Thije Harbers and Jeffrey Boom, you all made important contributions to this project. I also thank Ilena Isak for her help on the Py-GC/MS analysis, thank Stefan Hill for his support on the solid NMR spectroscopy, thank Laura Raymond for her work on the PCA and thank Lloyd Donaldson for his SEM work.

Finally I want to thank my family. My parents always support my decisions and motivate me to overcome any difficulties in my life, and most importantly, they are so proud of me. I wish my little brother good luck in his PhD study, you are so close to catching me up! Special thanks to my wife, Vivien, for her still be willing to marry me after I gave up a stable job and decided to

pursue a life I am passionate about. Gratefully, we reunite in New Zealand and have a lovely baby. In the very end I express my love to my baby boy, Luke. Your birth and thriving have proved that being a PhD is even harder than being a daddy.

Executive summary

Fast pyrolysis is a thermochemical process that converts biomass, the only carbon-based source of renewable energy, into bio-oil as the main product. Catalytic fast pyrolysis has been a promising pathway to improve the bio-oil quality. Biomass pretreatments have been employed to improve the yield and/or the quality of bio-oil in fast pyrolysis. The combination of biomass pretreatment with catalytic fast pyrolysis can be a potential process to achieve the optimum outcome. However, catalytic fast pyrolysis of pretreated biomass is not well understood yet. The objective of this study is to investigate the effects of biomass pretreatments on the product yields and composition in catalytic fast pyrolysis. Based on the results of this study, it is aimed to improve bio-oil yield and quality.

In this study, biomass pretreatments were first conducted including acid-leaching and torrefaction, and then the constitutive compositions and characteristics were analysed both for raw wood and treated wood. The acid-leaching was performed using 1 wt.% acetic acid solution and the torrefaction was done at the mild thermal conditions of 260 ^{o}C. A combined pretreatment of acid-leaching followed by torrefaction was also employed.

Following the above study, fast pyrolysis of these pretreated woods was conducted on two fluidised bed reactors, one at University of Canterbury and one at Scion, to understand the effects of the wood pretreatment on the outcomes in fast pyrolysis. However, fast pyrolysis of acid-leached pine wood suffered from bed material agglomeration in the fluidised bed reactor. The bed material adhered to the char and causing agglomeration. This issue had been frequently reported, but no solution had been demonstrated. Thus this issue was investigated in this study and the morphology of char samples was examined using scanning electron microscope.

Approaches to overcome this issue were investigated and the mechanism of bed agglomeration was proposed.

A spray-dried HZSM-5 catalyst was applied for catalytic fast pyrolysis, and a hot filter was built as a modification to the reactor to capture dust caused by catalyst attrition. Methods for catalytic fast pyrolysis were developed to optimize the operating conditions. Following the developed methods, the catalyst remained active during the entire reaction time of 90 minutes and the total recovery of products (mass balance) was between 91-99 wt.%.

Catalytic fast pyrolysis of acid-leached wood was conducted at three temperatures (360 ^{o}C, 450 ^{o}C and 500 ^{o}C) and at three catalyst to biomass ratios (2.5, 4 and 6). Catalytic fast pyrolysis of torrefied wood and acid-leached-torrefied wood was conducted at three catalyst to biomass ratios (2.5, 4 and 6) at 500 ^{o}C. The effects of biomass pretreatments on the outcomes in catalytic fast pyrolysis were investigated in terms of the distribution of products and the quality of oil product. The bed agglomeration occurred in catalytic fast pyrolysis of acid-leached wood, hence this issue was further discussed and the solutions were proposed.

Finally, a pyrolysis-gas chromatography/mass spectrometry (Py-GC/MS) study complemented the understanding of the effects of biomass pretreatments in catalytic pyrolysis. The Py-GC/MS tests were conducted at four temperatures from 360 to 550 °C and four catalyst to biomass ratios from 0:1 to 6:1. The Py-GC/MS results were evaluated by two methods. Firstly, forty five identified products were grouped according to their chemical functionalities and the area percentages of the groups were compared. Secondly, principal components analysis (PCA) was employed to identify variances in the distribution of the products. These findings in the Py-

GC/MS study were in agreement with those using a fluidised bed reactor. The chemical mechanism in catalytic pyrolysis of pretreated wood was discussed.

The key outcomes and findings of this study were:

(1) The issue of bed material agglomeration in pyrolysis of acid-leached pine wood on a fluidised bed reactor was overcome by the proposed approaches, thus catalytic fast pyrolysis of demineralised biomass on a fluidised bed reactor can be explored;
(2) The acid-leaching pretreatment mildly impeded deoxygenation in catalytic fast pyrolysis, nevertheless it removed the ash from biomass which are deleterious to the zeolite catalyst;
(3) The torrefaction pretreatment led to an increase in the yield of oil product in catalytic fast pyrolysis, and caused insignificant changes in the quality of the oil product;
(4) The combined pretreatment, acid-leaching followed by torrefaction, was able to remove the ash from the biomass without introducing negative effects associated with the acid-leaching pretreatment on the catalytic fast pyrolysis, including bed agglomeration and impeded deoxygenation.

Chapter 1

Literature review and introduction

Abstract

Climate change is a global challenge due to greenhouse gas emissions mainly from extensive use of fossil fuels. The use of renewable energy should be widely encouraged as it is friendly to the environment. Biomass, the only carbon-based source of renewable energy, can be converted into liquid fuels through multiple processes including fast pyrolysis.

Fast pyrolysis is a thermochemical process that converts biomass into bio-oil as the main product. The advantages of fast pyrolysis technology are high liquid yield, low energy consumption, easy operation and scaling-up potential. Bio-oil is usually dark-brown and comprised of numerous highly oxygenated compounds. Due to its complex chemical composition, bio-oil is difficult to be used directly in combustion engines. Bio-oil upgrading is a necessary process to improve its properties as fuels. Catalytic fast pyrolysis has been an encouraging pathway to produce upgraded oil product.

Biomass pretreatment methods have been investigated to improve the yield or the quality of bio-oils produced by fast pyrolysis. The combination of biomass pretreatment with catalytic fast pyrolysis can potentially produce bio-oil with further improved yield and quality. However,

catalytic fast pyrolysis of pretreated biomass is not well understood yet. The objective in this study is to investigate the effects of biomass acid-leaching and torrefaction on catalytic fast pyrolysis process operability, and product yield and quality.

1.1 Bioenergy and biomass

World energy consumption has been increasing in past decades and most of this energy consumed is derived from fossil fuels which induces serious concerns on security of future energy supply and CO_2 emissions. The extensive carbon emission from the fossil fuel consumption results in significant risk of climate-change [1]. Renewable energy can be continuously supplied and used without negative impacts on the environment and future generations of human being. For example, the solar, wind, geothermal, hydropower and bioenergy are all originated from solar or nature which are renewable [1].

Biomass is defined as organic matter of plant or animal origin, and bioenergy is the chemical energy stored in such biomass. The resource of bioenergy can be forestry, agricultural and municipal bio-solid wastes, additionally it includes sugar, grain, and vegetable oil crops [2].

In 2017, New Zealand produced around 80 % of its electricity from renewable sources such as hydropower, wind, geothermal and biomass [3]. However, 40 % of total energy consumption was associated with transport, which was mainly derived from petroleum [3]. Because biomass, the only carbon-based renewable energy, can be converted into liquid fuels using thermochemical or biochemical process, it is a good option to replace fossil fuel used in transportation.

Approximately 60 % of available productive land in New Zealand is hilly area which is not suitable for cropping and 23 % is unsuitable for pasture [4]. Hence the use of steep hilly land to grow forests for bioenergy is a potentially large-scale solution to a low-carbon energy supply for New Zealand.

Currently, New Zealand's wood production is 99.8 % from plantation forests of exotic tree species, 89 % of this is radiata pine, which is grown on an approximately 28-year rotation [5]. Woody material, such as sawdust and wood waste, from the planation forests is the main source of bioenergy in New Zealand. Therefore this kind of biomass is mainly discussed in this study.

The major components of plant biomass are carbohydrate polymers including cellulose and hemicelluloses, and lignin. Other minor components include organic extractives and inorganic minerals. The three major components of various lignocellulosic biomass are presented in Table 1-1 [6, 7].

Table 1-1: Lignocellulose contents of typical plant biomass [6, 7].

Biomass	Components (wt.%, dry basis)		
	Cellulose	Hemicellulose	Lignin
Orchard grass	32	40	5
Rice straw	34	27	14
Birch wood	40	26	16
Radiata pine	40	21	27

Cellulose comprises 40-50 wt.% of dry wood, and is the basic structural composition of plants [8]. Cellulose is a linear polymer of β-*(1→4)-D-glucopyranose* units, with a molecular weight of more than 10^6 g.mol^{-1} [7]. Hydrogen bonds link the long cellulosic chains together forming a network. This network has a three-dimensional structure, which leads to a variety of complex fibres. The structure of cellulose makes it thermally more stable than hemicellulose.

Hemicellulose is a mixture of many different polymerised monosaccharides. Hemicellulose typically constitutes 25 to 35 wt.% of dry wood, with higher concentrations in hardwoods (e.g. eucalyptus) than in softwoods (e.g. radiata pine) [7]. Hemicellulose has a lower molecular

weight than cellulose, with the number of repeating monomers approximately 150, compared to 5000-10000 in cellulose. Another difference is the presence of side branches along the main chain.

Lignin accounts for 23-33 wt.% of the dry mass in softwoods and 16-25 wt.% in hardwoods [8]. It has an amorphous cross-linked polyphenolic structure with random molecule arrangement. It functions as a binder for the agglomeration of fibre and shield against microbial or fungal destruction of wood [7]. There are three monomeric phenylpropane units, *p*-coumaryl alcohol, coniferyl alcohol and sinapyl alcohol that are the building blocks for lignin. Softwood lignin is mainly derived from coniferyl alcohol units. The major linkages between these lignin units are ether bonds, although carbon-carbon bonds exist as well.

Plant biomass contains a small fraction of inorganic matter and organic extractives. Organic extractives in softwoods comprise of about 3-4 wt.% [7]. Woody biomass contains less than 1 wt.% of inorganic matter, whereas grasses contain up to 25 wt.% [9]. The inorganic matter includes mostly minerals, such as potassium, sodium, phosphorus, calcium and magnesium [7].

1.2 Biomass fast pyrolysis

Biomass fast pyrolysis is a technology aiming to produce bio-oil, also known as pyrolysis oil, which can be used as transportation fuel or source of chemicals after upgrading and/or refining. The main advantages of fast pyrolysis technology are high liquid yield, low energy consumption, easy operation, and scaling-up potential. Normally, fast pyrolysis process includes the following steps [10]:

(1) Drying the feedstock to moisture content below 10 wt.%;

(2) Grinding the feedstock to particle sizes less than 3 mm;

(3) Fast pyrolysis;

(4) Separating char rapidly before condensation of pyrolysis vapours;

(5) Rapid quenching of the hot vapour to a bio-oil.

In order to optimise this process, several conditions are required in fast pyrolysis: high temperature, a high heating rate, a short vapour residence time, and rapid condensation of the hot vapour [10]. Under the preferred operating conditions, the yield of bio-oil can be up to 75 wt.% on a dry basis [11]. The by-products char and non-condensable gases, which mainly comprises of CO, CO_2, H_2, and CH_4 can be burnt to provide heat for pyrolysis process and feedstock drying [11, 12].

The pyrolysis temperature plays an important role in bio-oil production. Generally, pyrolysis temperature of 450-550 ^{o}C maximizes the yield of bio-oil [13]. Lower temperature leads to more char and less liquid and gas. Higher temperature increases the cracking severity, leading to more gas and less liquid and char.

The individual biomass components behave differently under fast pyrolysis. Cellulose degradation happens at 240-350 ^{o}C with anhydrocellulose and levoglucosan as intermediate products. Hemicellulose decomposes in the temperature range 200 to 260 ^{o}C, producing more volatiles and less char than cellulose [14]. Lignin decomposes at temperature from 280 to 500 ^{o}C, it leads to phenols and more char than the pyrolysis of cellulose or hemicelluloses [7].

The moisture content of feedstock also has impacts on the outcomes of fast pyrolysis. When the moisture content of the feedstock decreases from 20 to 0 wt.%, the yields of char and gas

decrease, the yield of produced water increases, and the yield of organics in bio-oil increases slightly [15].

There are many pyrolysis reactors types, including bubbling fluid bed, circulating fluid bed and rotating cone. Ablative pyrolysis and microwave pyrolysis also use particular reactors to realise fast pyrolysis. A good review of pyrolysis reactors was reported by Bridgwater [11].

Bubbling fluid bed is a well-developed reactor, which is simple for construction and operation, easy to control at a stable temperature and efficient in heat transfer. A typical facility using a bubbling fluidised bed reactor and recycling non-condensable gas as the carrier gas is shown in Figure 1-1A. In order to increase the economic potential, the pyrolysis heat is obtained by burning char which is obtained in about 15 wt.% yield and 25 % of total energy based on biomass feed [11].

Circulating fluid bed is another type of fast pyrolysis reactor which has many similar features with bubbling fluid bed. The typical circulating fluid bed is showed in Figure 1-1B. The bed material is circulated between reactor and combustor. The char is burnt in combustor with bed material, then the heated bed material is sent back to reactor to provide pyrolysis heat. As a widely used technology in the petrochemical industry, circulating fluid bed reactors have an advantage over other reactors in terms of the potential for large throughputs. Multiple pilot and commercial plants have been built and operated. Ensyn built its first commercial “Rapid Thermal Processing/RTP” [16] plant in 1989 and has designed and commissioned 15 RTP facilities for various applications and feedstocks, at different scales. Six RTP facilities are currently in commercial operation [17].

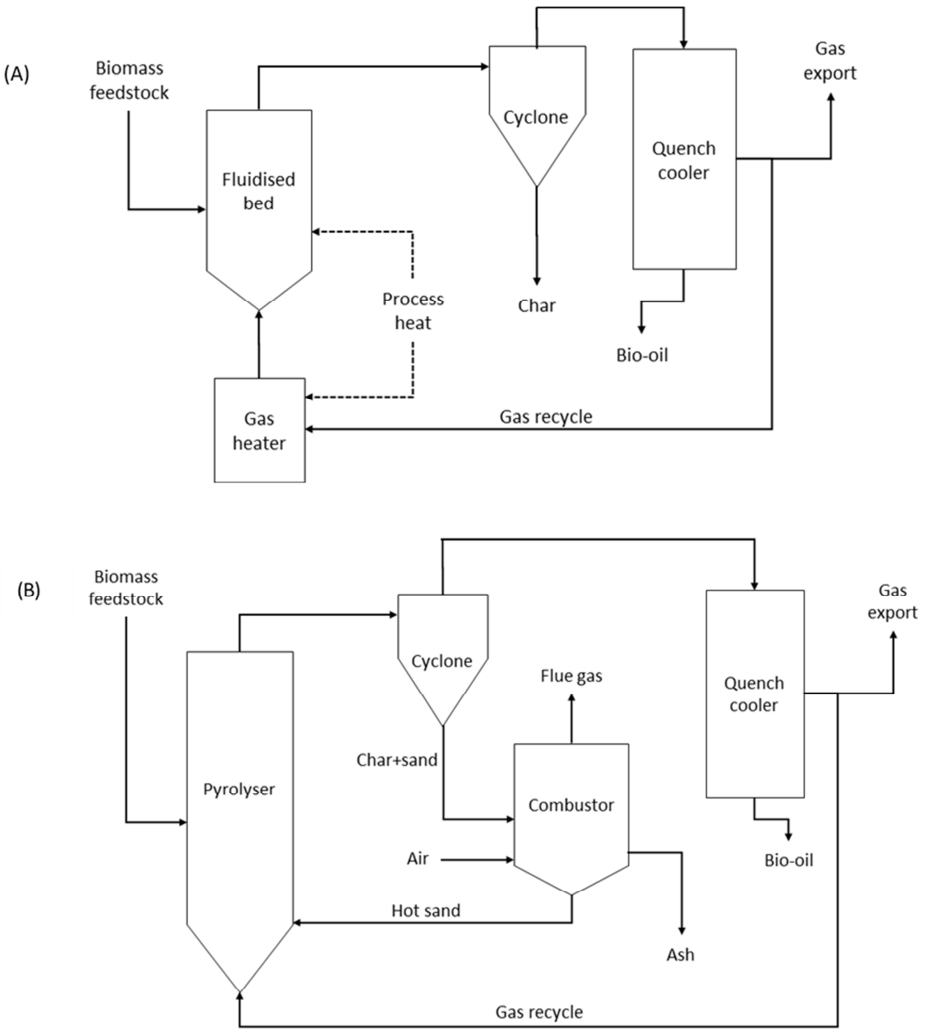

Figure 1-1: Bubbling fluidised bed reactor (A) and circulating fluidised bed reactor (B).

Other reactors for biomass fast pyrolysis have been developed as well, such as rotating cone, ablative pyrolysis and microwave pyrolysis [11, 18]. The rotating cone requires much less carrier gas than circulated fluid bed, however this integrated operation is more complex. Microwave pyrolysis is essentially different from all other pyrolysis reactor as the heat source is not from

external heat transfer but from molecular vibration by microwaves. Penetration of the microwaves into the biomass is only 1-2 cm depth, therefore scaling-up the technology is a challenge.

1.3 Bio-oil

1.3.1 Chemical composition

Bio-oil is usually dark-brown and comprised of oxygenated components [7]. It contains many reactive species because it is formed by fragmenting lignocellulosic polymers in fast pyrolysis. Only 40-50 % composition of bio-oil, normally small cracked molecules, has been structurally characterized [7]. The identified components can be classified according to their functional groups and include acids, alcohols, esters, ketones, aldehydes, furans, sugars, phenols, guaiacols, syringols and miscellaneous oxygenates [19, 20]. Figure 1-2 shows the chemical composition of a typical bio-oil as an approximate distribution of functional groups derived from the pyrolysis of lignin, hemicellulose and cellulose.

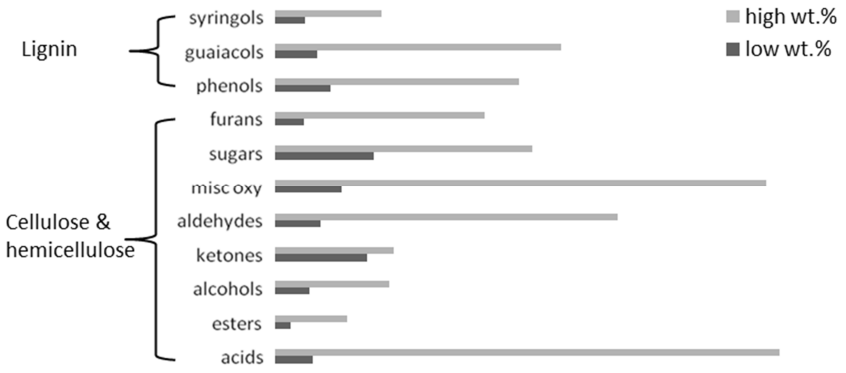

Figure 1-2: Chemical composition of bio-oil [20].

1.3.2 Bio-oil properties

Bio-oil is obtained by quenching hot pyrolysis vapours with the many reactive species in the bio-oil contributing to its characteristics. Some properties of bio-oil and heavy fuel oil are showed in Table 1-2. The undesirable properties, such as high water content, acidity, high oxygen content, high viscosity and high levels of distillation residue make bio-oil difficult to use directly. Bio-oil can be combusted without flame due to its high content of non-volatile components [21]. In addition, bio-oil combustion requires ignition before it continues as self-sustaining burning.

Table 1-2: Comparison of properties of bio-oil and heavy fuel oil [21, 22].

Properties	Bio-oil	Heavy fuel oil
Density at 15 °C (g/mL)	1.05-1.25	0.86-0.92
Viscosity at 50 °C (cP)	40-100	180
High heating value (MJ/kg)	16-19	40-44
Solids (wt.%)	0.2-1.0	1
Distillation residue (wt.%)	up to 50	1
Pour point (°C)	-33	-18
Water content (wt.%)	15-30	<0.1
Ash content (wt.%)	<0.02	0.03
pH	2.5-3.8	N/A
Elemental composition (wt.%, wet basis)		
C	55-65	83-86
H	5.5-7.0	11
O	28-40	<1
N	<0.4	<1
S	N/A	0.5-3

1.3.3 The challenges of bio-oil use

Bio-oil contains a lower amount of sulphur and nitrogen compared to petroleum oil or coal [23]. However, use of bio-oil as fuel directly in engines or turbines is difficult due to its high viscosity, poor volatility, corrosiveness and coking problem. In addition, storage of bio-oil leads to aging

which further deteriorates its properties [21]. Generally the undesirable properties causing problems in its use are related to the high oxygen content and reactivity of the bio-oil.

Water content in bio-oil (single phase) varies from 15 to 30 wt.% depending on feedstock and process conditions [21]. The high water content lowers its heating value and flame temperature, delays ignition and decreases combustion efficiency. On the other hand, water reduces oil viscosity and NO_X emissions during combustion [21].

Oxygen content in bio-oil is similar to that of the biomass, for example pine wood has an oxygen content of 47 wt.% [24]. Many application problems are related to its high oxygen content, such as poor thermal stability and low heating value. A high oxygen content makes bio-oil polar, so it is miscible with polar solvents like methanol, ethanol. But it is only partially miscible with petroleum-derived oil and it can only tolerate a limited addition of water before phase separation occurs [12].

The acidity of bio-oil is derived mainly from the volatile acids, and there are also other groups of compounds that influence acidity, such as phenols [25]. The pH of bio-oil is normally about 2.5. High acidity can cause corrosion of containers and pipes [12], hence corrosion-resistant material, such as polyolefin or stainless steel, is needed. Bio-oil esterification, which is still under development, is one solution to neutralize the acid and improve bio-oil stability [26, 27].

The viscosity of bio-oil varies over a wide range, 35-1000 *cP* at 40 °C, and is affected by water content, feedstock and process conditions [21]. Increasing its temperature leads to viscosity reduction, however, the rate of polymerization increases. The high viscosity also causes problems such as high pressure drops and high pumping costs. Therefore, the use of polar solvents has been proposed to improve viscosity. Diebold and Czernik [28] discovered that

addition of 10 wt.% methanol in bio-oil can lower the viscosity by 20 times. Similar results have been achieved using ethanol and acetone [29].

Bio-oil cannot be distilled completely because the unstable compounds can react under the distillation conditions, producing solid residues. Additionally the instability worsens with the rising of temperature [30]. Bio-oil normally starts to evaporate below 100 °C and the distillation range stops at 250-280 °C [21]. During distillation the bio-oil reacts rapidly and 35-50 wt.% of the oil is carbonised as solid residue. The distillate includes original volatile and secondary cracked products [12]. At present, upgrading bio-oil appears to be the only way to reduce the proportion of undistillable components.

Some small char particles and the inorganics in the char can pass through the solid separation system (typically cyclones) before the oil is condensed and end up in the liquid product. Bio-oil typically contains less than 0.5 wt.% solids with an average particle size of approximately 5 μm [25]. The presence of solid and ash in bio-oil is highly undesirable because the solid may cause blockages in equipment when combusting the bio-oil. Alkali metals deposition can cause damage in some applications such as combustors [29]. One effective method to minimise char and ash content is hot vapour filtration, however this reduces the liquid yield [12]. Hot vapour filtration also leads to reduced viscosity of the bio-oil and lowers its average molecular weight since char accumulated on the filter surface has a catalytic effect on the vapour.

Aging refers to polymerization and condensation of bio-oil components with time, and this process can be accelerated by higher temperatures, exposure to oxygen or UV light [23]. Aging results in increased viscosity and water content as well as phase separation. This instability is believed to result from continuing chemical reactions after the rapid vapour quenching. For

instance, aldehydes, ketones, and other molecules can react to form larger components during bio-oil storage [24].

Due to the challenges of bio-oil use as discussed above, it is important to upgrade bio-oil for its application as transportation fuels.

1.4 Bio-oil upgrading

Generally bio-oil can be upgraded by physical, chemical and catalytic methods into chemicals, hydrocarbons or intermediates for further refining [12]. The methods include blending with additives, solvent fractionation, hydrotreating, catalytic cracking. Hydrotreating and catalytic cracking are two main pathways to remove oxygen from bio-oil. Upgrading bio-oil to intermediate products, which can be compatible and blended with petroleum refinery streams, is also one promising method to produce partial green fuels.

1.4.1 Physical and chemical methods

Blending bio-oil with other liquids is a simple way to stabilize it and improve its properties. Addition of some solvents can lower its viscosity, while the addition of water causes reduction in the heating value and, eventually, phase separation [12]. Bio-oil is not miscible with petroleum-derived fuel because of the difference in polarity, unless surfactants are used to emulsify the bio-oil [31]. Emulsification can also reduce bio-oil aging during storage [28]. Upgrading of bio-oil through emulsification provides a short-term approach to the use of bio-oil in diesel engines. But fuel properties such as heating value, octane number and corrosivity are still unsatisfactory [27].

Another simple way to upgrade bio-oil is solvent fractionation. Polar solvents used as extraction agents include water, acids, methylene chloride, and alcohol, and nonpolar solvents used include toluene and hexane [7].

Zheng *et al*. [32] investigated reduced pressure distillation of bio-oil from fast pyrolysis of rice husk. The experiment was conducted at 80 °C with a residual pressure of 15 mm Hg. The first fraction of distillate was water phase (29 wt.%), the second fraction was distilled bio-oil (61 wt.%), the last fraction was residue (10 wt.%). Comparing with bio-oil, moisture content of the distilled bio-oil decreased to 0.1 wt.% from 25.2 wt.%, while the pH value increased to 6.8 from 2.8. Correspondingly, heating value of the distilled bio-oil increased to 34.2 MJ/kg from 17.4 MJ/kg, and the oxygen content decreased to 9.2 wt.% from 50.3 wt.%. GC/MS was applied to test the composition of bio-oil and distilled bio-oil. The result indicated that the carboxylic acids and heterocyclic substances were relatively low in distilled bio-oil while hydrocarbon contents of distilled bio-oil was higher than bio-oil. Organic acids and other oxygenated chemicals with low molecular weight were mostly transferred into the water phase. The stability of distilled bio-oil was determined by variation of viscosity over time. The result showed the viscosity of the distilled bio-oil hardly changed during storage. It revealed that polymerization and condensation reactions that typically happen in bio-oil storage disappeared due to lack of unstable oxygenated organic chemicals.

Xu *et al.* [33] investigated bio-oil upgrading by ozone oxidation followed by esterification with alcohols. Bio-oil oxidation was carried out in a stirred batch at 20 ^{o}C with continuous ozone introducing into for 10 h. Esterification was operated on a continuous distillation of the butanol-water azeotrope at 116 ^{o}C with solid $NaHSO_4$ as a catalyst. The two phase condensate was

composed of lower aqueous phase which was removed and upper butanol phase which was returned to distillation. After bio-oil oxidation, total acid number was increased from 45.4 to 118.4 mg KOH/g, which indicated that reducible components, such as aldehydes, were converted to acids. FT-IR spectra analysis revealed C=O stretching was intensified after oxidation, indicating carboxylic acids were increased. The following esterification decreased the acid value to 14.5 mg KOH/g. The bio-oil's water content was decreased from 44.75 wt.% to 2.38 wt.% after oxidation and azeotropic distillation. GC/MS analysis results showed that carboxylic acids were converted into butyl esters such as butylacetate, butyl propionate, and dibutyl succinate. The molecular weight distribution suggested that oligomerization reactions during esterification was significantly decreased when the aldehydes were oxidized first.

1.4.2 Hydrodeoxygenation

Hydrodeoxygenation (HDO) of bio-oil is a process to reduce the amount of oxygen in bio-oil via catalytic reactions with hydrogen. It closely related to the hydrodesulphurization (HDS) used in the refinery industry to eliminate sulphur from petroleum hydrocarbons [34]. This process is generally operated in a hydrogen environment under high pressure (up to 20 MPa) and at temperatures ranging from 200 to 400 °C [12]. During hydrodeoxygenation the bio-oil's oxygen is removed as water and unsaturated bonds are hydrogenated [20]. Hydrocarbons are produced and further refining can produce conventional transport fuels.

A two-step hydrotreating process was developed by Elliott *et al*. [20, 35-38] using sulphided Co-Mo/Al_2O_3 or sulphided Ni-Mo/Al_2O_3 catalyst for both steps. The first step was at a low temperature (170 °C) at a pressure of 13.6 MPa to hydrogenate thermally unstable compounds which would form coke at higher temperatures. The second step was at a higher temperature of

400 °C under the same pressure (13.6 MPa) to achieve deep deoxygenation. The volume yield of upgraded bio-oil is about 40 %. The properties of bio-oil and upgraded oil (HDO oil) are shown in Table 1-3. Upgraded bio-oil has higher energy content, lower oxygen content and lower viscosity. Hence its properties and stability are significantly improved.

Table 1-3: Properties of bio-oil and HDO oil [20].

	Bio-oil	HDO oil
Carbon (wt.%)	43.5	85.3-89.2
Hydrogen (wt.%)	7.3	10.5-14.1
Oxygen (wt.%)	49.2	0.0-0.7
H/C atom ratio (dry basis)	1.23	1.40-1.97
Density (g/mL)	24.8	0.796-0.926
Moisture (wt.%)	24.8	0.001-0.008
Higher heating value (MJ/kg)	22.6	42.3-45.3
Viscosity (cP)	59 (40 °C)	1.0-4.6 (23 °C)
Aromatic/aliphatic carbon	-	38/62-22/78
Research octane number (RON	-	77
Distillation range (wt.%)		
IBP-225 °C	44	36-97
225-350 °C	coked	0-41

1.4.3 Catalytic cracking

Catalytic cracking in this study is referred to as a bio-oil upgrading method via cracking and other thermochemical reactions in the presence of zeolite catalyst. The catalytic cracking can be realized by upgrading the re-vapourised bio-oil. One key difference between catalytic cracking and HDO is the absence of a high pressure hydrogen environment [11].

In catalytic cracking , the reaction temperature (typically 300 to 600 ^{o}C) and contact time of vapour and catalyst affect the yield and quality of the oil product [34]. An increased temperature results in a decrease in the oil yield and an increase in the gas yield [39]. However,

the high temperature is required in order to decrease the oxygen content to a significant degree. Similarly, a sufficient contact time should be carried out to ensure a satisfying degree of deoxygenation. However, the extent of carbon formation increases when increasing the contact time [40]. Hence the best compromise between oil yield and deoxygenation needs to be found.

Catalytic cracking involves multiple reactions including cracking, dehydration, decarbonylation, decarboxylation, aromatization, and polymerization [22]. Dehydration leads to formation of water and dehydrated compounds, such as ketones and aldehydes [41]. Decarboxylation and decarbonylation produce hydrocarbons and gases, CO_2 and CO. Polymerization reactions can convert bio-oil into undesirable by-products, such as coke and tar.

A comparison of bio-oil and the upgraded oils via HDO and catalytic cracking is reported as shown in Table 1-4 [34]. Due to the addition of hydrogen, HDO oil can be produced in a larger yield and in a higher fuel grade compared to catalytic cracking oil. The main product from catalytic cracking is coke, and the catalytic cracking oil contains a large elemental fraction of oxygen. Although catalytic cracking avoids the use of a high pressure hydrogen environment, the outcome is not as good as HDO process in terms of the yield and quality of the oil.

Table 1-4: Comparison of characteristics of bio-oil, HDO oil and catalytic cracking oil [34].

	Bio-oil	HDO	Catalytic cracking
Upgraded bio-oil (wt%)			
Yield of oil	100	21–65	12–28
Yield of water	–	13–49	24–28
Yield of gas	–	3–15	6–13
Yield of coke	–	4–26	26–39
Oil characteristics			
HHV [MJ/kg]	6–19	42–45	21–36
H/C	0.9–1.5	1.3–2.0	0.3–1.8
O/C	0.3–0.5	<0.1	0.1–0.3

1.5 Catalytic fast pyrolysis

Catalytic fast pyrolysis (CFP) is a thermochemical conversion route comprising fast pyrolysis of biomass and catalytic cracking of the vapours before condensing the oil. The advantage of CFP is the low cost due to its similar reaction conditions to fast pyrolysis, such as the atmospheric pressure and the operating temperature [20].

There are two process configurations based on how the catalyst is used, either inside the pyrolysis reactor or outside it. The process with catalyst packed/fed together with the biomass feedstock in the pyrolysis reactor is referred to as *in situ* CFP, while the process where the catalyst is located in a separate reactor following the pyrolysis reactor is referred to as *ex situ* CFP [42]. Typically, the *in situ* CFP is operated on a (circulating) fluidised bed using catalyst as bed material and heat carrier so that the hot vapour is cracked directly after the biomass being pyrolysed.

For *in situ* CFP, the catalyst is intimately mixed with the biomass and the catalytic cracking temperature is always the same as the fast pyrolysis temperature. A circulating fluidized bed reactor is ideal for *in situ* CFP as this reactor can realise frequent and continuous regeneration of the catalyst, which is rapidly deactivated in catalytic cracking by coke deposition. In this research *in situ* catalytic fast pyrolysis is considered.

Catalysts such as metal oxides (MnO, FeO, ZnO, CaO, CuO) have been studied in catalytic fast pyrolysis [43-45]. However, zeolite catalysts are more widely used in catalytic fast pyrolysis of biomass, and are recognized as the most efficient catalysts in bio-oil catalytic cracking. Research using zeolite catalysts is considered below.

1.5.1 Zeolite catalyst

Zeolites, also called molecular sieves, are widely used in petroleum industry for refining [46]. Zeolites have very high surface area which contain active sites as they have crystalline microporous structures on the order of 5-12 Å. Their active sites and adsorption properties can be tailored for special applications. Zeolite catalysts include HZSM-5, HY, SiO_2-Al_2O_3, silicate, SAPO-5. Zeolites should have correct pore size and acidic sites to promote desired reactions while minimizing coking [34].

HZSM-5, one of the most widely used zeolites, is relatively rich in both Lewis and Brønsted acid sites, the acidity is linked to the Si/Al ratio with a low ratio indicating high acidity [47]. Many studies have demonstrated that HZSM-5 can convert biomass pyrolysis vapour to hydrocarbons, mainly aromatics, while generating the least coke on the catalyst [48-51]. One study on catalytic fast pyrolysis of pine wood with zeolites HBeta-25, HY-12, HZSM-5-23, and HMOR-20 was conducted in a fluidized bed reactor at 450 °C, using quartz sand as the control [52]. HZSM-5 produced more liquid and less coke than other zeolites, and more ketone and aromatics were produced in the bio-oil.

The synthesis of zeolite ZSM-5 is usually performed under hydrothermal conditions [53]: a silica source, an alumina source and an exchangeable cation are dissolved in water and the synthesis is realised via crystallization under heating from 80-200°C. ZSM-5 synthesis produces the catalyst “ZSM-5” in ammonia form, which can be converted to “HZSM-5” form by calcination. After catalyst synthesis, it is prepared with a binder (silica sol, an aqueous silicic acid solution) by granulation or spray drying to produce the pellet or particle catalyst used in fixed bed or fluidised bed reactors [54]. The purpose of adding binder is to increase the catalyst’s attrition

resistance, otherwise nearly half the catalyst particles would be lost in fluidized bed reactor [55]. It is reported that higher binder content leads to higher attrition resistance [56]. However too much binder can increase the ratio of matrix to zeolite activity, leading to higher coke and gas production, so a trade-off exists between the mechanical strength and the reaction selectivity of the catalyst [57].

1.5.2 Product distribution

The products from CFP using zeolites as the catalyst include liquid, non-condensable gas, coke and char. The liquid product usually contains an organic phase and an aqueous phase, which are named oily liquid and aqueous liquid in this study. The coke is a carbon-rich solid depositing in the catalyst pores causing deactivation [11]. The compounds in the oil liquid are mainly aromatics, and the non-condensable gas contains CO_2, CO, light olefins and alkanes [20]. The product distribution is variable due to the differences in the feedstock, reaction temperature, process type (*in situ* or *ex situ*) or weight hourly space velocity (WHSV). For instance, the oil yield is as high as 58.2 wt.% on an *in situ* reactor using alkaline lignin as feedstock, while it can be as low as 4.4 wt.% on an *ex situ* reactor using rice husk as the feedstock [58].

Iisa *et al.* [59] compared *in situ* and *ex situ* CFP of pine wood in a system with two bubbling fluidized bed reactors. The catalyst, HZSM-5 (Si/Al=30) was placed either in the first (pyrolysis) reactor or the second (upgrading) reactor. Both the pyrolysis and upgrading temperatures operated at 500 ^{o}C, and the weight hourly space velocity was 1.1 h^{-1}. No significant differences between *in situ* and *ex situ* catalytic pyrolysis were observed in coke and gas yields, or oil composition. Similar oil oxygen contents (15−17 wt.%), oil yields (14−17 wt.%), and carbon efficiencies (21−26 %) could be obtained by both *in situ* and *ex situ* catalytic pyrolysis. The *in situ*

configuration produced slightly more oil product, but it contained a higher oxygen content, than the *ex situ* configuration. It was concluded that the catalyst deactivated faster in the *in situ* configuration. Analysis by inductively coupled plasma atomic emission spectroscopy of the spent catalysts confirmed higher accumulation of metals on the catalyst in the *in situ* experiment.

Jae *et al.* [60] studied *in situ* CPF of wood using a spray-dried HZSM-5 catalyst on a bubbling fluidized bed reactor with continual catalyst addition and removal. It was found the yields for aromatics and olefins were dependent on operating parameters: temperature, biomass WHSV, and catalyst to biomass ratio. The aromatic yield increased from 9.6 % to 14.2 % (carbon mole percentage) as temperature increased from 500 ^{o}C to 600 ^{o}C, it then decreased to 10.3 % with a further increased in temperature to 650 ^{o}C. The yields of all the gaseous products, including olefins, CO, CO_2, and methane increased with temperature, and the combined yield of coke and char decreased with temperature. In the WHSV range from 0.15 h^{-1} to 0.9 h^{-1}, the aromatic yield reached a maximum of 14.2 % at WHSV 0.3 h^{-1}. Further increasing the WHSV to 0.9 h^{-1} decreased the aromatic yield to 10.2 %. In contrast, the olefin yield initially decreases from 8.7 % to 8.1 % with increasing WHSV from 0.15 h^{-1} to 0.3 h^{-1} and then increased again. The catalyst to biomass ratio in this study is defined as the mass flow rate of catalyst feed in divided by the mass flow rate of wood feed. The catalyst to biomass ratio was controlled in the range of 3-9 by changing the catalyst mass flow rate. The aromatic yield went through a maximum of 14.2 % at a catalyst to biomass ratio of 6, and the coke yield increased from 28.9 % to 33 % as the catalyst to biomass ratio increased from 3 to 9. However, the gaseous product yield did not change with the catalyst to biomass ratio. Additionally an investigation of fluidization gas flowrate suggested that a lower fluidization gas velocity, which means a longer vapour residence time, had a positive effect on the CFP chemistry, increasing the aromatic yield.

1.5.3 Catalyst deactivation

The high yield of coke and low yield of oil restrict the application of catalytic fast pyrolysis [20]. Another challenge in CFP is the rapid deactivation of catalyst. Deactivation of catalyst is mainly attributed to deposition of coke, deposition of ash originally present in the biomass, and dealumination of the zeolite Si/Al framework by hydrolysis in the presence of acids and steam [61].

It has been reported that the coke precursors form via an initial build-up of high molecular weight compounds, mainly aromatic structures [62]. These compounds are formed in the pores of the zeolite and then expand, resulting in blocking and deactivating the catalyst, which is so called coking. Acid sites of the zeolites are not only the essential part of the mechanism for the deoxygenating reactions, but also the coke forming mechanisms [63]. Hence coking accompanied with deoxygenation in CFP is unavoidable.

Similar to conventional fluid catalytic cracking (FCC) process, the deactivated catalyst can be regenerated by a high temperature oxidative treatment, burning the coke off the catalyst. Studies [52, 64-66] on regeneration and reuse of zeolite catalyst in CFP found that the catalyst activity decreases with regeneration cycles due to a decrease in the availability of acid sites. The decrease of zeolite acid sites is mainly due to the exposure to the steam leading to dealumination, as well as the metals deposition on the acid sites leading to irreversible deactivation [67-69]. The cost of zeolite catalyst in CFP process must be considered as the catalyst lifetime is limited due to the loss of acid sites during regenerations.

1.6 Combining biomass pretreatment with fast pyrolysis

1.6.1 Biomass pretreatment

Carpenter *et al.* [70] summarised the biomass pretreatment methods, which can help improving both the yield and quality of bio-oils produced by fast pyrolysis. These methods include process such as washing/leaching, steam explosion, or torrefaction.

Water, inorganic acids (such as HCl), organic acids (such as acetic acid) and alkalis (such as ammonia) are used for biomass washing/leaching. In general, leaching with dilute acids only removes soluble metals, while dilute alkali are required to disrupt cell walls and release ash components that are physiologically bound to the plant tissue [70]. The removal of minerals in biomass, especially alkali and alkaline earth metals (AAEMs) has positive effects on fast pyrolysis product yields [71]. Studies demonstrate that acetic acid , which can be derived from bio-oil [72] or the liquid of biomass torrefaction [73, 74], can be used as acid leachate to remove most of AAEMs. Hence biomass acid-leaching prior to fast pyrolysis can be a self-sufficient process when using an aqueous fraction produced from the biomass itself for demineralising the biomass.

Thermal pretreatment of biomass is conducted in the temperature range of 50 °C to 320 °C, including torrefaction in the range from 200 °C to 320 °C [75, 70]. The structural and chemical compositional changes of biomass during thermal pretreatment are summarised in Figure 1-3 [70, 76].

Torrefaction is a mild pyrolysis process [75, 70]. The benefits include increasing the energy density of the biomass for more efficient transportation, handling and storage. This is because the biomass dries and partially devolatilizes during torrefaction, decreasing its mass while

largely preserving its energy content. Torrefied biomass absorbs less moisture than fresh biomass during storage, as the hygroscopic property of biomass is decreased by torrefaction because of the destruction of OH groups through dehydration. Torrefaction causes biomass to lose its fibrous nature and become brittle so that specific grinding energy requirements decrease and grinding rates increase.

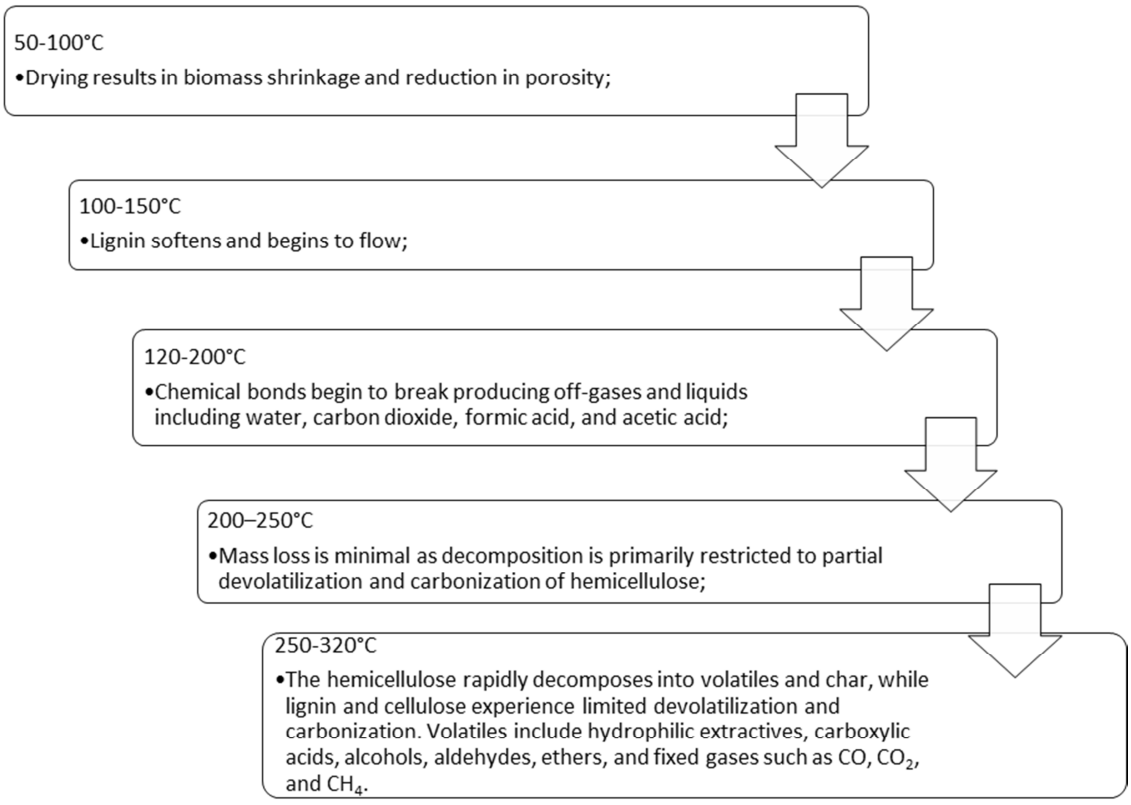

Figure 1-3: Structural and chemical compositional changes of biomass during thermal pretreatment.

1.6.2 Fast pyrolysis of pretreated biomass

The purpose of biomass pretreatment is to improve the quality of biomass, so that the reaction pathways in the following fast pyrolysis process are altered in order to obtain a better outcome. Acid-leaching and torrefaction are two popular biomass pretreatments as they can improve the fast pyrolysis process.

Minerals in biomass can act as cracking catalysts in fast pyrolysis processes, leading to less liquid yield, more produced water and loss of surfactants which are helpful for bio-oil stability. Carpenter *et al.* [70] summarized the effect of ash on pyrolysis: even 0.1 wt.% ash can alter both the thermal degradation rate and chemical pathways. There is a negative correlation between total ash content and bio-oil yield. Hence fast pyrolysis of acid-leached is investigated by many researchers. It has been found that the bio-oil yield is increased when using acid-leaching as a biomass pretreatment before fast pyrolysis [9, 72, 77-80]. In terms of bio-oil composition, acid-leaching pretreatment results in an increase of sugars and lignin-derived oligomers and a decrease of water and light organic compounds in the bio-oil [71, 81, 82].

Oudenhoven *et al.* reported detailed research on fast pyrolysis of organic acid-leached wood [72]. They demonstrated that washing pine wood with an aqueous acetic acid solution, produced in the fast pyrolysis process, effectively removed the minerals initially present in feedstock. Fast pyrolysis was performed at 530 °C in a 1 kg/h fluidised bed pilot plant. The results showed that the organic oil yield increased from 48.2 wt.% to 56.2 wt.%, while the produced water and char yields slightly decreased. Acid-leaching also resulted in increased yield of heavier molecules (e.g. levoglucosan) at the expense of lighter molecules.

Fast pyrolysis of acid-leached wood at different temperatures (360-580 °C) was also investigated by Oudenhoven *et al.* [78]. Generally the gas yield increased and the char yield decreased with increasing reactor temperature. Acid-leached pine wood produced more organic oil and less reaction water and char than the untreated wood over the whole temperature range. The organic oil yield reached the optimum around 480 °C for both untreated and acid-leached pinewood. A large increase in the glucose, xylose and mannose yields was obtained for acid-leached pine wood with the maximum sugar yield obtained around 480 °C. The analysis by gel permeation chromatography showed that with increasing fast pyrolysis temperature the bio-oil contained larger molecular weight components for both the untreated and acid-leached wood. The researchers also reported a bed agglomeration problem with acid-leached wood. The acid-leached wood went through a melt phase when the fast pyrolysis temperature was above 430 °C. Bed agglomeration can cause blockages and defluidisation in a fluidised bed reactor.

Raveendrana *et al*. [9] observed a higher yield of organic liquid and a lower yield of char with acid-leached biomass on both a thermogravimeteric analyser (TGA) and a fast pyrolysis reactor. Hassan *et al*. [77] pretreated debarked loblolly pine with several acids and found that the acid pretreatment increased the bio-oil molecular weight compared to untreated pine. Scott *et al.* [80] studied the effect of alkali metals on properties of bio-oil produced by fast pyrolysis. Potassium and calcium were removed by ion exchange using dilute acid. The properties of bio-oil derived from poplar wood and the deionized wood were compared, and it revealed that the levoglucosan content increased dramaticaly, while the acetic acid and hydroxyacetaldehyde contents decreased when alkali metals were removed.

Studies [73, 83-86] on biomass torrefaction followed by fast pyrolysis are also reported. Generally, the results indicate the bio-oil quality is improved in terms of lower water content and oxygen content. Zheng *et al*. [86] investigated the influence of the temperature of torrefaction pretreatment on bio-oil production. Although the yield of bio-oil decreased significantly by 20 wt.%, less water and acetic acid were produced with increasing the torrefaction pretreatment temperature from 240 to 320 °C.

Wigley *et al.* [73] proposed a pretreatment sequence combining acid-leaching and torrefaction prior to fast pyrolysis. Because the acidic liquid produced during torrefaction is rich in acetic and formic acid, this solution can be recovered as the acid leachate for removing the undesirable minerals in biomass. The bio-oil from fast pyrolysis of acid-leached and torrefied biomass was depleted in organic acids, pyrolytic lignin, and water but was rich in levoglucosan and aromatics.

1.6.3 Catalytic fast pyrolysis of pretreated biomass

It is reasonable to consider catalytic fast pyrolysis of pretreated biomass because of the benefits of applying biomass pretreatment before the bio-oil production process. However, combining biomass pretreatment with catalytic fast pyrolysis is not well understood. Hernando *et al.* [87] tested acid-washed wheat straw as the feedstock in an *ex situ* CFP study to investigate the deoxygenation pathways and energy yields using a downdraft fixed bed reactor. To the author's knowledge, there is no more reports about catalytic fast pyrolysis of acid-leached biomass. Studies [84, 88] on catalytic fast pyrolysis of torrefied biomass are reported using a Py-GC/MS instrument, but not using a pilot system. There is a knowledge gap in the catalytic fast pyrolysis of pretreated biomass.

1.7 Objectives and thesis outline

The main objective of this study is to examine the effects of biomass pretreatments, acid-leaching and torrefaction, on the outcomes of *in situ* catalytic fast pyrolysis. The details of this thesis outline are described as follows. There is some overlap of the results presented in Chapter 2 and Chapter 3, and in Chapter 4 and Chapter 5 for the convenience of discussion.

In **Chapter 2,** fast pyrolysis of acid-leached wood, torrefied wood and acid-leached-torrefied wood is studied under the same conditions. The aim of this study is to understand the effects of acid-leaching and torrefaction pretreatments in fast pyrolysis.

In **Chapter 3,** the bed material agglomeration in fast pyrolysis of acid-leached wood is investigated. The bed agglomeration issue has attracted attention due to the difficulty of fast pyrolysis operation when using acid-leached wood as feedstock in fluidised bed reactors. Approaches to overcoming this issue are discussed.

In **Chapter 4,** method development for catalytic fast pyrolysis on a bubbling fluidised bed reactor is presented. Afterwards catalytic fast pyrolysis of raw wood is conducted to be used as control experiments. The influence of catalyst to biomass ratio and reaction temperature is studied.

In **Chapter 5,** catalytic fast pyrolysis of acid-leached wood, torrefied wood and acid-leached-torrefied wood is studied. Different temperatures and catalyst/biomass ratios are applied to understand the effects of acid-leaching and torrefaction pretreatments in catalytic fast pyrolysis, and further investigate bed agglomeration.

In **Chapter 6,** analytic pyrolysis of pretreated woods with and without catalyst using a Py-GC/MS instrument is conducted. Pretreated woods are pyrolysed at different catalyst to biomass ratios and different temperatures. The chemistry in catalytic pyrolysis of pretreated woods is discussed.

In **Chapter 7** the main conclusions and recommendations are presented.

References

[1] Chu, S. and A. Majumdar, *Opportunities and challenges for a sustainable energy future.* Nature, 2012. **488**(7411): p. 294-303.

[2] Bauen, A., G. Berndes, M. Junginger, M. Londo, F. Vuille, R. Ball, T. Bole, C. Chudziak, A. Faaij, and H. Mozaffarian, *Bioenergy: a sustainable and reliable energy source. A review of status and prospects.* Bioenergy: a sustainable and reliable energy source. A review of status and prospects., 2009.

[3] *Energy Policies of IEA Countries-New Zealand-2017 Review*.

[4] Hall, P. and J. Gifford, *BIOENERGY OPTIONS FOR NEW ZEALAND, situation analysis of biomass resources and conversion technologies*. 2009, Scion.

[5] Hall, P., *Bioenergy options for New Zealand: key findings from five studies.* Wiley Interdisciplinary Reviews: Energy and Environment, 2013. **2**(6): p. 587-601.

[6] Butt, D., *Formation of phenols from the low-temperature fast pyrolysis of radiata pine (Pinus radiata).* Journal of Analytical and Applied Pyrolysis, 2006. **76**(1-2): p. 48-54.

[7] Mohan, D., C.U. Pittman, and P.H. Steele, *Pyrolysis of Wood/Biomass for Bio-oil: A Critical Review.* Energy & Fuels, 2006. **20**(3): p. 848-889.

[8] Rowell, R.M. and American Chemical Society. Cellulose Paper and Textile Division., *The Chemistry of solid wood*. Advances in chemistry series,. 1984, Washington, D.C.: American Chemical Society. x, 614 p.

[9] Raveendran, K., A. Ganesh, and K.C. Khilar, *Influence of mineral matter on biomass pyrolysis characteristics.* Fuel, 1995. **74**(12): p. 1812-1822.

[10] Bridgwater, A.V., D. Meier, and D. Radlein, *An overview of fast pyrolysis of biomass.* Organic Geochemistry, 1999. **30**(12): p. 1479-1493.

[11] Bridgwater, A.V., *Review of fast pyrolysis of biomass and product upgrading.* Biomass and Bioenergy, 2012. **38**: p. 68-94.

[12] Bridgwater, A.V., *Upgrading biomass fast pyrolysis liquids.* Environmental Progress & Sustainable Energy, 2012. **31**(2): p. 261-268.

[13] Elliot, D.C., *Analysis and comparison of biomass pyrolysis/gasification condensates*. 1986.

[14] Tang, W.K. and W.K. Neill, *Effect of Flame Retardants on Pyrolysis + Combustion of Alpha-Cellulose.* Journal of Polymer Science Part C-Polymer Symposium, 1964(6pc): p. 65-&.

[15] Westerhof, R.J.M., N.J.M. Kuipers, S.R.A. Kersten, and W.P.M. van Swaaij, *Controlling the Water Content of Biomass Fast Pyrolysis Oil.* Industrial & Engineering Chemistry Research, 2007. **46**(26): p. 9238-9247.

[16] Müller, S. *Ensyn Technologies*. IEA Bioenergy Agreement Task 34 Newsletter — PyNe 27, June 2010. 11-12.

[17] http://www.ensyn.com/overview.html.

[18] Peacocke, G.V.C. and A.V. Bridgwater, *Ablative Plate Pyrolysis of Biomass for Liquids.* Biomass & Bioenergy, 1994. **7**(1-6): p. 147-154.

[19] Branca, C., P. Giudicianni, and C. Di Blasi, *GC/MS characterization of liquids generated from low-temperature pyrolysis of wood.* Industrial & Engineering Chemistry Research, 2003. **42**(14): p. 3190-3202.

[20] George W. Huber, S.I., and Avelino Corma, *Synthesis of Transportation Fuels from Biomass Chemistry, Catalysts, and Engineering.* Chem. Rev., 2006. **106**: p. 4044-4098.
[21] Czernik, S. and A.V. Bridgwater, *Overview of applications of biomass fast pyrolysis oil.* Energy & Fuels, 2004. **18**(2): p. 590-598.
[22] Al-Sabawi, M., J. Chen, and S. Ng, *Fluid Catalytic Cracking of Biomass-Derived Oils and Their Blends with Petroleum Feedstocks: A Review.* Energy & Fuels, 2012. **26**(9): p. 5355-5372.
[23] Diebold, J.P. *A Review of the Chemical and Physical Mechanisms of the Storage Stability of Fast Pyrolysis Bio-Oils*. 2000; Report No. NREL/SR-570-27613;].
[24] Oasmaa, A. and S. Czernik, *Fuel oil quality of biomass pyrolysis oils - State of the art for the end user.* Energy & Fuels, 1999. **13**(4): p. 914-921.
[25] Oasmaa, A. and C. Peacocke, *Properties and fuel use of biomassderived fast pyrolysis liquids. A Guide*, in *VTT Publication 731*. 2010, VTT.
[26] Junming, X., J. Jianchun, S. Yunjuan, and L. Yanju, *Bio-oil upgrading by means of ethyl ester production in reactive distillation to remove water and to improve storage and fuel characteristics.* Biomass and Bioenergy, 2008. **32**(11): p. 1056-1061.
[27] Xiu, S. and A. Shahbazi, *Bio-oil production and upgrading research: A review.* Renewable and Sustainable Energy Reviews, 2012. **16**(7): p. 4406-4414.
[28] Diebold, J.P. and S. Czernik, *Additives to lower and stabilize the viscosity of pyrolysis oils during storage.* Energy & Fuels, 1997. **11**(5): p. 1081-1091.
[29] Bridgwater, A.V., *Principles and practice of biomass fast pyrolysis processes for liquids.* Journal of Analytical and Applied Pyrolysis, 1999. **51**(1-2): p. 3-22.
[30] Bridgwater, A.V., *Renewable fuels and chemicals by thermal processing of biomass.* Chemical Engineering Journal, 2003. **91**(2-3): p. 87-102.
[31] Ikura, M., M. Stanciulescu, and E. Hogan, *Emulsification of pyrolysis derived bio-oil in diesel fuel.* Biomass & Bioenergy, 2003. **24**(3): p. 221-232.
[32] Zheng, J.-L. and Q. Wei, *Improving the quality of fast pyrolysis bio-oil by reduced pressure distillation.* Biomass and Bioenergy, 2011. **35**(5): p. 1804-1810.
[33] Xu, J., J. Jiang, W. Dai, T. Zhang, and Y. Xu, *Bio-oil upgrading by means of ozone oxidation and esterification to remove water and to improve fuel characteristics.* Energy and Fuels, 2011. **25**(4): p. 1798-1801.
[34] Mortensen, P.M., J.D. Grunwaldt, P.A. Jensen, K.G. Knudsen, and A.D. Jensen, *A review of catalytic upgrading of bio-oil to engine fuels.* Applied Catalysis A: General, 2011. **407**(1-2): p. 1-19.
[35] Elliott, D.C., E.G. Baker, J. Piskorz, D.S. Scott, and Y. Solantausta, *Production of liquid hydrocarbon fuels from peat.* Energy & Fuels, 1988. **2**(2): p. 234-235.
[36] Elliott, D.C. and A. Oasmaa, *Catalytic hydrotreating of black liquor oils.* Energy & Fuels, 1991. **5**(1): p. 102-109.
[37] Elliott, D.C.N., G. G., *In DeVelopments in Thermochemical Biomass Conversion.* Blackie Academic and Professional: London, 1996. **Vol.1**.
[38] Elliott, D.C.S., G. F., *Preprints of Papers-American Chemical Society.* Division of Fuel Chemistry, 1989. **Vol 34**: p. 1160.
[39] Williams, P.T. and P.A. Horne, *Characterisation of oils from the fluidised bed pyrolysis of biomass with zeolite catalyst upgrading.* Biomass and Bioenergy, 1994. **7**(1-6): p. 223-236.

[40] Vitolo, S., M. Seggiani, P. Frediani, G. Ambrosini, and L. Politi, *Catalytic upgrading of pyrolytic oils to fuel over different zeolites.* Fuel, 1999. **78**(10): p. 1147-1159.
[41] Corma, A., G.W. Huber, L. Sauvanaud, and P. O'Connor, *Processing biomass-derived oxygenates in the oil refinery: Catalytic cracking (FCC) reaction pathways and role of catalyst.* Journal of Catalysis, 2007. **247**(2): p. 307-327.
[42] Wan, S. and Y. Wang, *A review on ex situ catalytic fast pyrolysis of biomass.* Frontiers of Chemical Science and Engineering, 2014. **8**(3): p. 280-294.
[43] Lu, Q., Z.-F. Zhang, C.-Q. Dong, and X.-F. Zhu, *Catalytic Upgrading of Biomass Fast Pyrolysis Vapors with Nano Metal Oxides: An Analytical Py-GC/MS Study.* Energies, 2010. **3**(11): p. 1805.
[44] Nokkosmäki, M.I., E.T. Kuoppala, E.A. Leppämäki, and A.O.I. Krause, *Catalytic conversion of biomass pyrolysis vapours with zinc oxide.* Journal of Analytical and Applied Pyrolysis, 2000. **55**(1): p. 119-131.
[45] Zhang, X., L. Sun, L. Chen, X. Xie, B. Zhao, H. Si, and G. Meng, *Comparison of catalytic upgrading of biomass fast pyrolysis vapors over CaO and Fe(III)/CaO catalysts.* Journal of Analytical and Applied Pyrolysis, 2014. **108**: p. 35-40.
[46] Corma, A., M.E. Domine, and S. Valencia, *Water-resistant solid Lewis acid catalysts: Meerwein-Ponndorf-Verley and Oppenauer reactions catalyzed by tin-beta zeolite.* Journal of Catalysis, 2003. **215**(2): p. 294-304.
[47] Adjaye, J.D. and N.N. Bakhshi, *Catalytic Upgrading of a Wood-Derived Fast Pyrolysis Oil over Various Catalysts.* 29th Intersociety Energy Conversion Engineering Conference, Pts 1-4, 1994: p. 1578-1583.
[48] French, R. and S. Czernik, *Catalytic pyrolysis of biomass for biofuels production.* Fuel Processing Technology, 2010. **91**(1): p. 25-32.
[49] Jackson, M.A., D.L. Compton, and A.A. Boateng, *Screening heterogeneous catalysts for the pyrolysis of lignin.* Journal of Analytical and Applied Pyrolysis, 2009. **85**(1–2): p. 226-230.
[50] Katikaneni, S.P.R., J.D. Adjaye, and N.N. Bakhshi, *Catalytic Conversion of Canola Oil to Fuels and Chemicals over Various Cracking Catalysts.* Canadian Journal of Chemical Engineering, 1995. **73**(4): p. 484-497.
[51] Mihalcik, D.J., C.A. Mullen, and A.A. Boateng, *Screening acidic zeolites for catalytic fast pyrolysis of biomass and its components.* Journal of Analytical and Applied Pyrolysis, 2011. **92**(1): p. 224-232.
[52] Aho, A., N. Kumar, K. Eränen, T. Salmi, M. Hupa, and D.Y. Murzin, *Catalytic pyrolysis of woody biomass in a fluidized bed reactor: Influence of the zeolite structure.* Fuel, 2008. **87**(12): p. 2493-2501.
[53] Van der Gaag, F.J., *ZSM-5 type zeolites: Synthesis and use in gasphase reactions with ammonia.* 1987.
[54] Ding, Y., J. Liang, Y. Fan, Y. Wang, and X. Bao, *Synergisms between matrices and ZSM-5 in FCC gasoline non-hydrogenating upgrading catalysts.* Catalysis today, 2007. **125**(3): p. 178-184.
[55] Cook, B., D. Mousko, W. Hoelderich, and R. Zennaro, *Conversion of methane to aromatics over Mo2C/ZSM-5 catalyst in different reactor types.* Applied Catalysis A: General, 2009. **365**(1): p. 34-41.
[56] Teng, L.-h., *Attrition resistant catalyst for dimethyl ether synthesis in fluidized-bed reactor.* Journal of Zhejiang University-SCIENCE A, 2008. **9**(9): p. 1288-1295.

[57] Harding, R.H., A.W. Peters, and J.R.D. Nee, *New developments in FCC catalyst technology.* Applied Catalysis A: General, 2001. **221**(1–2): p. 389-396.
[58] Liu, C., H. Wang, A.M. Karim, J. Sun, and Y. Wang, *Catalytic fast pyrolysis of lignocellulosic biomass.* Chemical Society Reviews, 2014. **43**(22): p. 7594-7623.
[59] Iisa, K., R.J. French, K.A. Orton, M.M. Yung, D.K. Johnson, J. ten Dam, M.J. Watson, and M.R. Nimlos, *In Situ and ex Situ Catalytic Pyrolysis of Pine in a Bench-Scale Fluidized Bed Reactor System.* Energy & Fuels, 2016. **30**(3): p. 2144-2157.
[60] Jae, J., R. Coolman, T.J. Mountziaris, and G.W. Huber, *Catalytic fast pyrolysis of lignocellulosic biomass in a process development unit with continual catalyst addition and removal.* Chemical Engineering Science, 2014. **108**: p. 33-46.
[61] Yildiz, G.r., T. Lathouwers, H.E. Toraman, K.M. van Geem, G.B. Marin, F. Ronsse, R. van Duren, S.R. Kersten, and W. Prins, *Catalytic fast pyrolysis of pine wood: effect of successive catalyst regeneration.* Energy & fuels, 2014. **28**(7): p. 4560-4572.
[62] Guo, X., Y. Zheng, B. Zhang, and J. Chen, *Analysis of coke precursor on catalyst and study on regeneration of catalyst in upgrading of bio-oil.* Biomass and Bioenergy, 2009. **33**(10): p. 1469-1473.
[63] Huang, J., W. Long, P.K. Agrawal, and C.W. Jones, *Effects of acidity on the conversion of the model bio-oil ketone cyclopentanone on H− Y zeolites.* The Journal of Physical Chemistry C, 2009. **113**(38): p. 16702-16710.
[64] Aho, A., N. Kumar, A. Lashkul, K. Eränen, M. Ziolek, P. Decyk, T. Salmi, B. Holmbom, M. Hupa, and D.Y. Murzin, *Catalytic upgrading of woody biomass derived pyrolysis vapours over iron modified zeolites in a dual-fluidized bed reactor.* Fuel, 2010. **89**(8): p. 1992-2000.
[65] Triantafillidis, C.S., A.G. Vlessidis, L. Nalbandian, and N.P. Evmiridis, *Effect of the degree and type of the dealumination method on the structural, compositional and acidic characteristics of H-ZSM-5 zeolites.* Microporous and Mesoporous Materials, 2001. **47**(2): p. 369-388.
[66] Vitolo, S., B. Bresci, M. Seggiani, and M. Gallo, *Catalytic upgrading of pyrolytic oils over HZSM-5 zeolite: behaviour of the catalyst when used in repeated upgrading–regenerating cycles.* Fuel, 2001. **80**(1): p. 17-26.
[67] Cerqueira, H., G. Caeiro, L. Costa, and F.R. Ribeiro, *Deactivation of FCC catalysts.* Journal of Molecular Catalysis A: Chemical, 2008. **292**(1): p. 1-13.
[68] Mullen, C.A. and A.A. Boateng, *Accumulation of Inorganic Impurities on HZSM-5 Zeolites during Catalytic Fast Pyrolysis of Switchgrass.* Industrial & Engineering Chemistry Research, 2013. **52**(48): p. 17156-17161.
[69] Paasikallio, V., C. Lindfors, E. Kuoppala, Y. Solantausta, A. Oasmaa, J. Lehto, and J. Lehtonen, *Product quality and catalyst deactivation in a four day catalytic fast pyrolysis production run.* Green Chemistry, 2014. **16**(7): p. 3549-3559.
[70] Carpenter, D., T.L. Westover, S. Czernik, and W. Jablonski, *Biomass feedstocks for renewable fuel production: a review of the impacts of feedstock and pretreatment on the yield and product distribution of fast pyrolysis bio-oils and vapors.* Green Chemistry, 2014. **16**(2): p. 384-406.
[71] Mourant, D., Z. Wang, M. He, X.S. Wang, M. Garcia-Perez, K. Ling, and C.-Z. Li, *Mallee wood fast pyrolysis: Effects of alkali and alkaline earth metallic species on the yield and composition of bio-oil.* Fuel, 2011. **90**(9): p. 2915-2922.

[72] Oudenhoven, S.R.G., R.J.M. Westerhof, N. Aldenkamp, D.W.F. Brilman, and S.R.A. Kersten, *Demineralization of wood using wood-derived acid: Towards a selective pyrolysis process for fuel and chemicals production.* Journal of Analytical and Applied Pyrolysis, 2013. **103**: p. 112-118.

[73] Wigley, T., A.C.K. Yip, and S. Pang, *Pretreating biomass via demineralisation and torrefaction to improve the quality of crude pyrolysis oil.* Energy, 2016. **109**: p. 481-494.

[74] Wigley, T., A.C.K. Yip, and S. Pang, *The use of demineralisation and torrefaction to improve the properties of biomass intended as a feedstock for fast pyrolysis.* Journal of Analytical and Applied Pyrolysis, 2015. **113**: p. 296-306.

[75] Basu, P., *Chapter 3 - Pyrolysis and Torrefaction*, in *Biomass Gasification and Pyrolysis*, P. Basu, Editor. 2010, Academic Press: Boston. p. 65-96.

[76] Tumuluru, J.S., C.T. Wright, J.R. Hess, and K.L. Kenney, *Erratum: A review of biomass densification systems to develop uniform feedstock commodities for bioenergy application.* Biofuels, Bioproducts and Biorefining, 2011. **5**(6): p. 720-720.

[77] Hassan, E.-b., P. Steele, and L. Ingram, *Characterization of Fast Pyrolysis Bio-oils Produced from Pretreated Pine Wood.* Applied Biochemistry and Biotechnology, 2009. **154**(1-3): p. 3-13.

[78] Oudenhoven, S.R.G., C. Lievens, R.J.M. Westerhof, and S.R.A. Kersten, *Effect of temperature on the fast pyrolysis of organic-acid leached pinewood; the potential of low temperature pyrolysis.* Biomass and Bioenergy, 2016. **89**: p. 78-90.

[79] Oudenhoven, S.R.G., R.J.M. Westerhof, and S.R.A. Kersten, *Fast pyrolysis of organic acid leached wood, straw, hay and bagasse: Improved oil and sugar yields.* Journal of Analytical and Applied Pyrolysis, 2015. **116**: p. 253-262.

[80] Scott, D.S., L. Paterson, J. Piskorz, and D. Radlein, *Pretreatment of poplar wood for fast pyrolysis: rate of cation removal.* Journal of Analytical and Applied Pyrolysis, 2001. **57**(2): p. 169-176.

[81] Piskorz, J., D.A.G. Radlein, D. Scott, and S. Czernik, *Liquid Products from the Fast Pyrolysis of Wood and Cellulose*, in *Research in Thermochemical Biomass Conversion*, A.V. Bridgwater and J.L. Kuester, Editors. 1988, Springer Netherlands. p. 557-571.

[82] Piskorz, J., D.S. Scott, and D. Radlein, *Composition of Oils Obtained by Fast Pyrolysis of Different Woods.* Acs Symposium Series, 1988. **376**: p. 167-178.

[83] Meng, J., J. Park, D. Tilotta, and S. Park, *The effect of torrefaction on the chemistry of fast-pyrolysis bio-oil.* Bioresource Technology, 2012. **111**: p. 439-446.

[84] Neupane, S., S. Adhikari, Z. Wang, A.J. Ragauskas, and Y. Pu, *Effect of torrefaction on biomass structure and hydrocarbon production from fast pyrolysis.* Green Chemistry, 2015. **17**(4): p. 2406-2417.

[85] Westover, T.L., M. Phanphanich, M.L. Clark, S.R. Rowe, S.E. Egan, A.H. Zacher, and D. Santosa, *Impact of thermal pretreatment on the fast pyrolysis conversion of southern pine.* Biofuels, 2013. **4**(1): p. 45-61.

[86] Zheng, A., Z. Zhao, S. Chang, Z. Huang, F. He, and H. Li, *Effect of Torrefaction Temperature on Product Distribution from Two-Staged Pyrolysis of Biomass.* Energy & Fuels, 2012. **26**(5): p. 2968-2974.

[87] Hernando, H., S. Jiménez-Sánchez, J. Fermoso, P. Pizarro, J. Coronado, and D. Serrano, *Assessing biomass catalytic pyrolysis in terms of deoxygenation pathways and energy yields for the efficient production of advanced biofuels.* Catalysis Science & Technology, 2016. **6**(8): p. 2829-2843.

[88] Zheng, A., L. Jiang, Z. Zhao, Z. Huang, K. Zhao, G. Wei, X. Wang, F. He, and H. Li, *Impact of Torrefaction on the Chemical Structure and Catalytic Fast Pyrolysis Behavior of Hemicellulose, Lignin, and Cellulose.* Energy & Fuels, 2015. **29**(12): p. 8027-8034.

Chapter 2

Fast pyrolysis of pretreated wood

Abstract

In this part of study, radiata pine wood was pretreated to investigate the effects of the pretreatments on the outcomes of fast pyrolysis. The pretreatment methods were acid-leaching, torrefaction and the combination of acid-leaching and torrefaction. The acid-leaching used 1 wt.% acetic acid solution, while the mild torrefaction was conducted by heating up to 260 °C under nitrogen for 270 minutes. The samples from the three pretreated methods along with raw wood were pyrolysed afterwards.

To understand the effects of the wood pretreatment in fast pyrolysis, the wood samples were analysed for elemental composition and the contents of cellulose, hemicellulose, lignin and inorganics. These analyses showed that acid-leaching removed most of the inorganic material, but did not affect the cellulose, hemicellulose and lignin contents. Mild torrefaction caused hemicellulose decomposition, resulting in decrease in oxygen and hydrogen contents, therefore, carbon content and lignin content were increased for the two kinds of torrefied woods.

Fast pyrolysis was performed on a University of Canterbury (UC) fluidised bed reactor as well as a Scion fluidised bed reactor. They were both bubbling fluidised bed reactors but differed in how

the char product is removed from the bed. The char is carried out the bed with the hot vapour and is separated in the following cyclone in the UC reactor, while the char falls into an overflow vessel with the bed material (sand) in the Scion reactor. The experiments on the two reactors were conducted at the same temperature of 450 °C. The product distribution and bio-oil analysis results were similar for the two pyrolysis systems. The biomass pretreatments showed the same effects on both reactors. However, bed material agglomeration occurred when using the UC reactor for fast pyrolysis of acid-leached wood.

Acid-leached wood gave the highest bio-oil yield and the lowest char yield. On the other hand, torrefied wood gave the lowest bio-oil yield and the highest char yield. Raw wood, and acid-leached-torrefied wood gave a similar yield of bio-oil.

The bio-oil products were analysed by, elemental composition, water content, gel permeation chromatography and solvent fractionation. The results revealed that the acid-leaching pretreatment significantly increased the content of cellulose and hemicellulose-derived products in the bio-oil, while the torrefaction pretreatment reduced the content of oxygen and increased the content of lignin-derived products in the bio-oil. The accelerated aging test showed that the three bio-oils from pretreated wood samples all had better stability than the bio-oil from raw wood.

2.1 Introduction

There are multiple methods to carry out biomass pretreatments including washing/leaching, steam explosion, torrefaction [1]. The purpose of biomass pretreatment in this study was to alter the biomass properties so that it can be beneficial to fast pyrolysis and catalytic fast pyrolysis.

Removal of inorganics from the biomass by acid leaching prior to fast pyrolysis leads to increased bio-oil yield and improved bio-oil quality, such as a lower acid concentration [2-4]. The inorganics removed be acid leaching are typically alkali and alkali earth metals (AAEMs). It is reported that levoglucosan content increases, while acetic acid and hydroxyacetaldehyde decreases when AAEMs are removed [4]. The absence of AAEMs significantly suppresses the dehydration and ring fragmentation reactions of the sugars [5].

Torrefaction can increase the mass and energy density of biomass and decrease the moisture content and hygroscopicity of the biomass. Fast pyrolysis of torrefied wood leads to more production of aromatics, and less production of water and acids [1]. It has been reported that, at the expense of a decrease in bio-oil yield, the water, acids, and oxygen contents of bio-oil decrease with increasing torrefaction temperature [6-8]. It is also reported that the bio-oil produced from torrefied wood contains more pyrolytic lignin compared to the bio-oil from non-torrefied wood [6].

Wigley *et al.* [9, 10] combined biomass acid-leaching and torrefaction prior to fast pyrolysis, and found that the inorganics, acetyl and moisture contents of biomass were decreased. The bio-oil produced from this pretreated wood was depleted in organic acids, pyrolytic lignin and water, but was rich in levoglucosan and aromatics. Due to the compensating effect of acid-leaching on

torrefied wood, bio-oil yield from this combined-pretreated wood was as high as fast pyrolysis of non-treated wood.

An ideal pretreatment process is to use acid recovered from the biomass for the acid-leaching so that there is no need for additional chemicals. It is reported washing pine wood with 1 wt.% acetic acid solution can effectively remove the ash in the feedstock, especially the AAEMs [10, 11]. Approximately 1 wt.% acetic acid can potentially be recovered from the bio-oil or condensed torrefaction liquid [10, 12]. Hence acid-leaching with 1 wt.% acetic acid was applied in this study.

Severe torrefaction significantly decreases the overall bio-oil yield in fast pyrolysis because of the formation of cross-linked carbohydrate polymers in the torrefaction which are char precursors [10]. Due to the trade-off between total liquid yield and bio-oil quality, a mild torrefaction (240-270 °C) was suggested as a biomass pretreatment prior to fast pyrolysis [8, 9, 13].

The objective of this study was to understand the effects of wood acid-leaching and torrefaction on the outcomes of fast pyrolysis. The results can guide the following research on catalytic fast pyrolysis with pretreated wood.

2.2 Experimental

2.2.1 Biomass and the pretreatments

Fresh wood chips (radiata pine) were obtained from a local sawmill in Rotorua, New Zealand. Firstly, they were dried to decrease the moisture content to under 10 wt.% in a drying room.

The wood chips were ground with a knife mill to decrease the particle size to below 2 mm. Then, the wood particles smaller than 0.25 mm were removed with a sieve. Table 2-1 shows the particle size distribution of the non-treated feedstock (raw wood).

Table 2-1: Particle size distribution of raw wood.

Particle size (mm)	Weight fraction (wt.%)
1-2	25.9
0.5-1	58.7
0.25-0.5	15.4

Acid-leaching of the raw wood was treated in a 1 wt.% acetic acid solution for 4 hours at 30 °C. Figure 2-1 illustrates the 25 L bucket with a motor stirring at 300-400 Hz which was used for acid-leaching. Afterwards, the wood particles were washed with deionized water until the washings were pH neutral. Acid-leached wood was dried in an oven overnight at 60 °C, then dried at 105 °C overnight. This procedure is an optimal method according to the previous research in which a solid yield of 99.3 wt.% was found [14]. This research suggested that this acid-leaching condition was able to effectively remove the biomass minerals, while a higher concentration or longer residence time had minimal effect.

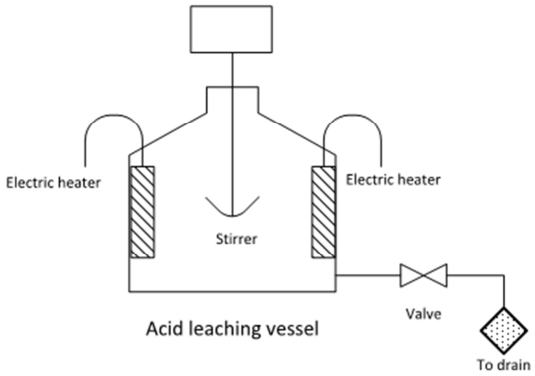

Figure 2-1: Acid-leaching setup.

In an industrial application, the wood feedstock would be torrefied before grinding. In order to simulate this scenario, the moisture content of feedstock was adjusted to 25 wt.% before torrefaction of the raw wood and acid-leached wood.

Torrefaction was carried out using the rig shown in Figure 2-2. This torrefaction vessel could treat 650-700 g of feedstock per run. It was constructed from 316 schedule 40, nominal bore 125 stainless steel pipe. The vessel was heated in a high temperature oven, and there was a steel tube inside the vessel to enhance thermal conductivity. During torrefaction a flow of nitrogen through the vessel carried the torrefaction vapour out. The condensed vapour was collected. Solid and liquid yields were measured, and the non-condensable gas composition was determined with an Agilent 3000A micro-GC. The details of configuration and operating conditions of the micro-GC has been reported previously [14]. Briefly this micro-GC was equipped with two TCD detectors and two columns (Molecular sieve 5A plot and Plot Q). The Molecular sieve 5A plot column was measuring H_2, O_2, N_2, CH_4 and CO, and the Plot Q column was measuring CO_2.

With the oven temperature set at 270 °C, the torrefaction vessel was heated with a steel tube inside the vessel to enhance thermal conductivity. The entire heating time was controlled precisely to 260 minutes, then the vessel was air-cooled to room temperature. The top temperature of the vessel was 258 ± 3 °C, the average heating rate was 0.9 °C/min and the average cooling rate was 2.0 °C/min. The average heating rate and cooling rate were calculated by dividing the temperature difference of the room temperature and the maximum torrefaction temperature by the heating or cooling time. This operating method was based on the previous

study [14]. This study suggested a torrefaction temperature between 250 and 280 °C to prevent significant biomass loss during torrefaction and to minimise the char yield during pyrolysis.

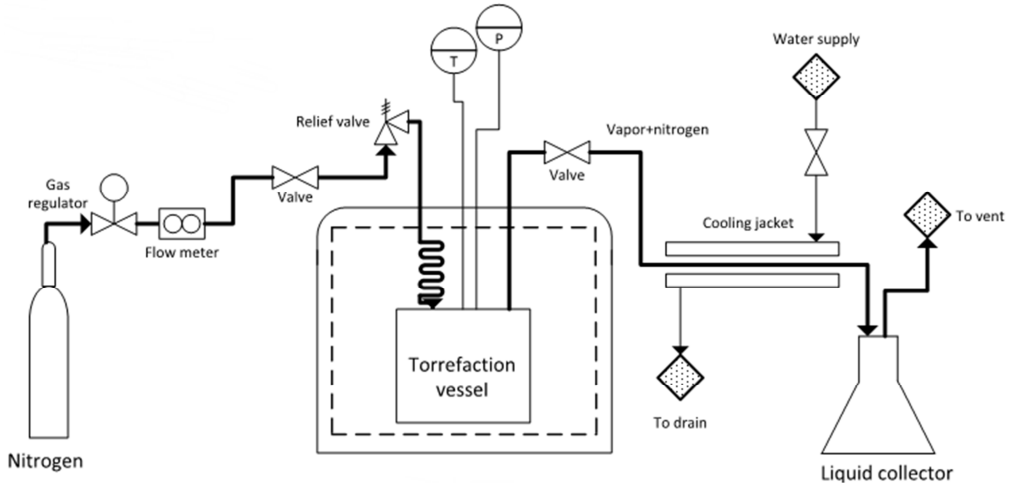

Figure 2-2: Torrefaction setup.

2.2.2 Biomass characterisation

Characterisation of the four biomass feedstocks, raw wood (Rwood), acid-leached wood (ALwood), torrefied wood (Twood) and acid-leached-torrefied wood (ALTwood), was undertaken at Scion in Rotorua, New Zealand. Wood samples were ground to powder then dried in an oven at 105 ^{o}C overnight before analysis. The analyses are described as follows.

Biomass ash content was determined by calcining the biomass in a muffle furnace at 575 ^{o}C for 12 hours to ensure ashing was completed and measuring the weight difference. Six replicate samples were tested. Elemental analysis was performed on a Thermo Scientific – FLASH 2000CHN analyser. Each sample was tested at least three times using approximately 3 mg of wood. A five-point calibration curve was constructed using acetanilide. The carbon, hydrogen and nitrogen content were determined by the analyser, and the oxygen content was calculated by difference. Wood samples were analysed for extractive, cellulose, hemicellulose and lignin

content by Scion's analytical chemistry laboratory, Veritec. Duplicate samples were tested. The wood samples were first extracted using dicholoromethane (DCM) solvent on a Soxtec apparatus to determine extractive content. The oven dried DCM-extracted samples were then analysed for contents of lignin and anhydrosugars using standard Veritec methodologies based on published methods [15-17]. Inductively coupled plasma mass spectrometry (ICP-MS) analysis was also performed by Veritec for measuring trace elemental contents of the wood samples.

2.2.3 Bubbling fluidised bed reactors

Two bubbling fluidised bed reactors were used for fast pyrolysis in this study. One was at the University of Canterbury (UC), and one at Scion. A diagram of the UC fluidised bed reactor is shown in Figure 2-3. Details of this reactor were reported in previous research [14]. A general description is presented below.

The UC reactor was composed of a biomass feeder, a nitrogen preheater, a bubbling fluidised bed, a cyclone, condensers which included a series of water coolers, an electrostatic precipitator (ESP), a vapour filter, and pressure and temperature control. Nitrogen was preheated before being fed into the fluidised bed. A copper gasket with a pore size of 56 μm was located at the bottom of the bed for the gas distribution. Five 500 W Watlow heating bands clamped directly in contact with the fluidised bed provided the pyrolysis heat for pyrolysis. Silica sand was preloaded in the reactor as the bed material. Biomass was fed into the fluidised bed via dual augers. Char was separated in a cyclone and fell into a storage vessel below the cyclone, while pyrolysis vapour exited the cyclone to pass through a set of condensers before entering the ESP. Finally a filter filled with about 40 grams cotton-wool collected any condensable materials no previously captured. The non-condensable gas (NCG) were exhausted after a gas sample port.

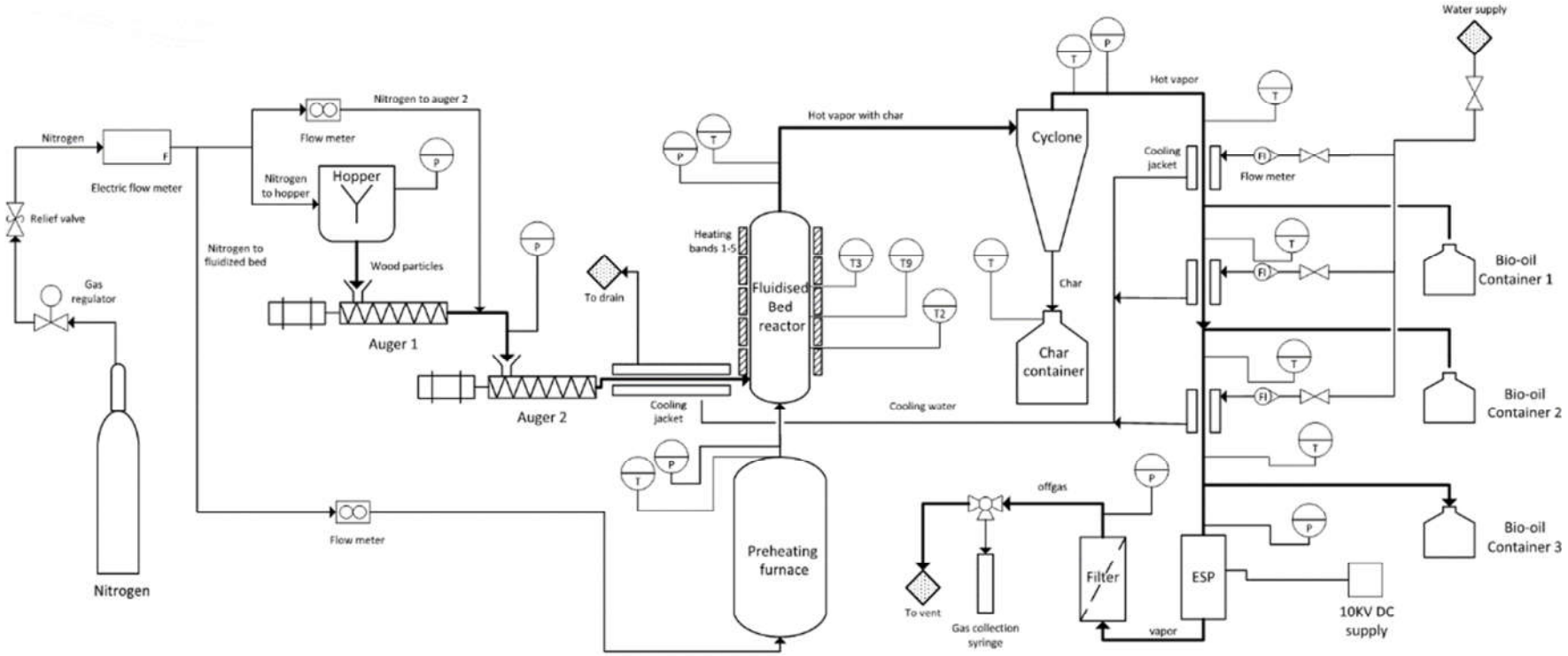

Figure 2-3: The UC fluidised bed reactor [14].

Figure 2-4: The front of Scion fluidised bed reactor (A), the ESP column, intense cooler and cartrige filter (B) and the gas cleaning set (C).

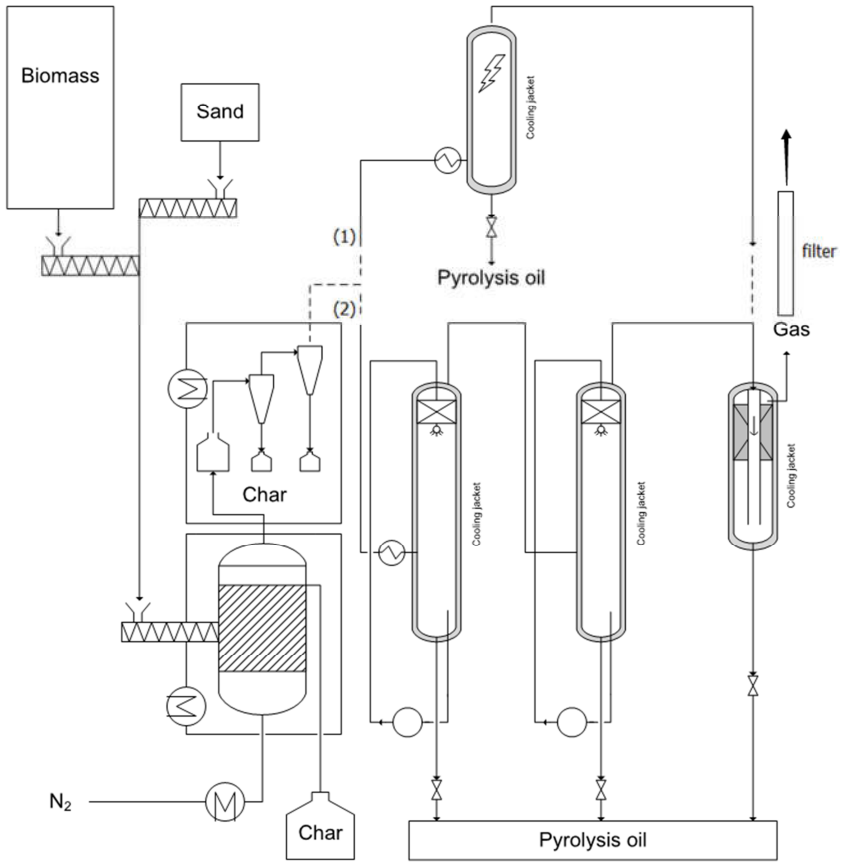

Figure 2-5: A brief scheme of the Scion fluidised bed reactor.

The design of the Scion fluidised bed reactor was based on a similar setup used by the Sustainable Process Technology group of the University of Twente in The Netherlands. This Scion fluidised bed reactor was built by Head Consultancy BV in 2015 for Scion (Figure 2-4). A brief schematic drawing is shown in Figure 2-5.

Three screw feeders provided a continuous flow of biomass and bed material to the fluidised bed reactor. A calibrated screw transported the biomass to a mixing tube. A rotating stirrer inside the biomass hopper prevented the biomass particles from forming bridges. The bed material (sand or catalyst) was fed with another calibrated feeding screw to the mixing tube.

The third screw transported the mixture of biomass and bed material from the mixing tube into the fluidised bed. A water-cooled jacket at the end of this screw prevented the biomass from pyrolysing before entering the bed. A small nitrogen flow was fed to the biomass hopper, which prevented backflow of pyrolysis vapour from the bed.

This bubbling fluidised bed had a conical-shaped bottom to ensure good distribution of the fluidisation gas (i.e. N_2). The gas flowrate was controlled by an electronic mass flow controller and was preheated before it was fed through a sintered metal plate (pore diameter 40 μm). Five thermocouples were located inside the fluidised bed at different heights to monitor the temperature profile of the bed. An overflow tube inside the bed kept the bed level constant. An overflow vessel with a water cooling coil collected char and bed material from the overflow tube. A small nitrogen flow was fed to this vessel, via a second electronic mass flow controller, and flowed from there to the bed. This nitrogen flow prevented vapours from the bed from condensing inside the cooled overflow vessel.

The solids removal and collection section (gas cleaning set) consisted of a knock-out vessel and two cyclones in series. The reactor, and the solids removal and collection section, were heated by two separately controlled ovens.

There were two options for liquid collection, which can be used alternatively:

(1) ESP + intensive cooler + gas filter;

(2) Two spray columns + intensive cooler + gas filter.

In this study, the first option was chosen as the ESP was better for catalytic fast pyrolysis (see Chapter 4 and Chapter 5). The ESP and intensive cooler were jacketed with coolant (water and

ethylene glycol). A cartridge filter was located after the intensive cooler to collect any remaining condensable material.

The total flow of the non-condensed gas was measured with a dry gas flow meter. The composition of non-condensed gas was analysed using an Agilent 490 Micro-GC with two analytical columns (10 m Molsieve 5 Å at 90 °C and 150 kPa and 10 m PPQ column at 70 °C at 150 kPa), with an analysis time of 120 s. It was calibrated to measure gases including N_2, O_2, H_2, CH_4, CO and CO_2.

The following table summarises the details of the Scion reactor. The bed material can be silica sand or zeolite catalyst. The minimum run time of 0.5 hour was required to achieve an accurate mass balance.

Table 2-2: The details of the Scion fluidised bed reactor.

	Description	Value
Feedstock	Particle size	0.5-2 mm
	Load	0.5-6 kg
	Feeding rate	0.5-1 kg/h
Bubbling fluidized bed	Inner diameter	100 mm
	Height	420 mm
	Reaction temperature	300-580 ^{o}C
	U/U_{mf} (fluidisation velocity/minimum fluidisation velocity)	1-10
	Superficial velocity	0.04-0.25 m/s
Bed material	Particle size	80-400 µm
	Initial load in bed	2.2 kg (silica sand)
Cyclones	Temperature	300-580 ^{o}C
	Particle size of removable char	> 10 µm
Condensers	ESP temperature	> -25 ^{o}C
	Intensive cooler temperature	> -25 ^{o}C
The total vapour resident time		1-4 s
Nitrogen flowrate		0-50 L/min (N)
Pressure of this setup		0-1.25 bara
Run time		0.5-3 hours

2.2.4 Fast pyrolysis experiments

Fast pyrolysis experiments on the UC reactor were performed at 450 ^{o}C for 120 minutes using the four feedstocks: Rwood, ALwood, Twood, and ALTwood. Each experiment was operated under the same conditions for at least three times. The operating conditions are summarized in Table 2-3. The moisture content of each feedstock was set to approximately 10 wt.%. This was because it was found that fast pyrolysis of Twood led to incomplete condensation and blockage of the cotton-wool filter when water was mostly removed from the feedstock by torrefaction. Gas samples (5 ml) were taken every 5 minutes using a gas tight collection bag and then analysed on the Agilent 3000A micro-GC. After the reactor cooled down, the liquid product from the water-cooling condensers and ESP collector were gathered and stored in a freezer. While the bio-oil trapped in cotton-wool filter was not recovered for analysis, but it was accounted for the mass balance (approximately 10 wt.% of the total bio-oil yield). The gas yield was calculated by mass balance difference.

Fast pyrolysis experiments using the Scion reactor were also performed using the four feedstocks. The operation conditions are summarized in Table 2-4. Rwood was pyrolysed at 450 ^{o}C three times to determine experimental repeatability. ALwood, Twood and ALTwood were pyrolysed at 450 ^{o}C once. The moisture content of feedstock was measured after each experiment. The bio-oil products collected in the ESP container and intensive cooler were blended together and stored in a freezer. The char mixed with silica sand was stored in sealed bucket. Two gas samples were taken from a sample port after the cartridge filter. Gas composition was measured offline by the portable GC after each experiment.

Table 2-3: Fast pyrolysis operating conditions on the UC reactor.

Description		Value
Feedstock	Particle size	0.25-2 mm
	Load	0.5-1 kg
	Feeding rate	0.33-0.36 kg/h
Bubbling fluidised bed	Inner diameter	31.8 mm
	Reaction temperature	450 ^{o}C
Bed material	Bed material	silica sand
	Particle size	600 - 710 µm
	Load	75 g
The total vapour resident time		< 2 s
Cyclone temperature		425 ^{o}C
Nitrogen flowrate		23 L/min (N)
Nitrogen temperature after preheating		470 ^{o}C
Max pressure of this setup		0.65 bar

Table 2-4: Fast pyrolysis operating conditions on the Scion reactor

Description		Value
Feedstock particle size		0.5-2 mm
Fluidized bed	Reaction temperature	450 ^{o}C
	Bed material	Silica sand
	Sand particle size	220-300 µm
	Overall feeding ratio of sand to feedstock	> 5
	Residence time of gas	1-4 seconds
Cyclones temperature		445 ^{o}C
Nitrogen flowrate		17 L/min (N)
Temperature of preheated nitrogen		500 ^{o}C
Run time		90 minutes
ESP temperature		5 ^{o}C
Intense cooler temperature		-15 ^{o}C

2.2.5 Bio-oil analysis

Water content of bio-oils from Rwood, ALwood, Twood and ALTwood (Roil, ALoil, Toil and ALToil) was measured by Karl-Fischer titration (Metrohm 870 KF Titrino plus). The solvent used was a 3:1 (vol.) mixture of methanol and dichloromethane. The titrant was Hydranal Composite

5 (Riedel-de Haën). The measurement was repeated three times and the average values were obtained.

Elemental analysis was performed on the same Thermo Scientific – FLASH 2000CHN analyser as described above using approximately 3 mg of bio-oil. The measurement was done in triplicate.

High heating value and the pH value were measured by a LECO AC500 bomb calorimeter and a SCHOTT pH meter, respectively. The measurements were both repeated three times to obtain average values.

Molecular weight distribution was determined by gel permeation chromatography (GPC) analysis. Bio-oil samples were firstly dissolved in tetrahydrofuran to give a concentration of 5 mg mL^{-1}, and syringe filtered through a 0.45 µm PTFE filter. Samples were analysed using a Knauer/Polymer Standards Service GPC with a PSS SDV Lux 1000 Å column at 30 ^{o}C and using a refractive index detector. The system was calibrated using polystyrene standards. The number-average (Mn), weight-average (Mw), and size-average (Mz) molecular weights were determined using Polymer Standards Service Win GPC Unichrom software. Each sample was analysed twice and the average values were obtained.

Solvent fractionation of the bio-oils was carried out following the method developed by Oassmaa *et al.* [18]. The procedure is briefly described as follows: 3 grams of bio-oil was separated into water-soluble (WS) and water-insoluble (WIS) fractions by water extraction with sonication in an ultrasonic bath. The WS fraction was then extracted by diethylether followed by dichloromethane (DCM) to give two fractions called ether insoluble and ether soluble. The WIS fraction was extracted with DCM to give two fractions called dichloromethane insoluble and

dichloromethane soluble. The solvents were removed and the bio-oil fractions weighted. Each sample was analysed twice and the average values were obtained.

2.2.6 Bio-oil accelerated aging test

Accelerated aging test was applied on the bio-oils from the Scion reactor. Duplicate samples of Roil, ALoil, Toil and ALToil were placed in 15 ml polypropylene tubes. The tubes were fully filled with the bio-oil samples and tightly capped to minimise oxygenation and loss of volatiles in the test. The samples were placed in an oven at 80 ^{o}C for 24 hours. The tube caps needed to be re-tightened after the first ten minutes of heating. The aged bio-oils were stored at -20 ^{o}C prior to analysis.

Water content was measured in triplicate by Karl-Fischer titration. Dynamic viscosity was measured by a CAP 1000+ Viscometer at 750 rpm and at 40 ^{o}C. The measure required less than 1 mL bio-oil sample and used a cone spindle (CAP-06). Bio-oil samples were heated to 40 ^{o}C before measurement due to the very high viscosity of bio-oil at lower temperature. The viscosity test was done in triplicate for both aged bio-oils and original bio-oils.

2.3 Results and discussion

2.3.1 Torrefaction pretreatment

The initial torrefaction pretreatment was conducted at 270 ^{o}C for 20 minutes. However the heating-up time was 250-280 minutes. This variable heating time led to a heterogeneous product as the biomass located near the vessel wall had a much longer torrefaction time than that in the centre of the vessel. Consequently the operating method was modified as described

in the experimental section. By this modified procedure, the colour of the torrefied woods was uniformly dark brown and the yields of solid and liquid products were stable (Table 2-5).

The product yields and gas composition in torrefaction of Rwood and ALwood, including the standard deviations of the averaged values, are shown in Table 2-5. The results of product yields show that this modified torrefaction method had a good repeatability as the standard deviation for solid and liquid yields were less than 1 wt.%. Afterwards the torrefied products from different batches were mixed in one container to give a homogeneous feedstock.

Table 2-5: Product yields and gas composition of wood torrefaction.

	Rwood	ALwood
Yield (wt.%, dry basis)		
Solid [a]	83.1	86.3
Liquid [a]	11.3	9.0
Gas [b]	5.6	4.7
Gas composition (vol.%) [c]		
CO	31.2	28.1
CO_2	68.8	71.9

[a] The standard deviations were no more than 0.9, based on more than 10 torrefaction experimental results; [b] by difference; [c] gas composition was normalized with carbon monoxide and carbon dioxide only, although trace amounts of other gases were detected.

Torrefaction of ALwood led to a higher yield of solid product, and lower yields of liquid and gas than torrefaction of Rwood. The non-condensable gas was mainly composed of carbon monoxide and carbon dioxide, although trace amounts of C_2 hydrocarbons were detected. It is reported torrefaction caused deacetylation of hemicellulose to produce carbon dioxide [13]. The concentration of carbon dioxide in the gas from Rwood torrefaction was lower than from ALwood torrefaction. Overall it appeared beneficial to acid-leach the wood prior to torrefaction as more mass was conserved in the solid product for the following fast pyrolysis.

2.3.2 Feedstock characteristics

The elemental and ash composition of Rwood, ALwood, Twood and ALTwood are shown in the Table 2-6. The results reveal that pretreating wood by acid-leaching effectively removed ash and torrefaction pretreatment decreased the oxygen content. Comparing the results for ALwood with Rwood shows that the elemental composition was similar, while the ash content was decreased substantially (88.5 wt.%) in ALwood. Comparing Twood and ALTwood with Rwood shows that torrefaction led to an increase in carbon content (approximately 5 wt.%) and a slight decrease in oxygen content. The results of ALTwood show the combining effect of acid-leaching and torrefaction on removing ash and decreasing oxygen content.

Table 2-6: Elemental and ash contents of feedstock.

wt.%	N [a]	C [a, b]	H [a, c]	O [a, d]	Ash [e]
Rwood	<0.5	50.1	6.3	43.2	0.26
ALwood	<0.5	48.6	6.1	44.8	0.03
Twood	<0.5	55.1	5.8	38.8	0.30
ALTwood	<0.5	53.3	5.7	40.6	0.07

[a] dry and ash free basis; [b] the standard deviations were no more than 0.9; [c] the standard deviations were no more than 0.1; [d] by difference; [e] dry biomass basis, the standard deviations were no more than 0.01.

Table 2-7 shows the biomass component composition of the four woody feedstocks. The analysis shows that ALwood and Rwood had similar compositions, but the ash content in the ALwood has been significantly reduced to 0.03 wt.% (Table 2-6). This implies acid-leaching just removed minerals from the woody feedstock while the biomass structural polymers were kept intact. This is further confirmed by ^{13}C NMR spectroscopy (see Chapter 3). The results show that the Klason lignin content was increased after torrefaction, mainly due to the loss of other components, namely hemicellulose. The decrease of hemicellulosic sugar units reveals that the hemicellulose was partially degraded in torrefaction. The result is consistent with the reports

claiming that torrefaction caused biomass thermal-decomposition and structure change [19, 20, 13]. The analysis results of ALTwood shows the hemicellulosic units were decreased to a lesser extent by the torrefaction. Possibly it was due to the removal of minerals by the acid-leaching, which could catalyse the thermal degradation.

Table 2-7: Biomass components of feedstock.

wt.% [a]		Rwood	ALwood	Twood	ALTwood
Extractives		0.7	0.4	0.7	0.6
Lignin	Acid-insoluble (Klason) [b]	26.8	27.0	42.7	39.6
	Acid-soluble [c]	0.5	0.5	0.9	0.8
Neutral carbohydrates as anhydrosugars [d]	Arabinosyl units	1.1	1.1	<LOD [e]	<LOD
	Galactosyl units	2.2	2.1	0.5	0.6
	Glucosyl units	45.0	45.1	41.9	44.4
	Xylosyl units	4.7	4.7	<LOD	1.4
	Mannosyl units	11.1	11.0	3.9	5.3
Total		92.2	91.8	90.4	92.7

[a] Results were average values of duplicate; [b] modified method based on TAPPI Standard Methods, T 222 om-88; [c] modified TAPPI Useful Method UM 250; [d] modified Wood Sugar Analysis by Anion Chromatography; [e] LOD (limit of the detection)=0.1;

Table 2-8: ICP-MS results of feedstock.

ppm	Al	As	B	Ba	Ca	Cd	Co	Cr	Cu
Rwood	14.3	0.4	2.7	3.0	383.7	0.1	<LOD	0.1	1.1
ALwood	6.6	0.3	1.9	1.4	98.9	<LOD	<LOD	0.1	3.6
Twood	13.8	0.1	1.9	3.7	481.0	0.1	<LOD	0.1	1.7
ALTwood	8.1	<LOD	1.3	1.8	180.0	<LOD	<LOD	0.1	3.7
ppm	Fe	K	Li	Mg	Mn	Mo	Na	Ni	P
Rwood	11.0	590.4	<LOD	91.8	27.9	1.0	5.4	0.1	76.0
ALwood	7.3	10.7	<LOD	12.1	4.0	0.5	1.2	0.1	18.6
Twood	7.3	729.3	<LOD	116.6	36.0	0.2	6.4	0.1	86.0
ALTwood	12.2	33.2	<LOD	14.8	5.3	<LOD	2.4	0.2	27.5
ppm	Pb	S	Se	Si	Sn	Sr	V	Zn	-
Rwood	<LOD	702.4	<LOD	9.2	2.8	1.8	<LOD	5.8	-
ALwood	0.2	686.4	<LOD	6.9	1.2	1.0	<LOD	2.5	-
Twood	0.1	701.9	<LOD	37.4	0.5	2.3	<LOD	7.9	-
ALTwood	0.3	689.4	<LOD	23.7	0.3	1.2	<LOD	3.7	-

* LOD (limit of detection)=0.05 ppm

The results of trace elements analysis are presented in Table 2-8. It shows Ca, K and S were the major trace elements in radiata pine. The alkali and alkaline earth metals (i.e. Ca and K) and phosphorus were removed mostly by acid-leaching, while sulphur was less affected by this pretreatment. Torrefaction led to some elements being concentrated, like Ca, K and Mg probably due to the loss of biomass components. Si content increased in the torrefied woods probably due to the silicone gel used for sealing the torrefaction vessel.

2.3.3 Experiments on the UC fluidised bed reactor

The fast pyrolysis experiments at 450 °C with Rwood, Twood and ALTwood on the UC reactor were successful.

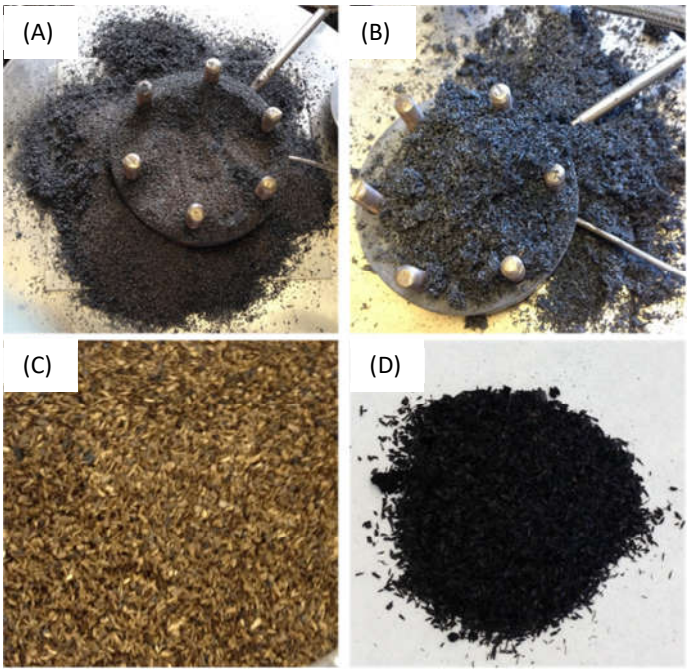

Figure 2-6: Bed agglomeration in ALwood fast pyrolysis at 450 °C, (A): agglomerated sand with the char, (B): agglomerated char from the reactor, (C): the solid product obtained in the char container, (D): The typical char from raw wood.

Fast pyrolysis of ALwood at 450 ^{o}C had a bed agglomeration problem causing defluidisation in the reactor after 20 minutes running. Figure 2-6 shows the bed materials from ALwood fast pyrolysis. Figure 2-6A shows the silica sand binding to the char, which developed to clumps causing defluidisation. Figure 2-6B shows the agglomerated char which caused blockage of the reactor. Figure 2-6C shows the solid product obtained in the char container, comparing to the typical char from fast pyrolysis of Rwood in Figure 2-6D. The brown colour in Figure 2-6C reveals the feedstock was not completely pyrolysed due to insufficient heat transfer as a result of defluidisation.

Two results of fast pyrolysis of ALwood were obtained, one for a 20 minutes experiment (stopping before bed agglomeration occurred); and one for a running time of 120 minutes (the same as other feedstocks), but with bed agglomeration occurring during the experiment.

The results from the fast pyrolysis experiments are summarized in Table 2-9. The product yields are presented on biomass dry basis and the gas yield was calculated by difference. Only CH_4, CO and CO_2 were accounted in the gas composition as the amounts of other gases, such as H_2, C_2H_4, C_2H_6, C_3H_6 and C_3H_8, were negligible. The two sets of experimental data for ALwood fast pyrolysis are also presented in the table.

Table 2-9: Products distribution of pretreated woods fast pyrolysis on the UC reactor.

	Rwood	ALwood [a]	ALwood [b]	Twood	ALTwood
Product yield (dry basis, wt.%) [c]					
Bio-oil	63	72	52	54	57
Char	17	9	38	30	28
Gas [d]	20	19	10	17	14
Gas composition [e] (vol.%)					
CH_4	3	8	trace	7	8
CO	57	65	76	62	64
CO_2	39	27	24	32	28

[a] A successful but short experiment stopping before bed agglomeration occurred, no standard deviation obtained; [b] a full length experiment but with bed agglomeration, including unconverted feedstock; [c] the standard deviations of product yields were no more than 0.8; [d] gas yield was calculated by difference; [e] fast pyrolysis gas compositions were normalized to 100 % based on CH_4, CO and CO_2 only, other gases, C_2H_4, C_2H_6, C_3H_6 and C_3H_8, were negligible.

The products distribution for ALwood fast pyrolysis without bed agglomeration occurring shows the bio-oil yield was increased to 72 wt.% and the char yield was decreased, compared to Rwood fast pyrolysis. After bed agglomeration occurred, the liquid yield decreased significantly. The high char yield of 38 wt.% and the images shown in Figure 2-6 indicate that the pyrolysis was not completed. The gas composition results show a higher carbon monoxide concentration in ALwood fast pyrolysis than in Rwood fast pyrolysis. It has been reported that ash in the wood can alter both the thermal degradation rate and chemical pathways of pyrolysis and can enhance char formation [1]. The changes in the composition of the gas from acid-leached wood indicate that the chemical pathways were altered in ALwood fast pyrolysis.

In the case of torrefaction pretreatment prior to fast pyrolysis, regardless of whether the wood was acid-leached or not, the yield of char increased and the yields of liquid and gas decreased. The product distribution results alone show no particular benefit of wood torrefaction for fast pyrolysis, however, oil quality is an important factor which can be improved by torrefaction pretreatment (see section 2.3.5).

2.3.4 Experiments on the Scion fluidised bed reactor

Fast pyrolysis of Rwood was performed three times to demonstrate the repeatability of pyrolysis experiments on the Scion reactor. Typically yield of 63-64 wt.% bio-oil, 15-16 wt.% char and 19 wt.% gas was produced from Rwood (Table 2-10). The standard deviations for the oil, char and gas yields were respectively 0. 5, 0.4 and 0.5. The mass balance for the three experiments was above 97 wt.%. The results indicate a high degree of repeatability of the Scion reactor. Also the results are consistent with the fast pyrolysis results for Rwood on the UC reactor.

Fast pyrolysis of Twood and ALTwood was successfully carried out. Fast pyrolysis of ALwood using this plant was also successful with no bed agglomeration occurring during the 90 minutes run time. The occurrence and prevention of bed agglomeration in ALwood fast pyrolysis is further explored in Chapter 3.

Table 2-10: Product distribution of pretreated woods fast pyrolysis on the Scion reactor.

	Rwood1	Rwood2	Rwood3	ALwood	Twood	ALTwood
Mass balance, biomass dry basis (wt.%)						
Bio-oil	63.4	62.9	64.0	74.9	54.4	63.4
Char	15.7	15.1	16.1	9.5	26.1	25.9
Gas	18.7	19.1	19.7	13.2	16.1	13.4
Total	97.8	97.1	99.8	97.6	96.6	102.7
Gas composition (vol.%)*						
H_2	2.0	2.0	2.2	3.9	1.7	2.2
CH_4	6.0	5.6	3.8	8.4	8.3	8.7
CO	58.5	57.4	58.4	63.2	59.5	63.0
CO_2	33.5	35.0	35.6	24.5	30.5	26.1

*The gas composition was analysed and normalised including hydrogen, methane, carbon monoxide and carbon dioxide as the gaseous species, the amounts of other gases, such as C_2H_4, C_2H_6, C_3H_6 and C_3H_8, were negligible.

Fast pyrolysis of ALwood gave the highest yield of bio-oil (74.9 wt.%) and the lowest yields of gas and char. Fast pyrolysis of Twood produced the most char at 26.1 wt.%. Overall the results were

similar to those findings on the UC reactor: acid-leaching pretreatment increased the yield of bio-oil and decreased the yield of char; torrefaction pretreatment had the opposite effect on the yields of bio-oil and char; both pretreatments led to a decreased yield of gas.

2.3.5 Bio-oil properties

Analysis results of the properties of bio-oils produced from the UC reactor are presented in Table 2-11 with the bio-oils labelled accordingly, i.e. Roil is the bio-oil from Rwood. The ALoil in this table represents the bio-oil sample obtained from ALwood when bed agglomeration occurred. The results for ALoil obtained without bed agglomeration are not presented as there was not enough oil produced for analysis. It should be noted that about 10 wt.% of the bio-oil trapped in cotton-wool filter after the ESP was not recovered. This part of bio-oil was believed to contain the small molecular weight compounds and water, so the bio-oil samples analysed in the table contained less of the light fraction of the bio-oil.

The water contents of the four bio-oils were relatively similar (17-18 wt.%) as the moisture contents of the four feedstocks were controlled at about 10 wt.%, so were the pH values. The heating values of bio-oils were consistent with the elemental compositions with lower oxygen content leading to higher heating value.

Table 2-11: Properties of bio-oils made on the UC reactor.

	Roil	ALoil [a]	Toil	ALToil
Water content (wt.%) [b]	17.2	18.4	18.0	17.4
pH [b]	2.4	2.7	2.4	2.6
HHV (MJ/kg) [b]	17.7	16.6	17.7	16.7
Elemental composition (wt.%), dry basis				
C [c]	53.9	51.2	54.4	53.7
H [b]	5.9	5.7	6.3	5.9
O, by difference	40.2	43.1	39.3	40.4
Solvent fractionation (wt.%), dry basis [d]				
High MW lignin [e]	6.7	5.1	6.1	5.9
Low MW lignin [f]	16.8	11.7	19.1	11.8
Sugars [g]	31.6	50.0	28.9	53.2
Volatiles [h]	44.8	33.3	45.9	29.1
GPC results (g/mol) [d]				
Mn	203	195	192	181
Mw	312	279	285	248
Mz	487	427	440	370

[a] Oil sample obtained from ALwood fast pyrolysis when bed agglomeration occurred; [b] the standard deviations (STDs) were no more than 0.2; [c] STDs<0.9; [d] the results were average values of duplicate; [e] fraction containing high molecular weight lignin and solids (water insoluble – DCM insoluble); [f] fraction containing low molecular weight lignin and extractives (water insoluble – DCM soluble); [g] fraction containing sugars and hydroxyl-acids (water soluble – diethylether & DCM insoluble); [h] fraction containing volatile acids, aldehydes, ketones, lignin monomers (water soluble – diethylether & DCM soluble)

The solvent fractionation results give an indication of the bio-oil's composition. The high MW lignin and low MW lignin fractions contain mainly compounds derived from lignin; the sugars fraction contains compounds which chemically behaved like sugars such as anhydrosugars and hydroxyl acids; the volatiles group contains mainly small organic molecules with water, such as acids, aldehydes, ketones, pyrans and furans [18]. As shown in Table 2-11 the ALoil was rich in sugars and low in the two lignins fractions comparing to the Roil. Toil's low MW lignins fraction was the highest at 19.1 wt.%. This result agrees with other reports indicating that torrefaction pretreatment produces more aromatics in the bio-oil [6, 13]. The ALoil and ALToil contained more sugars (50.0 and 53.2 wt.%) comparing to the other bio-oils. This result indicates acid-

leaching pretreatment enhances sugar production in fast pyrolysis. This is also in agreement with the literature [9, 11].

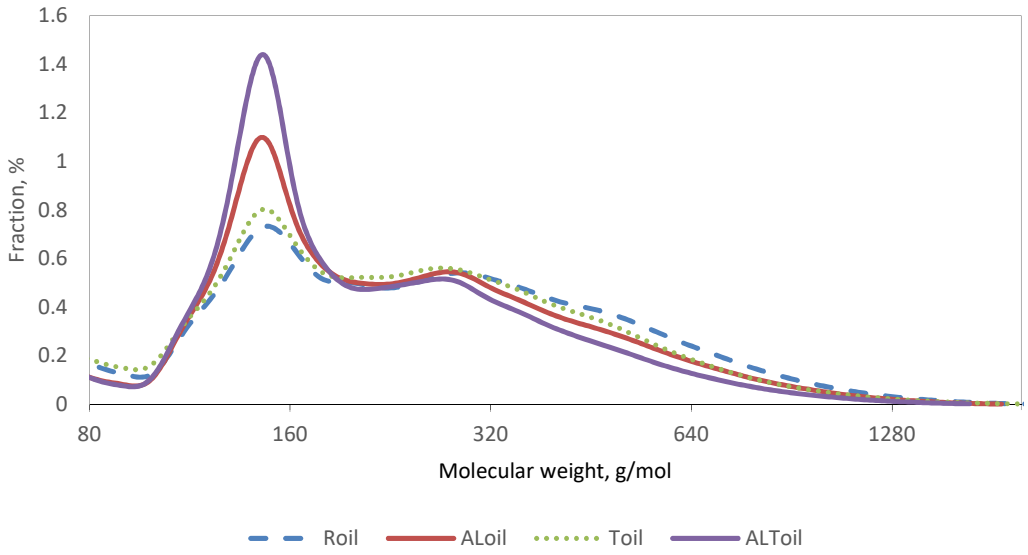

Figure 2-7: Molecular weight distribution profiles for the bio-oils from the UC reactor.

The GPC results can be used to calculate three kinds of average molecular weight value for the bio-oils: the number-average molecular weight (Mn), the weight-average molecular weight (Mw) and the size-average molecular weight (Mz). It should be noted that GPC analysis provides separation of molecules by size and the values are translated to molecular weight using a calibration with standards. As the relationship between size and molecular weight is different between the standards and the bio-oil, the calculated averages are only indicative [21]. The average molecular weights of the bio-oils from all the pretreated woods were lower compared to Roil. The GPC profiles in Figure 2-7 illustrate the molecular weight distributions of the three pretreated bio-oils were shifted slightly to the left side (to low MW) comparing with the distribution of the Roil, with more intensive signal around 150 g/mol. This peak is likely associated with the higher sugars content of the ALoil and ALToil (Table 2-11). It indicates that

acid-leaching and torrefaction both have the positive effect on bio-oil quality in terms of less oligomeric material.

Table 2-12: Properties of bio-oils made on the Scion reactor.

	Roil	ALoil	Toil	ALToil
Water content (wt.%) [a]	36.7	18.9	27.5	21.8
Elemental composition (wt.%), dry basis				
C [b]	51.5	51.7	58.0	53.8
H [a]	6.0	5.7	6.1	5.2
O, by difference	41.6	41.9	35.2	40.5
N	<1.0	<1.0	<1.0	<1.0
Solvent fractionation (wt.%), dry basis [c]				
High MW lignin	10	8	8	8
Low MW lignin	14	10	20	13
Sugars	45	52	43	59
Volatiles	31	30	29	21
GPC results (g/mol) [d]				
Mn	182	169	180	174
Mw	245	220	237	225
Mz	355	301	327	302

[a] The standard deviations (STDs) were no more than 0.2; [b] STDs<0.9; [c] see Table 2-11 for the details; [d] the results were average values of duplicate.

Analysis results of properties of bio-oil produced using the Scion reactor are presented in Table 2-12. The water content of Roil was the highest as 36.7 wt.%. This was partially due to Rwood having the highest moisture content at 9.4 wt.%, while the moisture contents of ALwood, Twood and ALTwood were 3.7 wt.%, 2.2 wt.% and 3.2 wt.%, respectively. Comparing the elemental composition of pretreated oils to Roil, acid-leaching pretreatment had little effect, while torrefaction pretreatment caused an increase in the carbon content and a decrease in oxygen content.

The solvent fractionation results (Table 2-12) show that acid-leaching pretreatment led to a higher sugars content, and torrefaction pretreatment led to a higher content of low MW

pyrolytic lignin in the bio-oils compared to Roil. The GPC results and the curves in Figure 2-8 show that both acid-leaching and torrefaction pretreatments produced lower molecular weight bio-oil compared to Roils. While torrefaction pretreatment lowered the bio-oil's molecular weight to a lesser extent than acid-leaching. It is also noteworthy to mention that the bio-oils from the UC reactor were more monodisperse than those from the Scion reactor by comparing the GPC curves. It is because about 10 wt.% of bio-oil was trapped in the cotton-wool filter and not recovered on the UC reactor. On the other hand, the Scion reactor was able to recover almost the entire oil product. As a result, the GPC curves of the Scion bio-oils show more peaks than those of the UC bio-oils.

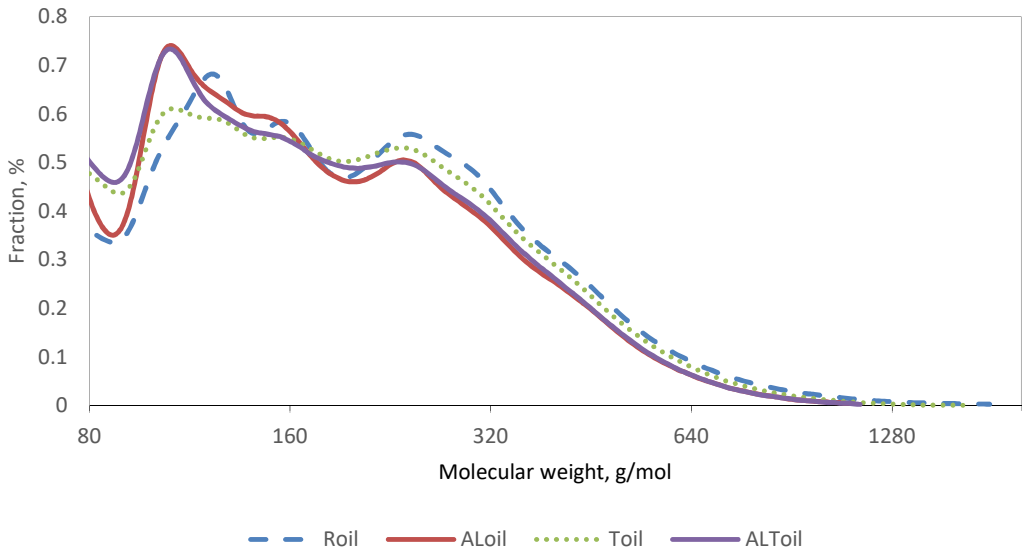

Figure 2-8: Molecular weight distribution profiles for the bio-oils from the Scion reactor.

2.3.6 Bio-oil stability

Accelerated aging was applied to analyse the stability of the bio-oils. The analysis results of water content and dynamic viscosity shown in Table 2-13 provide indicators of bio-oil aging. Pictures of original bio-oils and aged bio-oils are illustrated in Figure 2-9.

Table 2-13: Bio-oil aging analysis of the samples from the Scion reactor.

	Roil	ALoil	Toil	ALToil
Phase behaviour after aging	two phases	single phase	resin-like residue	resin-like residue
Mass loss (wt.%) [a]	0.7	0.3	0.4	0.4
Water content increase (wt.%) [b]	9.6	1.4	4.0	1.9
Dynamic viscosity at 40 ^{o}C initial (mPa.s) [c]	NA [d]	89	30	64
Dynamic viscosity at 40 ^{o}C after aging (mPa.s) [c]	NA	181	40 [e]	121 [e]

[a] The results were average values of duplicate; [b] the standard deviations (STDs) were no more than 0.7; [c] STDs<5; [d] no available results due to high water content making measurement impractical; [e] the solid was removed before viscosity measurement.

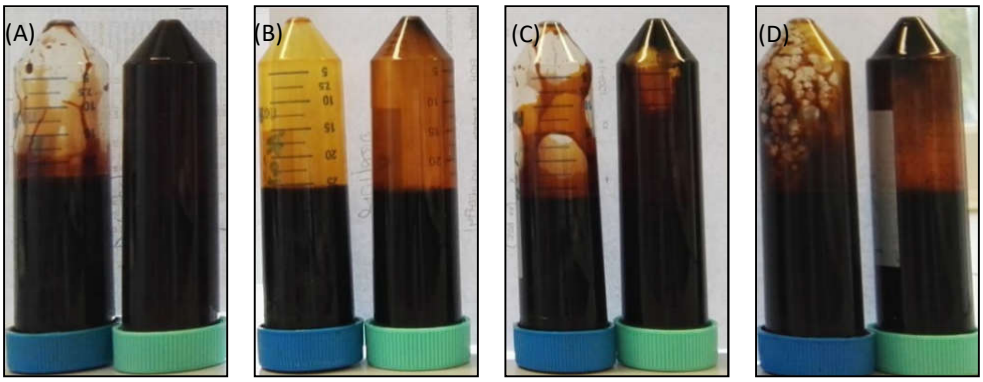

Figure 2-9: The comparison of initial bio-oils (left) and aged bio-oils (right): (A)-Roil, (B)-ALoil, (C)-Toil and (D)-ALToil.

The Roil had the largest increase in water content and phase separation occurred after the aging test. Because of the high water content of the Roil and aged Roil, no reliable viscosity results could be provided for these bio-oils. A visual assessment (Figure 2-9A) indicates the viscosity of the aged Roil appeared to be higher than the original Roil.

Roil, Toil and ALToil formed multi-phases after accelerated aging, whereas the ALoil remained a single phase. Roil and Toil had relatively high increases in water content. The ALoil and ALToil had substantially increases in dynamic viscosity after aging, possibly due to polymerisation and oligomerisation of the carbonhydrate derived products.

Generally, bio-oil from ALwood shows good performance in terms of phase stability and less dehydration in the aging test, while the bio-oil from Twood shows viscosity stability.

2.3.7 Comparison of the performance of the two reactors

The two pyrolysis systems were both bubbling fluidised bed reactors. One key difference between the reactors was the operation of using the bed material. In the UC reactor, silica sand was preloaded into the reactor and fluidised during running. The char was purged out of the reactor to the cyclones and the sand remained behind. While in the Scion reactor, fresh silica sand was co-fed with biomass continuously into reactor and the extra sand and char in the reactor dropped into the overflow vessel via the tube inside the reactor. This difference in operation was possibly the reason that ALwood could be successful pyrolysed on the Scion reactor. The quick removal of the sand and char may have prevented bed agglomerating in the Scion reactor. While in the UC reactor, the melt material accumulated in the reactor leading to agglomeration and eventually defluidisation.

Another difference between the operations of the two reactors was the moisture content of pretreated woods. It was controlled at around 10 wt.% for the UC reactor, whereas the three pretreated woods was used for the Scion reactor were drier (2-4 wt.%). The final difference was the condensation system. The condensers on the UC reactor include a series of water coolers, an ESP and a cotton-wool filter. Due to the limited capability of the upstream condensers, about

10 wt.% of bio-oil was trapped in the cotton-wool filter and not recovered for analysis (it was counted for mass balance). On the Scion reactor, the ESP column and intensive cooler, both jacketed with coolant, were capable of capturing and quenching almost all the pyrolysis vapours. Consequently, the bio-oil samples obtained on the Scion reactor were more representative.

The comparison of product distribution for the four feedstocks in the two reactors is presented in Figure 2-10. It shows consistent results between the two reactors, especially on Rwood fast pyrolysis: the oil yield was respectively 63.0 wt.% and 64.1 wt.%, the char yield was 16.7 wt.% and 16.1 wt.%, and the gas yield was 20.3 wt.% and 19.7 wt.%. However, all the oil yields from the pretreated wood produced by the Scion reactor were higher than the UC reactor. As it is reported water is auto-catalytic in pyrolysis [22], and it can promote the production of reaction water [9]. Probably the lower moisture content (2-4 wt.%) of pretreated woods contributed to the higher oil yield.

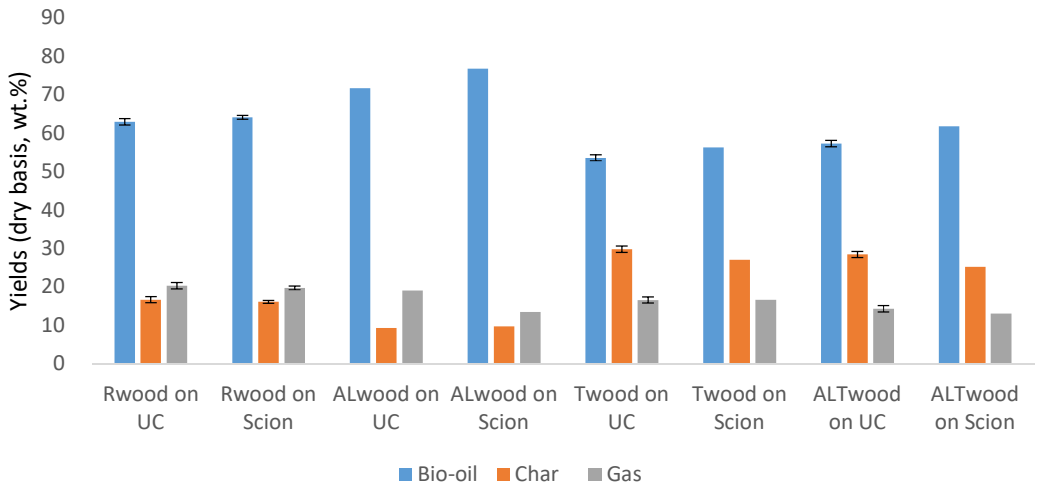

Figure 2-10: Comparison of product yields on the two reactors (UC-UC reactor,Scion-Scion reactor).

The comparison of water content and elemental contents for the bio-oils obtained from the two reactors is illustrated in Figure 2-11. Comparing the carbon and oxygen contents, the elemental composition was similar to each other. However, the water content of the bio-oils obtained on the UC reactor was relatively low due to the loss of the bio-oil's light fraction (including water not recovered from the cotton-wool filter). GPC results shown in Table 2-11 and Table 2-12 confirm that the average molecular weights of bio-oils obtained on the UC reactor were higher than those produced at Scion.

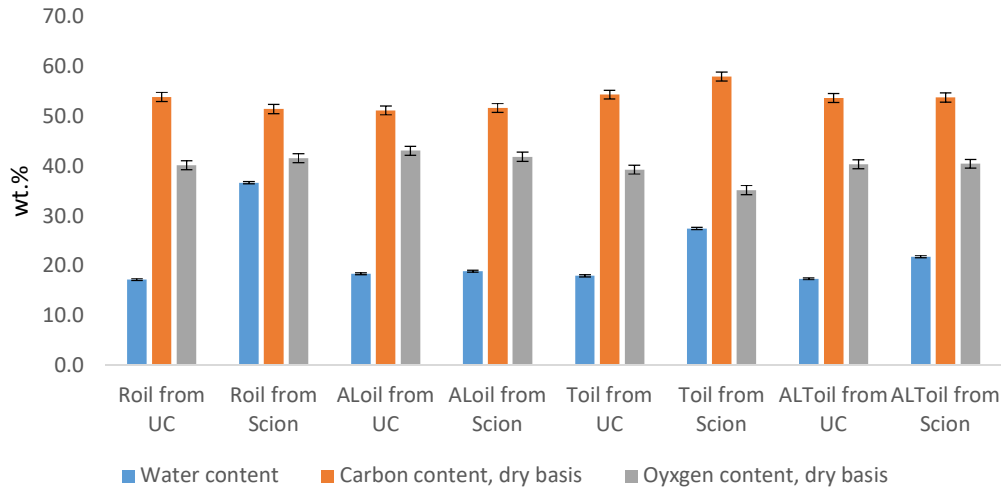

Figure 2-11: Comparison of water content and elemental content of bio-oils obtained on the two reactors (ALoil from UC reactor obtained when bed agglomeration ocurred).

2.4 Conclusion

The results of fast pyrolysis experiments performed in two bubbling fluidised bed reactors (UC reactor and Scion reactor) showed the same trends when evaluating different biomass pretreatments on product distribution and bio-oil properties. Acid-leaching pretreatment enhanced bio-oil production and suppressed carbonisation, while torrefaction pretreatment

enhanced carbonisation. While the combined pretreatment showed combined effects of acid-leaching and torrefaction in fast pyrolysis.

The acid-leaching pretreatment effectively reduced ash content of pine wood from 0.26 wt.% to 0.03 wt.%, especially potassium and calcium, while it did not impact on the other biomass components such as cellulose or lignin. This decrease in ash content led to an increase in bio-oil yield, but caused a bed agglomeration issue in the fast pyrolysis using the UC reactor. The bio-oil from acid-leached wood contained higher a content of carbohydrate derived products, although the elemental composition was similar to bio-oil from the raw wood. According to the GPC analysis of the bio-oil, the average molecular weight of the bio-oil was slightly decreased by acid-leaching. The bio-oil from acid-leached wood also had good stability in terms of phase stability and less dehydration during the accelerated aging test.

The torrefaction pretreatment altered the biomass constitutive composition, especially causing degradation of the hemicellulose. The elemental analysis revealed that the torrefaction pretreatment led to increased carbon content and decreased oxygen content. In fast pyrolysis, char yield was increased and bio-oil yield was decreased. However, the torrefied wood had positive effects on the bio-oil properties in terms of decreasing oxygen content and increasing the content of lignin derived products. The bio-oil from torrefied wood had lower average molecular weights in comparison with that from raw wood. The bio-oil produced from torrefied wood showed good viscosity stability after accelerated aging.

References

[1] Carpenter, D., T.L. Westover, S. Czernik, and W. Jablonski, *Biomass feedstocks for renewable fuel production: a review of the impacts of feedstock and pretreatment on the yield and product distribution of fast pyrolysis bio-oils and vapors.* Green Chemistry, 2014. **16**(2): p. 384-406.

[2] Hassan, E.-b., P. Steele, and L. Ingram, *Characterization of Fast Pyrolysis Bio-oils Produced from Pretreated Pine Wood.* Applied Biochemistry and Biotechnology, 2009. **154**(1-3): p. 3-13.

[3] Raveendran, K., A. Ganesh, and K.C. Khilar, *Influence of mineral matter on biomass pyrolysis characteristics.* Fuel, 1995. **74**(12): p. 1812-1822.

[4] Scott, D.S., L. Paterson, J. Piskorz, and D. Radlein, *Pretreatment of poplar wood for fast pyrolysis: rate of cation removal.* Journal of Analytical and Applied Pyrolysis, 2001. **57**(2): p. 169-176.

[5] Fuentes, M., D. Nowakowski, M. Kubacki, J. Cove, T. Bridgeman, and J. Jones, *Survey of influence of biomass mineral matter in thermochemical conversion of short rotation willow coppice.* Journal of the Energy Institute, 2008. **81**(4): p. 234-241.

[6] Meng, J., J. Park, D. Tilotta, and S. Park, *The effect of torrefaction on the chemistry of fast-pyrolysis bio-oil.* Bioresource Technology, 2012. **111**: p. 439-446.

[7] Westover, T.L., M. Phanphanich, M.L. Clark, S.R. Rowe, S.E. Egan, A.H. Zacher, and D. Santosa, *Impact of thermal pretreatment on the fast pyrolysis conversion of southern pine.* Biofuels, 2013. **4**(1): p. 45-61.

[8] Zheng, A., Z. Zhao, S. Chang, Z. Huang, F. He, and H. Li, *Effect of Torrefaction Temperature on Product Distribution from Two-Staged Pyrolysis of Biomass.* Energy & Fuels, 2012. **26**(5): p. 2968-2974.

[9] Wigley, T., A.C.K. Yip, and S. Pang, *Pretreating biomass via demineralisation and torrefaction to improve the quality of crude pyrolysis oil.* Energy, 2016. **109**: p. 481-494.

[10] Wigley, T., A.C.K. Yip, and S. Pang, *The use of demineralisation and torrefaction to improve the properties of biomass intended as a feedstock for fast pyrolysis.* Journal of Analytical and Applied Pyrolysis, 2015. **113**: p. 296-306.

[11] Oudenhoven, S.R.G., R.J.M. Westerhof, and S.R.A. Kersten, *Fast pyrolysis of organic acid leached wood, straw, hay and bagasse: Improved oil and sugar yields.* Journal of Analytical and Applied Pyrolysis, 2015. **116**: p. 253-262.

[12] Oudenhoven, S.R.G., R.J.M. Westerhof, N. Aldenkamp, D.W.F. Brilman, and S.R.A. Kersten, *Demineralization of wood using wood-derived acid: Towards a selective pyrolysis process for fuel and chemicals production.* Journal of Analytical and Applied Pyrolysis, 2013. **103**: p. 112-118.

[13] Neupane, S., S. Adhikari, Z. Wang, A.J. Ragauskas, and Y. Pu, *Effect of torrefaction on biomass structure and hydrocarbon production from fast pyrolysis.* Green Chemistry, 2015. **17**(4): p. 2406-2417.

[14] Wigley, T., *Improving the quality of bio-oil by fast pyrolysis of acid leached and torrefied Pinus radiata: a thesis submitted in full fulfilment of the requirements for the degree of Doctor of Philosophy in Chemical and Process Engineering at the University of Canterbury*. 2015.

[15] *TAPPI Standard Methods, T 222 om-88*.

[16] *TAPPI Useful Method UM 250*.
[17] Pettersen, R.C., *Wood sugar analysis by anion chromatography.* Journal of Wood Chemistry and Technology, 1991. **11**(4): p. 495-501.
[18] Oasmaa, A., E. Kuoppala, and D.C. Elliott, *Development of the Basis for an Analytical Protocol for Feeds and Products of Bio-oil Hydrotreatment.* Energy & Fuels, 2012. **26**(4): p. 2454-2460.
[19] Hill, S.J., W.J. Grigsby, and P.W. Hall, *Chemical and cellulose crystallite changes in Pinus radiata during torrefaction.* Biomass and Bioenergy, 2013. **56**: p. 92-98.
[20] Melkior, T., S. Jacob, G. Gerbaud, S. Hediger, L. Le Pape, L. Bonnefois, and M. Bardet, *NMR analysis of the transformation of wood constituents by torrefaction.* Fuel, 2012. **92**(1): p. 271-280.
[21] Hoekstra, E., S.R.A. Kersten, A. Tudos, D. Meier, and K.J.A. Hogendoorn, *Possibilities and pitfalls in analyzing (upgraded) pyrolysis oil by size exclusion chromatography (SEC).* Journal of Analytical and Applied Pyrolysis, 2011. **91**(1): p. 76-88.
[22] Kasparbauer, R.D., *The effects of biomass pretreatments on the products of fast pyrolysis*. 2009: Iowa State University.

Chapter 3

Understanding and overcoming bed material agglomeration in fast pyrolysis of acid-leached pine wood

Abstract

Acid-leaching of pine wood particles before fast pyrolysis can increase bio-oil yield. However, fast pyrolysis of the acid-leached pine wood suffers from bed material agglomeration in a fluidised bed reactor. The bed material (silica sand) adheres to the char and causes agglomeration. In this study, approaches to overcome this issue were investigated using a bubbling fluidised bed reactor. Firstly, experiments at different pyrolysis temperatures found that pyrolysing at a lower temperature, i.e. 360 ^{o}C, prevented bed agglomeration. Secondly, fast pyrolysis at a higher sand feeding rate was shown to overcome this issue. Thirdly, a torrefaction step after acid-leaching pretreatment was performed and this combined pretreatment was also successful in overcoming bed agglomeration.

The mechanism of bed agglomeration in the fast pyrolysis of acid-leached wood was discussed. It was concluded that melting behaviour of biomass was the precursor of bed agglomeration. Acid-leaching pretreatment caused biomass melting due to its suppression of carbonisation which are normally catalysed by the alkali and alkaline earth metals in biomass during fast

pyrolysis. This suppressed carbonisation led to melting behaviour and subsequent agglomeration. Torrefaction pretreatment had the effect of enhancing carbonisation, which hindered this melting behaviour and prevented bed agglomeration.

3.1 Introduction

Fast pyrolysis of pretreated biomass has been investigated in Chapter 2 of this thesis. This study and the results of other references have found that acid-leaching pretreatment can increase bio-oil yield and improve the bio-oil quality, especially the yield of cellulose derived products including levoglucosan [1-4]. The presence of ash in biomass can alter both the thermal degradation rate and chemical pathways during pyrolysis. The ash components, particularly alkali and alkaline earth metals, can have different effects in pyrolysis [5]. But the removal of the ash by acid-leaching pretreatment led to a decrease in the yield of char in fast pyrolysis [6, 4], which indicates that the biomass carbonisation was suppressed. Although promising results have been found using acid-leaching as a pretreatment method for biomass fast pyrolysis, bed agglomeration can be an important issue [3, 7]. Bed agglomeration can cause operational malfunction due to the defluidisation and blockage of the fluidised bed reactor.

In order to avoid the bed agglomeration issue, a low pyrolysis temperature was used by Oudenhovven *et al.* [3] who found that pyrolysing acid-leached wood at 360 °C prevented bed agglomeration. However, the bio-oil yield was reduced from 72 wt.% at the standard temperature of 480 °C to 65 wt.% at 360 °C. Bed agglomeration also occurred in fast pyrolysis of acid-infused wood and it was found that the bed agglomeration could be reduced by addition of a small amount of oxygen in the nitrogen sweep gas [8]. Bed agglomeration was also observed in fast pyrolysis of pure lignin extracted from lignocellulosic biomass [9, 10]. Calcium hydroxide pretreatment of lignin was found to prevent the bed agglomeration [10]. This was believed to be due to the catalytic effect of calcium in the fast pyrolysis of lignin. In a study of Wigley *et al.* on fast pyrolysis of pretreated wood [7], radiata pine wood was pretreated by dilute acid-leaching

followed by torrefaction. The fast pyrolysis was conducted in a continuous fluidised bed reactor at various temperatures from 400 °C to 525 °C. But it was not reported if bed agglomeration occurred.

In this study, bed agglomeration in fast pyrolysis of acid-leached pine wood particles was investigated and approaches to overcome it were developed. The possible mechanism of bed agglomeration was also discussed.

3.2 Experimental

3.2.1 Feedstock

Four types of woody biomass feedstocks presented in Chapter 2 were used in this study, which were raw wood without pretreatment (Rwood), acid-leached wood (ALwood), torrefied wood (Twood) and acid-leached and torrefied wood (ALTwood).

3.2.2 The reactor and operation

The Scion fluidised bed reactor was used, the configuration and operational procedure can be found in Chapter 2.

3.2.3 Fast pyrolysis experiments

In this study, experiments were conducted at different conditions as summarised in Table 3-1. The aim of these experiments was to investigate the effect of operating conditions and biomass pretreatment on bed agglomeration during fast pyrolysis. Variables of the experiments included pyrolysis temperature, sand feeding rate and an additional torrefaction pretreatment step. The

biomass feeding rate was kept at 0.5 kg/h in every experiment. Experiments were labelled as indicated in Table 3-1.

Table 3-1: A summary of fast pyrolysis experiments.

ID	Feedstock	Temperature (°C)	Sand feeding rate (kg/h)	Experiment
RFP450	Rwood	450	3	Chapter 2
ALFP360	ALwood	360	3	New
ALFP450	ALwood	450	3	Chapter 2
ALFP500	ALwood	500	3	New
ALFP450L	ALwood	450	1	New
ALFP500M	ALwood	500	4	New
ALFP500H	ALwood	500	5	New
TFP450	Twood	450	3	Chapter 2
ALTFP450	ALTwood	450	3	Chapter 2
ALTFP500	ALTwood	500	3	New

Control pyrolysis experiments for Rwood and Twood samples were conducted at 450 °C with a feeding rate of bed material (silica sand) at 3 kg/h.

To investigate the effect of pyrolysis temperature on bed agglomeration, ALwood fast pyrolysis was operated at 360 °C, 450 °C and 500 °C with a feeding rate of silica sand of 3 kg/h. Afterwards, fast pyrolysis experiments were conducted for the ALwood at 500 °C with sand feeding rates of 4 kg/h and 5 kg/h in order to investigate the feasibility of preventing agglomeration by using a higher feeding rate. Fast pyrolysis of ALwood at a lower temperature (450 °C) and a lower feeding rate of sand (1 kg/h) was also conducted to observe agglomeration.

Fast pyrolysis experiments of ALTwood were conducted at 450 °C and 500 °C with the feeding rate of sand at 3 kg/h in order to understand the effect of torrefaction pretreatment following the acid-leaching on bed agglomeration.

3.2.4 Bio-oil analysis

Water content and elemental contents of the bio-oil products were measured following the methods presented in Chapter 2.

Analysis of the bio-oils by ^{1}H-NMR spectroscopy was performed to determine the chemical functionality of the bio-oils. A Bruker Avance III 400 MHz spectrometer equipped with a 5 mm BBO probe was used. The spectra was obtained at 300 K in acetone-d6. At least 64 transients were collected. A presaturation pulse was applied during acquisition to suppress the signal of water. The spectrum were reprocessed, and the hydrogens in the bio-oil organics were divided into six groups based on their chemical shifts. The resonance signals assigned to different hydrogen types were described elsewhere [11] . Briefly, the chemical shift region from 0.5-1.5 ppm represents aliphatic hydrogens in bio-oil. The chemical shifts from 1.5-3.0 ppm is assigned to aliphatic hydrogens that are alpha (or on one carbon removed) from a C=C double bond or a heteroatom. Water in bio-oil also resonates in this region, but it was suppressed as described above. The chemical shift region from 3.0-4.4 ppm represents hydrogens on carbons next to aliphatic alcohols or ethers, and methoxy and methylene-dibenzene hydrogens. The chemical shift region from 4.4-6.0 ppm represents mainly the hydrogens of carbohydrates or carbohydrate derivatives, such as levoglucosan. The chemical shift region from 6.0-8.5 ppm contains resonances from aromatics and heteroaromatics hydrogens. The chemical shift region from 9.5-10.1 ppm represents the hydrogens from aldehydes and carboxylic acids functionalities.

3.2.5 Solid analysis

The feedstock analysis has been presented in Chapter 2. In this study, analysis of the biomass using solid-state CP/MAS ^{13}C NMR spectroscopy was also carried out using a Bruker 200 DRX spectrometer at 50.3 MHz. The magic-angle spinning speed was set at 5 kHz. For the standard cross-polarisation each 1.5 s pulse delay was followed by a hydrogen preparation pulse of duration t_p=4.6 μs, a 1 ms contact time and a 30 ms acquisition time. The hydrogen transmitter power was increased to a value corresponding to a 90^o pulse width of 2.8 μs for hydrogen decoupled during ^{13}C data acquisition. The spectras had a Gaussian line broadening of 25 Hz applied prior to Fourier transform. All spectras were calibrated by assigning the C-4 cellulose (ordered) peak to a value of 89.3 ppm [12].

For char analysis, images of char particles were obtained using scanning electron microscope (SEM). Since it was difficult to mechanically separate char from the mixture of sand and melt char, the mixtures were firstly sieved to remove fine sand. After this, the char-rich portion was ground into powder and transferred into a centrifuge tube filled with deionized water. This sludge was centrifuged at 3000 rpm for ten minutes so that the sand residue settled at the bottom and the char fines remained suspended in the water. The suspension was then transferred to another vial and freeze-dried to obtain purified char. The purified char samples were labelled in the same way as for bio-oil. The solid-state CP/MAS ^{13}C NMR spectroscopy was used for the char analysis in the same way as for the feedstock analysis.

3.3 Results and discussion

3.3.1 Feedstock characterisation

The resonance signals in ^{13}C solid-state NMR spectroscopy assign to carbon atoms in different chemical environments in wood have been described elsewhere [12-16]. Briefly, the signals in the region between 105 ppm and 160 ppm are associated to carbons of aromatic units in lignin (Figure 3-1). The signal #1 at 153 ppm is assigned to guaiacyl ether units involving in β-O-4 structures and the signal #2 at 147 ppm is assigned to free phenolic units. In the region ranging between 60 and 105 ppm, signals #3 to #9 are predominantly assigned to cellulose, and to a lesser extent to hemicelluloses carbohydrates. The signal #4 at 88.7 ppm is assigned to crystalline (or highly ordered) cellulose. The resonance #10 at 55.7 ppm can be specifically assigned to methoxy groups in lignin. The signal #11 at 21 ppm is assigned to the CH_3 carbons of the hemicelluloses acetyl units.

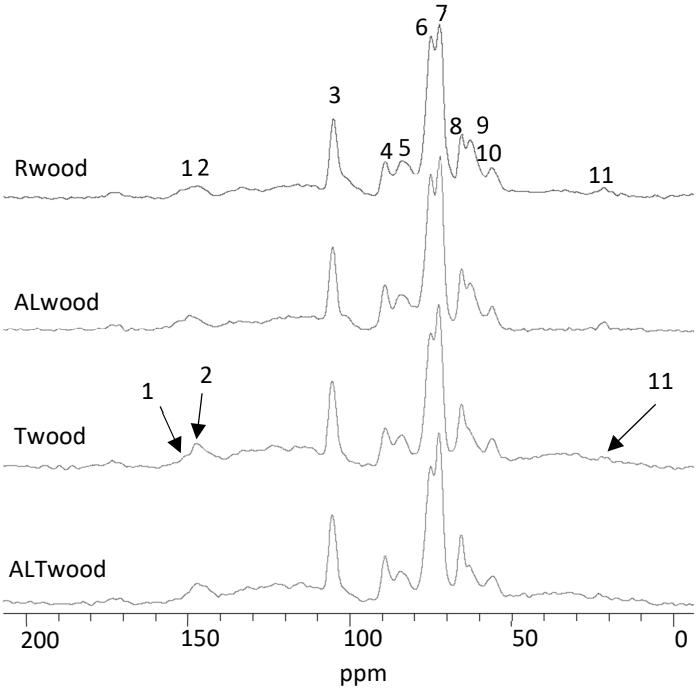

Figure 3-1: ^{13}C solid state NMR spectra of four types of feedstocks.

Comparing the spectra of the two torrefied woods with Rwood, the intensified signal at peak #2 in the spectra of Twood and ALTwood indicates a decrease in the β-O-4 linkages inside the lignin polymers. This is because the signal #2 at 147 ppm is assigned to free phenolic units and the signal #1 at 153 ppm is assigned to guaiacyl ether units involving in β-O-4 structures [12, 17]. The decrease of signal #11, along with the decrease in signal #9, in the spectra of Twood and ALTwood indicate the loss of hemicellulose due to torrefaction as signal #11 is assigned to the CH_3 carbons of the hemicelluloses acetyl units.

These results are consistent with the feedstock characterisation results presented in Chapter 2, in which the acid-leaching pretreatment removed the ash by 80 wt.% or more, while the main components of the pretreated wood were remained unchanged. Unless, torrefaction pretreatment caused some of the hemicellulose to be partially degraded and this is confirmed from the ^{13}C solid NMR spectrum.

3.3.2 Operational performance

3.3.2.1 Fast pyrolysis of acid-leached wood under different temperatures

The results from pyrolysis experiments using acid-leached wood at different temperatures, as identified by ALFP360, ALFP450 and ALFP500 are presented and discussed. The results using raw wood (RFP450) are also presented as the control for comparison. During the pyrolysis of acid-leached wood at lower temperatures (360 °C and 450 °C), bed agglomeration was not observed. However, bed agglomeration happened in pyrolysis at 500 °C, causing defluidisation in the reactor in one minute. When the defluidisation happened, the silica sand and char deposited on the reactor bottom as shown in Figure 3-2A. Consequently, the heat transfer through the reactor wall was reduced and the local temperature at the sand inlet rapidly decreased from the

reaction temperature to less than 100 °C. In this way the gas velocity was reduced and the silica sand could not be dispersed due to the agglomeration problem. The temperature drop in the reactor was an indicator of the occurrence of bed agglomeration.

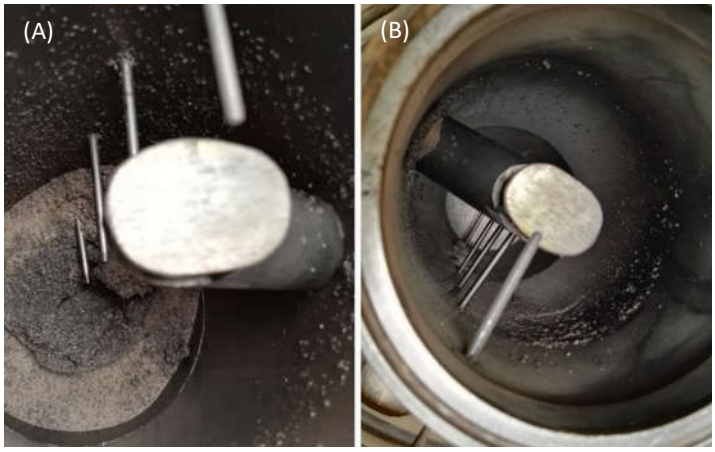

Figure 3-2: Deposited silica sand and char from bed agglomeration in fast pyrolysis of acid-leached wood at 500 °C (A) compared with a cleaned reactor in fast pyrolysis of the same wood at 450 °C (B).

Figure 3-3 shows SEM images of mixtures of sand and char residue from ALFP360, ALFP450, ALFP500 and RFP450. In the figure, the chars from RFP450 and ALFP360 were not melted and clearly show fibrous structure with rigid morphology, which indicates that melting behaviour did not occur under these conditions.

In pyrolysis of acid-leached wood at 450 °C, the melting behaviour was found as the sand was attached to the char although fibrous structure on the char could still be observed. The char from pyrolysis of acid-leached wood at 500 °C were agglomerated with the sand, forming solid lumps of sand particles. This indicates severe melting behaviour at a pyrolysis temperature of 500 °C. This melting is most likely caused bed agglomeration.

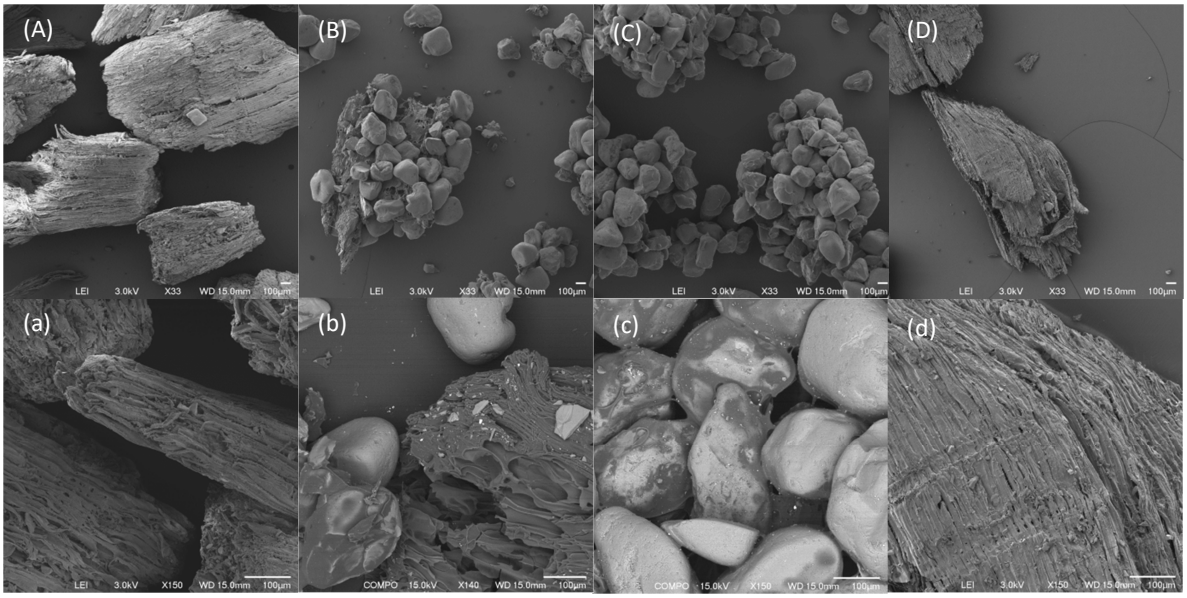

Figure 3-3: SEM images of mixtures of sand and char from fast pyrolysis experiments, (A&a) - ALFP360, (B&b) - ALFP450, (C&c) - ALFP500, (D&d) - RFP450.

3.3.2.2 Fast pyrolysis of acid-leached wood with different sand feeding rate

Bed agglomeration has been reported to occur during pyrolysis of acid-leached wood at 450 °C causing operational problems [3, 7]. In the present study, fast pyrolysis of acid-leached wood at 450 °C (ALFP450) was successful over a period of 90 minutes without any issue, but bed agglomeration occurred during pyrolysis at 500 °C (ALFP500). This successful operation (ALFP450) could be due to the high sand feeding rate, in which case the char was quickly removed from the fluidised bed before it could cause bed agglomeration.

In order to prove the effect of bed material feeding rate, pyrolysis experiments at 500 °C with higher sand feeding rates were conducted as a way of overcoming bed agglomeration. When increasing the sand feeding rate from 3 to 4 kg/h (ALFP500M), bed agglomeration occurred at around 20 minutes and operation had to be stopped. Although the operation time was longer than ALFP500, bed agglomeration still occurred. When increasing the sand feeding rate to 5 kg/h, the max capacity of this reactor (ALFP500H), the operation was smooth without

agglomeration occurring. However, the pyrolysis temperature gradually decreased from 500 °C to 465 °C over the 90 minutes run time. This was because this pyrolysis reactor could not provide enough heat to maintain this temperature within the reactor at this maximum sand feeding rate.

Furthermore, a pyrolysis experiment was conducted at 450 °C with a low feeding rate of 1 kg/h (ALFP450L) to observe bed agglomeration. This resulted in the agglomeration and defluidisation in 30 minutes, thereby confirming that the high sand feeding rate prevented bed agglomeration in ALFP450.

3.3.2.3 Fast pyrolysis of acid-leached and torrefied wood

Experiments on fast pyrolysis of acid-leached and torrefied wood at 450 °C (ALTFP450) and 500 °C (ALTFP500) were both successful over 90 minutes. As the SEM images show in Figure 3-4, the melting behaviour in fast pyrolysis of ALTwood occurred to a certain extent, and the severity of this melting increased with temperature. However, bed agglomeration did not occur in either of these experiments. It was also noticed that this melting behaviour in fast pyrolysis of ALTwood was less severe than that found in fast pyrolysis of ALwood. This indicates that the torrefaction pretreatment hindered the melting behaviour and thus prevented bed agglomeration. For comparison, an experiment on fast pyrolysis of torrefied wood was also conducted at 450 °C (TFP450), and the SEM image is also included in Figure 3-4C. From this image, it is observed that TFP450 char shows a fibrous structure with defined morphology, confirming that there was no melting behaviour during the pyrolysis.

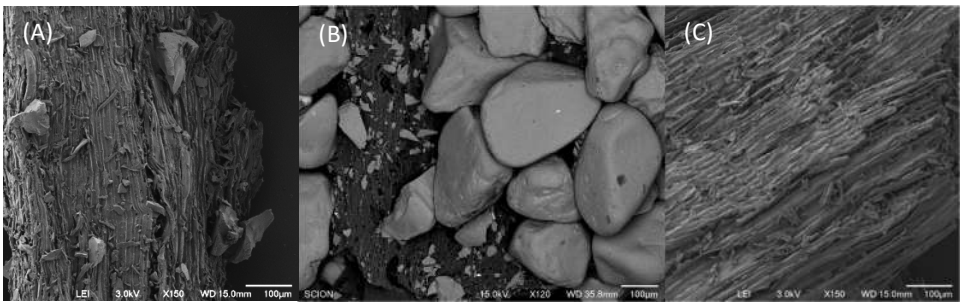

Figure 3-4: SEM images of mixed sand and char from fast pyrolysis experiments, (A)-ALTFP450, (B)-ALTFP500, (C)-TFP450.

3.3.3 Pyrolysis product distribution and characterisation

3.3.3.1 Experimental and analysis results

The results of product yields and gas composition from fast pyrolysis of pretreated and raw wood samples are given in Table 3-2. No mass balance was obtained in the experiment of ALFP500 due to the short operating time. Instead, the results of product distribution from experiment of ALFP500M using a higher sand feeding rate are discussed. In the analyses, it was assumed that silica sand was inert and the sand feeding rate had insignificant effect on the results of product distribution and properties. These results will be further discussed in the following sections.

Table 3-2: The pyrolysis product yields and the gas composition.

	RFP450 [b]	ALFP360	ALFP450 [b]	ALFP500M	TFP450 [b]	ALTFP450 [b]	ALTFP500
Yields (wt.%) [a]							
Bio-oil	63.4	65.0	74.9	70.8	54.4	63.4	63.8
Char	15.6	25.3	9.5	8.5	26.1	25.9	18.8
Gas	19.1	8.6	13.2	15.2	16.1	13.4	14.9
Mass balance	98.2	98.9	97.6	94.4	96.6	102.7	97.5
Gas composition (vol.%)							
H_2	2.1	1.2	3.9	5.4	1.7	2.2	4.6
CH_4	5.1	1.9	8.4	11.9	8.3	8.7	14.4
CO	58.1	46.8	63.2	64.9	59.5	63.0	60.0
CO_2	34.7	50.2	24.6	17.8	30.5	26.1	21.0

[a] dry biomass basis; [b] results from Chapter 2.

The results from analysis of bio-oil properties are given in Table 3-3. Hydrogen atoms of the products in the bio-oils were classified into six functional groups based on ^{1}H NMR analysis. This analysis provides a representation of the bio-oil compositions for each experiment. As mentioned above, the analysis results of ALFP500M bio-oil are presented for discussion. These results will be discussed alongside the product distribution results in the following sections.

Table 3-3: Bio-oil properties for each experiment using pretreated and raw wood.

	RFP450 bio-oil [a]	ALFP360 bio-oil	ALFP450 bio-oil [a]	ALFP500M bio-oil	TFP450 bio-oil [a]	ALTFP450 bio-oil [a]	ALTFP500 bio-oil
Water content (wt.%) [b]	36.7	22.5	18.9	16.6	27.5	21.8	19.5
Elemental composition (wt.%), dry basis							
N	<1.0	<1.0	<1.0	<1.0	<1.0	<1.0	<1.0
C [c]	51.5	51.0	51.7	51.6	58.0	53.8	52.8
H [b]	6.0	5.9	5.7	5.6	6.1	5.2	5.4
O, by difference	41.6	42.5	41.9	42.8	35.2	40.5	41.8
^{1}H NMR results (%) [d]							
Aldehydes, carboxylic acids	1.5	1.6	1.2	1.2	1.5	1.1	1.3
Aromatics, heteroaromatics	18.6	14.0	12.4	13.8	17.4	13.5	13.0
Carbohydrates	12.2	22.7	20.0	17.3	12.5	18.2	19.8
Aliphatic alcohols, methoxy	23.7	24.2	42.4	35.8	27.8	38.4	37.7
Hydrogen α to heteroatom, unsaturation	33.9	29.6	18.4	25.2	31.8	22.1	22.6
Alkanes	10.1	7.9	5.7	6.7	9.1	6.7	5.6

[a] Results from Chapter 2; [b] the standard deviations (STDs) were no more than 0.2; [c] STDs<0.9; [d] average values of duplicate.

3.3.3.2 Effect of acid-leaching pretreatment

From Table 3-2, it is found that the bio-oil yield in pyrolysis of acid-leached wood at 450 °C (ALFP450) was 74.9 wt.%, which was much higher than that in pyrolysis of raw wood (RFP450), i.e. 63.4 wt.%. The higher bio-oil yield in ALFP450 indicates that depolymerisation and fragmentation of the biomass were enhanced by the acid-leaching pretreatment. In addition, the lower char and gas yields in ALFP450 shows that carbonisation and gasification were suppressed.

Comparison of ^{1}H NMR analysis results shows that acid-leaching pretreatment enhanced the formation of products with carbohydrate and alcohols/methoxy functionality in the bio-oil. The bio-oils from ALwood appeared to have less aromatic/heteraromatic functionality compared to the bio-oil from Rwood (Table 3-3). This is consistent with the solvent fractionation results described in Chapter 2 and the finding of others who have reported increased carbohydrate-derived products in bio-oils from acid-leached woods [3, 7]. It has been reported that the percentage of aromatic/heteroaromatic organics in the bio-oil is not correlated to the lignin content of the feedstock but is more related to the pyrolysis process [11]. The minerals in Rwood may enhance the production of products with aromatics/heteroaromatics functionality.

Similar results have also been observed by comparison of the results of ALTFP450 and TFP450 bio-oils, which shows again the effect of acid-leaching pretreatment on increasing the bio-oil yield and decreasing the yield of gas. Acid-leaching pretreatment also increased the content of products with carbohydrates and alcohols/methoxys functionality in ALTFP450 bio-oil in comparison with the TFP450 bio-oil.

3.3.3.3 Effect of torrefaction pretreatment

Comparing the results of TFP450 with those from RFP450 (Table 3-2), the yields of bio-oil and gas were decreased while the char yield was increased when a torrefaction pretreatment was applied. This reveals that the torrefaction pretreatment can enhance carbonisation/charring in fast pyrolysis.

The comparison of properties of TFP450 bio-oil with those of RFP450 bio-oil (Table 3-3) reveals that the torrefaction pretreatment decreased the oxygen content, but increased the carbon content of the bio-oil. However, torrefaction pretreatment had little impact on the bio-oil

composition as analysed by ^{1}H NMR spectroscopy. The slight increasing proportion of the products with alcohols/methoxy functionality in the bio-oil was probably due to the higher lignin content in torrefied wood.

Similarly, the effect of torrefaction pretreatment on enhancing carbonisation can also be found by comparing the char yields from acid-leached and torrefied wood (ALTFP450, ALTFP500) with those from acid-leached only wood (ALFP450, ALFP500M) in Table 3-2. The carbon content in ALTFP450 bio-oil was also higher than that in the ALFP450 bio-oil in Table 3-3. The same trend was also observed by comparing the ALTFP500 bio-oil with the ALFP500M bio-oil.

3.3.3.4 Effect of reaction temperature in pyrolysis of acid-leached wood

Comparing the results of ALFP360, ALFP450 and ALFP500M, it showed that the highest bio-oil yield was 74.9 wt.% for ALFP450. When increasing temperature from 360 °C to 500 °C in fast pyrolysis of acid-leached wood, the char yield was decreased and the gas yield was increased. The concentration of fuel gases (carbon monoxide, hydrogen and methane) was increased with the temperature, while the concentration of carbon dioxide was reduced. This was in agreement with the study of Oudenhoven *et al*. [3].

The reason of the high char yield (25.3 wt.%) in ALFP360 was clarified by the solid state ^{13}C NMR analysis of the char samples. The ^{13}C NMR spectra in Figure 3-5 presented signals corresponding to the carbon atoms in different chemical environments in the char. The spectra were similar to each other except the spectrum of ALFP360 char. In the spectrum of ALFP360 char, peaks associated to biomass components still remain. For instance, signal #2 at 105 ppm was assigned to the anomeric C-1 carbon of sugars and signal #3 at 56 ppm corresponds to carbons in the methoxy groups in lignin [13]. This indicates that the cellulose and lignin were not fully

converted in ALFP360, leading to a high yield of char (with unconverted biomass) and relatively low yield of bio-oil. It is evident when comparing the spectra of ALFP360 char (Figure 3-5) and ALwood (Figure 3-1) that the polysaccharides are pyrolysed preferentially at 360 °C compared to the lignin, as the polysaccharide signals are greatly reduced compared to an enrichment in the lignin signals in the spectrum of ALFP360 char.

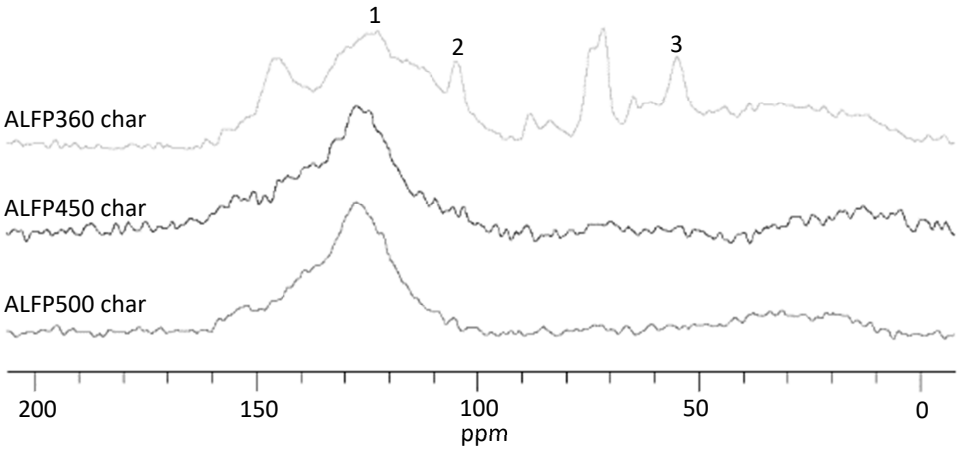

Figure 3-5: ^{13}C NMR spectras of chars from ALwood.

The broad peak #1 at 128 ppm in the spectra was dominant, which was associated to aromatic carbons [13], suggesting the chars were mainly composed of fused aromatic rings. This result was agreed with the study of Bardet *et al.* [13], which showed the ^{13}C NMR spectra of char did not show any lignocellulose features when the pyrolysis temperature was above 400 °C.

In terms of bio-oil properties, the pyrolysis temperature had no significant impact on the elemental composition (Table 3-3). However the bio-oil composition was strongly affected by pyrolysis temperature. ALFP360 bio-oil contained more compounds with hydrogen functionality α to heteroatom/unsaturation and less compounds with hydrogens with aliphatic alcohols/methoxy functionality than the ALFP450 and ALFP500 bio-oils. Also, the "carbohydrates" hydrogens were decreased when the temperature increased.

3.3.4 Possible mechanism of bed material agglomeration

The SEM images shown in Figure 3-3 confirm that melting behaviour was the precursor of bed agglomeration in fast pyrolysis of acid-leached pine wood. The severity of melting increased with pyrolysis temperature, and severe melting behaviour can lead to bed agglomeration (i.e. 450 ^{o}C). This finding agrees with the studies of other researchers. Dufour *et al.* [18, 19] studied the mobility of cellulose, xylan, lignin, *Miscanthus* and demineralised *Miscanthus* in pyrolysis at temperature of up to 450 ^{o}C. It was found that the mobility of all the substrates increased with temperature before being carbonised. But only lignin was completely mobile and demineralised *Miscanthus* also showed a high mobility (80 %). In another study, it was reported that cellulose has a melting point at 467 °C [20].

Based on those findings, biomass components could show melting behaviour before they were carbonised and their mobility could be related to the melting behaviour. As discussed previously, acid-leaching pretreatment suppressed carbonisation in fast pyrolysis, therefore, providing less resistance to the biomass melting behaviour. The severity of the melting increased with temperature because the mobility of biomass components increased. This melting was strongly intensified at 500 °C and caused bed agglomeration in ALFP500. The carbonisation in pyrolysis, promoted via torrefaction or the catalytic effect of minerals in raw wood, on the other hand, hindered the melting behaviour. In fast pyrolysis of ALTwood, torrefaction pretreatment reversed the acid-leaching effect of suppressing carbonisation, and thereby prevented bed agglomeration.

Lignin in the ALwood may be an important component for the melting behaviour and bed agglomeration, as lignin has higher mobility in pyrolysis than the other biomass polymers [18,

19]. In this study, it was found that more unconverted lignin remained than unconverted polysaccharides at the pyrolysis temperature of 360 °C (Figure 3-5), where no melting behaviour was observed (Figure 3-3). When the pyrolysis temperature increased to 450 °C, all the lignin was completely pyrolysed and the SEM image of ALchar450 showed evidence of melting behaviour. Thus lignin melting may be a significant contributing factor in bed agglomeration in fast pyrolysis of ALwood at 450 °C. Bed agglomeration has been observed in fast pyrolysis of pure lignin extracted from lignocellulosic biomass [9, 10]. Furthermore, calcium hydroxide pretreatment of the lignin feedstock prevented the melting behaviour and consequently bed agglomeration at the same pyrolysis temperature [10]. The calcium hydroxide pretreatment possibly had the same effect as the minerals in biomass on enhancing carbonisation in pyrolysis.

3.3.5 Approaches of overcoming bed agglomeration

The first approach demonstrated in this study to overcome bed agglomeration was to operate fast pyrolysis at a relatively low temperature, i.e. 360 ^{o}C. The melting behaviour and the agglomeration were avoided. However, the bio-oil yield was fair, and the char yield high because the feedstock was not fully pyrolysed. This approach can be applied when the process is aimed to produce sugar-rich bio-oil or the process has a high requirement of heating or power, because the byproduct char can be used as the fuel and the char yield is as high as 25 wt.%.

The second approach was to operate fast pyrolysis at an optimal temperature, i.e. 450 ^{o}C, along with relatively high feeding rate of sand. The bio-oil production was optimised as high as 74.9 wt.% and the yields of the rest products were minimised. The sand feeding rate should be high enough so that the melted residue would not lead to bed agglomeration. This approach can be a good option in (catalytic) fast pyrolysis of biomass using a circulated fluid bed, within which the

bed material is kept hot. The requirement for heating the sand is minimised as the sand is kept constantly hot by the pyrolysis-combustion circle.

The third approach was to apply torrefaction following acid-leaching pretreatment. The bed agglomeration was prevented due to the hindered melting behaviour. Although the bio-oil yield was decreased due to torrefaction pretreatment, the bio-oil properties were improved in terms of a higher carbon content. Because the process of biomass drying and torrefaction can be a combined process in commercialisation, the biomass torrefaction requires little increase in capital and operating costs. This approach is attractive when the pyrolysis reactor is difficult to operate as the other approaches suggested.

3.4 Conclusion

In this chapter, bed agglomeration in fast pyrolysis of acid-leached pine wood was investigated and the morphology of char samples was examined using SEM. Melting behaviour could be related to the melting behaviour of biomass components in pyrolysis before they are carbonised. The severity of biomass melting increases with pyrolysis temperature, and severe melting behaviour leads to increased possibility of bed agglomeration. Acid-leaching pretreatment can suppress carbonisation in pyrolysis leading, to the biomass melting behaviour and eventually bed agglomeration. Torrefaction pretreatment, on the other hand, can enhance carbonisation in pyrolysis. Hence a combined pretreatment of acid-leaching and torrefaction can reverse the suppressed carbonisation due to acid-leaching, and thereby prevent bed agglomeration.

Three approaches to overcome bed agglomeration have been proposed and successfully demonstrated. Operating at a lower temperature or applying a torrefaction pretreatment both prevented bed agglomeration. However both approaches reduced bio-oil yield and made acid-leaching pretreatment less attractive. Operational adjustment might be a better way to optimise bio-oil production as well as prevent bed agglomeration. A high sand feeding rate in the fluidised bed reactor can also prevent bed agglomeration by quickly moving the melted residue out of the reactor.

References

[1] Das, P., A. Ganesh, and P. Wangikar, *Influence of pretreatment for deashing of sugarcane bagasse on pyrolysis products.* Biomass and Bioenergy, 2004. **27**(5): p. 445-457.

[2] Fahmi, R., A.V. Bridgwater, I. Donnison, N. Yates, and J.M. Jones, *The effect of lignin and inorganic species in biomass on pyrolysis oil yields, quality and stability.* Fuel, 2008. **87**(7): p. 1230-1240.

[3] Oudenhoven, S.R.G., C. Lievens, R.J.M. Westerhof, and S.R.A. Kersten, *Effect of temperature on the fast pyrolysis of organic-acid leached pinewood; the potential of low temperature pyrolysis.* Biomass and Bioenergy, 2016. **89**: p. 78-90.

[4] Oudenhoven, S.R.G., R.J.M. Westerhof, and S.R.A. Kersten, *Fast pyrolysis of organic acid leached wood, straw, hay and bagasse: Improved oil and sugar yields.* Journal of Analytical and Applied Pyrolysis, 2015. **116**: p. 253-262.

[5] Carpenter, D., T.L. Westover, S. Czernik, and W. Jablonski, *Biomass feedstocks for renewable fuel production: a review of the impacts of feedstock and pretreatment on the yield and product distribution of fast pyrolysis bio-oils and vapors.* Green Chemistry, 2014. **16**(2): p. 384-406.

[6] Oudenhoven, S.R.G., R.J.M. Westerhof, N. Aldenkamp, D.W.F. Brilman, and S.R.A. Kersten, *Demineralization of wood using wood-derived acid: Towards a selective pyrolysis process for fuel and chemicals production.* Journal of Analytical and Applied Pyrolysis, 2013. **103**: p. 112-118.

[7] Wigley, T., A.C.K. Yip, and S. Pang, *Pretreating biomass via demineralisation and torrefaction to improve the quality of crude pyrolysis oil.* Energy, 2016. **109**: p. 481-494.

[8] Kim, K.H., R.C. Brown, and X. Bai, *Partial oxidative pyrolysis of acid infused red oak using a fluidized bed reactor to produce sugar rich bio-oil.* Fuel, 2014. **130**: p. 135-141.

[9] Nowakowski, D.J., A.V. Bridgwater, D.C. Elliott, D. Meier, and P. de Wild, *Lignin fast pyrolysis: Results from an international collaboration.* Journal of Analytical and Applied Pyrolysis, 2010. **88**(1): p. 53-72.

[10] Zhou, S., R.C. Brown, and X. Bai, *The use of calcium hydroxide pretreatment to overcome agglomeration of technical lignin during fast pyrolysis.* Green Chemistry, 2015. **17**(10): p. 4748-4759.

[11] Mullen, C.A., G.D. Strahan, and A.A. Boateng, *Characterization of various fast-pyrolysis bio-oils by NMR spectroscopy†.* Energy & Fuels, 2009. **23**(5): p. 2707-2718.

[12] Hill, S.J., W.J. Grigsby, and P.W. Hall, *Chemical and cellulose crystallite changes in Pinus radiata during torrefaction.* Biomass and Bioenergy, 2013. **56**: p. 92-98.

[13] Bardet, M., S. Hediger, G. Gerbaud, S. Gambarelli, J.F. Jacquot, M.F. Foray, and A. Gadelle, *Investigation with 13C NMR, EPR and magnetic susceptibility measurements of char residues obtained by pyrolysis of biomass.* Fuel, 2007. **86**(12–13): p. 1966-1976.

[14] Brewer, C.E., K. Schmidt-Rohr, J.A. Satrio, and R.C. Brown, *Characterization of biochar from fast pyrolysis and gasification systems.* Environmental Progress & Sustainable Energy, 2009. **28**(3): p. 386-396.

[15] David, K., Y. Pu, M. Foston, J. Muzzy, and A. Ragauskas, *Cross-Polarization/Magic Angle Spinning (CP/MAS) 13C Nuclear Magnetic Resonance (NMR) Analysis of Chars from Alkaline-Treated Pyrolyzed Softwood.* Energy & Fuels, 2009. **23**(1): p. 498-501.

[16] Neupane, S., S. Adhikari, Z. Wang, A.J. Ragauskas, and Y. Pu, *Effect of torrefaction on biomass structure and hydrocarbon production from fast pyrolysis.* Green Chemistry, 2015. **17**(4): p. 2406-2417.
[17] Melkior, T., S. Jacob, G. Gerbaud, S. Hediger, L. Le Pape, L. Bonnefois, and M. Bardet, *NMR analysis of the transformation of wood constituents by torrefaction.* Fuel, 2012. **92**(1): p. 271-280.
[18] Dufour, A., M. Castro-Diaz, N. Brosse, M. Bouroukba, and C. Snape, *The Origin of Molecular Mobility During Biomass Pyrolysis as Revealed by In situ 1H NMR Spectroscopy.* ChemSusChem, 2012. **5**(7): p. 1258-1265.
[19] Dufour, A., M. Castro-Díaz, P. Marchal, N. Brosse, R. Olcese, M. Bouroukba, and C. Snape, *In Situ Analysis of Biomass Pyrolysis by High Temperature Rheology in Relations with 1H NMR.* Energy & Fuels, 2012. **26**(10): p. 6432-6441.
[20] Krumm, C., J. Pfaendtner, and P.J. Dauenhauer, *Millisecond Pulsed Films Unify the Mechanisms of Cellulose Fragmentation.* Chemistry of Materials, 2016. **28**(9): p. 3108-3114.

Chapter 4

Method development for catalytic fast pyrolysis in a fluidised bed reactor

Abstract

Experimental methods were developed for catalytic fast pyrolysis of biomass for Scion's fluidised bed reactor. As catalytic fast pyrolysis experiments had never been conducted at Scion, this chapter focused on the development of the experimental methods, and the first validation tests using raw wood. The details of catalytic fast pyrolysis of pretreated woods are discussed in the next chapter.

A commercial spray-dried HZSM-5 was employed as the catalyst in this study. Catalyst dust generated by attrition in the fluidised bed passed through the gas cleaning system of the existing Scion reactor and contaminated the liquid product. In order to overcome this problem, a hot filter was built to capture the catalyst dust. It was composed of wire-mesh as filtration material and steel shell as container. This self-designed filter performed well in operation.

An operational method was developed so that the catalyst to biomass ratio could be controlled. It was found that the catalyst remained active during the entire operation of 90 minutes.

Triplicate experiments demonstrated good repeatability, with the total product recovery (mass balance) between 91- 99 wt.%.

Catalytic fast pyrolysis experiments using raw wood were conducted to understand the impacts of reaction temperature and catalyst to biomass ratio on product yields and properties. Three experiments were carried out at 360 ^{o}C, 450 ^{o}C and 500 ^{o}C, while keeping the catalyst to biomass ratio at 2.5. The results indicate that catalyst activity was increased with the increased temperature. The properties of oil product was the most improved at the pyrolysis temperature of 500 ^{o}C with a small loss in the yield of oil product.

In a second set of experiments, the temperature was set at 500 ^{o}C, and the catalyst to biomass (C/B) ratio was varied at 1.2, 2.5, 4 and 6. The results reveal that the product yields and oil properties were less impacted by the C/B ratio in this range compared to the effect temperature. Although the highest yield of oil product was obtained at a ratio of 1.2, the selectivity for aromatics was increased with the increased C/B ratio. This increase in selectivity was limited when increasing the ratio from 2.5 to 6, indicating that a C/B ratio of 2.5 was sufficient for catalytic conversion in this study.

4.1. Introduction

To carry out catalytic fast pyrolysis (CFP) of biomass, there are multiple catalysts available and reactor types studied. Granulated HZSM-5 zeolite has been widely used for CFP of biomass on fluidised bed reactors in early studies [1, 2]. A disadvantage of this catalyst type is that it has to be ground and sieved before using it as the bed material, with the associated material loss. Recently, spray-dried catalyst has become more popular [3-5], as the particle size of the catalyst can be specified for the application on a fluidised bed reactor, and it does not require grinding and sieving of the catalyst before use.

Similar to this study, fluidised bed reactors have been used to study catalytic fast pyrolysis of biomass in literature [3, 6, 7]. While in this study it was found that a large amount of catalyst dust can pass though the cyclones typically used for fast pyrolysis and contaminate the oil product, this issue is rarely discussed in the literature. To prevent excessive catalyst in the oil product, a wire-mesh hot filter (hot filter) can be used before quenching the hot vapour.

The impacts of a wire-mesh hot filter in catalytic fast pyrolysis have not been reported, but Hoekstra *et al*. [8] reported its impacts in fast pyrolysis of biomass. They observed that the bio-oil yield was reduced when using a hot filter comparing to that when only cyclone was used, but this yield was still fair. The hot filter led to a bio-oil containing less solids, and the molecular weight of this bio-oil was marginally reduced. The elemental composition of the bio-oils was not significantly affected by the hot filter.

The catalyst feeding rate is crucial in catalytic fast pyrolysis as it can change the catalyst to biomass ratio, and consequently affect the product distribution and the oil quality [3]. The

control of catalyst to biomass ratio was realised by following an operational method in this study. Typically, the liquid product from catalytic fast pyrolysis is composed of two phases, an organic-rich liquid (referred to as oily liquid in this study) and water-rich liquid (referred to as aqueous liquid in this study). This study developed a procedure to separate this two-phase liquid product.

To validate the new hot filter, catalytic fast pyrolysis experiments using raw wood were conducted at different reaction temperatures and catalyst to biomass ratios, to investigate their effects on the product distribution, and the properties and chemical composition of the oil product.

4.2. Experimental method development

4.2.1. Catalyst selection

Previous studies have shown that HZSM-5 can effectively convert biomass pyrolysis vapour to hydrocarbons, mainly aromatics. Aho *et al.* [1] conducted catalytic fast pyrolysis of pine wood with zeolites HBeta-25, HY-12, HZSM-5-23, and HMOR-20 and found that HZSM-5 produced more liquid and less coke than the other zeolites. Thus HZSM-5 was chosen as the catalyst in this study. Two types of commercial HZSM-5 catalyst were tested, which were purchased from Nankai University's Catalyst Company (Tianjin, China) and Saint Chemical Material Company (Shanghai, China).

As shown in Figure 4-1A, the granulated catalyst was rod-shaped. It can be ground into particles to be used in a fluidised bed. However, it was found that nearly 60 % of this catalyst was lost as fine dust after grinding and sieving.

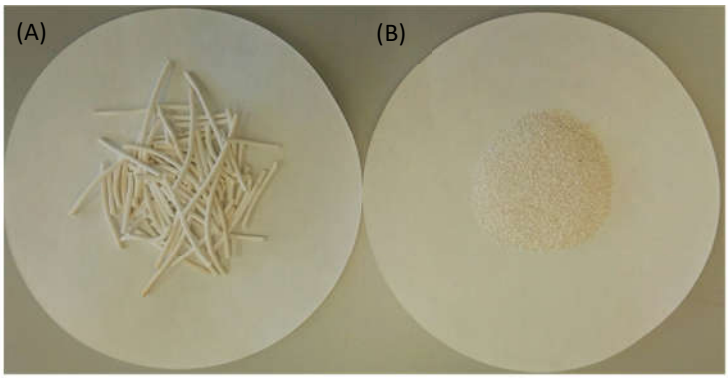

Figure 4-1: Granulated zeolite (A) and spray-dried zeolite (B).

The second type of HZSM-5 catalyst was spherical in shape and made by spray-drying (Figure 4-1B). The spray-dried catalyst was already converted to acidic form (HZSM-5) from the ammonia form (ZSM-5) by the supplier. 120 kg of this HZSM-5 catalyst was purchased for this project, and its specifications are shown in Table 4-1.

Table 4-1: Specifications of a commercial spray-dried HZSM-5 catalyst.

Specification*	Value
SiO_2/Al_2O_3	30 (molar ratio)
Pore size	5 Å
Silicon oxide	89.9-88.6 wt.%
Aluminium oxide	5.0-5.1 wt.%
Sodium oxide	≤0.02 wt.%
Iron oxide	0.35-1.25 wt.%
Specific surface area	≥350 m^2/g
Ignition loss (550 ^oC for 3h)	≤5 wt.%
Bulk density	0.65-0.85 g/cm^3
Purity	>99 %
Comparative crystallinity	≥98 %
Catalyst composition	50% (HZSM-5), 50% (binder)
Particle size distribution	0.3-0.4 mm (>95 wt.%)

*Information provided by the supplier.

4.2.2. Materials preparation

The catalyst was calcined at 525 ^oC in a muffle furnace for three hours before each experiment to remove the moisture and activate the zeolite. The calcination was following the procedure suggested by the supplier.

Raw wood (Rwood) was used as the feedstock in catalytic fast pyrolysis, and its characteristics have been described in Chapter 2. The moisture content of Rwood was measured before each experiment to calculate the mass balance on a dry basis.

4.2.3. Operational issues on using the original reactor

The configuration of the Scion fluidised bed reactor has been described in Chapter 2. The gas cleaning system of the reactor was comprised of a knock-out vessel and two cyclones. The attrition resistance of the catalyst is not as good as silica sand, even when the zeolite catalyst was customised with 50 % binder for a high attrition resistance. Consequently, catalyst dust was generated during the pyrolysis experiment. The existing gas cleaning system could not capture the fine dust, which ended up in both condensation units, i.e. the electrostatic precipitator (ESP) and the intensive cooler (IC), and in the oil product.

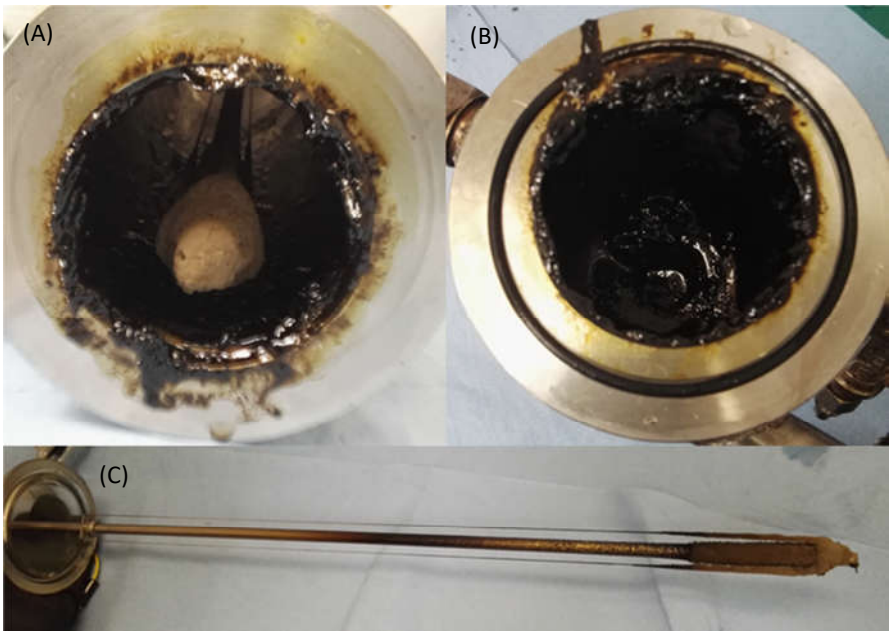

Figure 4-2: Catalyst dust captured by the ESP column (A: column body, B: column bottom, C: ESP rod).

As shown in Figure 4-2, the dust captured in the ESP column absorbed the liquid product and formed a dark sludge. It was impossible to obtain reliable mass balance because the loss of catalyst dust was not able to be quantified.

The liquid product/catalyst dust sludge was centrifuged to separate and recover the liquid product. However, some oil was still found in the catalyst dust after the centrifugation. It appeared that the catalyst dust had to be separated from the hot vapour before the quenching stage.

4.2.4. Building a hot filter

To prevent catalyst dust from reaching the condensation units, it was decided to build a hot vapour filtration unit using wire-mesh as the filter material.

The particle size of the catalyst dust was measured before deciding the pore size of the wire-mesh. The dust captured in the cyclone and that entered the ESP column were analysed by light scattering at the University of Waikato. The analysis results are shown in Table 4-2. Therefore, a wire-mesh with the pore size of 2 micron was chosen as the filter material. This wire-mesh was made of 5 layers of sintered of stainless 316 (the same steel as the Scion reactor).

Table 4-2: The size range of catalyst dust.

	dust size (micron)
Captured in the cleaning set	37-1190
Captured in the ESP column	2-710

The first prototype was a round-plate filter (diameter 10 cm) placed at the outlet position of the reactor as shown in Figure 4-3. This simple modification was tried first. But the pressure in the reactor increased rapidly and, consequently, it reached the reactor pressure limit of 0.4 barg in 10 minutes. As shown in Figure 4-3B, the filter was covered with catalyst dust and this led to the rapid rise of the pressure.

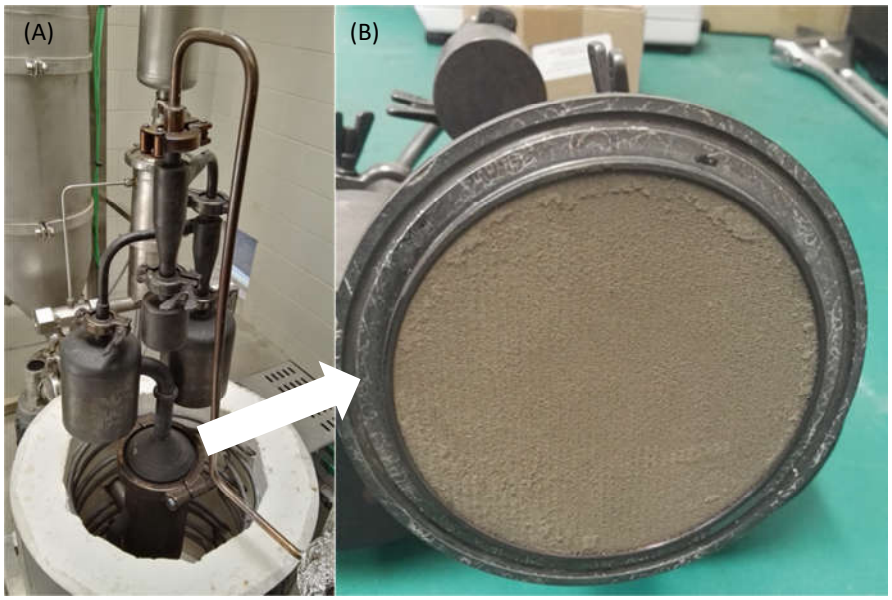

Figure 4-3: A plate filter placed at the reactor outlet.

The second filter was based on the configuration of a cartridge filter. As shown in Figure 4-4, a cylinder-shaped wire-mesh (length 300 mm, diameter 50 mm) and a shell (length 380 mm, diameter 70 mm) was made. The two ends of the cylinder wire-mesh were sealed by welding (Figure 4-4C) to prevent the dust from bypassing the filter.

This filter replaced the second cyclone. During the operation, the knock-off vessel and the first cyclone captured the large solid particles and the filter captured the fine dust. Experimental

results showed that this filter was able to capture the catalyst dust without an overpressure issue.

Figure 4-4: The original gas cleaning system (A), the modified setup (B) and the cartridge filter with captured dust (C).

4.2.5. Operating procedure development

Once it was possible to have standard length experiments (90 minutes) without excessive pressure build-up or catalyst dust in the product, the next step was to develop an operating procedure to control the catalyst to biomass ratio (C/B) and the separation of the two phases of the liquid product.

Some catalyst must be loaded in the fluidised bed before operation. It was found that approximately 800 grams of bed materials (used catalyst and char) remained in the reactor after

the operation. Therefore, the preloaded catalyst should be no more than 800 g, otherwise extra fresh catalyst would be purged out of the reactor and lead to an inaccurate C/B ratio. The appropriate mass of preloaded catalyst was 700 g, with no fresh catalyst found in the overflow vessel.

By keeping the feeding rate of biomass and the running time constant in different operations, the feeding rate of catalyst can be determined for a given C/B ratio from the following equation.

$$R = (f_c \times t + P_c) / (f_b \times t) \qquad \text{(Equation 1)}$$

R – The ratio of catalyst to biomass (wt/wt)

f_c – The feed rate of catalyst (kg/h)

f_b – The feed rate of biomass (kg/h)

t – Running time (h)

P_c – The weight of preloaded catalyst (kg)

The weight hourly space velocity (WHSV), defined as the weight of biomass feeding rate per unit weight of the catalyst per hour, was controlled by the feeding rate of biomass, when the weight of preloaded catalyst was kept at 0.7 kg. It was calculated by the following equation:

$$WHSV = f_b / P_c \qquad \text{(Equation 2)}$$

f_b – The feed rate of biomass (kg/h)

P_c – The weight of preloaded catalyst (kg)

The liquid product was normally comprised of an aqueous phase at the top (aqueous liquid) and an organic phase at the bottom (oily liquid), as shown in Figure 4-5A. After CFP experiment, the liquid products from ESP column and intensive cooler were mixed and transferred to a cylinder in which the liquid was settled into two phases in one hour (Figure 4-5B). Then the oily liquid and aqueous liquid were separated using a syringe. After this crude separation, these two liquids were further separated using separating funnels (Figure 4-5C).

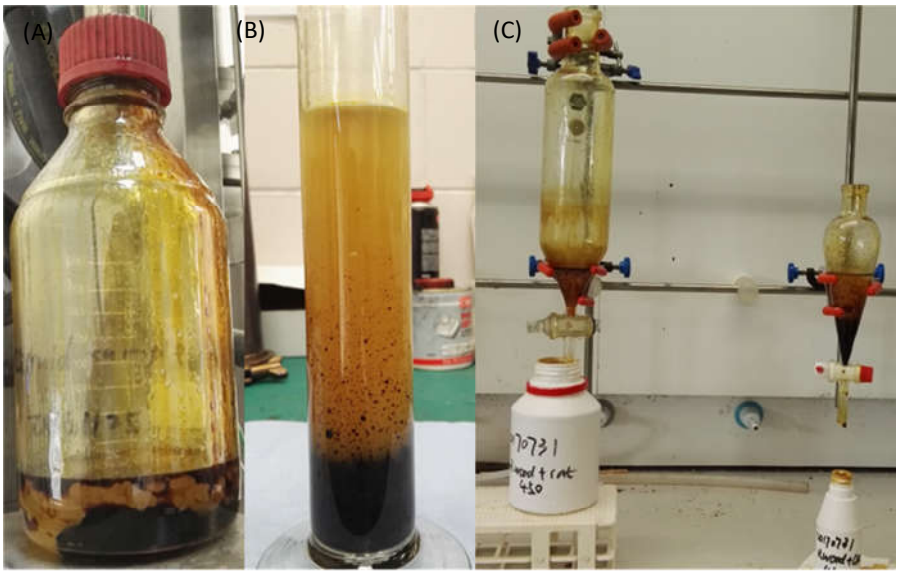

Figure 4-5: The two-phase liquid product (A) and separating procedure (B, C).

4.2.6. Catalytic fast pyrolysis experiments

The constant operating conditions for CFP experiments are summarized in Table 4-3. Every experiment was conducted for 90 minutes. The temperature in the gas cleaning system was kept at 440 ^{o}C. The temperatures in the ESP unit and the IC unit were controlled at -5 ^{o}C and -15 ^{o}C, respectively. The nitrogen flowrate was adjusted according to the temperature in order to maintain a constant gas velocity in the fluidised bed. In this way, the residence time of the hot vapour (3 seconds) in the fluidised bed was constant in different experiments.

Table 4-3: Constant operating conditions for catalytic fast pyrolysis of raw wood.

Description	Value
Constants	
Running time	90 minutes
Gas cleaning setup temperature	440 ^{o}C
ESP temperature	-5 ^{o}C
Intense cooler temperature	-15 ^{o}C
Calculated gas velocity in fluidised bed	0.086 m/s
WHSV	0.5

A summary of the experiments are shown in Table 4-4. CFP experiment was firstly conducted at 500 ^{o}C and this experiment was repeated three times to demonstrate experimental repeatability. The WHSV was kept at 0.5 (1/h) by setting the biomass feeding rate at 0.35 kg/h and the catalyst feeding rate at 0.43 kg/h, thus the C/B ratio was set at 2.5.

Experiments on the impact of temperature were conducted at 360 ^{o}C, 450 ^{o}C and 500 ^{o}C. In these experiments, WHSV was kept at 0.5 (1/h) and the C/B ratio was 2.5. Due to the limited heating capacity of this reactor, 500 ^{o}C was the highest reaction temperature it can maintain at a high feeding rate of catalyst.

The study of the impacts of C/B ratio was conducted at 500 ^{o}C, and the WHSV was kept constant at 0.5 (1/h). In these experiments, the C/B ratio was controlled at 1.2, 2.5, 4 and 6 by setting the catalyst feeding rate at 0 kg/h, 0.43 kg/h, 1 kg/h and 1.5 kg/h, respectively.

Table 4-4: A summary of catalytic fast pyrolysis experiments of raw wood.

Number	ID	Temperature (°C)	C/B ratio	nitrogen flowrate (L/min, N)
1	R_360_2.5	360	2.5	17.4
2	R_450_2.5	450	2.5	15.1
3	R_500_2.5	500	2.5	14.0
4	R_500_1.2	500	1.2	14.0
5	R_500_4	500	4	14.0
6	R_500_6	500	6	14.0

4.2.7. Product analysis

The liquid product was separated into two phases (aqueous liquid and oily liquid) following the method described above. After separation, the liquid products were stored in a freezer at -20 ^{o}C until analysis. Following the analytical methods for bio-oils described in Chapter 2 and Chapter 3, water content was measured for both the oily liquid and aqueous liquid. Elemental analysis, GPC and ^{1}H NMR spectroscopy analyses were performed for the oily liquid only.

Gas chromatography-mass spectrometry (GC/MS) analysis was applied on the oily liquids to determine the products in the oil. Prior to the GC/MS analysis, 100 mg of each oily liquid was dissolved in 5 mL dichloromethane (DCM), then this solution was filtered (Whatman 589/3 filter paper) to remove insoluble material, which was minimal. An aliquot (100 uL) of this filtered solution was mixed with 5 mL DCM to obtain a diluted solution sample with a concentration of 0.4 mg/mL. Duplicate samples of each oily liquid were prepared for analysis.

The GC/MS instrument was an Agilent 7890 GC equipped with a 5977B MS. The injector temperature was held at 260 ^{o}C and injection volume was 1 µL. High purity helium was used as carrier gas at constant flow rate of 1.0 mL/min. A split of the carrier gas (1:10) was used. Separation was carried out using an Ultra 2 capillary column (50 m × 0.2 mm × 0.33 µm). Temperature schedule of the oven was set as follows: 50°C for 2 min, 5°C/min to 130°C, 10°C/min to 300°C, held at 300°C for 5 min. MS data was collected in scan mode over a range of 50–350 amu.

Agilent MassHunter Quantitative Analysis software equipped with NIST 2011 database was used to analyse the chromatograms and mass spectra. Compounds were identified using the database and retention data from literature. The chromatographic peaks with areas larger than

5 % of the largest peak area in the chromatogram were included for identification. Only those peaks with a high degree of certainty (over 80%) were included and quantified based on the peak area percentage. In total 98 compounds were identified. The total area of the identified peaks accounted for 87-91 % of the area of all the peaks.

In each experiment, the non-condensable gas was sampled every 10 minutes during the operation and the samples were kept in syringes for gas chromatography (GC) analysis using a portable GC instrument Agilent 490 Micro GC equipped with a molecular sieve 5 Å column and a PoraPLOT Q column. The column temperature was kept at 80 ^{o}C, and it was calibrated using a standard gas mixture based on the reported composition of the non-condensable gas, including N_2, O_2, H_2, CH_4, CO, CO_2, C_2H_4, C_2H_6, C_3H_6 and C_3H_8. After analysis, the gas composition was normalised to N_2-free and O_2-free contents (vol.%). The volume based contents of gas species were then converted to mass-based contents, and then the yields (wt.%) of the individual gases were calculated.

The char and used catalyst was collected together as a mixture. The used catalyst (containing coke product) could not be completely separated from char, thus coke and char were reported together as carbon-residue.

4.3. Results and discussion

4.3.1 Operational performance

4.3.1.1 Performance of the hot filter

Figure 4-6 shows the change of pressure in the reactor (before the hot filter) during the reaction time. To start an experiment, the fluidised bed was first heated up and fluidised with nitrogen

flow in 30 minutes. The CFP reaction was then conducted for 90 minutes. The pressure in the reactor gradually increased from 0.06 barg to 0.2 barg due to catalyst dust accumulating in the filter during the reaction time. This was not a problem as the pressure limitation of this system was 0.4 barg.

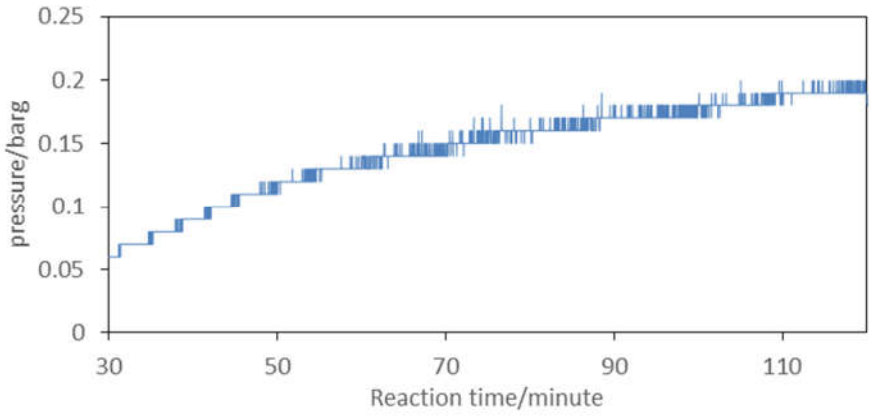

Figure 4-6: The pressure change in the fluidised bed during operation (reaction time) after initial heat-up period (30 minutes).

4.3.1.2 Catalyst activity

Fresh catalyst was preloaded in the reactor and thus the catalyst activity was high at the beginning of each experiment. This activity could be gradually deactivated during operation, even when extra fresh catalyst was fed into the reactor to maintain the catalyst activity. It was important to monitor the change of catalyst activity during operation.

The gas composition can be an indicator of change in catalyst activity. Figure 4-7 shows the change of the individual gases production during reaction time. The content of CO was the highest and relatively stable with reaction time. While the contents of H_2, CH_4, C_2H_6, and C_3H_6 increased slightly with reaction time, and the contents of CO_2, C_2H_4 and C_3H_8 slightly decreased.

The ratio of CO/CO_2 slightly increased from 2.4 to 2.8 during reaction time, indicating that the degree of deoxygenation was slightly decreased. An average ratio of CO/CO_2 of 2.9 has been reported in a catalytic fast pyrolysis run lasting four days [9]. Thus the catalyst was still active at deoxygenation in the end of the reaction time in this study.

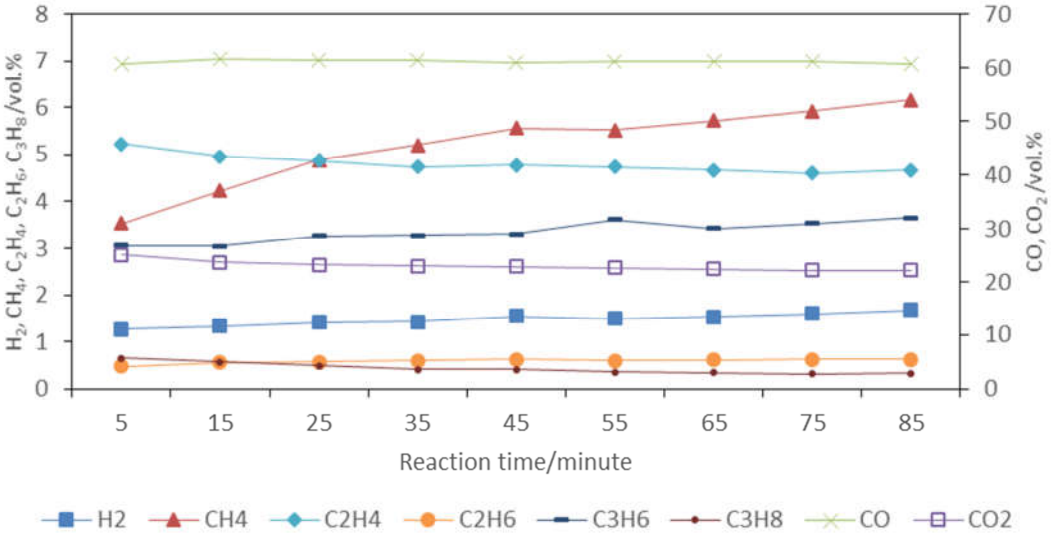

Figure 4-7: The change of non-condensable gas contents during reaction time.

4.3.1.3 Experimental repeatability

Figure 4-8 shows the mass balances for three runs of CFP of Rwood at 500 °C and a C/B ratio of 2.5. The stacked columns represent the yields of liquid, carbon-residue and gas. It shows that the mass balances for the three experiments were very close with values of 97.0 wt.%, 98.1 wt.% and 98.7 wt.%, respectively. This confirms that this system has reliable repeatability.

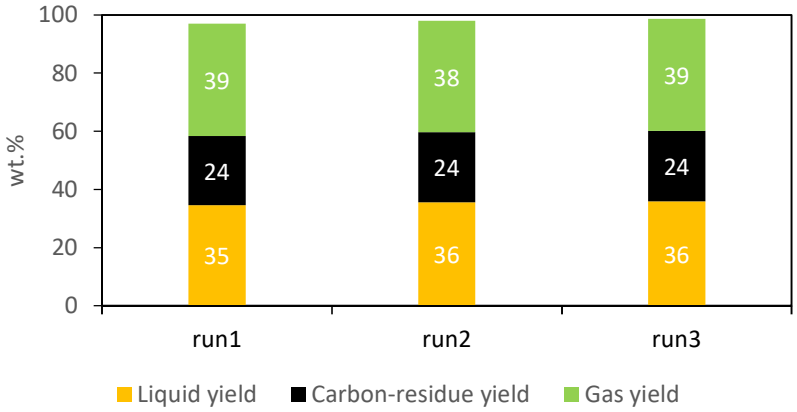

Figure 4-8: The mass balance from the reactor.

In Figure 4-9, the liquid recovery values for aqueous and oily liquids are presented. The liquid product was partially lost in the separating procedure as some liquid remained in the cylinder and separating funnels. The total recovery for the three experiments was 92.0 wt.%, 85.4 wt.% and 86.3 wt.%.

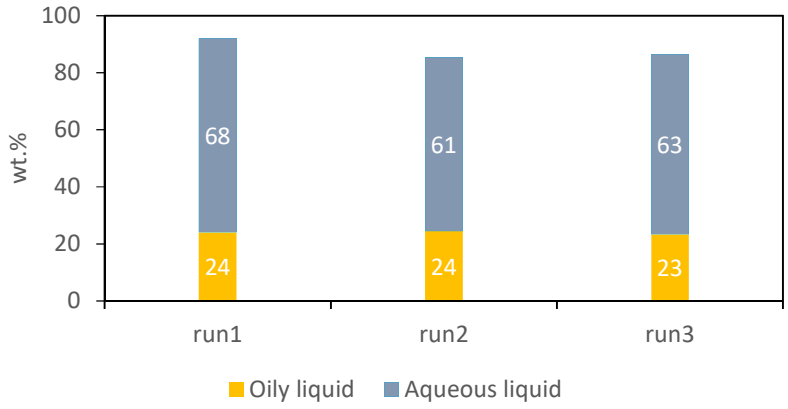

Figure 4-9: The liquid recovery after separation.

4.3.2 Distribution of the products

The distribution of the products (organics in the oily liquid, organics in the aqueous liquid, produced water, carbon-rich residue and non-condensable gas) are presented in Table 4-5. The

non-condensable gas was separated into individual gases. The comparison was focused on the two gaseous products CO and CO_2, as the yields of other gases are negligible.

Table 4-5: The products distribution in catalytic fast pyrolysis of Rwood.

	R_360_2.5	R_450_2.5	R_500_2.5	R_500_1.2	R_500_4	R_500_6
Product yield (wt.%) [a]						
Organics in oily liquid	8	10	8	12	7	8
Organics in aqueous liquid	4	- [b]	-	-	-	-
Produced water	21	23	24	22	23	21
Carbon-residue	43	27	24	22	24	29
Non-condensable gas	22	36	39	38	38	40
Total	98	96	94	93	91	99
Gas yields (wt.%) [a]						
H_2	-	-	-	-	-	-
CH_4	-	1	1	1	1	1
CO	13	20	21	21	20	22
CO_2	8	12	12	12	12	13
C_2H_4	-	1	2	2	2	2
C_2H_6	-	-	-	-	-	-
C_3H_6	-	1	2	2	2	2
C_3H_8	-	-	-	-	-	-

[a] dry basis; [b] trace amount, <1 wt.%.

4.3.2.1 Effect of reaction temperature

The highest yield of organics in oily liquid among the three experiments at temperatures of 360, 450 and 500 ^{o}C (C/B ratio 2.5) was 10 wt.% at 450 ^{o}C (see Table 4-5). The yield of carbon-residue significantly decreased with increasing temperature, and the yield of gas significantly increased. While the yield of produced water was slightly increased. This indicates that the dehydration in CFP is not significantly affected by temperature in this range. Similar trends of the products yields were reported by Olazar *et al.* [10] in a study of catalytic fast pyrolysis of sawdust using a conical spouted-bed reactor in the range from 400 ^{o}C to 500 ^{o}C.

The zeolite catalyst remained active at a low temperature of 360 ^{o}C, as the results show that the yield of gas was 22 wt.%. In the non-catalytic fast pyrolysis, the gas yield was less than 20 wt.% in all the experiments (see Chapter 2 and 3). In addition, the liquid product in CFP at 360 ^{o}C naturally separated into two phases, which was different from the bio-oil from the non-catalytic fast pyrolysis.

The yields of CO and CO_2 under different temperatures are also presented in Table 4-5. The yields were increased when increasing temperature from 350 °C to 450 °C. This indicates that the two deoxygenation pathways, decarboxylation and decarbonylation, were promoted in this temperature range. On the other hand, deoxygenation was not significantly affected in the range from 450 °C to 500 °C.

4.3.2.2 Effect of catalyst to biomass ratio

Table 4-5 also lists the product yields in catalytic fast pyrolysis of raw wood at C/B ratios of 1.2, 2.5, 4 and 6. The yield of organics in oily liquid was the highest at C/B ratio of 1.2, and this yield appears to be stable at 7-8 wt.% with increased C/B ratio from 2.5 to 6. The yield of carbon-residue was increased with increased the C/B ratio, and this yield was the highest at the C/B ratio of 6. Thus excessive catalyst loading led to the formation of solid product, probably coke.

There was no significant change in the yields of produced water, CO and CO_2 when increasing the C/B ratio. This indicates that the degree of deoxygenation was hardly affect by the C/B ratio in this range.

4.3.3 Properties of the liquids

The properties of liquid products are given in Table 4-6 including the water content, elemental composition, and the GPC results for oily liquid. The molar ratio of oxygen to carbon (O/C) for the organics in oily liquid are also presented. This table also shows the water content for the aqueous liquid. As it was very high, the elemental analysis and GC/MS analysis cannot be conducted for reliable results.

Table 4-6: Properties of liquid products in catalytic fast pyrolysis of Rwood.

	R_360_2.5	R_450_2.5	R_500_2.5	R_500_1.2	R_500_4	R_500_6
Oily liquid						
Water content (wt.%) [a]	4.3	2.6	2.1	2.3	1.5	1.2
Elemental composition (wt.%), dry basis						
C [b]	71.9	76.6	79.8	80.2	80.6	81.5
H [c]	6.6	6.6	7.0	7.4	7.0	7.0
O, by difference	21.5	16.8	13.2	12.5	12.5	11.5
O/C (mol/mol), dry basis	0.30	0.22	0.17	0.16	0.16	0.14
GPC results (g/mol) [d]						
Mn	123	112	113	118	109	109
Mw	166	142	145	161	141	137
Mz	291	242	258	302	265	241
Aqueous liquid						
Water content (wt.%) [a]	84.0	98.0	>LOD [e]	>LOD	>LOD	>LOD

[a] The standard deviations (STDs) were no more than 0.4; [b] STDs<2.0; [c] STDs<0.2; [d] average values of duplicate; [e] LOD (the limit of detection)=99.0 wt.%.

4.3.3.1 Effect of reaction temperature

As shown Table 4-6, the water content decreased in oily liquid when increasing temperature from 360 ^{o}C to 500 ^{o}C, and conversely it increased in the aqueous liquid. The O/C ratio of oily liquid decreased from 0.30 to 0.17 when increasing temperature. Hence the properties of oily liquid, in terms of water content and elemental content, were improved with the temperature.

The molecular weight profiles of oily liquids (Figure 4-10) show that the oily liquids from 450 °C and 500 °C pyrolysis are almost the same. The molecular weight profile of oily liquid from 360 °C pyrolysis is different, with its average molecular weight being higher than the other two oils (Table 4-6). It appears that the oily liquid from 360 °C pyrolysis contained relatively more compounds which were frequently detected in bio-oil from non-catalytic pyrolysis, as also observed by the higher oxygen content. These compounds contributed to a higher average molecular weight for the oily liquid from the 360 °C pyrolysis experiment.

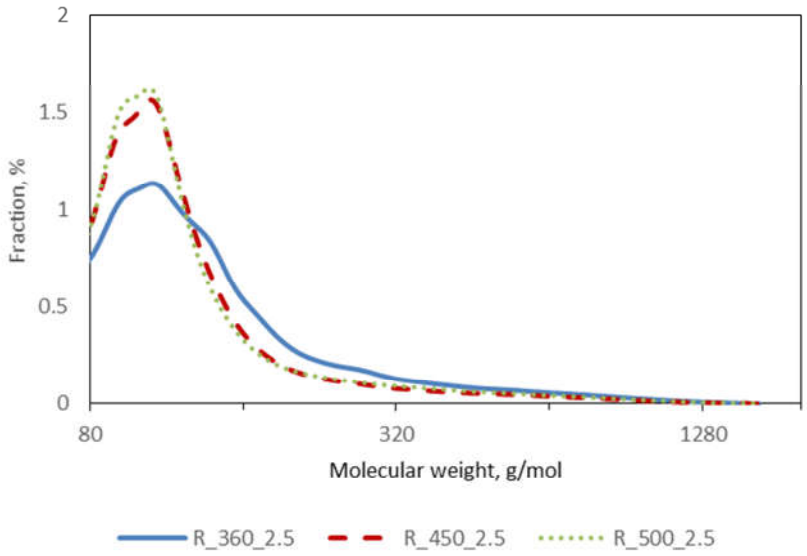

Figure 4-10: Molecular weight distribution profiles of oily liquids under different temperature.

4.3.3.2 Effect of catalyst to biomass ratio

As shown in Table 4-6, the water content of the oily liquid from 500 °C pyrolysis slightly decreased with the increased C/B ratio from 1.2 to 6. The results of elemental analysis show little difference and the O/C ratio was about 0.15 at all the C/B ratios. Thus C/B ratio in this range has little influence on the properties of oily liquid in terms of water content and elemental content.

The average molecular weights of oily liquids from GPC results (Table 4-6) slightly decreased with the increased C/B ratio. This trend is also confirmed by the GPC profiles as shown in Figure 4-11, in which the curves of the oily liquid produced at higher C/B ratios were slightly shifted to the left (to lower MW).

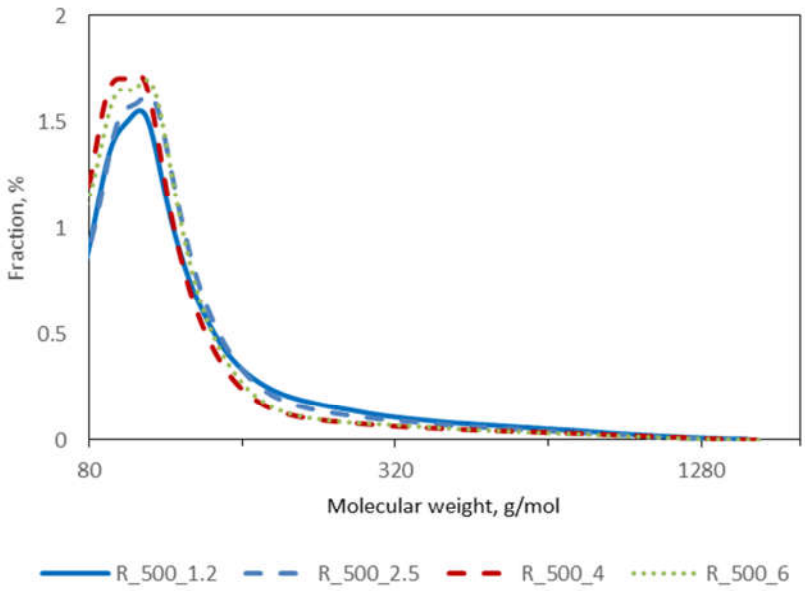

Figure 4-11: Molecular weight distribution profiles for oily liquid at different C/B ratios.

4.3.4 Chemical composition of the oily liquid

The oily liquid was analysed by ^{1}H NMR spectroscopy and GC/MS to determine the chemical composition, and the results are shown in Table 4-7. ^{1}H NMR analysis is able to give the composition of different organic groups whereas GC/MS analysis can identify GC volatile compounds. The ^{1}H NMR analysis classified the hydrogen atoms in the oily liquid compounds into six groups (see Chapter 3) [11]: namely “alkanes” (0.5-1.5 ppm), “hydrogen α to heteroatom/unsaturation” (1.5-3.0 ppm), “aliphatic alcohols/methoxy” (3.0-4.4 ppm), “carbohydrates” (4.4-6.0 ppm), “aromatics/heteroaromatics” (6.0-8.5 ppm) and “aldehydes”

(9.5-10.1 ppm). The identified compounds in GC/MS analysis were grouped as aromatics, oxygenated aromatics, benzofurans, furans, catechols, guaiacols, ketones and phenols based on their primary functionality. The aromatics group contains aromatic hydrocarbons without oxygen, while oxygenated aromatics group represents aromatics containing oxygen.

As the water content of the aqueous liquid was more than 84 wt.%, no more analysis was undertaken except ^{1}H NMR spectroscopy for the 360 ^{o}C aqueous liquid.

Table 4-7: The chemical composition of liquid products from catalytic fast pyrolysis of Rwood.

	R_360_2.5 [a]	R_360_2.5 [b]	R_450_2.5	R_500_2.5	R_500_1.2	R_500_4	R_500_6
^{1}H NMR analysis results (% of all hydrogens) [c]							
Aldehydes, carboxylic acids	1.2	0.3	0.1	0.0	0.1	0.0	0.0
Carbohydrates	7.7	3.5	1.2	1.1	1.7	1.0	0.9
Aliphatic alcohols, methoxy	9.2	12.7	6.0	5.0	6.6	4.7	3.9
Alkanes	6.4	9.7	6.1	4.2	5.5	3.8	3.7
Hydrogen α to heteroatom, unsaturation	65.5	38.9	38.6	35.2	34.8	34.5	37.5
Aromatics, heteroaromatics	10.0	34.9	48.0	54.5	51.4	55.9	54.0
GC/MS analysis results (% of peak area) [c, d]							
Aromatics	-	53.5	73.0	75.8	68.9	79.2	79.7
Aromatics, oxygenated	-	13.6	10.8	9.9	11.7	8.9	7.7
Furans	-	1.2	0.5	0.2	0.4	0.2	0.3
Catechols	-	2.2	0.4	0.1	0.3	0.0	0.0
Guaiacols	-	12.3	0.7	0.2	0.7	0.2	0.2
Ketones	-	6.7	0.8	0.3	0.7	0.2	0.3
Phenols	-	10.6	13.9	13.5	17.4	11.2	11.8

[a] Aqueous liquid; [b] oily liquid; [c] average values of duplicate; [d] details of the GC/MS results can be found in Table 4-A1 in Appendix A.

4.3.4.1 Effect of reaction temperature

According to the ^{1}H NMR analysis, only the content of hydrogen atoms associated to aromatics/ heteroaromatics functionality was increased with the increased temperature, while the contents of the rest hydrogens were decreased. Similarly, the GC/MS analysis results show the contents of aromatics, oxygenated aromatics, and phenols were increased with the temperature. These

results reveal that the main products were aromatics, and the activity of the zeolite catalyst increased when increasing the temperature.

Four dominant compounds in the oily liquid were identified in the GC/MS analysis: toluene, naphthalene, phenol, and 2-methoxy-phenol. Toluene and naphthalene are typical products in CFP using HZSM-5 as a catalyst [12]. 2-Methoxy-phenol, also known as guaiacol, is a typical lignin-derived product in thermal pyrolysis, and phenol is also a common product in fast pyrolysis largely derived from lignin [12].

The percentage changes of these four compounds with temperature are presented in Figure 4-12. The percentage of toluene increased substantially from 1.7 % at 360 °C to 6.5 % at 450 °C and then to 9.4 % at 500 °C. The percentage of naphthalene also increased with the temperature. The percentage of phenol slightly increased from 2.9 % to 5.0 % with the increased temperature from 360 to 500 °C. However, guaiacol almost completely disappeared when the temperature was 450 °C or higher.

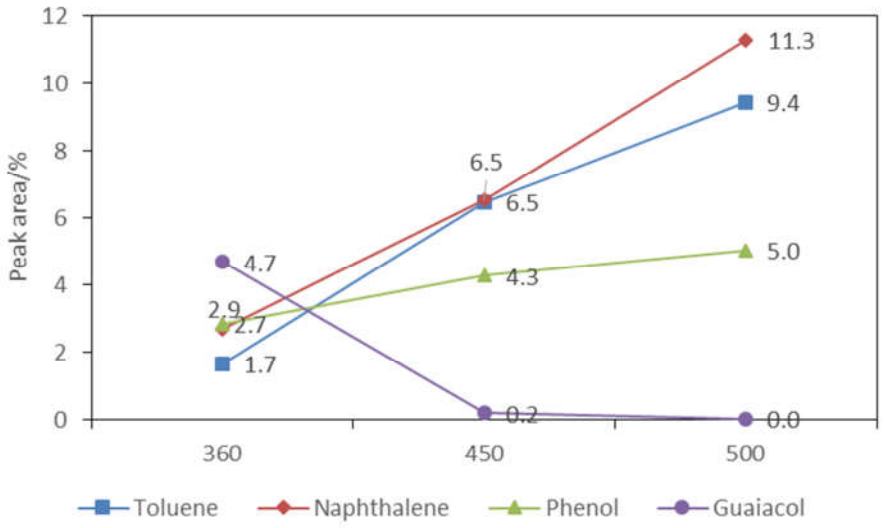

Figure 4-12: The product selectivity at different temperatures

In summary, the activity of the HZSM-5 catalyst increased with the increased temperature in the examined range of 360 to 500 °C. As the results indicated, the properties of the oily liquid, in terms of a low water content and O/C ratio, were improved with the increased temperature. Meanwhile, the selectivity of aromatics was increased. Similarly, a study of CFP of lignocellulosic biomass reported that the yield of aromatic carbon increased with the increased temperature up to 600 °C [3].

4.3.4.2 Effect of catalyst to biomass ratio

Table 4-7 also presents the changes in the chemical composition of the oily liquid with the increased C/B ratio from 1.2 to 6. The results of ^{1}H NMR analysis show that the hydrogen contents associated to carbohydrates, alcohols/methoxy and alkanes functionalities decreased with increasing C/B ratio. But this decrease was less significant when the C/B ratio was higher than 2.5. Similarly in GC/MS analysis, the percentage of guaiacols decreased with increasing C/B ratio and the decrease was less substantial when the C/B ratio was increased from 2.5 to 6. The production of aromatics increased with increased C/B ratio, in both the ^{1}H NMR and GC/MS analyses, and this increase was less substantial when the C/B ratio was increased from 2.5 to 6.

The percentage changes of toluene, naphthalene and phenol in GC/MS analysis are presented in Figure 4-13. The percentage of toluene gradually increased when increasing the C/B ratio from 1.2 to 6. The percentage of naphthalene increased when increasing the C/B ratio from 1.2 to 4, but it decreased slightly when further increasing the C/B ratio to 6. On the other hand, the percentage of phenol slightly decreased with increasing C/B ratio. This suggests that a C/B ratio at 2.5 provided enough catalyst loading for catalytic conversion, and higher catalyst loading results in limited improvement on aromatics production.

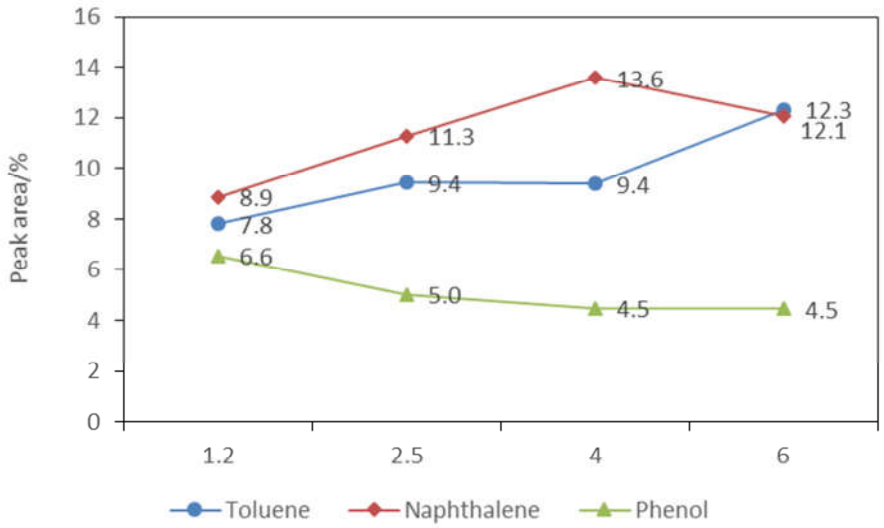

Figure 4-13: The product selectivity at different C/B ratios.

In summary, these results indicate that there is a certain catalyst loading (C/B ratio at 2.5) which is necessary for catalytic conversion, while further increasing catalyst loading (C/B ratio) resulted in limited changes in the chemical composition. Meanwhile, this resulted in a decrease in the yield of the oil product and an increase in the yield of the solid product.

Coke formation occurs in catalytic pyrolysis accompanied by the conversion of thermal pyrolysis products to aromatics [12]. Excessive catalyst loading may promote the formation of coke, rather than the catalytic conversion from oxygenated organics to aromatics.

4.4. Conclusion

The hot filter was able to effectively capture the catalyst dust generated by particle attrition in the fluidised bed reactor. Although the pressure in the reactor gradually increased during operation, the reactor was operated for 90 minutes below its pressure limitation. By following a developed operational method, the catalyst to feeding biomass (C/B) ratio can be controlled at required values and good catalyst activity can be maintained during the entire reaction time.

Triplicate experiments using Rwood at 500 ^{o}C and the C/B ratio of 2.5 confirmed good repeatability of the system in terms of the product yields. A total recovery (mass balance) of 91 - 99 wt.% can be achieved, and the mass loss mainly came from the liquid separation.

This study found that, in the ranged studied (360-500 °C), the reaction temperature had significant impacts on the product distribution and the chemical composition of the oil product (oily liquid). The yield of oily liquid was the highest at pyrolysis temperature of 450 ^{o}C. The yield of solid product (carbon-residue) decreased with the increased temperature, while the gas yield was increased. The abundance of aromatics in the oily liquid, such as toluene and naphthalene, increased with the increased temperature, while the contents of thermal decomposition products, such as guaiacols, decreased. As the catalyst activity was increased with the increased temperature, catalytic conversion was optimised at 500 ^{o}C with a little loss in the oil yield.

This study also showed that the C/B ratio in the examined range (1.2-6) affected the products distribution and the chemical composition of the oil product, to a less extent. The yields of carbon-residue and gas were increased with the increased C/B ratio. The yield of oily liquid was the highest at a C/B ratio of 1.2, and increasing C/B ratio led to a lower oil production. The C/B ratio had little influence on the properties of the oily liquid. The selectivity for aromatics was increased with the increased C/B ratio, this increase was limited when the C/B ratio increased from 2.5 to 6. Although a C/B ratio of 1.2 is the optimal ratio for raw wood, it may be not for acid-leached wood which produces more bio-oil in fast pyrolysis. In order to avoid insufficient catalytic conversion, a C/B ratio of 2.5 was applied in the following study with pretreated biomas.

References

[1] Aho, A., N. Kumar, K. Eränen, T. Salmi, M. Hupa, and D.Y. Murzin, *Catalytic pyrolysis of woody biomass in a fluidized bed reactor: Influence of the zeolite structure.* Fuel, 2008. **87**(12): p. 2493-2501.

[2] Zhang, H., R. Xiao, H. Huang, and G. Xiao, *Comparison of non-catalytic and catalytic fast pyrolysis of corncob in a fluidized bed reactor.* Bioresource Technology, 2009. **100**(3): p. 1428-1434.

[3] Jae, J., R. Coolman, T.J. Mountziaris, and G.W. Huber, *Catalytic fast pyrolysis of lignocellulosic biomass in a process development unit with continual catalyst addition and removal.* Chemical Engineering Science, 2014. **108**: p. 33-46.

[4] Yang, H., R. Coolman, P. Karanjkar, H. Wang, P. Dornath, H. Chen, W. Fan, W.C. Conner, T. Mountziaris, and G. Huber, *The effects of contact time and coking on the catalytic fast pyrolysis of cellulose.* Green Chemistry, 2017. **19**(1): p. 286-297.

[5] Yildiz, G.r., T. Lathouwers, H.E. Toraman, K.M. van Geem, G.B. Marin, F. Ronsse, R. van Duren, S.R. Kersten, and W. Prins, *Catalytic fast pyrolysis of pine wood: effect of successive catalyst regeneration.* Energy & fuels, 2014. **28**(7): p. 4560-4572.

[6] Azeez, A.M., D. Meier, J. Odermatt, and T. Willner, *Fast Pyrolysis of African and European Lignocellulosic Biomasses Using Py-GC/MS and Fluidized Bed Reactor.* Energy & Fuels, 2010. **24**(3): p. 2078-2085.

[7] Dayton, D.C., J.R. Carpenter, A. Kataria, J.E. Peters, D. Barbee, O.D. Mante, and R. Gupta, *Design and operation of a pilot-scale catalytic biomass pyrolysis unit.* Green Chemistry, 2015. **17**(9): p. 4680-4689.

[8] Hoekstra, E., K.J.A. Hogendoorn, X. Wang, R.J.M. Westerhof, S.R.A. Kersten, W.P.M. van Swaaij, and M.J. Groeneveld, *Fast Pyrolysis of Biomass in a Fluidized Bed Reactor: In Situ Filtering of the Vapors.* Industrial & Engineering Chemistry Research, 2009. **48**(10): p. 4744-4756.

[9] Paasikallio, V., C. Lindfors, E. Kuoppala, Y. Solantausta, A. Oasmaa, J. Lehto, and J. Lehtonen, *Product quality and catalyst deactivation in a four day catalytic fast pyrolysis production run.* Green Chemistry, 2014. **16**(7): p. 3549-3559.

[10] Olazar, M., R. Aguado, J. Bilbao, and A. Barona, *Pyrolysis of sawdust in a conical spouted-bed reactor with a HZSM-5 catalyst.* AIChE Journal, 2000. **46**(5): p. 1025-1033.

[11] Mullen, C.A., G.D. Strahan, and A.A. Boateng, *Characterization of various fast-pyrolysis bio-oils by NMR spectroscopy†.* Energy & Fuels, 2009. **23**(5): p. 2707-2718.

[12] Liu, C., H. Wang, A.M. Karim, J. Sun, and Y. Wang, *Catalytic fast pyrolysis of lignocellulosic biomass.* Chemical Society Reviews, 2014. **43**(22): p. 7594-7623.

Chapter 5

Catalytic fast pyrolysis of pretreated wood

Abstract

In this chapter, catalytic fast pyrolysis of pretreated woods was investigated on a fluidised bed reactor. Catalytic fast pyrolysis of acid-leached wood was conducted at three temperatures (360 ^{o}C, 450 ^{o}C and 500 ^{o}C) and at three catalyst to biomass ratios (2.5, 4 and 6). Catalytic fast pyrolysis of torrefied wood and acid-leached-torrefied wood was conducted at three catalyst to biomass ratios (2.5, 4 and 6) at 500 ^{o}C.

The experimental results show that with acid-leaching pretreatment, the yield of oil product in catalytic fast pyrolysis was not significantly affected and this is dissimilar to its effect in non-catalytic fast pyrolysis in which the yield of oil product was increased. This indicates that the acid-leaching pretreatment mildly impedes deoxygenation in catalytic fast pyrolysis. As a result, the oil product contains more oxygen and less aromatic hydrocarbons.

The experimental results also show that torrefaction pretreatment can lead to an increase in the yield of oil product in catalytic fast pyrolysis, but no significant change was found in properties and chemical composition of the oil product. This effect is different from that in non-catalytic fast pyrolysis, in which torrefaction pretreatment can decrease the oxygen content of bio-oil. The torrefaction pretreatment increases the yield of solid product (char and coke), and

decreases the yield of produced water in catalytic fast pyrolysis. This effect is similar to that in fast pyrolysis.

Bed material agglomeration can occur in catalytic fast pyrolysis of acid-leached wood on a fluidised bed reactor. The operational performance and SEM images of the char residues showed that it is a same phenomenon as that occurred in fast pyrolysis. The catalytic effect of zeolite HZSM-5 cannot prevent bed agglomeration. This issue is able to be overcome by the three approaches proposed in this study.

5.1. Introduction

Acid-leaching pretreatment can decrease the ash content of biomass, and consequently increases the yield of bio-oil in fast pyrolysis [1-3]. Torrefaction pretreatment can improve the properties of bio-oil, such as decreasing the oxygen content [4, 5]. Wigley *et al.* [6] proposed an integrated process in which the torrefaction and acid-leaching pretreatments are conducted before the fast pyrolysis. In such a process, the acidic condensate from torrefaction can be used for acid-leaching, thus avoiding any additional acid cost. Because of the benefits of acid-leaching and torrefaction pretreatments in fast pyrolysis, it is interesting to investigate a process which combines these biomass pretreatments with catalytic fast pyrolysis (CFP).

In CFP, the ash in biomass can cause catalyst deactivation by metals depositing on the acid sites of the zeolite [7, 8]. Mullen *et al.* [9] found that the amount of accumulated ash on zeolite catalyst was increased after successive use of the same catalyst in a fluidised bed reactor. Consequently, the level of deoxygenation of the oil product and the selectivity of aromatic hydrocarbons were decreased. When upscaling the CFP process to pilot or commercial scale, coked catalyst will be burnt for regeneration of the catalyst. After a few regeneration cycles, accumulated ash on the catalyst can lead to an irreversible deactivation of the catalyst. As demonstrated in Chapter 2, the acid-leaching pretreatment is able to efficiently remove biomass ash from the woody feedstock. Acid-leaching pretreatment is likely to be favourable for catalytic fast pyrolysis as it could extend the lifetime of the catalyst.

However, studies on CFP of acid-leached (demineralised) biomass are limited in the literature. Hernando *et al.* [10] tested acid-washed wheat straw as the feedstock in an *ex situ* CFP study using a downdraft fixed bed reactor. Bed material agglomeration (bed agglomeration) can occur

when pyrolysing acid-leached biomass in a fluidised bed reactor [11]. It may be difficult to conduct CFP of acid-leached biomass in a fluidised bed because of this operational problem. In this study, approaches were developed to overcome the bed agglomeration problem as described in Chapter 3, and CFP of the acid-leached biomass on a fluidised bed reactor will be investigated in this chapter.

Catalytic pyrolysis of torrefied biomass has been reported previously, but not in a fluidised bed reactor. Torrefaction pretreatment is reported to be an effective method to improve the selectivity of aromatic hydrocarbons in catalytic pyrolysis as reported [12-14]. Srinivasan *et al.* [13] studied the effect of torrefaction pretreatment on catalytic pyrolysis using a pyroprobe reactor and a fixed bed reactor. Pine wood samples were torrefied at 225 °C for 30 minutes. It was concluded that torrefaction pretreatment favours the production of aromatic hydrocarbons in catalytic pyrolysis. Zheng *et al.* [14] investigated catalytic pyrolysis of torrefied corncobs using a pyroprobe reactor. It was found that the optimal torrefaction conditions for catalytic pyrolysis were 210-240 °C for 40 minutes. Torrefaction pretreatment for shorter time (210-240 °C for 20 minutes) had little impact on the aromatic yield, while severe torrefaction (270-300 °C) led to a sharp increase of coke yield and a reduced yield of aromatic hydrocarbons. Studies on catalytic pyrolysis of torrefied cellulose [15] and torrefied lignin [16] also revealed that torrefaction pretreatment can enhance the production of aromatic hydrocarbons.

The effects of biomass pretreatments in catalytic pyrolysis are related to their effects in thermal pyrolysis, which is the first step in catalytic pyrolysis. The thermal pyrolysis products are decomposition oxygenates from cellulose, hemicellulose and lignin [17]. Some ash elements in the biomass play an active role as catalysts promoting fragmentation reactions [5]. Then these products from thermal pyrolysis undergo a series of catalytic reactions on the acid sites of the

zeolite, the catalytic reactions include deoxygenation, cracking, aromatisation, oligomerisation [10, 18]. Because the biomass pretreatments can affect the distribution of the thermal pyrolysis products, these changes can lead to the differences in catalytic pyrolysis.

In this chapter, CFP experiments using acid-leached wood, torrefied wood and acid-leached-torrefied wood as feedstocks were conducted. Based on the literature review, this is the first study to use a fluidised bed reactor for CFP of acid-leached wood or torrefied wood.

5.2. Experimental

5.2.1 Materials and configuration

Acid-leached wood (ALwood), torrefied wood (Twood) and acid-leached-torrefied wood (ALTwood) as described in Chapter 2 were used as the feedstocks. The commercial spray-dried HZSM-5 zeolite as described in Chapter 4 was used as the catalyst and bed material. The moisture contents of feedstock and catalyst were measured before each CFP experiment and used for mass balance analysis on a dry basis.

The Scion fluidised bed reactor modified with a hot filter was employed for the CFP experiments. As described in Chapter 4, this reactor has good repeatability and the catalyst was active over the reaction time of 90 minutes.

5.2.2 Catalytic fast pyrolysis experiments

Experimental operation followed the procedures described in Chapter 4. The operation time in each experiment was 90 minutes. For all of the experiments, the temperature of the gas cleaning set was kept at 440 ^{o}C, the temperatures of electrostatic precipitator (ESP) unit and the

intensive cooler (IC) unit were kept at -5 ^{o}C and -15 ^{o}C, respectively. The residence time of the hot vapour in the fluidised bed reactor was kept at approximately 3 seconds by adjusting nitrogen flowrate at different reaction temperature. The WHSV was kept at 0.5 by setting the biomass feeding rate at 0.35 kg/h.

The operation conditions and IDs for the CFP experiments in this chapter are summarized in Table 5-1. The control experiments using Rwood as the feedstock were previously described in Chapter 4.

Table 5-1: A summary of catalytic fast pyrolysis experiments.

Number	ID	Feedstock	Temperature (°C)	C/B ratio	Experiment
1	AL_500_2.5	ALwood	500	2.5	New
2	AL_500_4	ALwood	500	4	New
3	AL_500_6	ALwood	500	6	New
4	AL_450_2.5	ALwood	450	2.5	New
5	AL_360_2.5	ALwood	360	2.5	New
6	T_500_2.5	Twood	500	2.5	New
7	T_500_4	Twood	500	4	New
8	T_500_6	Twood	500	6	New
9	ALT_500_2.5	ALTwood	500	2.5	New
10	ALT_500_4	ALTwood	500	4	New
11	ALT_500_6	ALTwood	500	6	New
12	R_500_2.5	Rwood	500	2.5	Chapter 4
13	R_500_4	Rwood	500	4	Chapter 4
14	R_500_6	Rwood	500	6	Chapter 4
15	R_450_2.5	Rwood	450	2.5	Chapter 4
16	R_360_2.5	Rwood	360	2.5	Chapter 4

CFP experiments with ALwood were conducted at catalyst to biomass (C/B) ratios of 2.5, 4 and 6 by setting the catalyst feeding rate at 0.43 kg/h, 1.00 kg/h and 1.50 kg/h, respectively. The reaction temperature was kept at 500 ^{o}C as the catalyst was found to be the most active at this temperature in this study. Then CFP of ALwood experiments were conducted at 450 ^{o}C and 360 ^{o}C while the C/B ratio was kept at 2.5 by setting the catalyst feeding rate at 0.43 kg/h.

CFP experiments with Twood and ALTwood were conducted at C/B ratios of 2.5, 4 and 6, respectively. The reaction temperature was kept at 500 ^{o}C.

5.2.3 Product analysis

As discussed in Chapter 4, the products from biomass pyrolysis include liquid, solid (coke and char) and non-condensable gas. The liquid product from the CPF experiments were separated into two phases, oily liquid and aqueous liquid, following the procedure described in Chapter 4. The water content of both phases was measured following the method as described in Chapter 2. The oily liquids were further analysed by elemental analysis, GPC, ^{1}H NMR spectroscopy and gas chromatography-mass spectrometry (GC/MS) following the methods as described in Chapter 4.

The non-condensable gas was sampled every 10 minutes and analysed by a portable gas chromatography (GC) following the method as described in Chapter 4. The coke yield and char yield were reported together as carbon-rich residue yield, because the coked catalyst could not be completely separated from the char product.

5.3. Results

5.3.1 Operational performance

Bed agglomeration occurred in the experiment AL_500_2.5 causing immediate defluidisation in the reactor (Figure 5-1). As was observed with fast pyrolysis of ALwood at 500 ^{o}C, the temperature near the main auger in the reactor decreased rapidly indicating a problem with bed agglomeration (see Chapter 3).

Figure 5-1: Bed agglomeration in AL_500_2.5.

In order to overcome bed agglomeration at 500 °C, the reactor was operated with a higher C/B ratio. Bed agglomeration occurred after 35 minutes when the C/B ratio was increased to 4 (AL_500_4). When the C/B ratio was further increased to 6 (AL_500_6), a successful experiment with a 90 minutes runtime was achieved. Additionally, the CFP experiments with a C/B ratio of 2.5 at 450 °C (AL_450_2.5) and 360 °C (AL_360_2.5) were also successfully conducted. Therefore, bed agglomeration can be overcome by increasing the feeding rate of catalyst (increasing the C/B ratio) or reducing the reaction temperature.

The experiments using Twood and ALTwood with C/B ratios of 2.5, 4 and 6 at 500 °C were successfully conducted on the fluidised bed reactor. The success of the experiment ALT_500_2.5 suggests that torrefaction pretreatment can prevent the bed agglomeration in CFP of acid-leached wood.

The melting behaviour of the biomass in CFP was the same as that observed in fast pyrolysis of ALwood and ALTwood (see Chapter 3). Figure 5-2 (pictures A-C) shows SEM images of char residues from experiments AL_360_2.5, AL_450_2.5 and AL_500_2.5. The char from AL_360_2.5 clearly shows fibrous structure with rigid morphology. On the other hand, the melting behaviour was observed in experiments AL_450_2.5 and AL_500_2.5. The severity of the melting increased with temperature and this eventually led to bed agglomeration as observed in experiment AL_500_2.5.

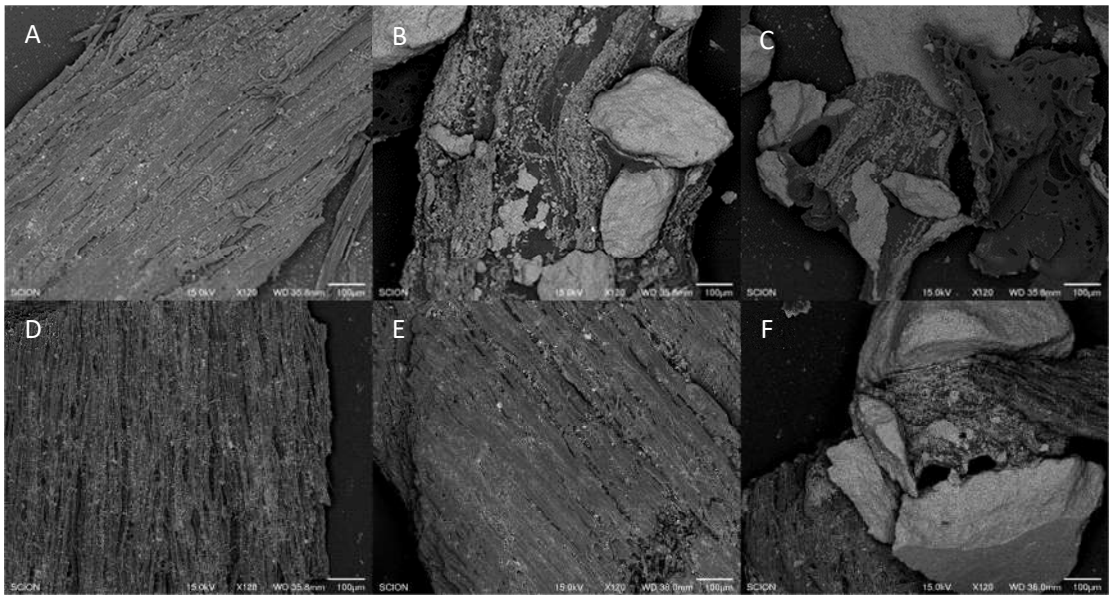

Figure 5-2: SEM images of char residue from catalytic fast pyrolysis experiments, AL_360_2.5 (A), AL_450_2.5 (B), AL_500_2.5(C), R_500_2.5(D), T_500_2.5 (E), ALT_500_2.5 (F).

Figure 5-2 (pictures D-F) also shows SEM images of char residues from experiments R_500_2.5, T_500_2.5 and ALT_500_2.5. The char samples from R_500_2.5 and T_500_2.5 show fibrous structure with rigid morphology. Conversely, the melting behaviour was observed in experiment ALT_500_2.5. In this case, bed agglomeration was prevented because the melting severity was hindered by the carbonisation effect of torrefaction pretreatment in thermal pyrolysis.

5.3.2 Distribution of the products

The yields of the products including organics in the oily liquid, organics in the aqueous liquid, produced water, carbon-rich residue, and non-condensable gas are presented in Table 5-2. The yields of the organics in the aqueous liquid were insignificant in most cases, thus the investigation was focused on the yields of the organics in the oily liquid. The non-condensable gas was separated into individual gases, so that the yields of the gaseous products in different experiments are comparable. The comparison was focused on the two gaseous products CO and CO_2, as the yields of other gases are negligible.

The results from Rwood are included as controls. As bed agglomeration occurred in CFP of ALwood at 500 ^{o}C with C/B ratios of 2.5 and 4, no results were available for these two experiments. In order to investigate the effects of biomass pretreatments in CFP, the comparison can be between the results from a pretreated wood and raw wood under the same conditions.

Generally, the mass balance closure across all experiments ranged from 91-99 wt.%. Over 90 wt.% was considered to be acceptable because of the challenges of recovering all the products from the fluidised bed reactor. The mass loss occurred mainly in the procedure of collecting and separating the liquid product. The unrecovered liquid mainly remained on the inner-wall of the ESP column and the separating funnels.

Table 5-2: The comparison of product yields from CFP of pretreated woods.

	R_360_2.5 [a]	R_450_2.5 [a]	R_500_2.5 [a]	R_500_4 [a]	R_500_6 [a]	AL_360_2.5	AL_450_2.5	AL_500_6	T_500_2.5	T_500_4	T_500_6	ALT_500_2.5	ALT_500_4	ALT_500_6
Yields of products, wt.% [b]														
Organics in oily liquid	8	10	8	7	9	11	12	9	12	8	8	10	7	7
Organics in aqueous liquid	4	1	- [c]	-	-	8	2	-	-	-	-	-	-	- [c]
Produced water	21	23	24	23	21	18	24	23	16	17	16	18	19	17
Carbon-rich residue	43	27	24	24	29	37	27	29	32	34	40	29	33	37
Gas	22	36	39	38	40	18	34	38	36	35	35	37	37	35
Total	98	96	94	91	99	92	98	99	96	94	99	94	96	96
Yields of gases, wt.%														
H_2	-	-	-	-	-	-	-	-	-	-	-	-	-	- [c]
CH_4	-	1	1	1	1	-	1	1	1	1	1	1	1	1
CO	13	20	21	20	22	11	21	27	20	20	20	22	23	22
CO_2	8	12	12	12	13	6	10	7	11	11	10	10	10	9
C_2H_4	-	1	2	2	2	-	1	1	2	2	2	1	1	1
C_2H_6	-	-	-	-	-	-	-	-	-	-	-	-	-	- [c]
C_3H_6	-	2	2	2	2	-	1	1	2	2	2	2	1	2
C_3H_8	-	-	-	-	-	-	-	-	-	-	-	-	-	- [c]

[a] Results from Chapter 4; [b] dry basis; [c] trace amount.

5.3.2.1. Effect of acid-leaching pretreatment

The yields of organics in oily liquid and carbon-rich residue were similar between experimental run of AL_500_6 and that of R_500_6. Although the yields of the produced water and the gas were slightly different, the product distribution from CFP was not strongly affected by acid-leaching pretreatment. This trend was different from the results in fast pyrolysis, in which the yield of bio-oil from ALwood was significantly increased (see Chapter 3). However, in CFP of ALwood, the yield of CO was 5 wt.% higher, and that of CO_2 was 6 wt.% lower than those from CFP of Rwood. This reveals that acid-leaching pretreatment promoted decarbonylation and suppressed decarboxylation in CFP.

By comparing the results of AL_450_2.5 with those of R_450_2.5, it was found that the yields of organics in oily liquid and produced water were slightly increased by acid-leaching pretreatment. The yields of carbon-rich residue were similar. However, the yield of CO was increased while that of CO_2 was decreased in a similar trend as for CFP at 500 °C.

The comparison of AL_360_2.5 results with R_360_2.5 results shows that acid-leaching pretreatment increased the yields of organics in oily and aqueous liquids, but decreased the yields of produced water, carbon-rich residue and gas. The yields of both CO_2 and CO were lower in AL_360_2.5 than those in R_360_2.5. These results reveal that the yields of the products in CFP at low temperature (360 ^{o}C) were strongly affected by acid-leaching pretreatment. Similar trends were also found for fast pyrolysis regarding the bio-oil yield (increasing) and yields of char and non-condensable gas (decreasing), as observed in Chapter 2. Because the catalyst had limited activity at 360 °C, the effects of acid-leaching pretreatment in thermal pyrolysis became more important in CFP.

5.3.2.2. Effect of torrefaction pretreatment

Comparing T_500_2.5 results with R_500_2.5 results shows that torrefaction pretreatment increased the yield of organics in oily liquid from 8 wt.% to 12 wt.% and that of carbon-rich residue from 24 wt.% to 32 wt.%. The torrefaction pretreatment also decreased the yield of the produced water from 24 wt.% to 16 wt.% and that of gas from 39 wt.% to 36 wt.%. Correspondingly, the torrefaction pretreatment slightly decreased the yields of CO and CO_2. The above observations are consistent with the results of fast pyrolysis as described in Chapter 2 except in CFP, the torrefaction pretreatment can increase the yield of oil product.

From the results of experiments of T_500_2.5, T_500_4 and T_500_6, it was found that with C/B ratio increasing from 2.5 to 6, the yield of carbon-rich residue was increased while the yield of organics in oily liquid was decreased. The influence of C/B ratio in the range of 2.5-6 on the yields of produced water and the gas were negligible, indicating the degree of deoxygenation was not affected in this C/B ratio range.

5.3.2.3. Effect of the combined pretreatment

Comparing ALT_500_2.5 and R_500_2.5 results in Table 5-2 shows that the yield of organics in oily liquid was slightly increased from 8 to 10 wt.% by the combined pretreatment of acid-leaching followed by torrefaction. The yield of produced water was decreased from 24 to 18 wt.% and the carbon-rich residue yield was increased from 24 to 29 wt.%. These observed changes on the product yields were likely due to the effect of torrefaction pretreatment as described above. On the other hand, the CO yield was slightly higher and the CO_2 yield was slightly lower in ALT_500_2.5 than in R_500_2.5. This was likely due to the effect of acid-

leaching pretreatment as described in the comparison of AL_500_6 results with R_500_6 results.

The comparison of results of ALT_500_2.5, ALT_500_4 and ALT_500_6 shows a similar effect of C/B ratio on the product distribution as the trends seen with the Rwood or Twood results. Briefly, the yield of organics in oily liquid was slightly decreased and the carbon-rich residue yield was increased with the increasing C/B ratio. While the yields of produced water, CO and CO_2 were barely changed.

5.3.3 Properties of liquid products

The properties of liquid products are given in Table 5-3, in which the results of elemental analysis and molar ratio of oxygen to carbon (O/C) for the organics in oily liquid are also presented. The O/C ratio indicates the level of deoxygenation. The profiles of the molecular weight distribution from GPC analysis are presented in Figure 5A-1 in the Appendix B. The GPC profiles are illustrated in 4 graphs, one for each pretreated wood and Rwood as control. Those profiles show no significant difference with the exception of the results from AL_360_2.5 and R_360_2.5. Those profiles reveal that the molecular weight of the compounds in oily liquid were mostly below 350 g/mol, indicating that the GC/MS analysis (Table 5-4) can detect most of the compounds in the oily liquid.

Table 5-3 also shows the water content of aqueous liquid. As the aqueous liquid contained largely water in most experiments, the elemental analysis and GC/MS analysis could not be conducted with reliable results. Although the aqueous liquid products from AL_360_2.5 and R_360_2.5 were analysed by ^{1}H NMR spectroscopy, no significant difference between these

experiments were found. The ^{1}H NMR result of the aqueous liquid from R_360_2.5 was presented in Chapter 4, and not further discussed in this chapter.

5.3.3.1. Effect of acid-leaching pretreatment

The comparison of the AL_500_6 and R_500_6 results shows that the water content was very low (1.2 wt.% and 1.6 wt.%) for both oily liquids. The carbon content of organics in oily liquid was decreased from 81.5 wt.% to 77.8 wt.% and the oxygen content was increased from 12.5 wt.% to 15.6 wt.% when acid-leaching pretreatment was applied. Correspondingly, the O/C ratio was increased from 0.11 to 0.15. The water content of the aqueous liquid from AL_500_6 was 98.4 wt%. It reveals that this aqueous liquid contained a small amount of water-soluble organics. In comparison, the aqueous liquid from R_500_6 contained trace amount of organics, which were beyond the limit of detection.

In CFP experiments at 360 and 450 °C, the trends of effect of acid-leaching pretreatment were found to be similar to those observed above for CFP experiment at 500 °C at the same C/B ratio. For instance, the water content of AL_360_2.5 oily liquid was 2.3 wt.% higher than that of R_360_2.5 oily liquid. AL_360_2.5 oily liquid was 2.9 wt.% higher in oxygen content and slightly lower in carbon content than R_360_2.5 oily liquid. The water content of aqueous liquid from R_360_2.5 and AL_360_2.5 was 84.0 wt.% and 69.0 wt.%, respectively. Hence more water-soluble organics were produced due to acid-leaching pretreatment.

Table 5-3: The properties of liquid products from CFP of pretreated woods.

	R_360_2.5 [a]	R_450_2.5 [a]	R_500_2.5 [a]	R_500_4 [a]	R_500_6 [a]	AL_360_2.5	AL_450_2.5	AL_500_6	T_500_2.5	T_500_4	T_500_6	ALT_500_2.5	ALT_500_4	ALT_500_6
Oily liquid														
Water content (wt.%) [b]	4.3	2.4	2.1	1.5	1.2	6.6	2.4	1.6	1.6	1.7	1.6	1.9	1.9	1.6
Elemental composition (wt.%), dry basis														
C [c]	71.9	76.6	79.8	80.6	81.5	69.2	74.2	77.8	78.4	78.6	79.6	79.6	80.7	80.7
H [d]	6.6	6.6	7.0	7.0	7.0	6.3	6.4	6.6	6.7	6.6	6.8	6.8	6.3	5.9
O	21.5	16.8	13.2	12.5	11.5	24.4	19.4	15.6	14.9	14.8	13.6	13.7	13.0	13.4
O/C (mol/mol)	0.22	0.16	0.12	0.12	0.11	0.26	0.20	0.15	0.14	0.14	0.13	0.13	0.12	0.12
Aqueous liquid														
Water content (wt.%) [b]	84.0	98.0	>LOD [e]	>LOD	>LOD	69.0	93.8	98.4	>LOD	>LOD	>LOD	>LOD	>LOD	>LOD

[a] Results from Chapter 4; [b] the standard deviations (STDs) were no more than 0.4; [c] STDs<2.0; [d] STDs<0.2; [e] LOD (the limit of detection)=99.0 wt.%.

5.3.3.2. Effect of torrefaction pretreatment

The comparison of T_500_2.5 and R_500_2.5 results shows that water content was low for both oily liquids (2.1 wt.% and 1.6 wt.%). The carbon content of organics in oily liquid was slightly decreased by torrefaction pretreatment, along with an increase in the O/C ratio from 0.12 to 0.14. The comparison of results of T_500_2.5, T_500_4 and T_500_6 shows that the C/B ratio caused no changes to the properties of the oily liquid. The water content remained constant at 1.6-1.7 w.%, the O/C ratio was 0.13-0.14. Overall, torrefaction pretreatment had little influence on the properties of the oily liquid.

5.3.3.3. Effect of the combined pretreatment

The comparison of ALT_500_2.5 results with R_500_2.5 results shows no significant difference in the properties of the oily liquid due to the combined pretreatment of acid-leaching followed by torrefaction. The water content of the oily liquid from ALT_500_2.5 was 1.9 wt.%, the carbon content was 79.6 wt.% and the O/C ratio was 0.13. Comparing the results of ALT_500_2.5, ALT_500_4 and ALT_500_6 shows that water content remained at 1.6-1.9 w.% and the O/C ratio was 0.12-0.13. In a similar way to torrefaction pretreatment rather than acid-leaching pretreatment, this combined pretreatment had little influence on the properties of the oily liquid.

5.3.4 Chemical composition of the oily liquid

The oily liquids were analysed by GC/MS and ^{1}H NMR spectroscopy to determine the chemical composition, and the results are shown in Table 5-4. The GC/MS analysis can identify GC volatile compounds up to a molecular weight of approximately 350 atomic mass units. In total 98 compounds were identified, they are presented in Table 5A-1 in the Appendix B. Four examples

of chromatograms are illustrated in Figure 5A-2 in the Appendix B. The total area of the identified peaks accounts for 87-91 % of the area of all the peaks with an exception for AL_360_2.5 (79 %). The area percentages of the identified peaks were also presented in 5A-1 in the Appendix B. These identified compounds were classified to seven groups based on their main functionalities. These groups were aromatics, oxygenated aromatics, furans, catechols, guaiacols, ketones and phenols. The aromatics group contained aromatic hydrocarbons without oxygen, whereas the oxygenated aromatics group contained aromatics with oxygen. Any water-soluble products such as acids and carbohydrates and water were removed in GC/MS sample preparation (see Chapter 4).

The ^{1}H NMR analysis classified the hydrogen atoms of the organics in the oily liquid into six groups following the method proposed by Mullen *et al.* [19]: namely “alkanes” (0.5-1.5 ppm); “hydrogen α to heteroatom/unsaturation” (1.5-3.0 ppm); “aliphatic alcohols/methoxy” (3.0-4.4 ppm); “carbohydrates” (4.4-6.0 ppm); “aromatics/heteroaromatics” (6.0-8.5 ppm) and “aldehydes” (9.5-10.1 ppm). ^{1}H NMR analysis is able to give an overview of the chemical composition by quantifying the proportion of hydrogen atoms in each of these groups. This was useful when looking for differences in the chemical functionalities of the bio-oil (Chapter 3). However this analysis was not effective at differentiating the oily liquids from CFP, because most of the compounds are related to the same chemical functionalities such as the “aromatics/ heteroaromatics” and “hydrogen α to heteroatom/unsaturation”. Hence the discussion is mainly focused on the results of the GC/MS analysis. ^{1}H NMR analysis can provide supporting information for the GC/MS results.

Table 5-4: The chemical composition of oily liquids from CFP of pretreated woods as analysed by GC/MS and ^{1}H NMR spectroscopy.

	R_360_2.5 [a]	R_450_2.5 [a]	R_500_2.5 [a]	R_500_4 [a]	R_500_6 [a]	AL_360_2.5	AL_450_2.5	AL_500_6	T_500_2.5	T_500_4	T_500_6	ALT_500_2.5	ALT_500_4	ALT_500_6
GC/MS analysis results (% of total identified peak area) [b, c]														
Aromatics	53.5	73.0	75.8	79.2	79.7	37.6	68.8	73.4	76.7	75.7	78.5	75.8	75.6	76.6
Aromatics, oxygenated	13.6	10.8	9.9	8.9	7.7	14.8	10.7	9.9	8.7	8.3	7.2	8.5	8.2	7.8
Furans	1.2	0.5	0.2	0.2	0.3	4.7	0.5	0.4	0.2	0.3	0.2	0.2	0.3	0.2
Catechols	2.2	0.4	0.1	0.0	0.0	1.8	0.9	0.1	0.2	0.1	0.1	0.2	0.2	0.1
Guaiacols	12.3	0.7	0.2	0.2	0.2	17.0	1.2	0.2	0.6	0.6	0.4	0.6	0.6	0.5
Ketones	6.7	0.8	0.3	0.2	0.3	9.8	2.0	0.7	0.5	0.6	0.4	0.6	0.7	0.6
Phenols	10.6	13.9	13.5	11.2	11.8	14.3	16.0	15.4	13.2	14.5	13.2	14.1	14.5	14.2
^{1}H NMR analysis results (% of all hydrogen) [c]														
Aldehydes, carboxylic acids	0.3	0.1	0.0	0.0	0.0	0.8	0.1	0.1	0.1	0.1	0.1	0.1	0.1	0.0
Carbohydrates	3.5	1.2	1.1	1.0	0.9	5.4	1.6	1.3	1.3	1.3	1.1	1.5	1.5	1.3
Aliphatic alcohols, methoxy	12.7	6.0	5.0	4.7	3.9	13.8	6.7	5.1	6.1	5.5	4.7	6.4	5.7	4.9
Alkanes	9.7	6.1	4.2	3.8	3.7	8.9	6.0	4.4	4.9	4.4	4.0	4.6	4.5	4.1
Hydrogen α to heteroatom, unsaturation	38.9	38.6	35.2	34.5	37.5	38.3	38.4	36.1	35.3	36.2	36.4	34.8	36.2	37.3
Aromatics, heteroaromatics	34.9	48.0	54.5	55.9	54.0	32.8	47.3	53.1	52.3	52.6	53.8	52.7	52.1	52.4

[a] Results from Chapter 4; [b] details of the GC/MS results for oily liquids composition can be found in Table 5A-1 with the examples of chromatographs illustrated in Figure 5A-2 in Appendix B; [c] average values of duplicate.

5.3.4.1. Effect of acid-leaching pretreatment

From the GC/MS analysis results of experiment AL_500_6, it is found that aromatics accounted for 73.4 % of the identified products in the oily liquid. While the corresponding value was increased to 79.7 % in the experiment R_500_6. The oily liquid from AL_500_6 was comprised of more oxygenated organics, such as oxygenated aromatics, benzofurans, furans, catechols, guaiacols, ketones and phenols. The comparison of ^{1}H NMR analysis results of AL_500_6 with R_500_6 shows that AL_500_6 oily liquid contained slightly more hydrogen atoms associated to the groups of "aliphatic alcohols/methoxy" and "carbohydrates", but slightly less hydrogens associated to the group of "aromatics/heteroaromatics". Hence both analysis results indicate that acid-leaching pretreatment led to more oxygenated organics in the oily liquid.

At pyrolysis temperatures lower than 500 °C and C/B ratio of 2.5, the same trends were observed for the comparison of AL_450_2.5 and R_450_2.5 results. These trends were more obvious in the comparison of results of AL_360_2.5 and R_360_2.5. The comparison of GC/MS results of AL_360_2.5 and R_360_2.5 shows that the content of aromatics was decreased by acid-leaching pretreatment from 53.5 % to 37.6 %. Meanwhile, acid-leaching pretreatment increased the contents of furans, guaiacols, ketones and phenols. Correspondingly in ^{1}H NMR analysis results, the proportion of hydrogens related to the groups of "carbohydrates " and "alcohols/methoxy" were increased by acid-leaching pretreatment, from 3.5 % to 5.4 % and from 12.7 % to 13.8 %, respectively. The proportion of hydrogens in the "aromatics" group was decreased from 34.9 % to 32.8 %. These findings are in agreement with the elemental analysis as previously discussed, that acid-leaching pretreatment led to a higher O/C ratio of organics in oily liquid.

5.3.4.2. Effect of torrefaction pretreatment

The comparison of T_500_2.5 and R_500_2.5 results shows that at the C/B ratio of 2.5, the chemical composition of the oily liquid were barely affected by torrefaction pretreatment. With the increase in C/B ratio from 2.5 to 6, the effect of torrefaction pretreatment on the chemical composition of oily liquid was also insignificant based on comparison of results of T_500_2.5, T_500_4 and T_500_6 with the results of raw wood. The contents of aromatics in the above experiments were 76.7-78.5 % from the GC/MS results. In ^{1}H NMR analysis results, the proportion of hydrogens associated to “aromatics/heteroaromatics” group was 52.0-53.8 % when the C/B ratio increased from 2.5 to 6. Therefore, it is concluded that the torrefaction pretreatment has negligible effect of the chemical composition of the oily liquid from catalytic fast pyrolysis. This finding is in agreement with the results previously discussed in section 5.3.3.2.

5.3.4.3. Effect of the combined pretreatment

The comparison of ALT_500_2.5 and R_500_2.5 results shows that the chemical composition of the two oily liquids was similar. The comparison of the results of ALT_500_2.5, ALT_500_4 and ALT_500_6 shows that the chemical composition of oily liquid was not significantly affected by increasing the C/B ratio, except that the proportion of hydrogen atoms associated to “aliphatic alcohols/ methoxy” in ^{1}H NMR analysis was slightly decreased. These trends were the same as observed in the comparison of the results for Twood and Rwood.

5.4. Discussion

5.4.1 The effects of acid-leaching pretreatment in CFP

The results showed that acid-leaching pretreatment did not change the yield of carbon-rich residue (char and coke) at a temperature of 450 ^{o}C and a C/B ratio of 2.5. But this pretreatment decreased the yield of char by 6 wt.% in fast pyrolysis at a temperature of 450 ^{o}C, as demonstrated in Chapter 3. Since thermal pyrolysis occurs prior to catalytic reactions, acid-leaching pretreatment is likely to have decreased the yield of char in CFP. It follows then that the yield of coke in CFP might be increased by acid-leaching pretreatment.

The ash in biomass can catalyse cracking of pyrolysis products to smaller molecules, which then become accessible to the zeolite pores [20]. Because acid-leaching pretreatment removes most of the ash, the effect of this cracking is weakened. Therefore it is hypothesised that more pyrolysis products, which are inaccessible to the zeolite pores, are produced from acid-leached biomass. These molecules may deposit on the zeolite surface resulting in coke. Consequently there is only a small improvement in the yield of the oily liquid, compared to the large improvement in bio-oil yield observed in fast pyrolysis of acid-leached wood.

Acid-leaching pretreatment increased the yield of CO and decreased yield of the CO_2 in CFP, meanwhile it barely affected the yield of produced water. In the three deoxygenation pathways, namely decarboxylation, decarbonylation and dehydration [10], decarbonylation is not as efficient as decarboxylation for deoxygenation. As decarboxylation is decreased, it follows that the degree of deoxygenation in CFP was decreased by acid-leaching pretreatment. Consequently, the O/C ratio of the oily liquid and the content of oxygenated organics in the oil were both increased.

CFP of acid-leached wood produce oily liquid at similar yield as raw wood, but with higher oxygen content. Although this higher oxygen content is a negative consequence of acid-leaching pretreatment, the anticipated extended catalyst lifetime due to the removal of inorganic material from biomass that would accumulate in the catalyst and reduces its activity [9] might be beneficial for the overall process.

5.4.2 The effects of torrefaction pretreatment in CFP

Torrefaction pretreatment increased the yield of oil product in CFP at 500 °C and C/B ratio of 2.5. On the other hand, this pretreatment did not have noticeable effect on the properties and chemical composition of the oil product. Torrefaction pretreatment actually can increase the yield of the aromatics by increasing the overall yield of the oil product. It was reported that torrefaction pretreatment can improve the selectivity of aromatics in catalytic pyrolysis on pyroprobe reactors, such as Py-GC/MS [16, 17, 21]. In these studies, it was claimed that thermal pyrolysis products from torrefied biomass contained more lignin-derived molecules, which could be easily converted to aromatic hydrocarbons in the presence of zeolite catalyst [4, 21].

As demonstrated in Chapter 3, torrefaction pretreatment enhanced carbonisation in fast pyrolysis. Here, it was found that this pretreatment led to a significant increase in the yield of carbon-rich residue. Since the carbonisation occurs in the stage of thermal pyrolysis prior to catalytic reactions, torrefaction pretreatment can also enhance carbonisation in CFP. It may lead to an increase in the yield of char, rather than the yield of coke.

In Chapter 6, pyrolysis-gas chromatography/mass spectrometry (Py-GC/MS) will be employed to investigate the distribution of the products in catalytic pyrolysis of pretreated woods. The chemical mechanism in catalytic pyrolysis of pretreated wood will be further discussed.

5.4.3 Overcoming bed agglomeration

The SEM images of the char residue reveal that the severity of the melting behaviour in CFP of acid-leached wood increased with increasing pyrolysis temperature and it could lead to bed agglomeration. Meanwhile the catalytic effect of zeolite HZSM-5 could not prevent this melting behaviour or bed agglomeration. As suggested in Chapter 3, this melting phenomenon is likely due to rheological behaviour of the biomass components in pyrolysis. Hence the issue of bed agglomeration in catalytic fast pyrolysis could also be prevented by the three methods demonstrated in Chapter 3.

Firstly, operating the reactor at a lower temperature (360 ^{o}C and 450 ^{o}C) is able to avoid bed agglomeration, because the melting severity is decreased, possibly associated with lignin melting. However, deoxygenation in zeolite upgrading is restricted at lower pyrolysis temperatures due to the reduced catalyst activity. Secondly, operating the reactor at a high catalyst feeding rate (C/B ratio of 6) is also able to overcome this issue by removing the melted material out of the reactor quickly. But excessive catalyst loading is required leading to a decrease in the yield of the oil product. Torrefaction following acid-leaching pretreatment is the third approach which prevents this issue, likely by the enhanced carbonisation of the torrefaction pretreatment. This combined pretreatment compensates for the negative effects of acid-leaching pretreatment on the oil quality, while removing the ash from the biomass that can cause catalyst deactivation.

5.5. Conclusion

The strong influence of acid-leaching pretreatment in fast pyrolysis disappears in catalytic fast pyrolysis, as the zeolite upgrading dominates the outcomes in catalytic fast pyrolysis of acid-leached wood. The yield of oil product from acid-leached wood at a temperature of 500 ^{o}C is equal to that from raw wood. This pretreatment changes the yields of CO and CO_2, thus the deoxygenation in zeolite upgrading is mildly impeded. As a result, the oil product contains a relatively high oxygen content and a low content of aromatic hydrocarbons compared to oil from raw wood. However, the deleterious ash in the biomass is removed potentially extending zeolite catalyst lifetime.

Torrefaction pretreatment can lead to an increase in the yield of oil product in catalytic fast pyrolysis, while the properties and chemical composition of the oil product are little changed. Meanwhile this pretreatment decreases the yield of produced water, and possibly increases the yield of char.

The acid-leaching pretreatment can cause bed agglomeration in catalytic fast pyrolysis on a fluidised bed reactor. The same phenomenon that occurs in fast pyrolysis, is likely caused by the melting behaviour of the biomass components at elevated temperatures. This issue can be overcome by the three approaches proposed in this study, namely lowering the temperature, increasing the feeding rate of catalyst and applying torrefaction after acid-leaching pretreatment.

References

[1] Oudenhoven, S.R.G., R.J.M. Westerhof, N. Aldenkamp, D.W.F. Brilman, and S.R.A. Kersten, *Demineralization of wood using wood-derived acid: Towards a selective pyrolysis process for fuel and chemicals production.* Journal of Analytical and Applied Pyrolysis, 2013. **103**: p. 112-118.

[2] Oudenhoven, S.R.G., R.J.M. Westerhof, and S.R.A. Kersten, *Fast pyrolysis of organic acid leached wood, straw, hay and bagasse: Improved oil and sugar yields.* Journal of Analytical and Applied Pyrolysis, 2015. **116**: p. 253-262.

[3] Wigley, T., A.C.K. Yip, and S. Pang, *The use of demineralisation and torrefaction to improve the properties of biomass intended as a feedstock for fast pyrolysis.* Journal of Analytical and Applied Pyrolysis, 2015. **113**: p. 296-306.

[4] Meng, J., J. Park, D. Tilotta, and S. Park, *The effect of torrefaction on the chemistry of fast-pyrolysis bio-oil.* Bioresource Technology, 2012. **111**: p. 439-446.

[5] Wigley, T., A.C.K. Yip, and S. Pang, *Pretreating biomass via demineralisation and torrefaction to improve the quality of crude pyrolysis oil.* Energy, 2016. **109**: p. 481-494.

[6] Wigley, T., A.C. Yip, and S. Pang, *A detailed product analysis of bio-oil from fast pyrolysis of demineralised and torrefied biomass.* Journal of Analytical and Applied Pyrolysis, 2017. **123**: p. 194-203.

[7] Cerqueira, H., G. Caeiro, L. Costa, and F.R. Ribeiro, *Deactivation of FCC catalysts.* Journal of Molecular Catalysis A: Chemical, 2008. **292**(1): p. 1-13.

[8] Paasikallio, V., C. Lindfors, E. Kuoppala, Y. Solantausta, A. Oasmaa, J. Lehto, and J. Lehtonen, *Product quality and catalyst deactivation in a four day catalytic fast pyrolysis production run.* Green Chemistry, 2014. **16**(7): p. 3549-3559.

[9] Mullen, C.A. and A.A. Boateng, *Accumulation of Inorganic Impurities on HZSM-5 Zeolites during Catalytic Fast Pyrolysis of Switchgrass.* Industrial & Engineering Chemistry Research, 2013. **52**(48): p. 17156-17161.

[10] Hernando, H., S. Jiménez-Sánchez, J. Fermoso, P. Pizarro, J. Coronado, and D. Serrano, *Assessing biomass catalytic pyrolysis in terms of deoxygenation pathways and energy yields for the efficient production of advanced biofuels.* Catalysis Science & Technology, 2016. **6**(8): p. 2829-2843.

[11] Oudenhoven, S.R.G., C. Lievens, R.J.M. Westerhof, and S.R.A. Kersten, *Effect of temperature on the fast pyrolysis of organic-acid leached pinewood; the potential of low temperature pyrolysis.* Biomass and Bioenergy, 2016. **89**: p. 78-90.

[12] Adhikari, S., V. Srinivasan, and O. Fasina, *Catalytic pyrolysis of raw and thermally treated lignin using different acidic zeolites.* Energy & Fuels, 2014. **28**(7): p. 4532-4538.

[13] Srinivasan, V., S. Adhikari, S.A. Chattanathan, and S. Park, *Catalytic Pyrolysis of Torrefied Biomass for Hydrocarbons Production.* Energy & Fuels, 2012. **26**(12): p. 7347-7353.

[14] Zheng, A., Z. Zhao, Z. Huang, K. Zhao, G. Wei, X. Wang, F. He, and H. Li, *Catalytic Fast Pyrolysis of Biomass Pretreated by Torrefaction with Varying Severity.* Energy & Fuels, 2014. **28**(9): p. 5804-5811.

[15] Srinivasan, V., S. Adhikari, S.A. Chattanathan, M. Tu, and S. Park, *Catalytic pyrolysis of raw and thermally treated cellulose using different acidic zeolites.* BioEnergy Research, 2014. **7**(3): p. 867-875.

[16] Mahadevan, R., S. Adhikari, R. Shakya, K. Wang, D.C. Dayton, M. Li, Y. Pu, and A.J. Ragauskas, *Effect of torrefaction temperature on lignin macromolecule and product*

distribution from HZSM-5 catalytic pyrolysis. Journal of Analytical and Applied Pyrolysis, 2016. **122**: p. 95-105.
[17] Wang, K., K.H. Kim, and R.C. Brown, *Catalytic pyrolysis of individual components of lignocellulosic biomass.* Green Chemistry, 2014. **16**(2): p. 727-735.
[18] Liu, C., H. Wang, A.M. Karim, J. Sun, and Y. Wang, *Catalytic fast pyrolysis of lignocellulosic biomass.* Chemical Society Reviews, 2014. **43**(22): p. 7594-7623.
[19] Mullen, C.A., G.D. Strahan, and A.A. Boateng, *Characterization of various fast-pyrolysis bio-oils by NMR spectroscopy†.* Energy & Fuels, 2009. **23**(5): p. 2707-2718.
[20] Yildiz, G., F. Ronsse, R. Venderbosch, R. van Duren, S.R. Kersten, and W. Prins, *Effect of biomass ash in catalytic fast pyrolysis of pine wood.* Applied Catalysis B: Environmental, 2015. **168**: p. 203-211.
[21] Neupane, S., S. Adhikari, Z. Wang, A.J. Ragauskas, and Y. Pu, *Effect of torrefaction on biomass structure and hydrocarbon production from fast pyrolysis.* Green Chemistry, 2015. **17**(4): p. 2406-2417.

Chapter 6

A Py-GC/MS study: The impacts of biomass pretreatments, temperature and catalyst to biomass ratio in catalytic pyrolysis

Abstract

Catalytic pyrolysis of raw wood, acid-leached wood, torrefied wood and acid-leached-torrefied wood was conducted using pyrolysis-gas chromatography/mass spectrometry (Py-GC/MS). The aim was to investigate the impacts of biomass pretreatments, temperature, and catalyst to biomass ratio on the distribution of the products in catalytic pyrolysis.

The experimental conditions were varied including four reaction temperatures from 360 to 550 °C and four catalyst to biomass ratios from 0:1 to 6:1. Sixty four experiments were conducted in total. The results were evaluated by two methods. Firstly, forty five identified products were grouped according to their chemical functionalities and the area percentages of the groups were compared. Secondly, principal components analysis (PCA) was employed to identify variances in the distribution of the products.

The effects of biomass pretreatments in non-catalytic pyrolysis and catalytic pyrolysis were further explored following the studies in previous chapters. In general, the findings agreed with those using a fluidised bed reactor. The acid-leaching pretreatment enhances the production of

sugars in thermal pyrolysis, while torrefaction pretreatment enhances the formation of catechols. These effects of biomass pretreatments can change the distribution of the products in catalytic pyrolysis.

The impacts of temperature in non-catalytic pyrolysis and catalytic pyrolysis were investigated at four temperatures from 360 °C to 550°C. Then the impacts of catalyst to biomass (C/B) ratio were studied at 550° and 360 °C. It was concluded that increasing the reaction severity (i.e. the temperature or the C/B ratio) promotes the conversion of thermal pyrolysis products to aromatic hydrocarbons. It was found that even at a temperature as low as 360 °C, this conversion is able to be enhanced by increasing the C/B ratio.

Principal component analysis (PCA) of the Py-GC/MS results confirmed the findings obtained by the first method. PCA visually showed that temperature and C/B ratio are two important factors in catalytic pyrolysis. Acid-leaching and torrefaction pretreatments have considerably less influence on the distribution of the products in catalytic pyrolysis than temperature or C/B ratio.

6.1. Introduction

In previous chapters, the effects of biomass pretreatments, acid-leaching and torrefaction, on the outcomes of fast pyrolysis and catalytic fast pyrolysis had been investigated using fluidised bed reactors. A limited set of experimental conditions could be tested on a fluidised bed reactor, as this reactor was designed with limits on operation conditions, and takes several days to run one experiment and analyse its results. For instance, the Scion fluidised bed reactor was not able to operate at temperatures of 500 °C or above at high feeding rates of silica sand (i.e. ≥5 kg/h). Pyrolysis-gas chromatography/mass spectrometry (Py-GC/MS) was employed as a supplementary tool to understand the effects of biomass pretreatment in catalytic pyrolysis. Instead of using it as a pre-screening tool before pyrolysis experiments on a fluidised bed, this study conducted Py-GC/MS experiments under largely varied conditions and compared the results with the ones obtained on the Scion reactor.

Py-GC/MS can be used as a rapid technique to investigate the distribution of the products in biomass pyrolysis with or without catalyst. A precise quantitative analysis by Py-GC/MS requires the amount of the identified product to be calibrated using a chemical standard. Due to the number of products produced and the fact that the products are usually not available as calibration standards, this type of quantification is not practical. However, information can be obtained on the relative change in the yield of a particular product by the change in its peak area percentage under different reaction conditions [1]. Therefore these trends under varied conditions were investigated in this study.

Py-GC/MS technique can investigate the impacts of variable conditions, including feedstock, temperature and C/B ratio, in biomass pyrolysis [1-3]. Mihalcik *et al.* [2] employed Py-GC/MS as a tool to screen zeolite catalysts and biomass feedstocks for catalytic pyrolysis. Promising

catalysts and biomass feedstocks were found which could potentially produce desirable chemicals. Lu *et al.* [1] applied Py-GC/MS to investigate the influence of temperature and pyrolysis time on the distribution of the products in cellulose pyrolysis. Thangalazhy-Gopakumar *et al.* [3] carried out a Py-GC/MS study on catalytic pyrolysis of algal biomass at different catalyst to biomass (C/B) ratios.

Interpretation of Py-GC/MS results can be difficult because hundreds of produced compounds can be detected. Two methods can be used to interpret Py-GC/MS data. In the first method, the identified compounds can be classified into a few groups based on their chemical functionalities [4]. The area percentage changes in the groups can be evaluated to understand the influence of the varied conditions. In the second method, principal component analysis (PCA) can be used to evaluate the Py-GC/MS results [5-7]. PCA, as a multivariate technique, is able to extract hidden details from complex data sets. Pattiya *et al.* [6] conducted Py-GC/MS experiments with a variety of catalysts, and used PCA models to evaluate the distributions of the products. They investigated the performance of fifteen catalysts, and used PCA to visualise the promising candidates.

In order to understand the chemical mechanism in catalytic pyrolysis, the reaction pathways for transforming lignocellulosic biomass to aromatic hydrocarbons are illustrated in a simplified way in Figure 6-1. It is notable to mention that the figure only shows the pathways to produce aromatic hydrocarbons as the main products and the actual reactions in catalytic pyrolysis are more complex than this illustration. The by-products including non-condensable gases, water, char and coke are not illustrated for the purpose of simplifying the illustration.

In catalytic pyrolysis of lignocellulosic biomass, thermal pyrolysis occurs first releasing pyrolytic products from cellulose, hemicellulose and lignin [8]. Cellulose and hemicellulose are pyrolysed

to various sugars and sugar derivatives, furans, light oxygenates and other compounds [9-12], meanwhile lignin is pyrolysed to phenolic compounds including guaiacols, catechols and phenols [13, 14].

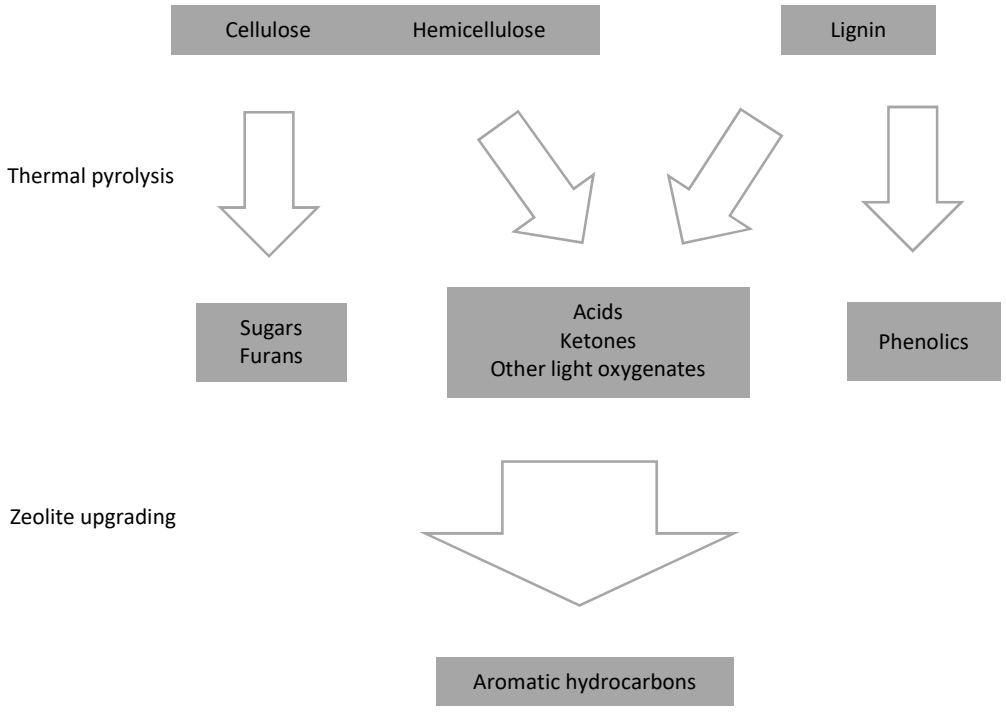

Figure 6-1: The pathways for transforming lignocellulosic biomass to aromatic hydrocarbons in catalytic pyrolysis on HZSM-5.

In zeolite upgrading, the products from thermal pyrolysis undergo a series of reactions on the acid sites of the zeolite forming aromatic hydrocarbons [13]. The sugars can form furans via deoxygenation and hydrogen transfer [15]. The furans can be further transformed to aromatic hydrocarbons [16]. Guaiacols, such as guaiacol and 2-methoxy-4-methylphenol, can enter the pores of HZSM-5 and be transformed to aromatics [17]. The light oxygenates including acids and ketones are converted to aromatics within the zeolite, the reactions involve oligomerization, aromatization, hydrogen transfer, deoxygenation [8, 13].

6.2. Experimental

6.2.1 Materials and preparation

The four types of feedstocks used previously in this study on the fluidised bed reactors were tested using the Py-GC/MS technique, i.e. raw wood (Rwood), acid-leached wood (ALwood), torrefied wood (Twood) and acid-leached-torrefied wood (ALTwood). The feedstock samples were first sieved to pass a 50 mesh screen to obtain fine particles and then oven-dried before mixing with catalyst or sand.

The commercial zeolite catalyst, HZSM-5 (Si/Al=30:1), as used previously in this study, was also applied here. It was ground and sieved through a 50 mesh screen to obtain a fine powder, which was calcinated at 525 °C for three hours in a furnace. Silica sand was ground and sieved through a 50 mesh screen to obtain a fine powder.

For tests of thermal pyrolysis, the ground sand was mixed with the four feedstocks at a weight ratio of 2.5:1. The test runs were labelled as R00, AL00, T00 and ALT00, respectively, for feedstocks of raw wood, acid-leached wood, torrefied wood and pretreated wood with acid-leaching followed by torrefaction. In these runs, '00' means no catalyst was added.

For the tests of catalytic pyrolysis, ground catalyst were mixed with the four feedstocks at catalyst to biomass (C/B) ratios of 2.5:1, 4:1 and 6:1, respectively. These ratios were the same as the C/B ratios used in Chapter 5. There were twelve runs for three C/B ratios and four types of feedstocks which were labelled as R25, AL25, T25, ALT25, R40, AL40, T40, ALT40, R60, AL60, T60 and ALT60. All of the four sand-wood samples and the twelve catalyst-wood samples were kept in a desiccator before the Py-GC/MS experiments.

6.2.2 Py-GC/MS experiment

The sixteen samples were tested at four different temperatures: 360 °C, 450 °C, 500 °C and 550 °C. Therefore, there were sixty-four experimental runs in total. These runs were labelled as [sample]_[temperature]. For example, R00_360 represents the experiment pyrolysing Rwood without catalyst (with sand) at 360 °C, and ALT25_550 represents the experiment pyrolysing ALTwood with a C/B ratio of 2.5 at 550 °C. Every experiment was repeated three times to obtain average values and standard deviations.

The Py-GC/MS instrument was composed of a Lab Frontier pyrolysis furnace with an auto-shot sampler (Pyrolysis), an Agilent 7890A gas chromatograph (GC) and a Waters GCT Premier TOF mass spectrometer (MS). Gas chromatography was performed on a 30 m Zebron WaxPlus column (Phenomenex) with 0.25 mm inner diameter and 0.25 µm film thickness. This Py-GC/MS instrument can analyse GC volatile compounds up to 550 atomic mass units (amu), however, it cannot detect heavier molecules such as lignin oligomers.

In each run, the test sample contained 0.6 ± 0.05 mg biomass, and the residence time in pyrolysis furnace was controlled at 6 seconds before the gas/vapour products were split at an injection split ratio 30:1 into the GC/MS. The injection temperature was set at 280 °C, the interface temperature was 280 °C and the ion source temperature was 250 °C. The carrier gas was helium at a constant flow rate of 1 ml/min. The oven temperature program was set as 2 minutes isothermal heating at 60 °C, followed by a 4 °C /min rate to 260 °C then a hold at this temperature for 26 minutes. The mass spectra were recorded at 0.2 scan per sec with an m/z 40-550 amu scanning range.

Chromatographic peaks with areas accounting for 5 % or more of the largest peak area in the chromatogram, were included for identification. The peaks were identified using the MS library NIST 2011. In this way, forty five peaks were identified peaks with a high degree of certainty (over 80%) and were included and quantified based on their peak area percentages. The area values of the identified peaks under the total ion chromatogram (TIC) mode were obtained. The area percentage relative to the total identified peak area were calculated and used for analysis. The total identified peak area represented 43-62 % of the total peak area (which included approximately 500 peaks in one chromatogram) for the sixty four Py-GC/MS experiments. Those excluded peaks were mostly very minor peaks, and therefore, they were not considered in order to make the analysis practical.

6.2.3 Principal component analysis

The SIMCA 15 software (Sartorius Stedim Data Analytics AB, Sweden) was employed for principal component analysis of the Py-GC/MS data, namely the peak area percentages of the identified products. This software used an orthogonal transformation to convert a set of observations of possibly correlated variables into a set of values of linearly uncorrelated variables called principal components. Three PCA models were created by this software, and each model had a score plot and a loading plot to visualise the correlations between the various experimental conditions and the distribution of products.

In the PCA models, the Py-GC/MS experiments were set as the samples, the area percentages of all the products were set as the variables. Each model generated a score plot and a loading plot, which were PCA maps of samples and variables, respectively. The score plot shows the dispersion of the samples, and the loading plot shows the contribution of the variables to the principal components. The first two principal components of the variance, PC1 and PC2, were

considered in this study. PC1 has the largest possible variance, and PC2 has the second highest variance. PC1 and PC2 are the horizontal and the vertical axes, respectively, in the score and loading plots.

6.3. Results and Discussion

6.3.1 The identified products in Py-GC/MS analysis

Table 6-1 lists the forty five identified products in the order of their retention times (RT) in the chromatograms. The retention times of some compounds were slightly shifted between the different tests but the sequence was the same. Therefore the RT sequence was presented in Table 6-1 instead of the actual RT. Two chromatogram examples, one for non-catalytic pyrolysis and the other for catalytic pyrolysis, are illustrated in Figure 6-2 in which the identified products (peaks) are labelled with their RT sequence. The chromatographic profiles can be substantially different due to the different conditions used among the experiments.

The important products, such as toluene, naphthalene and methyl-phenol (Appendix A), in the oil from catalytic fast pyrolysis appeared in Table 6-1. Additionally, the molecular weights of the oil products from catalytic fast pyrolysis were relatively low as GPC results shown in Figure 4-10, Figure 4-11 and Figure 5A-1. Therefore, most of the catalytic pyrolysis products can be identified by this Py-GC/MS instrument. On the other hand, a minor proportion of the bio-oil products from fast pyrolysis was beyond the detection range of the Py-GC/MS as shown in the GPC results in Figure 2-7 and Figure 2-8. For example, polymers from cellulose and lignin can be not detected in the Py-GC/MS analysis. Hence the Py-GC/MS results from experiments with catalyst were more reliable than those without catalyst.

Table 6-1: The identified Py-GC/MS products and their groups.

RT sequence	Compound	Group
1	Furan	Furans
2	Furan,2-methyl	Furans
3	Benzene	Aromatics
4	Toluene	Aromatics
5	Xylene-p/o/m	Aromatics
6	Benzene, 1-ethyl-(4/3/2)-methyl-	Aromatics
7	Styrene	Aromatics
8	Benzene, 1,2,4-trimethyl-	Aromatics
9	2-Propanone, 1-hydroxy-	Ketones
10	Cyclopentenone	Ketones
11	Indane	Aromatics
12	Acetic acid	Acid
13	Furfural	Furans
14	Indene	Aromatics
15	Benzofuran	Aromatics, oxygenated
16	Benzofuran, 2-methyl-	Aromatics, oxygenated
17	1H-Indene,(1/3)-methyl-	Aromatics
18	1H-Indene, 1,3-dimethyl-	Aromatics
19	Naphthalene	Aromatics
20	2(5H)-Furanone	Furans
21	1,2-Cyclopentanedione	Ketones
22	2-Cyclopenten-1-one, 2-hydroxy-3-methyl-	Ketones
23	Naphthalene, 2-methyl-	Aromatics
24	Guaiacol	Guaiacols
25	Naphthalene,2,7-dimethyl-	Aromatics
26	Creosol	Phenols
27	Phenol, p/m/o-methyl-	Phenols
28	4-ethyl-guaiacol	Guaiacols
29	Eugenol	Guaiacols
30	2-Methoxy-4-vinylphenol	Guaiacols
31	trans-Isoeugenol	Guaiacols
32	6-Methoxy-3-methylbenzofuran	Aromatics, oxygenated
33	5-Hydroxymethylfurfural	Furans
34	Vanillin	Guaiacols
35	4-Propylguaiacol	Guaiacols
36	Apocynin	Guaiacols
37	Guaiacylacetone	Guaiacols
38	1,2-Benzenediol, 3-methyl-	Catechols
39	Catechol	Catechols
40	1,2-Benzenediol, 4-methyl-	Catechols
41	Anthracene, 2-methyl-	Aromatics
42	Phenol, 4-(ethoxymethyl)-2-methoxy-	Guaiacols
43	Coniferyl aldehyde	Guaiacols
44	Mannose	Sugars
45	Levoglucosan	Sugars

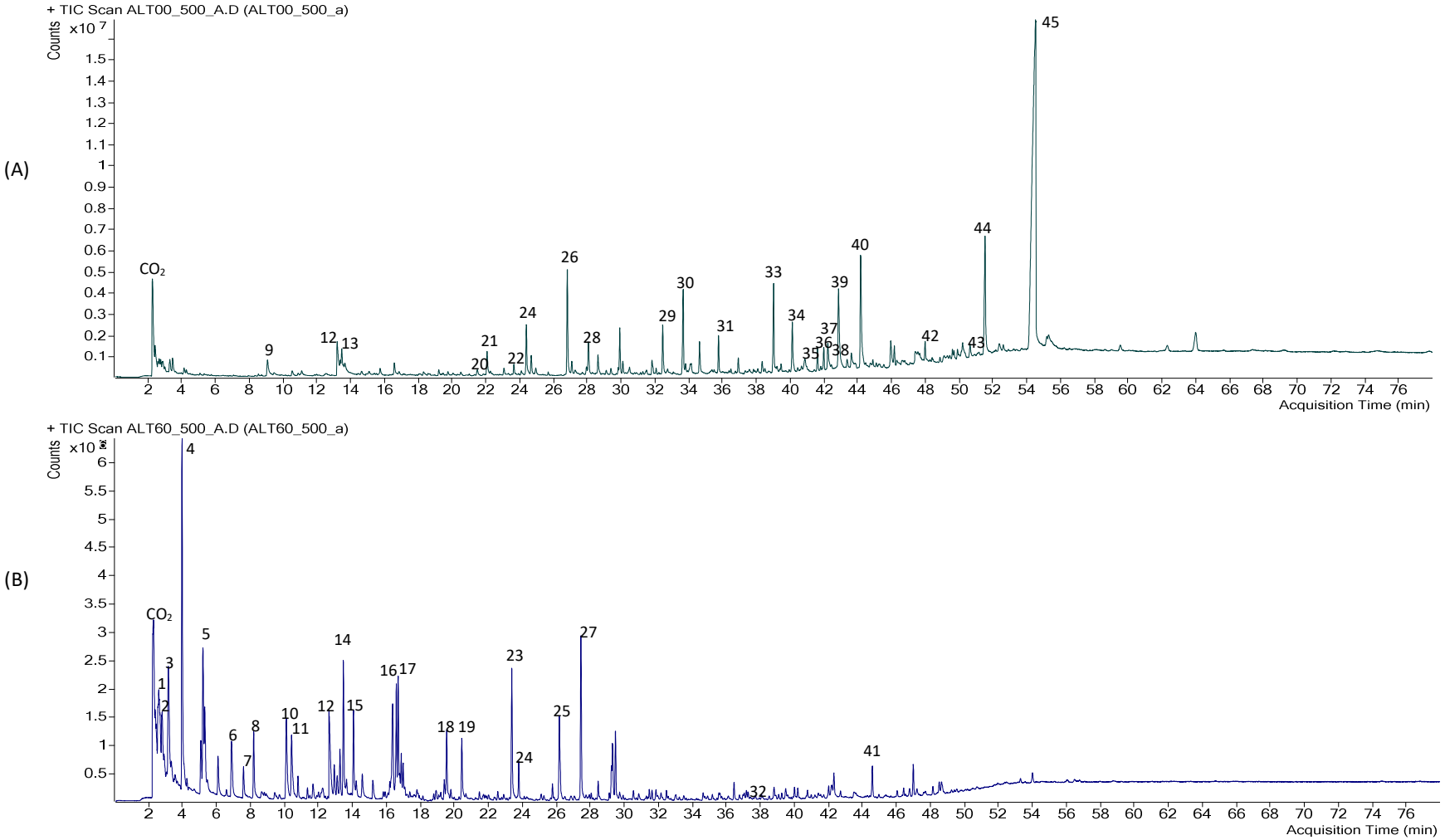

Figure 6-2: The chromatograms obtained by Py-GC/MS and chemical identification, ALT00_500 (A) and ALT60_500 (B).

The identified compounds in Table 6-1 were classified into nine groups based on their main functionalities and the biomass components from which they were derived [4, 13]. Furans, acetic acid (only acid identified), ketones and sugars (including sugar derivatives such as levogluconsan) are thermal pyrolysis products from cellulose and hemicellulose, while guaiacols, catechols and phenols are thermal pyrolysis products from lignin [13]. Catechols were separated from phenols as the effects of pyrolysis conditions on these two groups were found to be different among the experimental runs. Furans can also be products of catalytic pyrolysis, for example levoglucosan can undergo dehydration reaction to form hydroxymethylfurfural in catalytic pyrolysis [8].

The catalytic pyrolysis products were classified into aromatics and oxygenated aromatics. Aromatics include single ring aromatics and polycyclic aromatic hydrocarbons (PAHs). Oxygenated aromatics identified by this Py-GC/MS analysis include only benzofurans. The area percentage values of the products classified in the same groups were summed up to give values for comparisons in the following sections.

6.3.2 Impacts of acid-leaching and torrefaction pretreatments

6.3.2.1. Non-catalytic pyrolysis

The chart in Figure 6-3 shows the distribution of the products in non-catalytic pyrolysis at 450 ^{o}C using Rwood, ALwood, Twood and ALTwood as feedstocks. It is the same temperature as conducted in the fast pyrolysis experiments in Chapter 2. The relevant charts for non-catalytic pyrolysis at other temperatures (360 ^{o}C, 500 ^{o}C and 550 ^{o}C) are presented in Figure 6A-1 in the Appendix C. Similar trends can be found in those charts.

From Figure 6-3, it is found that the acid-leaching pretreatment significantly increased the percentage of sugars. This is the same trend as that in fast pyrolysis of pretreated woods as described in Chapter 2, as the content of sugars fraction in the solvent fractionation analysis was increased by this pretreatment. Figure 6-3 also shows that the percentage of ketones was significantly decreased by the acid-leaching, while it was only slightly reduced by torrefaction pretreatment. Therefore, this change was likely due to the absence of the ash in the biomass which was removed by the acid-leaching pretreatment. The ash (containing alkali and alkaline earth metals) can promote the conversion of sugars to light oxygenates via reactions like fragmentation, ring-opening and cracking [18]. Hence, ash removal by this acid-leaching reduced this catalytic effect for conversion of sugars to ketones in pyrolysis.

The acid-leaching pretreatment decreased the percentage of catechols, and the torrefaction pretreatment increased it. The percentage of phenols was slightly increased by this torrefaction. The percentage of guaiacols was marginally decreased by the three pretreatments. This reveals that torrefaction pretreatment actually promoted the formation of catechols rather than phenols or guaiacols. It has previously been reported that the torrefaction pretreatment can promote the formation of lignin-derived compounds [19, 20]. These studies included phenols, catechols and guaiacols all in one group.

The percentage of acetic acid was slightly decreased by both the acid-leaching and torrefaction pretreatments. Wigley *et al.* [21] also found that applying acid-leaching or torrefaction on pine wood before fast pyrolysis decreased the concentration of acetic acid in the bio-oil. Acetic acid contributes to the corrosivity of bio-oil, therefore decreasing its production is beneficial.

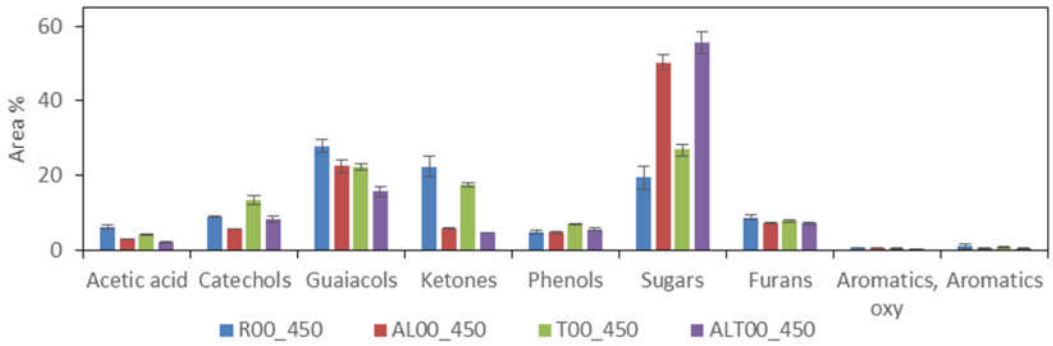

Figure 6-3: The impacts of biomass pretreatments in non-catalytic pyrolysis at 450 °C.

6.3.2.2. Catalytic pyrolysis

The chart in Figure 6-4 shows the distribution of the products in catalytic pyrolysis of Rwood, ALwood, Twood and ALTwood. The temperature was kept at 500 °C and the C/B ratio was 6. These conditions were the same as those in catalytic fast pyrolysis of pretreated woods as described in Chapter 5. The relevant charts for catalytic pyrolysis at 360 °C, 450 °C and 550 °C are presented in Figure 6A-2 in the Appendix C. Similar trends on the changes of the products distribution can be found in those charts.

The percentages of thermal pyrolysis products, acid, catechols, guaiacols, ketones, phenols and sugars, were all very low. Acid-leaching pretreatment decreased the percentage of aromatics, while it increased the percentages of furans and oxygenated aromatics although the experimental error was relatively high in the case of the furans. Torrefaction pretreatment only slightly increased the percentages of furans and slightly decreased the percentage of aromatics, while having not noticeable effect on other products. These findings are in agreement with the findings in Chapter 5, namely acid-leaching pretreatment led to a lower proportion of aromatics

in the oil product and torrefaction pretreatment only had insignificant effects on the chemical composition of liquid products.

It has been reported that torrefaction pretreatment promotes the formation of lignin derivatives, which can increase the selectivity of aromatic hydrocarbons in catalytic pyrolysis [20, 22]. The charts in Figure 6A-2 also show that the percentage of aromatics was slightly increased at 550 °C and possibly at 450 °C. But the results in this study indicate that this effect is not significant at 500 °C.

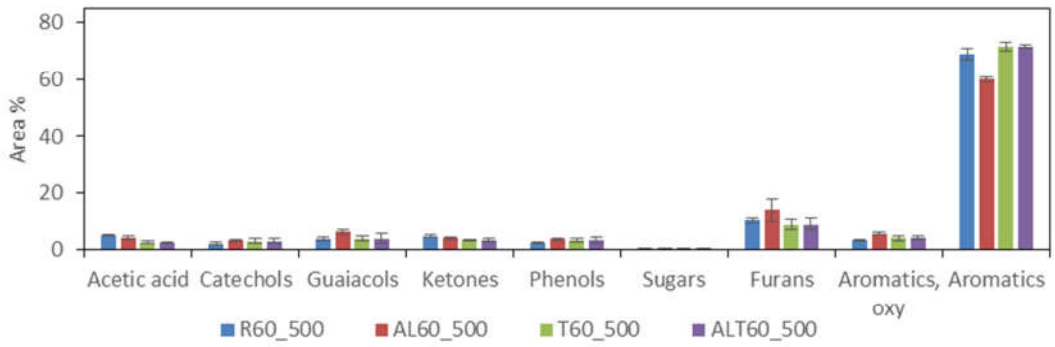

Figure 6-4: The impacts of biomass pretreatments in catalytic pyrolysis at 500 °C with a C/B ratio of 6.

6.3.3 Impacts of temperature

6.3.3.1. Non-catalytic pyrolysis

The impacts of temperature in non-catalytic pyrolysis were investigated without addition of catalyst in the test samples at pyrolysis temperatures from 360 °C to 550 °C. The distributions of the products are presented in Figure 6-5. The four charts in the figure illustrate the results for Rwood (chart A), ALwood (chart B), Twood (chart C) and ALTwood (chart D), respectively. It is noteworthy that the increase of the temperature can lead to producing more pyrolysis

products, which decreases the relative percentages of some products which are less produced with the increased temperature.

The percentage of catechols was clearly increased with increasing temperature from 360 ^{o}C to 550 ^{o}C for all of the four feedstocks. Conversely the percentage of guaiacols was decreased with increasing temperature. Amutio *et al.* [23] also found that the proportion of catechols increased when temperature was raised from 400 ^{o}C to 600 ^{o}C, while the proportion of guaiacols decreased. Possibly the guaiacols underwent breakdown at an elevated temperature, and this contributed to the increase of the catechols.

The percentage of sugars increased with increasing temperature for Rwood, and this percentage decreased for ALwood and ALTwood. This is consistent with the ^{1}H NMR analysis in Chapter 3 which showed that the content of hydrogen atoms related to carbohydrates in the bio-oil was decreased with increasing temperature when using ALwood and ALTwood.

The percentage of aromatics was less than 1 % at 360 ^{o}C for all four feedstocks. This percentage increased to 2-4 % across the four feedstocks when the temperature was increased to 550 ^{o}C, suggesting that an elevated temperature can promote the formation of aromatics in non-catalytic pyrolysis.

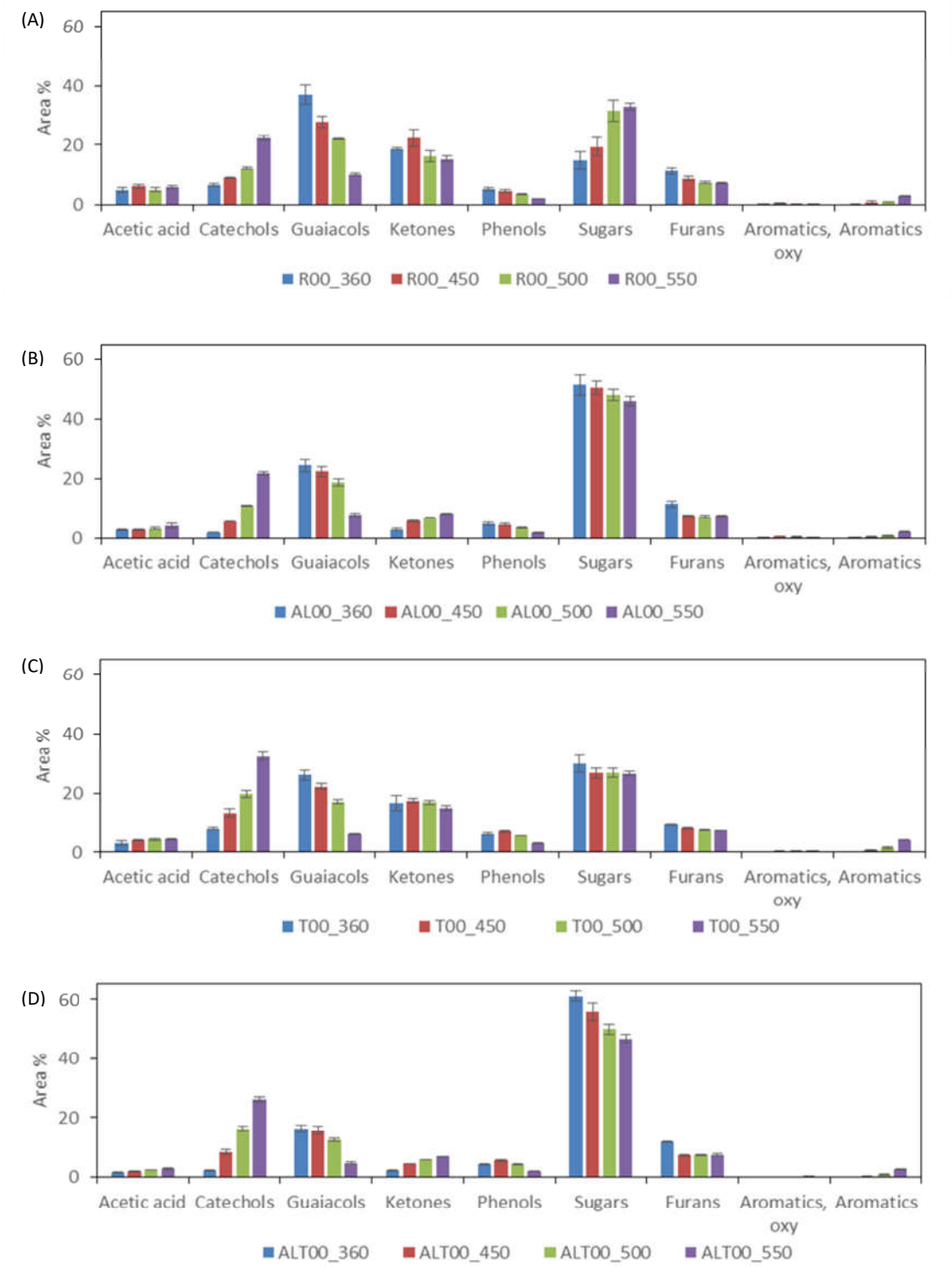

Figure 6-5: The impacts of temperature on the products distribution in non-catalytic pyrolysis, (A): Rwood, (B): ALwood, (C): Twood, (D): ALTwood.

6.3.3.2. Catalytic pyrolysis

The impacts of temperature in catalytic pyrolysis were investigated by increasing the temperature from 360 ^{o}C to 550 ^{o}C, the C/B ratio was kept at 6. The distributions of the products are presented in Figure 6-6. The four charts in the figure illustrate the results for Rwood (chart A), ALwood (chart B), Twood (chart C) and ALTwood (chart D), respectively.

The distributions of products in catalytic pyrolysis of all feedstocks show the following trends. The thermal pyrolysis products, including acetic acid, catechols, guaiacols and ketones, were decreased from a significant proportion (ranging from 8-20 %) to less than 4 % as the temperature increased from 360 ^{o}C to 550 ^{o}C. Correspondingly, the percentage of aromatics was significantly increased from 10-20 % to over 70 %.

In contrast to non-catalytic pyrolysis, the percentage of sugars in catalytic pyrolysis was as low as 1-5 % at 360 ^{o}C for all of the four feedstocks, and it was further decreased to less than 1 % when the temperature was 450 ^{o}C or higher. This reveals that the sugars detected by the GC/MS analysis were highly reactive to HZSM-5, even at a low temperature of 360 ^{o}C. It has been reported that levoglucosan has a high reactivity on HZSM-5 at 550 ^{o}C [2]. But to the author's knowledge, the high reactivity at a low temperature (360 ^{o}C) is not reported.

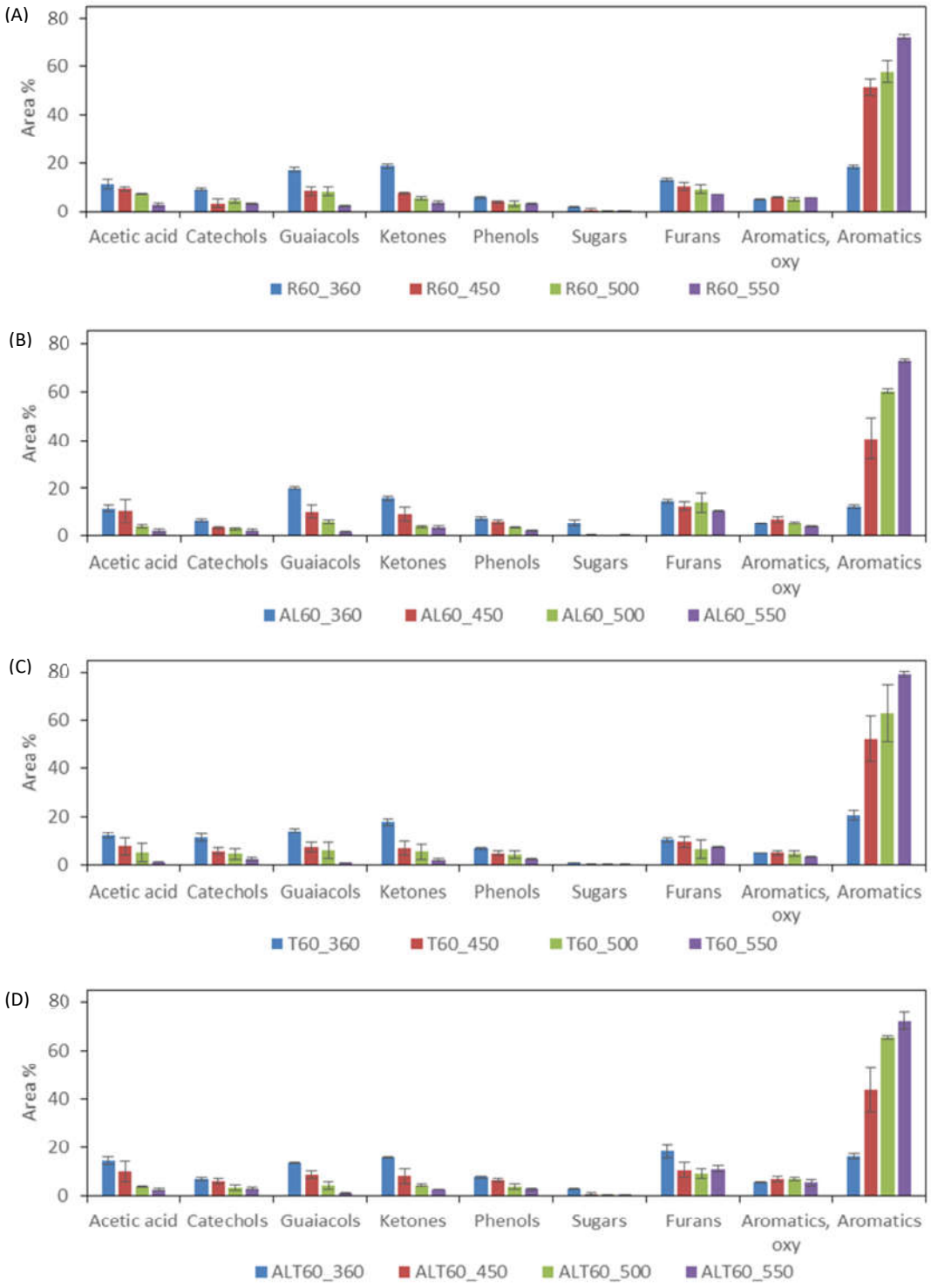

Figure 6-6: The impacts of temperature on the products distribution in catalytic pyrolysis at a C/B ratio of 6, (A): Rwood, (B): ALwood, (C): Twood, (D): ALTwood.

The percentages of furans and oxygenated aromatics in catalytic pyrolysis were always higher than those in thermal pyrolysis for all four feedstocks. Furans and oxygenated aromatics are intermediate products in catalytic pyrolysis, which can be further transformed to other low oxygen content products [16, 24]. The sugars are converted to furans in catalytic pyrolysis, these furans then undergo a series of reactions [8]. The products transformed from furan include olefins, benzofurans and aromatics [16]. The oxygenated aromatics identified by this GC/MS analysis were only benzofurans. Benzofurans can be catalytically converted from furans [16], and can further undergo deoxygenations to form aromatics [24].

6.3.4 Impacts of catalyst to biomass ratio

6.3.4.1. At a temperature of 550 ^{o}C

From above section, it is found that the distribution of products is strongly affected by the temperature, therefore, the impacts of C/B ratio at the two extreme temperature conditions (550 ^{o}C and 360 ^{o}C) are discussed in this section. Figure 6-7 shows the results of Py-GC/MS at 550 °C with Rwood (chart A), ALwood (chart B), Twood (chart C) and ALTwood (chart D). The C/B ratio was increased from 0:1 to 6:1.

Figure 6-7 shows that distributions of the products for the four feedstocks have similar trends. The percentages of catechols, guaiacols, ketones and sugars were significantly decreased with increasing C/B ratio from 0 to 2.5, and these percentages were further decreased, to a less extent, when increasing the C/B ratio from 2.5 to 6. Correspondingly, the percentage of aromatics substantially increased when increasing the C/B ratio from 0 to 2.5, and then further increased with increasing C/B ratio to 6. Thus the presence of zeolite catalyst (with C/B ratio of 2.5) strongly promoted the conversion of thermal pyrolysis products to aromatics, and this

extent of conversion increased with increasing C/B ratio. These results agreed with those of a study of Thangalazhy-Gopakumar *et al.* [3] who reported that the carbon yield of aromatics was increased with the increased C/B ratio ranging from 0:1 to 9:1. The zeolite activity is highly dependent on the availability of acid sites [25]. Increasing the C/B ratio can provide more acid sites for converting thermal pyrolysis products.

The percentage of furans was increased when increasing the C/B ratio from 0 to 2.5, then it decreased when increasing the C/B ratio from 4 to 6. Sugars are converted to furans on HZSM-5 zeolite, then furans are transformed to aromatics [15]. Furans as intermediate products in catalytic pyrolysis can be further deoxygenated when the catalyst loading is sufficient.

The percentage of phenols remained at a value between 2 % to 4 % when increasing C/B ratio from 0 to 6. This indicates that phenols were not affected by zeolite upgrading. Other researchers also found that phenols are resistant to HZSM-5 [17, 26]. It was speculated that the C-O bond between the aromatic ring and the hydroxyl group in the phenol molecule is refractory to HZSM-5 [27].

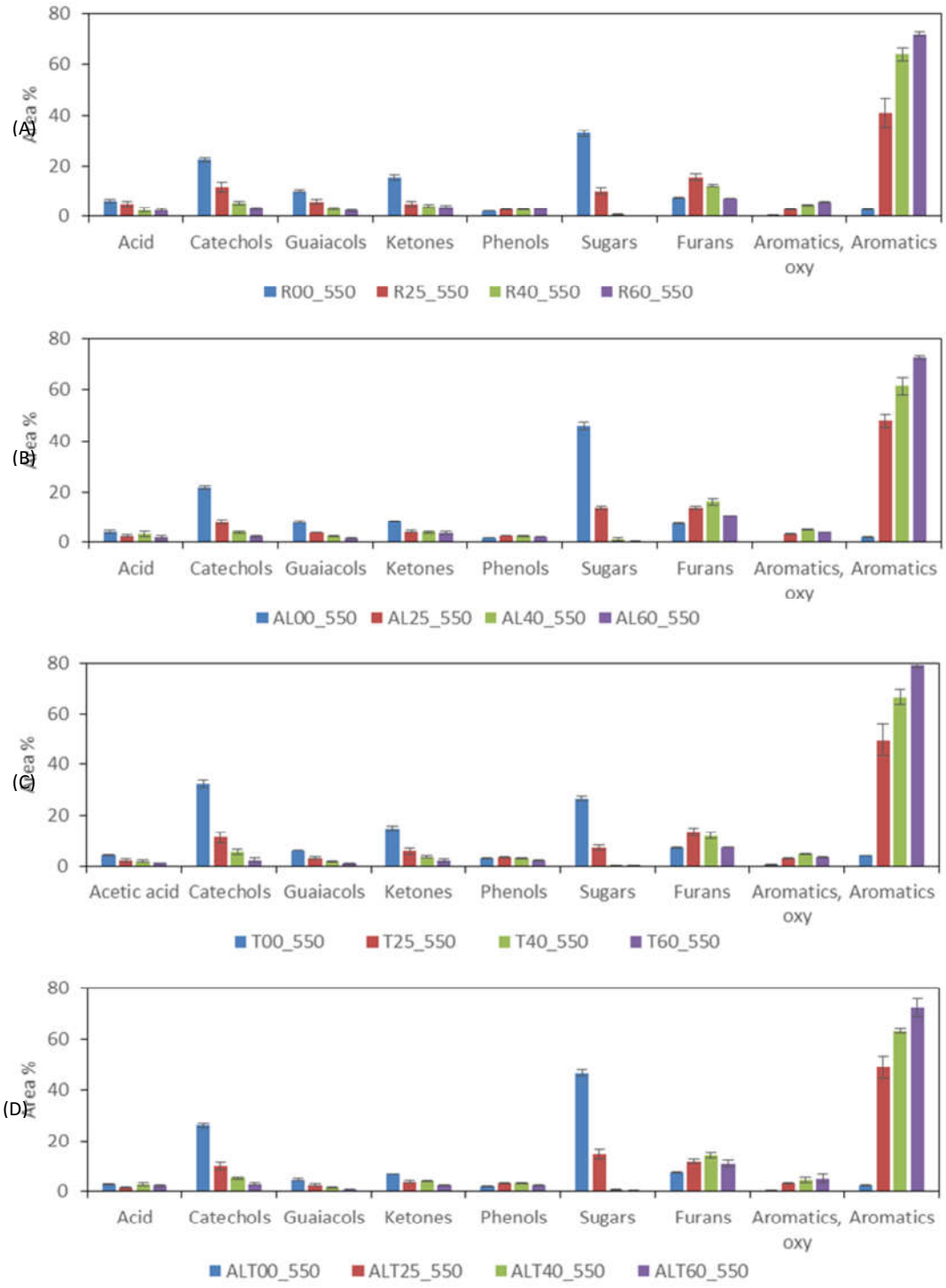

Figure 6-7: The impacts of C/B ratio on products distribution at 550 °C, (A): Rwood, (B): ALwood, (C): Twood, (D): ALTwood.

6.3.4.2. At a temperature of 360 ^{o}C

The study of catalytic fast pyrolysis described in Chapter 5 using the Scion fluidised bed reactor demonstrated that a low temperature of 360 ^{o}C can considerably activate the zeolite HZSM-5. Although the catalytic activity is less than optimal at this temperature, it was of interest to understand the impacts of C/B ratio at a low temperature. Operating at a low temperature can avoid the issue of bed agglomeration in catalytic fast pyrolysis of acid-leached biomass on a fluidised bed reactor. In Figure 6-8, the four charts illustrate the results for Rwood (chart A), ALwood (chart B), Twood (chart C) and ALTwood (chart D), respectively. The C/B ratio was increased from 0 to 6 and the temperature was kept at 360 ^{o}C.

For all four feedstocks, the percentage of sugars was significantly decreased with increasing C/B ratio. The percentage was less than 6 % at a C/B ratio of 6. Meanwhile, the percentage of furans was increased with increasing C/B ratio from 0 to 2.5 as more sugars were converted, then decreased when increasing the C/B ratio from 4 to 6 as furans were further transformed. These findings confirm the claim that sugars were reactive on zeolite HZSM-5 at a temperature as low as 360 ^{o}C.

For ALwood and ALTwood, the percentage of guaiacols was slightly decreased with increasing C/B ratio from 0 to 6. While in the case of Rwood and Twood, the percentage of guaiacols was significantly decreased with increasing the C/B ratio. Hence guaiacols, to a lesser extent than sugars, was reactive on the HZSM-5 zeolite at 360 ^{o}C.

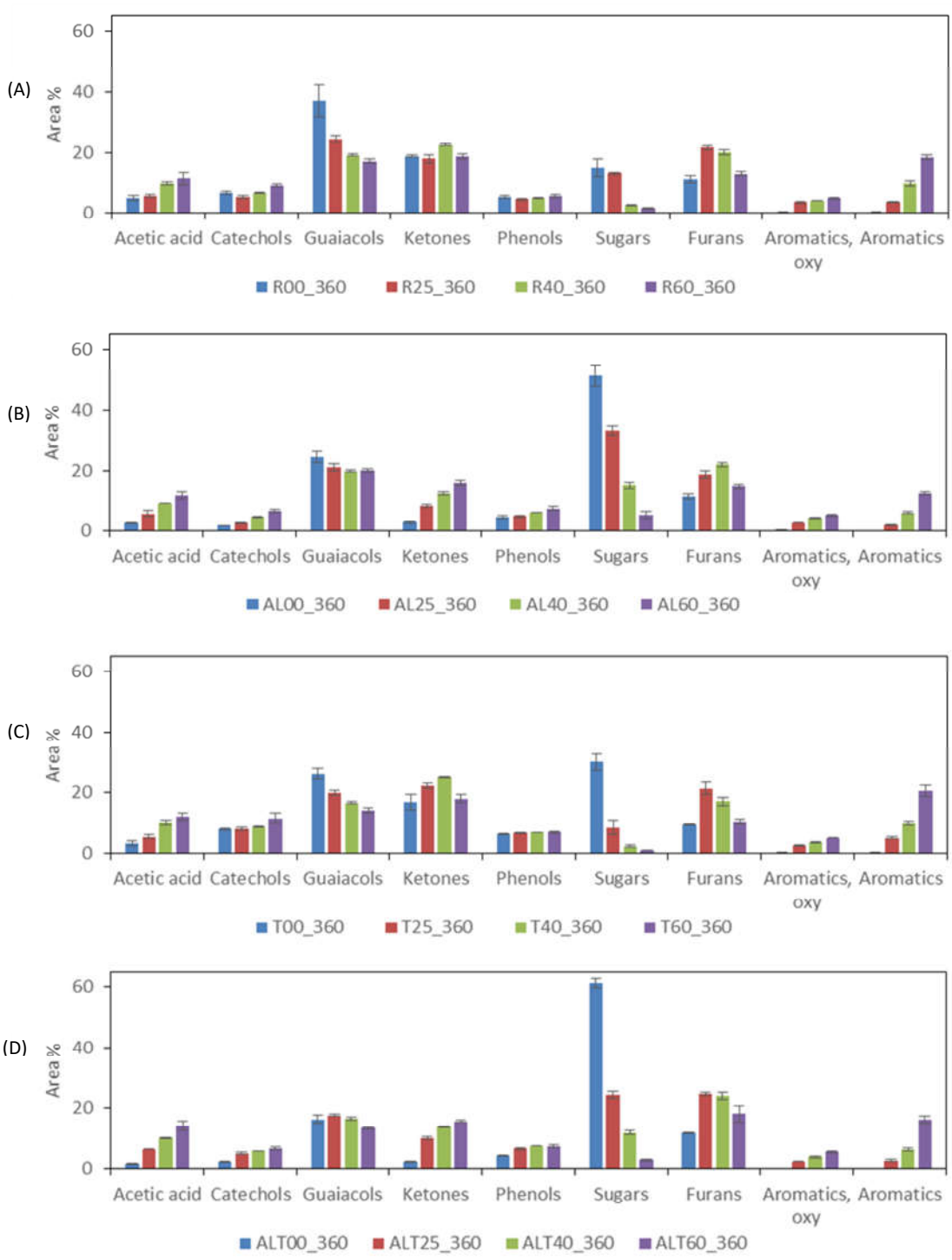

Figure 6-8: The impacts of C/B ratio on products distribution at 360 °C, (A): Rwood, (B): ALwood, (C): Twood, (D): ALTwood.

The percentages of aromatics and oxygenated aromatics were increased with increasing C/B ratio for all four feedstocks. This indicates that a high C/B ratio can compensate to some degree for the restriction in catalyst activity at a low temperature. Probably the reason is that more acid sites of the zeolite for catalytic conversion were provided by increasing the C/B ratio.

In contrast to the changes in sugars and guaiacols, the percentages of acetic acid and catechols were gradually increased with increasing C/B ratio from 0 to 6. The percentage of ketones was increased with increasing C/B ratio for ALwood and ALTwood, but remained relatively constant for Rwood. For the torrefied wood, the percentage of ketones was increased when the C/B ratio was increased from 0 to 4, but then decreased with further increase in the C/B ratio. These trends were opposite to those observed at the high temperature of 550 ^{o}C. This indicates that the reactivity of acetic acid, catechols and ketones on HZSM-5 was low at a low temperature of 360 ^{o}C.

6.3.5 Principal component analysis

Principal component analysis (PCA) can be used to evaluate the contribution of all the individual products to the variances, which can be an advantage over the first method of classifying the products into different groups. The score plot (e.g. plot A in Figure 6-9) shows the dispersion of the samples (the experiments under different conditions). Clustering of the samples indicates that they have a similar distribution of the products, while scattering of the samples indicates that their distributions of the products are different. The loading plot (e.g. plot B in Figure 6-9) shows the contribution of the variables (the area percentages of the pyrolysis products) to the principal components.

6.3.5.1. Impacts of pretreatments and temperature in non-catalytic pyrolysis

In the first PCA model, the impacts of biomass pretreatments and temperature in non-catalytic pyrolysis are considered. The sixteen samples represent experimental runs conducted in Py-GC/MS experiments which covered the four types of feedstocks and the four pyrolysis temperatures without catalyst. The score and loading plots are given in Figure 6-9. The two principal components together account for 75 % of the variance among the samples (PC1 at 56 %, PC2 at 19 %).

The score plot (plot A in Figure 6-9) shows that the samples with acid-leaching pretreatment are located on the positive side of the origin on PC1 axis, and the samples without acid-leaching pretreatment are located on the negative side. Therefore, acid-leaching pretreatment has a strong influence on the distribution of the products. On PC2 axis, the influences of the torrefaction pretreatment and temperature can be observed. As torrefaction pretreatment and increasing temperature both drive the samples up on PC2 axis. For instance, sample T00_550 is located above sample R00_550, and AL00_500 is located above sample AL00_450.

As observed in the loading plot (plot B in Figure 6-9), PC1 is in a positive relation with mainly levoglucosan. It indicates that the influence of acid-leaching pretreatment is mainly due to the contribution of the formation of levoglucosan. PC1 is in a negative relation with a number of compounds including mainly 1-hydroxy-2-propanone and 1,2-cyclopentanedione (products in the group of ketones). It was also found in Figure 6-3 that the percentage of ketones was higher for Rwood and Twood than that for ALwood and ALTwood. This indicates that removing ash from biomass suppresses the formation of ketones in thermal pyrolysis.

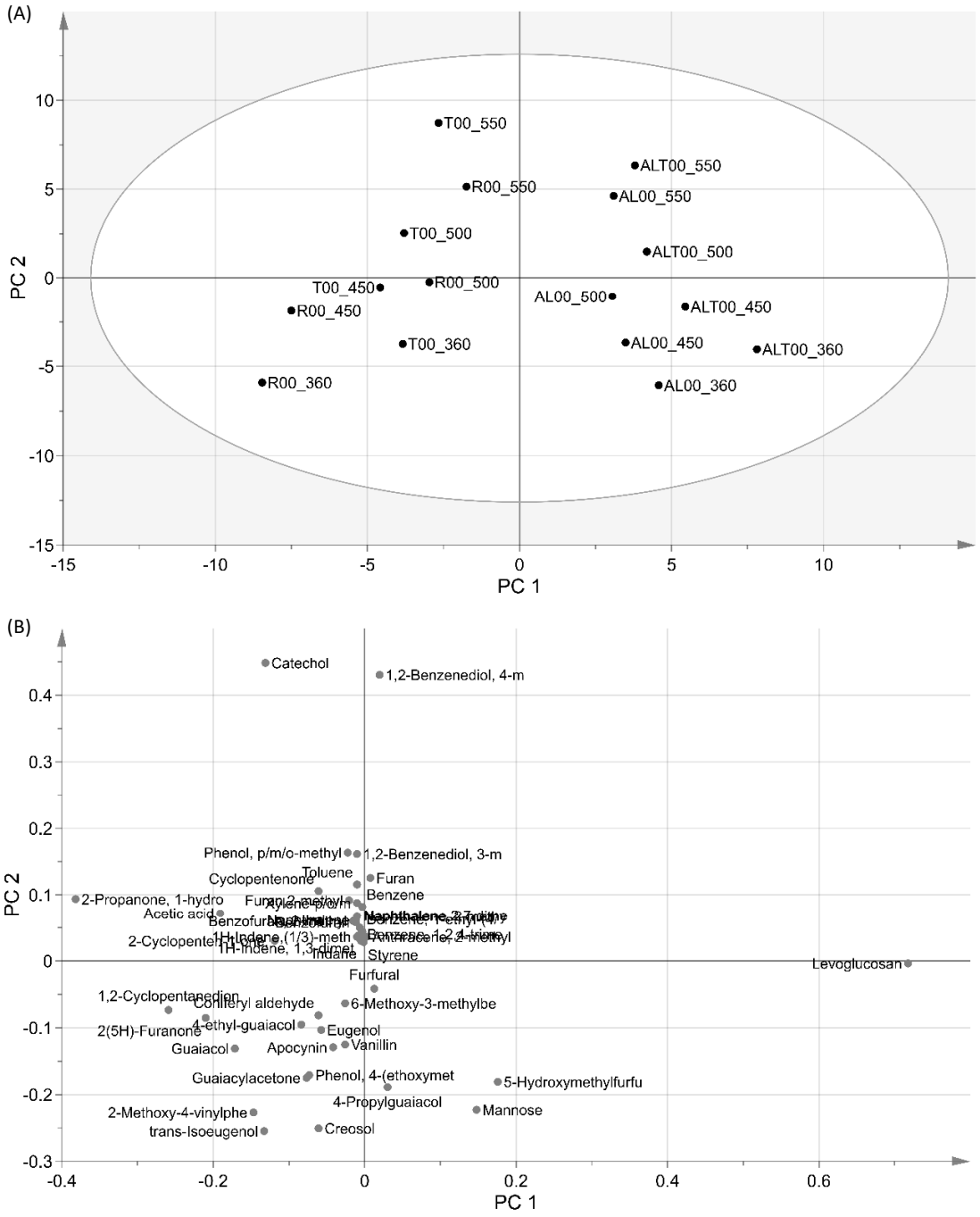

Figure 6-9: Score (A) and loading (B) plots of PC1 and PC2 for the model in Py-GC/MS analysis with all feedstocks at all temepratures and a C/B ratio of 0.

In the loading plot (plot B in Figure 6-9), PC2 is positively correlated with the catechols, especially catechol and 4-methyl-1, 2-benzenediol (4-methyl-catechol). While guaiacols, such as creosol and trans-isoeugenol, were negatively correlated with PC2. It indicates that the influence of torrefaction pretreatment or increasing temperature is contributed to the formation of catechols, which are possibly pyrolysis fragments of guaiacols.

From this PCA model, it is concluded that the acid-leaching pretreatment has the strongest influence in non-catalytic pyrolysis, meanwhile changing temperature and torrefaction pretreatment both can mildly affect the distribution of the products. These findings are consistent with trends observed in Figure 6-3 and **Figure 6-**5, which classified the products into different groups.

6.3.5.2. Impacts on pretreatment and temperature in catalytic pyrolysis

In order to visualise the influence of biomass pretreatments and temperature in catalytic pyrolysis, a PCA model with sixteen Py-GC/MS experimental results which covered the four types of feedstocks and the four temperatures at a constant C/B ratio of 4 was created (Figure 6-10). The two principal components explains 85 % of the variance among the samples (PC1 at 73 %, PC2 at 12 %). It is noticed that PC1 explains a high degree of the variance, while PC2 is less important. The discussion is mainly therefore focused on the variance in PC1.

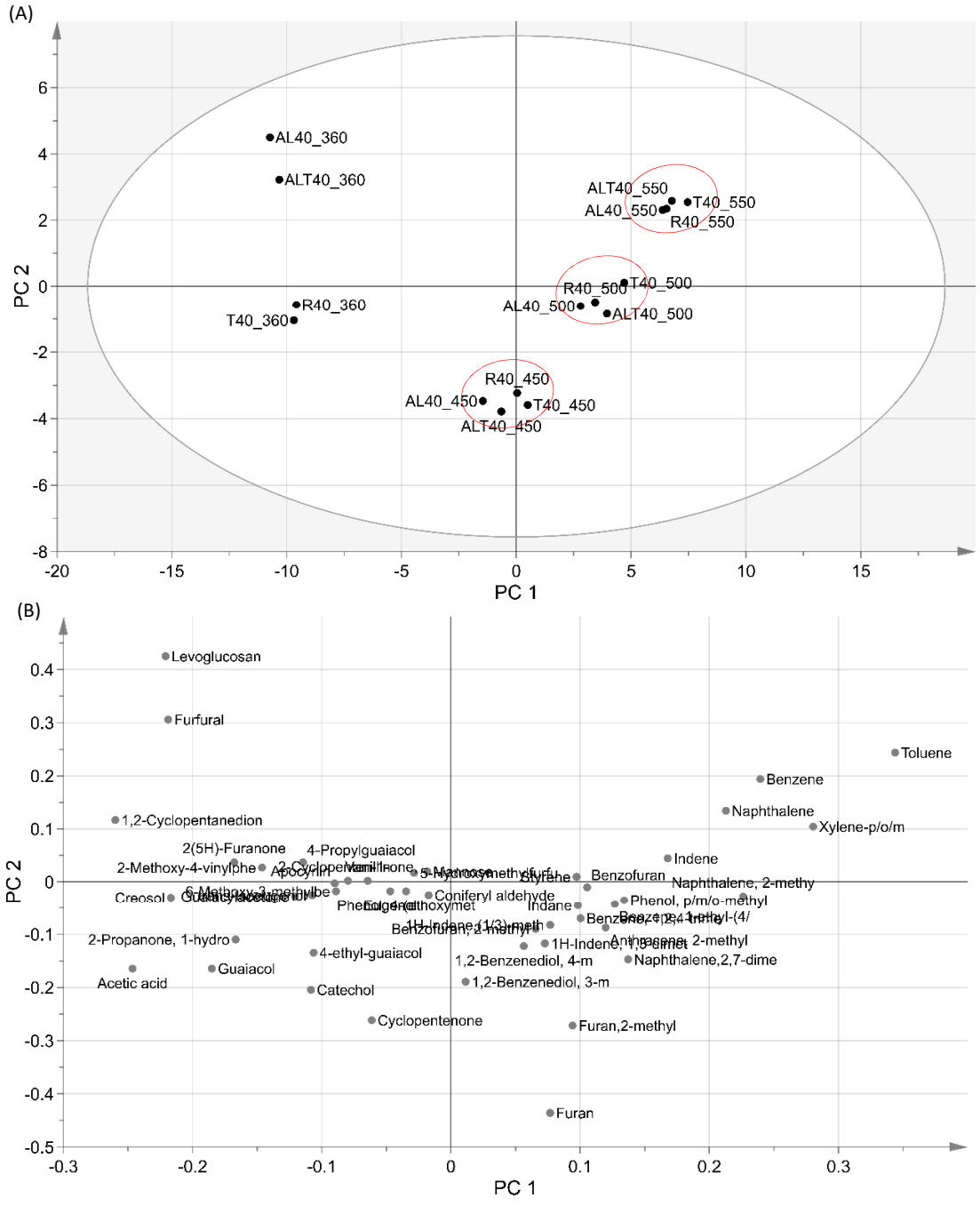

Figure 6-10: Score (A) and loading (B) plots of PC1 and PC2 for the model in Py-GC/MS analysis with all feedstocks at all temperatures and a C/B ratio of 4.

As illustrated in the score plot in Figure 6-10A, the samples with the same temperatures are clustered together except the ones for the temperature of 360 °C. Hence temperature was the most important factor in catalytic pyrolysis. The samples with the temperatures of 450 °C, 500 °C and 550 °C are grouped into 3 clusters (circled in the score plot) according to temperature. For these three groupings, the clusters are shifted in the positive direction on PC1 and PC2 axes with increasing temperature.

The exception is the four samples with a temperature of 360 °C, where the two samples with acid-leaching pretreatment are shifted up on PC2 axis. Because the activity of the catalyst is low at this temperature, the influence of acid-leaching pretreatment became relatively important.

The loading plot in Figure 6-10B shows that PC1 is in a positive relation with catalytic pyrolysis products, such as toluene, benzene and naphthalene, and in a negative relation with thermal pyrolysis products, such as 1,2-cyclopentanedione, acetic acid and creosol. Hence the influence of increasing temperature on the variance is due to the formation of aromatic hydrocarbons. Conversely the influence of decreasing temperature is due to the formation of thermal pyrolysis products.

The second PCA model shows that increasing temperature strongly promoted the formation of aromatics in catalytic pyrolysis. In comparison, the acid-leaching and torrefaction pretreatments had a much less influence when the temperature was 450 °C or higher. These findings are consistent with the trends observed by the first analysis method (Figure 6-6).

6.3.5.3. Comparison of the influence of temperature and C/B ratio

In the third PCA model, the sixteen samples represent the sixteen Py-GC/MS runs covering the four temperatures and the four C/B ratios with one feedstock (ALTwood). The model's score

and loading plots are shown in Figure 6-11. PC1 explains 61 % of the variance and PC2 explains 22 %.

As illustrated in the score plot in Figure 6-11A, the four samples without catalyst (a C/B ratio of 0) were clustered together. Samples for experiments at the same temperature are shifted in the negative direction on PC1 axis by increasing the C/B ratio. Meanwhile, samples for experiments at the same C/B ratio are also shifted in the negative direction on the PC1 axis by increasing the temperature. Additionally increasing temperature drives samples for experiments at the same C/B ratio in the negative direction on the PC2 axis. Therefore, the C/B ratio and the temperature both affect the distribution of products in catalytic pyrolysis.

As observed in the loading plot in Figure 6-11B, PC1 is positively correlated to thermal pyrolysis products, particularly levoglucosan, and it is negatively correlated to aromatics. Hence the influence of increasing C/B ratio on the variance is due to the formation of aromatics, likewise the influence of increasing temperature. PC2 is positively correlated to light oxygenates (acetic acid and ketones) and guaiacols, and negatively correlated to aromatic hydrocarbons and sugars, particularly levoglucosan. This indicates that increasing temperature favours the formation of aromatics and sugars, and decreasing temperature favours the formation of light oxygenates and guaiacols.

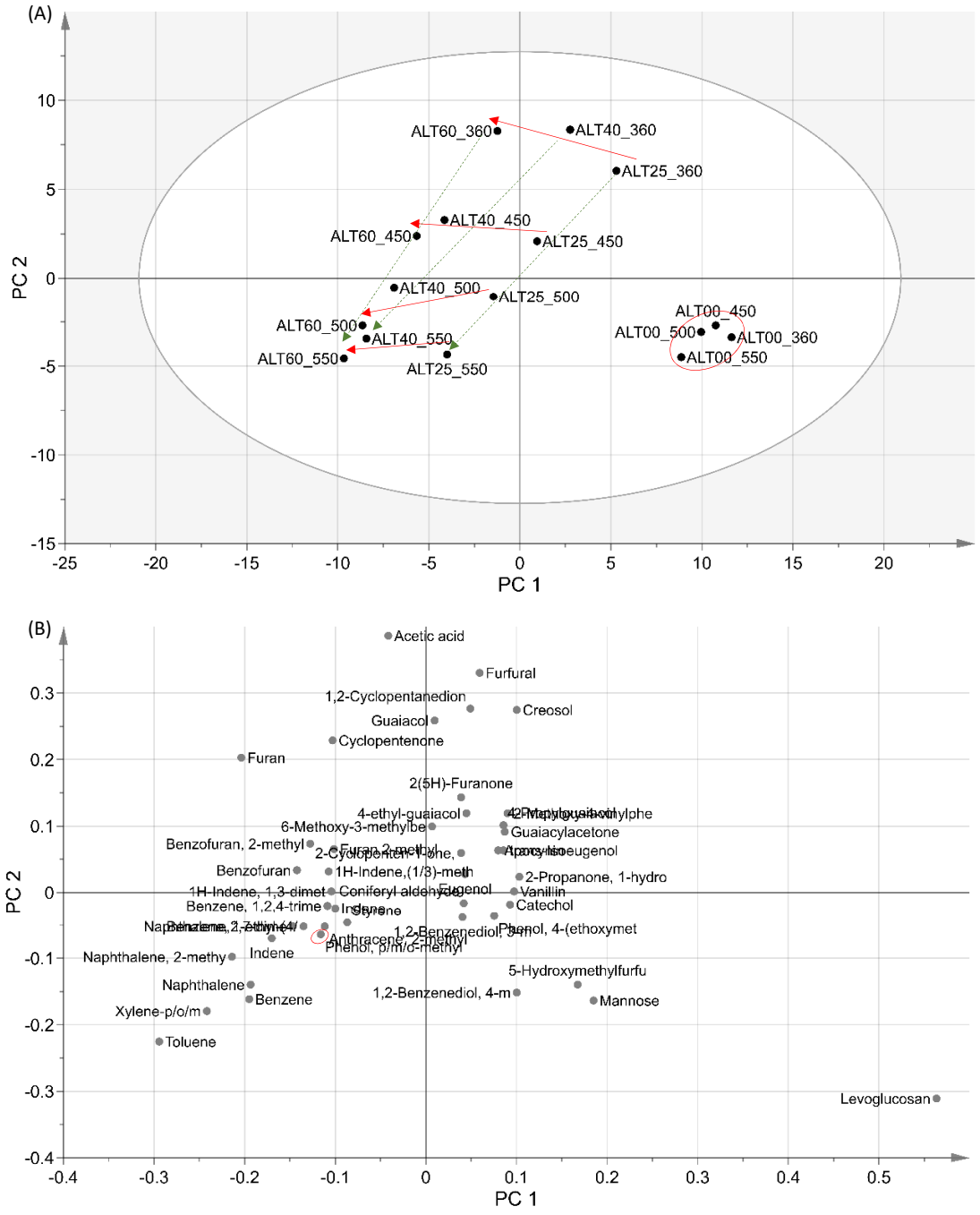

Figure 6-11: Score (A) and loading (B) plots of PC1 and PC2 for the model in ALTwood Py-GC/MS analysis at all temepratures and C/B ratios.

In Figure 6-11B, it is also observed the phenols were located close to the origin of the two axes, for instance methyl-phenol in the red circle. This suggests that changes in phenols made little contribution to PC1 and PC2, which is consistent with the fact that phenols are barely reactive on the zeolite catalyst.

From the third PCA model, it is concluded that the presence of zeolite catalyst strongly promoted the conversion of thermal pyrolysis products to aromatics at a high temperature. The temperature and C/B ratio are equally important in catalytic pyrolysis.

The score and loading plots of the other three models for Rwood, Twood and ALwood, are given in the Figure 6A-3, Figure 6A-4 and Figure 6A-5 in the Appendix C. In general the same trends, as discussed above, on the effects of pyrolysis temperature and C/B ratio can be demonstrated by these models.

6.3.6 The chemical mechanism in catalytic pyrolysis of pretreated woods

In catalytic pyrolysis of lignocellulosic biomass, thermal pyrolysis occurs initially releasing organic vapours [8]. The organic vapours then undergo a series of catalytic reactions (zeolite upgrading) on the zeolite forming aromatics and low-oxygen content products [13]. The results in this study reveal that acid-leaching and torrefaction pretreatments can affect the reaction pathways in thermal pyrolysis. Those changes in the distribution of thermal pyrolysis products as a result of biomass pretreatment can lead to changes in catalytic pyrolysis.

The acid-leaching pretreatment can significantly promote the formation of sugars in thermal pyrolysis as shown in Figure 6-3. In the subsequent zeolite upgrading, the sugars are transformed to furans [15], which are then further transformed to aromatics [16]. As a result, more acid sites of zeolite are required for catalytic conversion of sugars to aromatics, because a

substantial amount of sugars has to be converted to furans first. Therefore, acid-leaching pretreatment can restrict the formation of aromatics and promote the formation of furans if there are insufficient zeolite acid sites.

Torrefaction pretreatment hardly affected the distribution of products in catalytic pyrolysis (Figure 6-4), however it can lead to an increase in the yield of organics in catalytic fast pyrolysis (see Chapter 5). It was found in this study that this pretreatment promoted the formation of catechols rather than phenols or guaiacols in thermal pyrolysis (Figure 6-3). Meanwhile phenols are resistant to HZSM-5, and bulky guaiacols, such as 1,2,3-trimethoxybenzene, are too large to enter the pores of the zeolite for zeolite upgrading [17]. Thus the enhanced formation of catechols due to torrefaction pretreatment can be helpful to increase the yield of aromatics in catalytic pyrolysis.

6.4. Conclusion

A systematic study on catalytic pyrolysis of pretreated woods has been performed using Py-GC/MS. Products from the Py-GC/MS were classified into nine chemical groups and the results are compared to investigate the effects of wood pretreatment, pyrolysis temperature and catalyst loading (represented by catalyst to biomass ratio). Principal component analysis was employed to visually evaluate these effects on pyrolysis products. Both evaluation methods led to the same conclusions.

The investigation on the impacts of acid-leaching and torrefaction pretreatments in non-catalytic and catalytic pyrolysis confirms the conclusions made in Chapter 5. The acid-leaching pretreatment strongly enhances the formation of sugars in thermal pyrolysis, consequently it

hinders the formation of aromatics in zeolite upgrading. The possible reason is that transforming sugars to aromatics needs more acid sites of the zeolite than other thermal pyrolysis products. The torrefaction pretreatment enhances the formation of catechols rather than guaiacols or phenols in thermal pyrolysis. As a result, torrefaction pretreatment can lead to an increase of the yield of aromatics in catalytic pyrolysis.

Temperature is a key factor in catalytic pyrolysis as rising the temperature increases the activity of the zeolite catalyst. The sugars, and guaiacols to a lesser extent, are reactive to HZSM-5 at a temperature as low as 360 ^{o}C. While the catechols and light oxygenates need a higher temperature for zeolite upgrading. A sufficient catalyst load is necessary for effective catalytic conversion. Increasing C/B ratio can partially compensate for the restriction in catalyst activity at a low temperature of 360 ^{o}C. By increasing C/B ratio, more sugars and guaiacols are catalytically converted to aromatics at this temperature.

From principal component analysis, it was concluded that the presence or absence of the HZSM-5 catalyst has the greatest influence on the distribution of products. The temperature and C/B ratio are equally important in catalytic pyrolysis. Acid-leaching and torrefaction pretreatments have some influence on the distribution of products in catalytic pyrolysis, but their impacts are not as strong as the other factors.

References

[1] Lu, Q., X.-c. Yang, C.-q. Dong, Z.-f. Zhang, X.-m. Zhang, and X.-f. Zhu, *Influence of pyrolysis temperature and time on the cellulose fast pyrolysis products: Analytical Py-GC/MS study.* Journal of Analytical and Applied Pyrolysis, 2011. **92**(2): p. 430-438.

[2] Mihalcik, D.J., C.A. Mullen, and A.A. Boateng, *Screening acidic zeolites for catalytic fast pyrolysis of biomass and its components.* Journal of Analytical and Applied Pyrolysis, 2011. **92**(1): p. 224-232.

[3] Thangalazhy-Gopakumar, S., S. Adhikari, S.A. Chattanathan, and R.B. Gupta, *Catalytic pyrolysis of green algae for hydrocarbon production using H+ ZSM-5 catalyst.* Bioresource Technology, 2012. **118**: p. 150-157.

[4] Huber, G.W., S. Iborra, and A. Corma, *Synthesis of Transportation Fuels from Biomass: Chemistry, Catalysts, and Engineering.* Chem. Rev., 2006. **106**(9): p. 4044-4098.

[5] Meier, D., I. Fortmann, J. Odermatt, and O. Faix, *Discrimination of genetically modified poplar clones by analytical pyrolysis–gas chromatography and principal component analysis.* Journal of Analytical and Applied Pyrolysis, 2005. **74**(1-2): p. 129-137.

[6] Pattiya, A., J.O. Titiloye, and A.V. Bridgwater, *Evaluation of catalytic pyrolysis of cassava rhizome by principal component analysis.* Fuel, 2010. **89**(1): p. 244-253.

[7] Schwarzinger, C., *Identification of fungi with analytical pyrolysis and thermally assisted hydrolysis and methylation.* Journal of analytical and applied pyrolysis, 2005. **74**(1-2): p. 26-32.

[8] Wang, K., K.H. Kim, and R.C. Brown, *Catalytic pyrolysis of individual components of lignocellulosic biomass.* Green Chemistry, 2014. **16**(2): p. 727-735.

[9] Paine III, J.B., Y.B. Pithawalla, and J.D. Naworal, *Carbohydrate pyrolysis mechanisms from isotopic labeling: Part 4. The pyrolysis of d-glucose: The formation of furans.* Journal of analytical and applied pyrolysis, 2008. **83**(1): p. 37-63.

[10] Patwardhan, P.R., R.C. Brown, and B.H. Shanks, *Product distribution from the fast pyrolysis of hemicellulose.* ChemSusChem, 2011. **4**(5): p. 636-643.

[11] Ponder, G.R., G.N. Richards, and T.T. Stevenson, *Influence of linkage position and orientation in pyrolysis of polysaccharides: A study of several glucans.* Journal of Analytical and Applied Pyrolysis, 1992. **22**(3): p. 217-229.

[12] Shen, D., S. Gu, and A. Bridgwater, *The thermal performance of the polysaccharides extracted from hardwood: cellulose and hemicellulose.* Carbohydrate Polymers, 2010. **82**(1): p. 39-45.

[13] Liu, C., H. Wang, A.M. Karim, J. Sun, and Y. Wang, *Catalytic fast pyrolysis of lignocellulosic biomass.* Chemical Society Reviews, 2014. **43**(22): p. 7594-7623.

[14] Stefanidis, S.D., K.G. Kalogiannis, E.F. Iliopoulou, C.M. Michailof, P.A. Pilavachi, and A.A. Lappas, *A study of lignocellulosic biomass pyrolysis via the pyrolysis of cellulose, hemicellulose and lignin.* Journal of Analytical and Applied Pyrolysis, 2014. **105**: p. 143-150.

[15] Carlson, T.R., J. Jae, Y.-C. Lin, G.A. Tompsett, and G.W. Huber, *Catalytic fast pyrolysis of glucose with HZSM-5: the combined homogeneous and heterogeneous reactions.* Journal of Catalysis, 2010. **270**(1): p. 110-124.

[16] Cheng, Y.-T. and G.W. Huber, *Chemistry of Furan Conversion into Aromatics and Olefins over HZSM-5: A Model Biomass Conversion Reaction.* ACS Catalysis, 2011. **1**(6): p. 611-628.

[17] Yu, Y., X. Li, L. Su, Y. Zhang, Y. Wang, and H. Zhang, *The role of shape selectivity in catalytic fast pyrolysis of lignin with zeolite catalysts.* Applied Catalysis A: General, 2012. **447-448**: p. 115-123.
[18] Piskorz, J., D.S.A. Radlein, D.S. Scott, and S. Czernik, *Pretreatment of wood and cellulose for production of sugars by fast pyrolysis.* Journal of Analytical and Applied Pyrolysis, 1989. **16**(2): p. 127-142.
[19] Meng, J., J. Park, D. Tilotta, and S. Park, *The effect of torrefaction on the chemistry of fast-pyrolysis bio-oil.* Bioresource Technology, 2012. **111**: p. 439-446.
[20] Neupane, S., S. Adhikari, Z. Wang, A.J. Ragauskas, and Y. Pu, *Effect of torrefaction on biomass structure and hydrocarbon production from fast pyrolysis.* Green Chemistry, 2015. **17**(4): p. 2406-2417.
[21] Wigley, T., A.C.K. Yip, and S. Pang, *Pretreating biomass via demineralisation and torrefaction to improve the quality of crude pyrolysis oil.* Energy, 2016. **109**: p. 481-494.
[22] Zheng, A., Z. Zhao, Z. Huang, K. Zhao, G. Wei, X. Wang, F. He, and H. Li, *Catalytic Fast Pyrolysis of Biomass Pretreated by Torrefaction with Varying Severity.* Energy & Fuels, 2014. **28**(9): p. 5804-5811.
[23] Amutio, M., G. Lopez, M. Artetxe, G. Elordi, M. Olazar, and J. Bilbao, *Influence of temperature on biomass pyrolysis in a conical spouted bed reactor.* Resources, Conservation and Recycling, 2012. **59**: p. 23-31.
[24] Cheng, Y.T., J. Jae, J. Shi, W. Fan, and G.W. Huber, *Production of Renewable Aromatic Compounds by Catalytic Fast Pyrolysis of Lignocellulosic Biomass with Bifunctional Ga/ZSM-5 Catalysts.* Angewandte Chemie, 2012. **124**(6): p. 1416-1419.
[25] Mortensen, P.M., J.D. Grunwaldt, P.A. Jensen, K.G. Knudsen, and A.D. Jensen, *A review of catalytic upgrading of bio-oil to engine fuels.* Applied Catalysis A: General, 2011. **407**(1-2): p. 1-19.
[26] Gayubo, A.G., A.T. Aguayo, A. Atutxa, R. Aguado, and J. Bilbao, *Transformation of Oxygenate Components of Biomass Pyrolysis Oil on a HZSM-5 Zeolite. I. Alcohols and Phenols.* Ind. Eng. Chem. Res., 2004. **43**(11): p. 2610-2618.
[27] Horne, P.A. and P.T. Williams, *Reaction of oxygenated biomass pyrolysis model compounds over a ZSM-5 catalyst.* Renewable Energy, 1996. **7**(2): p. 131-144.

Chapter 7

Conclusions and recommendations

7.1. Conclusions

The effects of biomass pretreatments on the product yields and quality in fast pyrolysis and catalytic fast pyrolysis are related to the alterations of the biomass constitutive composition after the pretreatments. In this study, acid-leaching using an acetic acid solution effectively reduced ash content of pine wood. Mild torrefaction of biomass caused degradation of the hemicellulose leading to a mass loss.

Fast pyrolysis of pretreated wood was studied in two bubbling fluidised bed reactors (University of Canterbury reactor and Scion reactor). The results from the experiments using these two reactor showed similar trends regarding the effects of biomass pretreatments on fast pyrolysis. Acid-leaching pretreatment increased the bio-oil yield and decreased the char and gas yields. Acid-leaching pretreatment substantially increased the content of carbohydrate-derived products in the bio-oil, although the elemental composition was similar to bio-oil from the pyrolysis of raw wood. Torrefaction pretreatment increased the char yield and decreased the gas and bio-oil yields in fast pyrolysis, therefore it enhanced carbonisation in pyrolysis. Torrefaction pretreatment decreased the oxygen content and increased the content of lignin derived products in the bio-oil. The combined pretreatment, acid-leaching followed by

torrefaction, showed the effect of acid-leaching on increasing the content of carbohydrate derived products in bio-oil and the effect of torrefaction on enhancing carbonisation.

Bed material agglomeration typically observed during fast pyrolysis of acid-leached wood was successfully overcome by three different approaches: lower temperature, torrefaction, or quick renewal of bed material. Operating at a lower temperature or applying torrefaction after acid-leaching pretreatment prevented bed agglomeration, but bio-oil yield was reduced in both cases. A high sand (bed material) feeding rate in the fluidised bed reactor also prevented bed agglomeration by quickly moving the melted residue out of the reactor before it could cause complete bed defluidisation, and in this case, the bio-oil yield and composition were not affected.

Acid-leaching pretreatment can supress carbonisation in pyrolysis leading to biomass melting, and eventually bed agglomeration. The melting behaviour could be related to melting behaviour of biomass components, particularly the lignin, before they are pyrolysed. The severity of biomass melting increases with pyrolysis temperature, and severe melting behaviour leads to increased possibility of bed agglomeration. Torrefaction pretreatment can enhance carbonisation in pyrolysis. The combined pretreatment of acid-leaching and torrefaction can reverse the suppressed carbonisation due to acid-leaching, and thereby prevent bed agglomeration.

Pioneer research on *in situ* catalytic fast pyrolysis of pretreated wood was conducted on the Scion pyrolysis reactor. Experiments were conducted at multiple temperatures (360-500 °C) and catalyst to biomass ratios (2.5-6) using the three biomass pretreatments (acid-leaching, torrefaction, and their combination). This study showed that the strong influence of acid-

leaching pretreatment in fast pyrolysis disappeared in catalytic fast pyrolysis. The yield of oil product was not significantly increased by acid-leaching pretreatment, as observed in fast pyrolysis. Furthermore, the deoxygenation was mildly impeded, producing an oil product with higher oxygen content compared to the oil produced from raw wood. Torrefaction pretreatment led to an increase in the yield of oil product compared to raw wood, while changes in the properties and chemical composition of the oil product were insignificant. The combined pretreatment, acid-leaching followed by torrefaction, was able to remove the ash from the biomass, potentially extending catalyst lifetime, without introducing negative effects associated with the acid-leaching pretreatment on the catalytic fast pyrolysis, including bed agglomeration and impeded deoxygenation.

Similar to the phenomenon observed in fast pyrolysis, acid-leaching pretreatment also caused bed agglomeration in catalytic fast pyrolysis. The catalytic effect of zeolite HZSM-5 was not able to prevent this issue. Bed agglomeration was also overcome by the three approaches used in fast pyrolysis.

Assuming that catalytic pyrolysis consists of two steps: thermal pyrolysis of biomass generating vapours, and zeolite upgrading of such vapours in the catalyst, a pyrolysis-gas chromatography/mass spectrometry (Py-GC/MS) study was used to better understand the reaction pathways in catalytic pyrolysis of pretreated biomass. This study showed that the acid-leaching pretreatment strongly enhanced the formation of sugar products in thermal pyrolysis, consequently hindered the formation of aromatics in zeolite upgrading. A possible reason is that transforming sugars to aromatics needs more zeolite acid sites than other thermal pyrolysis products. Torrefaction pretreatment enhanced the formation of catechols rather than guaiacols or phenols in thermal pyrolysis. As a result, torrefaction pretreatment led to an increase of the

yield of aromatics in catalytic pyrolysis. The Py-GC/MS results also showed that sugars, and guaiacols to a lesser extent, were reactive with HZSM-5 at a temperature as low as 360 ^{o}C. Increasing the catalyst to biomass ratio was used to partially compensate for the reduced catalyst activity at a low temperature of 360 ^{o}C, resulting in more sugars and guaiacols being catalytically converted to aromatics at this temperature.

Principal component analysis of the Py-GC/MS data graphically revealed that the presence or absence of the HZSM-5 catalyst had the greatest influence on the products distribution. The temperature and catalyst to biomass ratio were equally important in catalytic pyrolysis. On the other hand, acid-leaching and torrefaction pretreatments mildly affected the results.

7.2. Recommendations for future work

Acid leaching effectively removes ash in biomass that can cause irreversible deactivation by metal elements accumulating on the zeolite catalyst [1]. More experimental work is needed to find out if applying acid-leaching pretreatment to the feedstock before catalytic fast pyrolysis can prolong the catalyst lifetime.

At the same time, acid leaching pretreatment can cause bed agglomeration during (catalytic) fast pyrolysis in a fluidised bed reactor. Torrefaction is able to prevent this issue and compensate the negative effects of acid-leaching pretreatment in catalytic fast pyrolysis. This study has led to insights into an integrated process, which combines acid leaching and torrefaction as biomass pretreatment with catalytic fast pyrolysis.

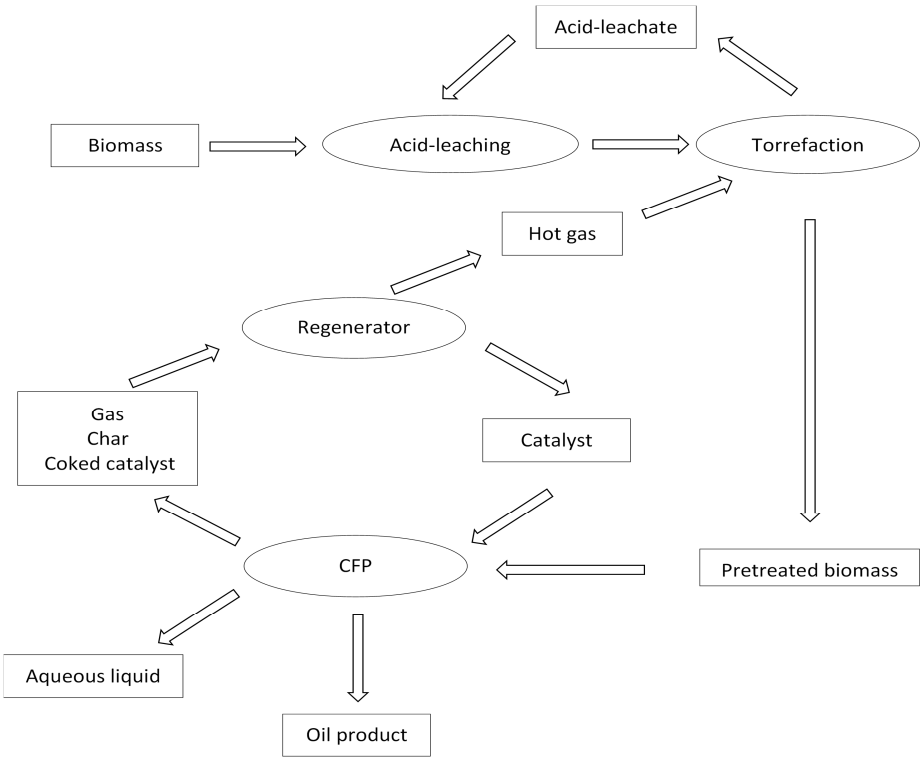

Figure 7-1: Proposed process integrating biomass pretreatment with catalytic fast pyrolysis.

An integrated process is proposed as illustrated in Figure 7-1. The biomass feedstock is pretreated by acid-leaching followed by torrefaction. The torrefaction process produces acidic liquid, which can be used as a low-cost acid leachate for the acid-leaching process [2]. This pretreated biomass is then fed to a fluidised bed reactor for catalytic fast pyrolysis. The coked catalyst and the by-products char and gas are transferred to another reactor for catalyst regeneration by combustion. The regenerated catalyst carries heat to the CFP reactor, while the exhaust gas can provide heat for the torrefaction pretreatment, as the temperature of exhaust gas is as high as 600 ^{o}C [3]. The oil product is separated from the aqueous liquid. This study showed that catalytic fast pyrolysis of pine wood can produce a significant amount of aqueous

liquid, approximately 20 wt.% on dry biomass basis. Since water is required to wash the biomass to remove any remaining ash after acid-leaching, the aqueous liquid from CFP can be used as the leachate instead of water in the acid-leaching process.

Future research could investigate if this integrated process can be economically and technically viable. Process simulation and techno-economic analysis can be realised by computer modelling using software such as Aspen Plus. The catalyst inventory contributes the most to the total process cost [4]. Applying acid-leaching pretreatment before catalytic fast pyrolysis may decrease the cost on catalyst supplement. On the other hand, the cost of treatment and disposal of the waste water in the acid-leaching process should also be considered, as it may cause extra cost [5]. In addition, the application of the oil product containing a significant amount of aromatic hydrocarbons can be considered in the techno-economic analysis. This oil product can be a renewable source of chemicals such as toluene and phenol, which are largely produced from fossil oil.

References

[1] Yildiz, G., F. Ronsse, R. van Duren, and W. Prins, *Challenges in the design and operation of processes for catalytic fast pyrolysis of woody biomass.* Renewable and Sustainable Energy Reviews, 2016. **57**: p. 1596-1610.

[2] Wigley, T., A.C.K. Yip, and S. Pang, *Pretreating biomass via demineralisation and torrefaction to improve the quality of crude pyrolysis oil.* Energy, 2016. **109**: p. 481-494.

[3] Jones, S., P. Meyer, L. Snowden-Swan, A. Padmaperuma, E. Tan, A. Dutta, J. Jacobson, and K. Cafferty, *Process design and economics for the conversion of lignocellulosic biomass to hydrocarbon fuels: fast pyrolysis and hydrotreating bio-oil pathway*. 2013, National Renewable Energy Laboratory (NREL), Golden, CO.

[4] Dutta, A., A. Sahir, E. Tan, D. Humbird, L.J. Snowden-Swan, P.A. Meyer, J. Ross, D. Sexton, R. Yap, and J. Lukas, *Process design and economics for the conversion of lignocellulosic biomass to hydrocarbon fuels: Thermochemical research pathways with in situ and ex situ upgrading of fast pyrolysis vapors*. 2015, Pacific Northwest National Laboratory (PNNL), Richland, WA (United States).

[5] Oudenhoven, S., *Improving the selectivity of pyrolysis by pyrolytic acid leaching of biomass: the role of AAEMS, anhydrosugar production and process design & evaluation.* 2016.

Appendix A

Table 4A-1: GC/MS analysis results of the oily liquid in catalytic fast pyrolysis of Rwood (to be continued).

RT order	RT (min)	Identified compound	Group	R_360_2.5	R_450_2.5	R_500_2.5	R_500_1.2	R_500_4	R_500_6
1	7.79	Toluene	Aromatics	1.7	6.5	9.4	7.8	9.4	12.3
2	9.63	3-Furaldehyde	Furans	0.7	0.0	0.0	0.0	0.0	0.0
3	9.67	2-Cyclopenten-1-one	Ketones	2.8	0.5	0.1	0.4	0.1	0.1
4	10.62	Ethylbenzene	Aromatics	0.7	2.7	1.9	2.1	1.5	2.3
5	10.87	Benzene, 1,3-dimethyl-	Aromatics	0.7	2.9	2.8	2.5	2.7	3.7
6	11.57	Styrene	Aromatics	0.2	0.3	0.4	0.5	0.3	0.4
7	11.65	p-Xylene	Aromatics	1.1	3.6	3.4	3.0	3.4	4.5
8	12.01	2-Cyclopenten-1-one, 2-methyl-	Ketones	1.1	0.1	0.0	0.1	0.0	0.0
9	12.48	2-Cyclopenten-1-one, 2-hydroxy-	Ketones	0.7	0.0	0.0	0.0	0.0	0.0
10	13.64	Benzene, propyl-	Aromatics	0.3	0.4	0.2	0.3	0.1	0.2
11	13.89	Benzene, (1-methylethyl)-	Aromatics	1.7	2.8	1.4	1.5	1.3	1.6
12	13.94	2-Cyclopenten-1-one, 3-methyl-	Ketones	0.8	0.1	0.0	0.1	0.0	0.0
13	13.95	Furan, 2,5-dimethyl-	Furans	0.2	0.2	0.1	0.1	0.1	0.1
14	13.95	Benzene, 1-ethyl-4-methyl-	Aromatics	2.1	2.4	1.1	1.5	0.9	1.2
15	14.23	Phenol	Phenols	2.9	4.3	5.0	6.6	4.5	4.5
16	14.98	Mesitylene	Aromatics	5.3	6.1	4.1	3.9	4.3	4.7
17	15.13	Benzofuran	Aromatics, oxygenated	1.9	1.9	1.8	2.1	1.7	1.8
18	15.90	2-Cyclopenten-1-one, 2-hydroxy-3-methyl-	Ketones	0.4	0.0	0.0	0.0	0.0	0.0
19	16.04	Benzene, 1-propenyl-	Aromatics	0.2	3.2	2.2	0.2	2.2	2.3
20	16.41	2-Cyclopenten-1-one, 2,3-dimethyl-	Ketones	0.3	0.0	0.0	0.0	0.0	0.0
21	16.45	Indane	Aromatics	2.4	3.2	2.2	2.5	2.2	2.3
22	16.54	4-Methyl-5H-furan-2-one	Ketones	0.5	0.0	0.0	0.0	0.0	0.0
23	16.70	Phenol, 2-methyl-	Phenols	1.5	2.2	2.2	2.8	2.0	2.0
24	16.75	Indene	Aromatics	2.1	3.3	4.4	4.5	4.4	4.3
25	16.83	Benzene, 1-methyl-3-propyl-	Aromatics	0.4	0.3	0.1	0.1	0.1	0.1
26	16.96	Benzene, 1-methyl-4-propyl-	Aromatics	0.7	0.3	0.1	0.2	0.1	0.1
27	16.99	o-Cymene	Aromatics	0.1	0.1	0.0	0.1	0.0	0.0
28	17.33	p-Cresol	Phenols	2.2	3.9	4.0	5.1	3.6	3.7
29	17.85	Benzofuran, 2,3-dihydro-	Aromatics, oxygenated	0.6	0.1	0.0	0.1	0.0	0.0

Table 4A-1: GC/MS analysis results of the oily liquid in catalytic fast pyrolysis of Rwood (continued).

30	17.90	Benzene, (2-methyl-1-propenyl)-	Aromatics	1.7	0.8	0.4	0.5	0.4	0.4
31	17.96	Benzene, 1-ethyl-2,4-dimethyl-	Aromatics	1.3	0.4	0.2	0.2	0.2	0.2
32	18.04	Phenol, 2-methoxy-	Guaiacols	4.7	0.2	0.1	0.1	0.0	0.0
33	18.73	Benzofuran, 2-methyl-	Aromatics, oxygenated	2.9	2.1	1.9	2.4	1.7	1.6
34	18.92	Benzene, 1,2,3,5-tetramethyl-	Aromatics	0.6	0.2	0.1	0.1	0.1	0.1
35	19.23	Benzyl methyl ketone	Aromatics, oxygenated	0.4	0.1	0.0	0.1	0.0	0.0
36	19.27	Phenol, 2-ethyl-	Phenols	0.3	0.2	0.7	0.1	0.1	0.1
37	19.61	Phenol, 2,3-dimethyl-	Phenols	1.3	2.3	1.3	2.1	0.9	1.3
38	19.63	Benzene, 4-ethenyl-1,2-dimethyl-	Aromatics	3.2	1.9	1.1	1.2	1.0	0.9
39	19.92	2-Methylindene	Aromatics	1.9	2.4	2.5	2.7	2.5	2.2
40	20.06	Benzene, (1-methyl-2-cyclopropen-1-yl)-	Aromatics	2.5	1.1	0.9	1.2	0.8	0.8
41	20.72	Catechol	Catechols	1.5	0.2	0.0	0.1	0.0	0.0
42	20.79	Benzaldehyde, 3-ethyl-	Aromatics	0.4	0.0	0.0	0.0	0.0	0.0
43	20.86	2-Methoxy-5-methylphenol	Guaiacols	2.8	0.2	0.1	0.2	0.1	0.0
44	20.88	Naphthalene	Aromatics	2.7	6.5	11.3	8.9	13.6	12.1
45	21.31	Ethyl-2-benzofuran	Aromatics, oxygenated	0.4	0.2	0.1	0.2	0.1	0.1
46	21.36	3-Isopropylbenzaldehyde	Aromatics, oxygenated	0.2	0.0	0.0	0.0	0.0	0.0
47	21.49	Benzofuran, 4,7-dimethyl-	Aromatics, oxygenated	2.2	1.1	0.6	0.9	0.5	0.5
48	21.72	2H-Inden-2-one, 1,3-dihydro-	Aromatics, oxygenated	0.1	0.1	0.1	0.1	0.1	0.1
49	21.76	Benzene, 1,1'-(oxydiethylidene)bis-	Aromatics, oxygenated	0.4	0.1	0.0	0.1	0.0	0.0
50	21.77	1,3-Cyclopentadiene, 1,2,3,4,5-pentamethyl-	Ketones	0.2	0.2	0.1	0.1	0.1	0.1
51	21.90	2-Ethyl-2,3-dihydro-1H-indene	Aromatics	0.1	0.1	0.0	0.1	0.0	0.0
52	21.95	2,2'-Bifuran	Furans	0.4	0.3	0.1	0.2	0.1	0.2
53	22.16	1H-Indene, 2,3-dimethyl-	Aromatics	0.2	0.2	0.1	0.2	0.1	0.1
54	22.18	1,2-Benzenediol, 3-methyl-	Catechols	0.2	0.1	0.0	0.1	0.0	0.0
55	22.41	Phenol, 2,3,5-trimethyl-	Phenols	0.2	0.1	0.1	0.1	0.0	0.1
56	22.44	Benzofuran, 7-methoxy-	Aromatics, oxygenated	0.1	0.1	0.1	0.1	0.1	0.1
57	22.48	1H-Indene, 1,3-dimethyl-	Aromatics	2.0	1.0	0.7	0.9	0.6	0.5
58	22.57	2-Ethyl-1-H-indene	Aromatics	0.5	0.2	0.2	0.2	0.1	0.2
59	22.73	1,2-Benzenediol, 4-methyl-	Catechols	0.5	0.1	0.0	0.1	0.0	0.0
60	22.73	Phenol, 4-ethyl-2-methoxy-	Guaiacols	2.9	0.2	0.1	0.1	0.0	0.0
61	22.90	Naphthalene, 1,2-dihydro-4-methyl-	Aromatics	0.2	0.2	0.1	0.1	0.1	0.1
62	22.92	1H-Inden-1-one, 2,3-dihydro-	Aromatics, oxygenated	0.8	0.1	0.1	0.2	0.1	0.1
63	23.25	Naphthalene, 2-methyl-	Aromatics	4.8	7.9	10.8	9.2	12.4	10.8
64	23.41	Ethanone, 1-(2-hydroxy-5-methylphenyl)-	Phenols	0.6	0.1	0.0	0.1	0.0	0.0

Table 4A-1: GC/MS analysis results of the oily liquid in catalytic fast pyrolysis of Rwood (continued).

65	23.45	Phenol, 2-(3-hydroxy-3-methyl-1-butenyl)-, (Z)-	Phenols	0.7	0.2	0.1	0.1	0.1	0.1
66	23.86	1H-Inden-5-ol, 2,3-dihydro-	Phenols	0.6	0.6	0.2	0.4	0.1	0.1
67	23.86	1,4-Benzenedicarboxaldehyde	Aromatics, oxygenated	0.6	0.6	0.2	0.4	0.1	0.1
68	24.12	1H-Indenol	Aromatics, oxygenated	0.6	1.3	0.8	1.7	0.6	0.5
69	24.49	1H-Indene, 1,1,3-trimethyl-	Aromatics	0.5	0.2	0.1	0.1	0.1	0.1
70	24.92	Vanillin	Guaiacols	0.2	0.0	0.0	0.0	0.0	0.0
71	24.99	Naphthalene, 2-ethyl-	Aromatics	0.8	1.0	1.1	1.1	1.2	1.0
72	25.03	Phenol, 2-methoxy-4-(1-propenyl)-, (Z)-	Phenols	0.3	0.0	0.0	0.0	0.0	0.0
73	25.17	Naphthalene, 1,6-dimethyl-	Aromatics	3.1	4.3	4.2	4.0	4.5	3.8
74	25.41	Naphthalene, 1,7-dimethyl-	Aromatics	3.1	0.2	0.5	0.3	0.8	0.8
75	25.48	Naphthalene, 1,5-dimethyl-	Aromatics	0.4	0.2	0.4	0.2	0.6	0.6
76	25.68	trans-Isoeugenol	Guaiacols	1.1	0.1	0.0	0.1	0.0	0.0
77	25.74	Naphthalene, 1,3-dimethyl-	Aromatics	0.4	0.3	0.2	0.2	0.2	0.2
78	25.85	1-Naphthalenol, 5,8-dihydro-	Aromatics, oxygenated	0.3	0.2	0.1	0.2	0.1	0.1
79	26.32	6-Methoxy-3-methylbenzofuran	Aromatics, oxygenated	0.3	0.0	0.0	0.0	0.0	0.0
80	26.44	Naphthalene, 1-propyl-	Aromatics	0.3	0.3	0.2	0.2	0.2	0.2
81	26.62	1-Naphthalenol	Aromatics, oxygenated	0.1	0.2	0.4	0.3	0.5	0.4
82	26.66	Naphthalene, 2-(1-methylethyl)-	Aromatics	1.1	1.0	0.8	0.8	0.7	0.6
83	26.74	Furan, 3-phenyl-	Aromatics	0.6	3.5	4.5	4.5	4.3	2.7
84	26.86	2-Propanone, 1-(4-hydroxy-3-methoxyphenyl)-	Guaiacols	0.6	0.0	0.0	0.0	0.0	0.0
85	26.93	Dibenzofuran	Aromatics, oxygenated	0.1	0.2	0.3	0.3	0.3	0.3
86	27.33	Naphthalene, 1,6,7-trimethyl-	Aromatics	0.7	0.4	0.2	0.3	0.2	0.2
87	27.93	Naphthalene, 2-methyl-1-propyl-	Aromatics	0.3	0.2	0.1	0.1	0.1	0.1
88	28.05	1-Naphthalenol, 2-methyl-	Aromatics, oxygenated	0.2	0.6	0.7	0.7	0.7	0.5
89	28.14	1-Naphthalenol, 4-methyl-	Aromatics, oxygenated	0.6	0.9	2.2	1.1	1.9	1.2
90	28.44	Fluorene	Aromatics	0.0	0.1	0.3	0.2	0.3	0.2
91	28.51	9H-Xanthene	Aromatics, oxygenated	0.1	0.1	0.2	0.2	0.2	0.2
92	28.78	7-Methoxy-1-naphthol	Aromatics, oxygenated	0.3	0.1	0.0	0.0	0.0	0.0
93	29.13	[1,1'-Biphenyl]-4-carboxaldehyde	Aromatics, oxygenated	0.2	0.1	0.1	0.1	0.1	0.0
94	29.25	2-Hydroxyfluorene	Aromatics, oxygenated	0.1	0.1	0.1	0.1	0.1	0.1
95	29.34	1-Naphthol, 5,7-dimethyl-	Aromatics, oxygenated	0.2	0.5	0.4	0.5	0.3	0.2
96	29.81	9H-Fluorene, 1-methyl-	Aromatics	0.1	0.1	0.1	0.1	0.1	0.1
97	30.47	9H-Fluorene, 9-methylene-	Aromatics	0.0	0.2	0.6	0.5	0.7	0.6
98	31.76	Phenanthrene, 2-methyl-	Aromatics	0.1	0.3	0.5	0.4	0.6	0.4

Appendix B

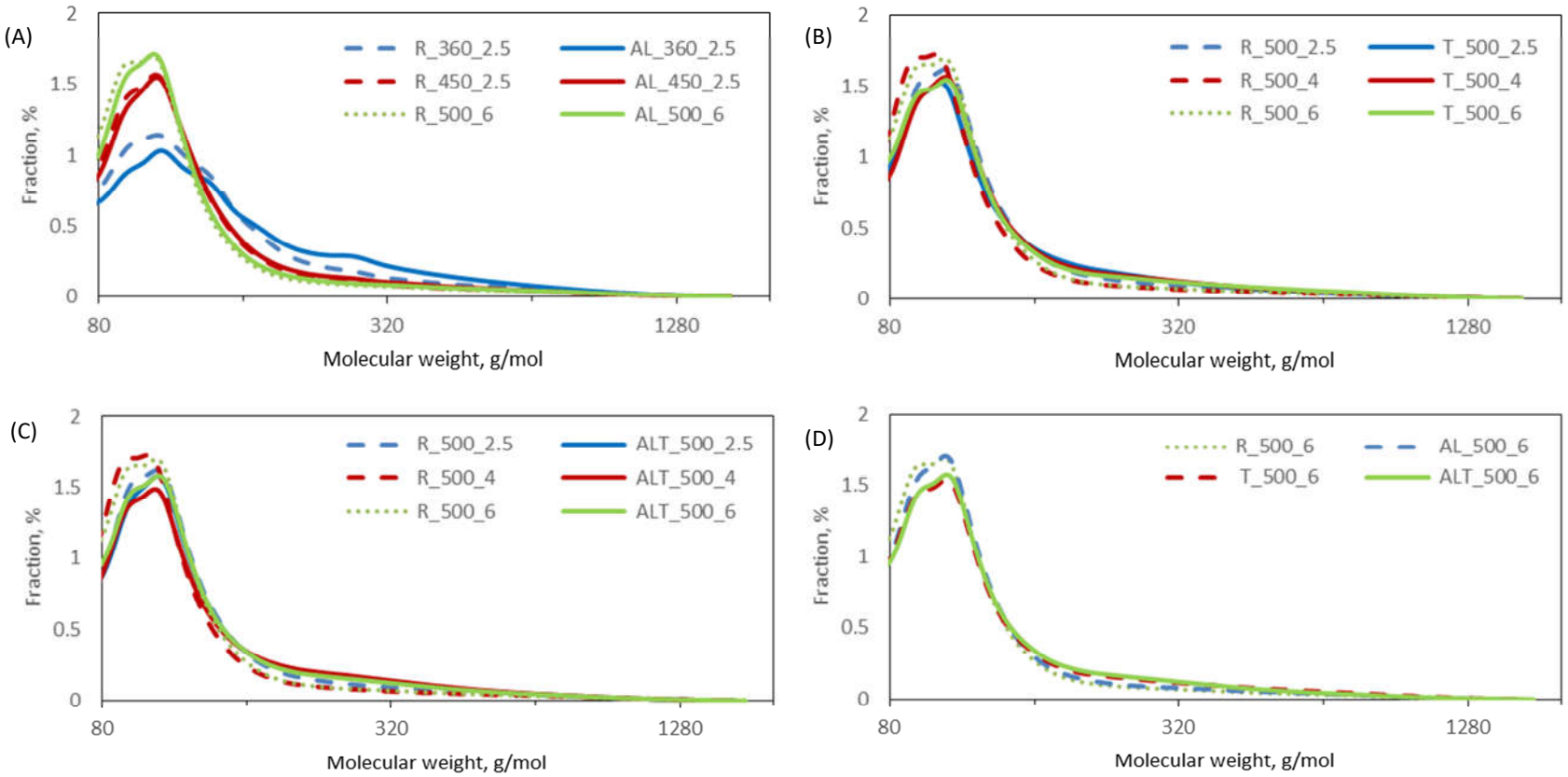

Figure 5A-1: Comparison of the molecular weight distribution profiles of oily liquids from CFP of pretreated woods.

Table 5A-1: GC/MS analysis results of oily liquid for CFP of pretreated woods (to be continued).

RT order	RT (min)	Identified compound	Group	% of total identified peak area								
				AL_360_2.5	AL_450_2.5	AL_500_6	T_500_2.5	T_500_4	T_500_6	ALT_500_2.5	ALT_500_4	ALT_500_6
1	7.79	Toluene	Aromatics	1.2	6.5	9.6	10.7	11.9	12.0	10.4	10.8	11.5
2	9.63	3-Furaldehyde	Furans	4.3	0.0	0.0	0.0	0.0	0.0	0.0	0.0	0.0
3	9.67	2-Cyclopenten-1-one	Ketones	4.3	1.4	0.4	0.3	0.3	0.2	0.4	0.5	0.4
4	10.62	Ethylbenzene	Aromatics	0.5	2.6	2.6	2.0	2.0	1.9	2.1	2.3	2.2
5	10.87	Benzene, 1,3-dimethyl-	Aromatics	0.4	2.6	2.8	2.9	2.9	3.2	2.6	2.7	3.2
6	11.57	Styrene	Aromatics	0.2	0.4	0.6	0.4	0.4	0.4	0.4	0.5	0.5
7	11.65	p-Xylene	Aromatics	0.7	3.4	3.2	3.4	3.5	3.9	3.1	3.3	3.9
8	12.01	2-Cyclopenten-1-one, 2-methyl-	Ketones	1.1	0.2	0.1	0.0	0.0	0.0	0.1	0.1	0.1
9	12.48	2-Cyclopenten-1-one, 2-hydroxy-	Ketones	1.3	0.0	0.0	0.0	0.0	0.0	0.0	0.0	0.0
10	13.64	Benzene, propyl-	Aromatics	0.2	0.4	0.3	0.2	0.2	0.1	0.2	0.2	0.2
11	13.89	Benzene, (1-methylethyl)-	Aromatics	1.2	2.3	1.7	1.3	1.4	1.3	1.3	1.5	1.5
12	13.94	2-Cyclopenten-1-one, 3-methyl-	Ketones	0.9	0.1	0.0	0.0	0.0	0.0	0.0	0.0	0.0
13	13.95	Furan, 2,5-dimethyl-	Furans	0.1	0.2	0.2	0.1	0.1	0.1	0.1	0.1	0.1
14	13.95	Benzene, 1-ethyl-4-methyl-	Aromatics	1.2	2.3	1.7	1.1	1.1	1.0	1.1	1.3	1.2
15	14.23	Phenol	Phenols	4.8	5.3	5.9	5.6	5.3	5.6	5.9	5.7	5.9
16	14.98	Mesitylene	Aromatics	3.6	5.1	3.9	3.8	4.0	4.1	3.4	3.7	4.0
17	15.13	Benzofuran	Aromatics, oxygenated	2.6	2.0	2.4	1.9	2.0	1.9	2.0	2.2	2.1
18	15.90	2-Cyclopenten-1-one, 2-hydroxy-3-methyl-	Ketones	0.6	0.0	0.0	0.0	0.0	0.0	0.0	0.0	0.0
19	16.04	Benzene, 1-propenyl-	Aromatics	0.2	0.2	0.1	2.4	2.2	2.2	2.4	2.1	1.2
20	16.41	2-Cyclopenten-1-one, 2,3-dimethyl-	Ketones	0.2	0.1	0.0	0.0	0.0	0.0	0.0	0.0	0.0
21	16.45	Indane	Aromatics	1.4	3.2	2.7	2.4	2.2	2.2	2.4	2.4	2.3
22	16.54	4-Methyl-5H-furan-2-one	Ketones	1.3	0.0	0.0	0.0	0.0	0.0	0.0	0.0	0.0
23	16.70	Phenol, 2-methyl-	Phenols	1.9	2.4	2.5	2.1	2.5	2.3	2.2	2.6	2.4
24	16.75	Indene	Aromatics	1.8	3.8	5.7	4.4	4.2	4.0	4.9	4.8	4.6
25	16.83	Benzene, 1-methyl-3-propyl-	Aromatics	0.2	0.3	0.1	0.1	0.1	0.1	0.1	0.1	0.1

Table 5A-1: GC/MS analysis results of oily liquid for CFP of pretreated woods (continued).

26	16.96	Benzene, 1-methyl-4-propyl-	Aromatics	0.3	0.3	0.2	0.1	0.1	0.1	0.1	0.1	0.1
27	16.99	o-Cymene	Aromatics	0.1	0.1	0.1	0.0	0.0	0.0	0.0	0.0	0.0
28	17.33	p-Cresol	Phenols	3.5	4.5	4.6	3.9	4.7	4.2	4.1	4.9	4.3
29	17.85	Benzofuran, 2,3-dihydro-	Aromatics, oxygenated	0.6	0.1	0.1	0.0	0.0	0.0	0.0	0.0	0.0
30	17.90	Benzene, (2-methyl-1-propenyl)-	Aromatics	1.0	0.8	0.5	0.4	0.4	0.4	0.4	0.4	0.4
31	17.96	Benzene, 1-ethyl-2,4-dimethyl-	Aromatics	0.8	0.4	0.2	0.2	0.2	0.2	0.1	0.2	0.2
32	18.04	Phenol, 2-methoxy-	Guaiacols	5.5	0.3	0.1	0.1	0.2	0.1	0.1	0.1	0.1
33	18.73	Benzofuran, 2-methyl-	Aromatics, oxygenated	4.2	2.2	2.1	1.6	1.7	1.5	1.7	1.8	1.6
34	18.92	Benzene, 1,2,3,5-tetramethyl-	Aromatics	0.4	0.2	0.1	0.1	0.1	0.1	0.0	0.1	0.1
35	19.23	Benzyl methyl ketone	Aromatics, oxygenated	0.3	0.1	0.1	0.0	0.0	0.0	0.0	0.0	0.0
36	19.27	Phenol, 2-ethyl-	Phenols	0.4	0.3	0.1	0.1	0.1	0.1	0.1	0.1	0.1
37	19.61	Phenol, 2,3-dimethyl-	Phenols	1.2	2.4	1.8	1.1	1.6	0.9	1.4	1.7	1.2
38	19.63	Benzene, 4-ethenyl-1,2-dimethyl-	Aromatics	1.8	1.7	1.1	1.1	1.0	0.9	1.1	1.0	0.9
39	19.92	2-Methylindene	Aromatics	1.4	2.5	2.9	2.5	2.3	2.1	2.7	2.5	2.3
40	20.06	Benzene, (1-methyl-2-cyclopropen-1-yl)-	Aromatics	2.1	1.4	1.3	0.9	0.9	0.8	1.1	1.1	0.9
41	20.72	Catechol	Catechols	1.2	0.5	0.0	0.1	0.0	0.0	0.1	0.1	0.0
42	20.79	Benzaldehyde, 3-ethyl-	Aromatics	0.3	0.0	0.0	0.0	0.0	0.0	0.0	0.0	0.0
43	20.86	2-Methoxy-5-methylphenol	Guaiacols	5.6	0.4	0.1	0.2	0.2	0.1	0.3	0.3	0.2
44	20.88	Naphthalene	Aromatics	2.4	5.7	10.3	11.5	11.5	13.4	11.3	10.8	12.5
45	21.31	Ethyl-2-benzofuran	Aromatics, oxygenated	0.5	0.3	0.2	0.1	0.2	0.1	0.2	0.2	0.2
46	21.36	3-Isopropylbenzaldehyde	Aromatics, oxygenated	0.2	0.0	0.0	0.0	0.0	0.0	0.0	0.0	0.0
47	21.49	Benzofuran, 4,7-dimethyl-	Aromatics, oxygenated	2.4	1.3	0.9	0.5	0.6	0.5	0.6	0.7	0.6
48	21.72	2H-Inden-2-one, 1,3-dihydro-	Aromatics, oxygenated	0.1	0.1	0.1	0.1	0.1	0.1	0.1	0.1	0.1
49	21.76	Benzene, 1,1'-(oxydiethylidene)bis-	Aromatics, oxygenated	0.3	0.1	0.1	0.0	0.0	0.0	0.0	0.0	0.0

Table 5A-1: GC/MS analysis results of oily liquid for CFP of pretreated woods (continued).

50	21.77	1,3-Cyclopentadiene, 1,2,3,4,5-pentamethyl-	Ketones	0.2	0.2	0.1	0.1	0.1	0.1	0.1	0.1	0.1
51	21.90	2-Ethyl-2,3-dihydro-1H-indene	Aromatics	0.1	0.1	0.0	0.0	0.0	0.0	0.0	0.0	0.0
52	21.95	2,2'-Bifuran	Furans	0.2	0.3	0.2	0.1	0.2	0.1	0.1	0.2	0.1
53	22.16	1H-Indene, 2,3-dimethyl-	Aromatics	0.1	0.2	0.2	0.1	0.1	0.1	0.1	0.1	0.1
54	22.18	1,2-Benzenediol, 3-methyl-	Catechols	0.2	0.2	0.0	0.1	0.0	0.0	0.1	0.1	0.0
55	22.41	Phenol, 2,3,5-trimethyl-	Phenols	0.2	0.2	0.1	0.1	0.1	0.1	0.0	0.1	0.1
56	22.44	Benzofuran, 7-methoxy-	Aromatics, oxygenated	0.1	0.1	0.1	0.1	0.1	0.0	0.1	0.1	0.1
57	22.48	1H-Indene, 1,3-dimethyl-	Aromatics	1.4	1.1	0.8	0.7	0.6	0.5	0.7	0.7	0.6
58	22.57	2-Ethyl-1-H-indene	Aromatics	0.4	0.2	0.2	0.2	0.1	0.2	0.2	0.2	0.2
59	22.73	1,2-Benzenediol, 4-methyl-	Catechols	0.5	0.2	0.0	0.1	0.0	0.0	0.1	0.1	0.0
60	22.73	Phenol, 4-ethyl-2-methoxy-	Guaiacols	3.1	0.3	0.0	0.1	0.1	0.1	0.1	0.1	0.1
61	22.90	Naphthalene, 1,2-dihydro-4-methyl-	Aromatics	0.1	0.2	0.1	0.1	0.1	0.1	0.1	0.1	0.1
62	22.92	1H-Inden-1-one, 2,3-dihydro-	Aromatics, oxygenated	0.6	0.2	0.1	0.1	0.1	0.0	0.1	0.1	0.1
63	23.25	Naphthalene, 2-methyl-	Aromatics	3.8	7.0	9.8	11.1	10.7	11.7	11.1	10.4	11.2
64	23.41	Ethanone, 1-(2-hydroxy-5-methylphenyl)-	Phenols	0.7	0.1	0.0	0.1	0.1	0.0	0.1	0.1	0.0
65	23.45	Phenol, 2-(3-hydroxy-3-methyl-1-butenyl)-, (Z)-	Phenols	0.8	0.3	0.1	0.1	0.1	0.1	0.1	0.1	0.1
66	23.86	1H-Inden-5-ol, 2,3-dihydro-	Phenols	0.5	0.5	0.2	0.1	0.1	0.1	0.1	0.1	0.1
67	23.86	1,4-Benzenedicarboxaldehyde	Aromatics, oxygenated	0.5	0.5	0.2	0.1	0.1	0.1	0.1	0.1	0.1
68	24.12	1H-Indenol	Aromatics, oxygenated	0.5	1.1	0.7	0.4	0.4	0.3	0.4	0.4	0.3
69	24.49	1H-Indene, 1,1,3-trimethyl-	Aromatics	0.3	0.2	0.1	0.1	0.1	0.1	0.1	0.1	0.1
70	24.92	Vanillin	Guaiacols	0.5	0.0	0.0	0.0	0.0	0.0	0.0	0.0	0.0
71	24.99	Naphthalene, 2-ethyl-	Aromatics	0.5	0.9	0.9	1.1	1.0	1.0	1.1	1.0	0.9
72	25.03	Phenol, 2-methoxy-4-(1-propenyl)-, (Z)-	Phenols	0.4	0.0	0.0	0.0	0.0	0.0	0.0	0.0	0.0
73	25.17	Naphthalene, 1,6-dimethyl-	Aromatics	2.3	3.9	4.0	4.2	3.9	3.9	4.2	4.0	3.9
74	25.41	Naphthalene, 1,7-dimethyl-	Aromatics	2.3	3.9	0.5	0.5	0.6	1.0	0.4	0.6	0.8
75	25.48	Naphthalene, 1,5-dimethyl-	Aromatics	0.3	0.3	0.3	0.3	0.5	0.7	0.3	0.4	0.6
76	25.68	trans-Isoeugenol	Guaiacols	1.5	0.1	0.0	0.0	0.0	0.0	0.0	0.0	0.0

Table 5A-1: GC/MS analysis results of oily liquid for CFP of pretreated woods (continued).

77	25.74	Naphthalene, 1,3-dimethyl-	Aromatics	0.3	0.3	0.2	0.2	0.2	0.3	0.2	0.2	0.2
78	25.85	1-Naphthalenol, 5,8-dihydro-	Aromatics, oxygenated	0.3	0.2	0.1	0.1	0.1	0.1	0.1	0.1	0.1
79	26.32	6-Methoxy-3-methylbenzofuran	Aromatics, oxygenated	0.2	0.0	0.0	0.0	0.0	0.0	0.0	0.0	0.0
80	26.44	Naphthalene, 1-propyl-	Aromatics	0.1	0.2	0.2	0.2	0.2	0.2	0.2	0.2	0.2
81	26.62	1-Naphthalenol	Aromatics, oxygenated	0.1	0.2	0.3	0.3	0.3	0.4	0.3	0.3	0.3
82	26.66	Naphthalene, 2-(1-methylethyl)-	Aromatics	0.7	0.9	0.7	0.7	0.7	0.6	0.7	0.7	0.6
83	26.74	Furan, 3-phenyl-	Aromatics	0.4	2.4	2.5	3.5	2.6	2.0	3.3	2.4	2.0
84	26.86	2-Propanone, 1-(4-hydroxy-3-methoxyphenyl)-	Guaiacols	0.8	0.1	0.0	0.0	0.0	0.0	0.0	0.0	0.0
85	26.93	Dibenzofuran	Aromatics, oxygenated	0.2	0.2	0.4	0.3	0.3	0.3	0.3	0.3	0.4
86	27.33	Naphthalene, 1,6,7-trimethyl-	Aromatics	0.6	0.5	0.3	0.2	0.2	0.2	0.2	0.3	0.2
87	27.93	Naphthalene, 2-methyl-1-propyl-	Aromatics	0.2	0.2	0.1	0.1	0.1	0.1	0.1	0.1	0.1
88	28.05	1-Naphthalenol, 2-methyl-	Aromatics, oxygenated	0.1	0.4	0.4	0.6	0.5	0.5	0.6	0.5	0.4
89	28.14	1-Naphthalenol, 4-methyl-	Aromatics, oxygenated	0.3	0.7	1.3	1.8	1.3	0.9	1.2	1.2	1.0
90	28.44	Fluorene	Aromatics	0.0	0.1	0.2	0.2	0.2	0.2	0.2	0.2	0.2
91	28.51	9H-Xanthene	Aromatics, oxygenated	0.1	0.2	0.2	0.2	0.2	0.2	0.2	0.2	0.2
92	28.78	7-Methoxy-1-naphthol	Aromatics, oxygenated	0.4	0.1	0.0	0.0	0.0	0.0	0.0	0.0	0.0
93	29.13	[1,1'-Biphenyl]-4-carboxaldehyde	Aromatics, oxygenated	0.1	0.1	0.1	0.1	0.1	0.0	0.1	0.1	0.1
94	29.25	2-Hydroxyfluorene	Aromatics, oxygenated	0.1	0.1	0.1	0.1	0.1	0.1	0.1	0.1	0.1
95	29.34	1-Naphthol, 5,7-dimethyl-	Aromatics, oxygenated	0.1	0.4	0.2	0.3	0.2	0.1	0.2	0.2	0.1
96	29.81	9H-Fluorene, 1-methyl-	Aromatics	0.0	0.1	0.1	0.1	0.1	0.1	0.1	0.1	0.1
97	30.47	9H-Fluorene, 9-methylene-	Aromatics	0.0	0.2	0.5	0.6	0.5	0.7	0.6	0.5	0.6
98	31.76	Phenanthrene, 2-methyl-	Aromatics	0.1	0.2	0.4	0.5	0.4	0.5	0.4	0.4	0.4

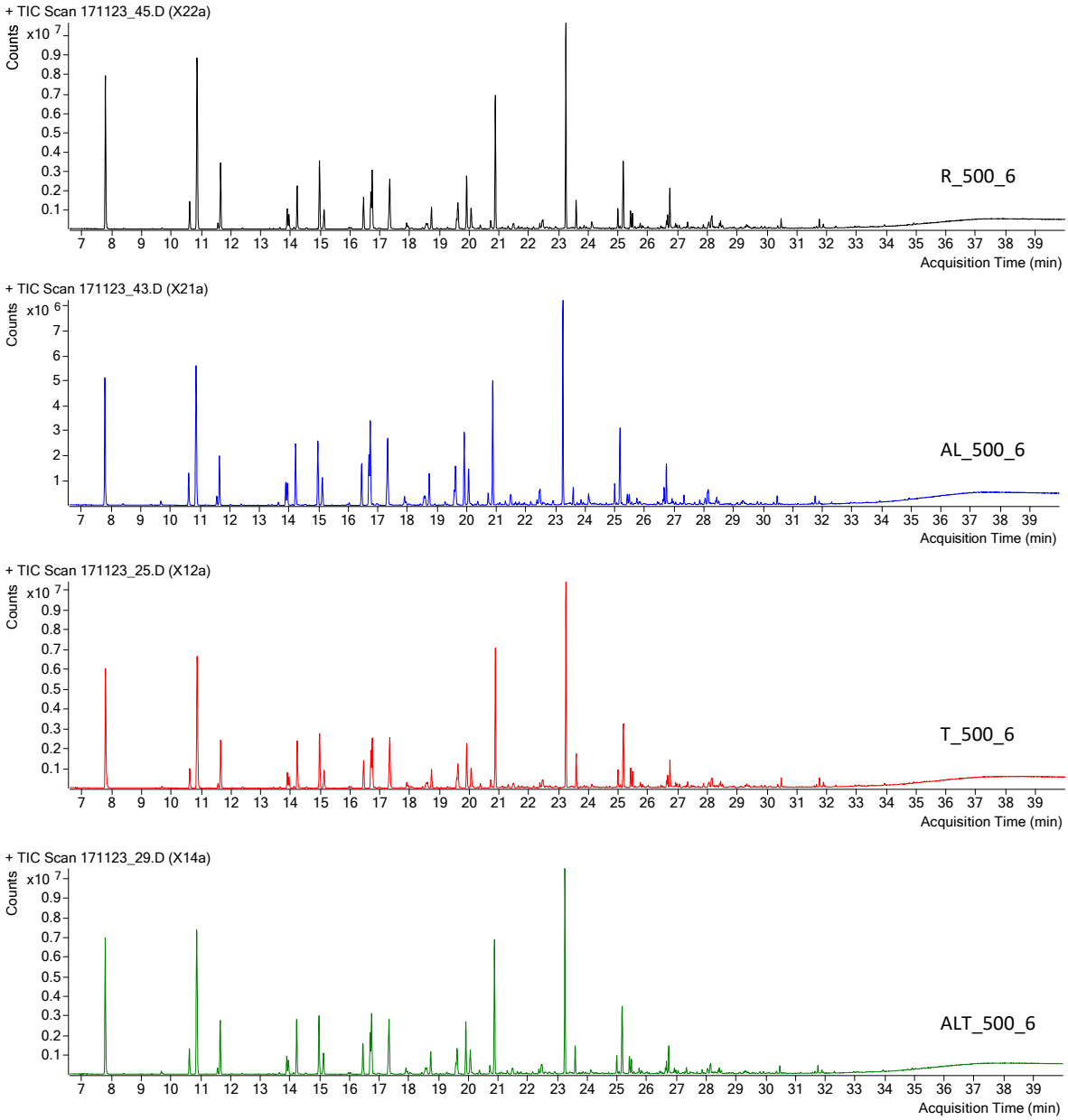

Figure 5A-2: Chromatographs of oily liquids in GC/MS analysis.

Appendix C

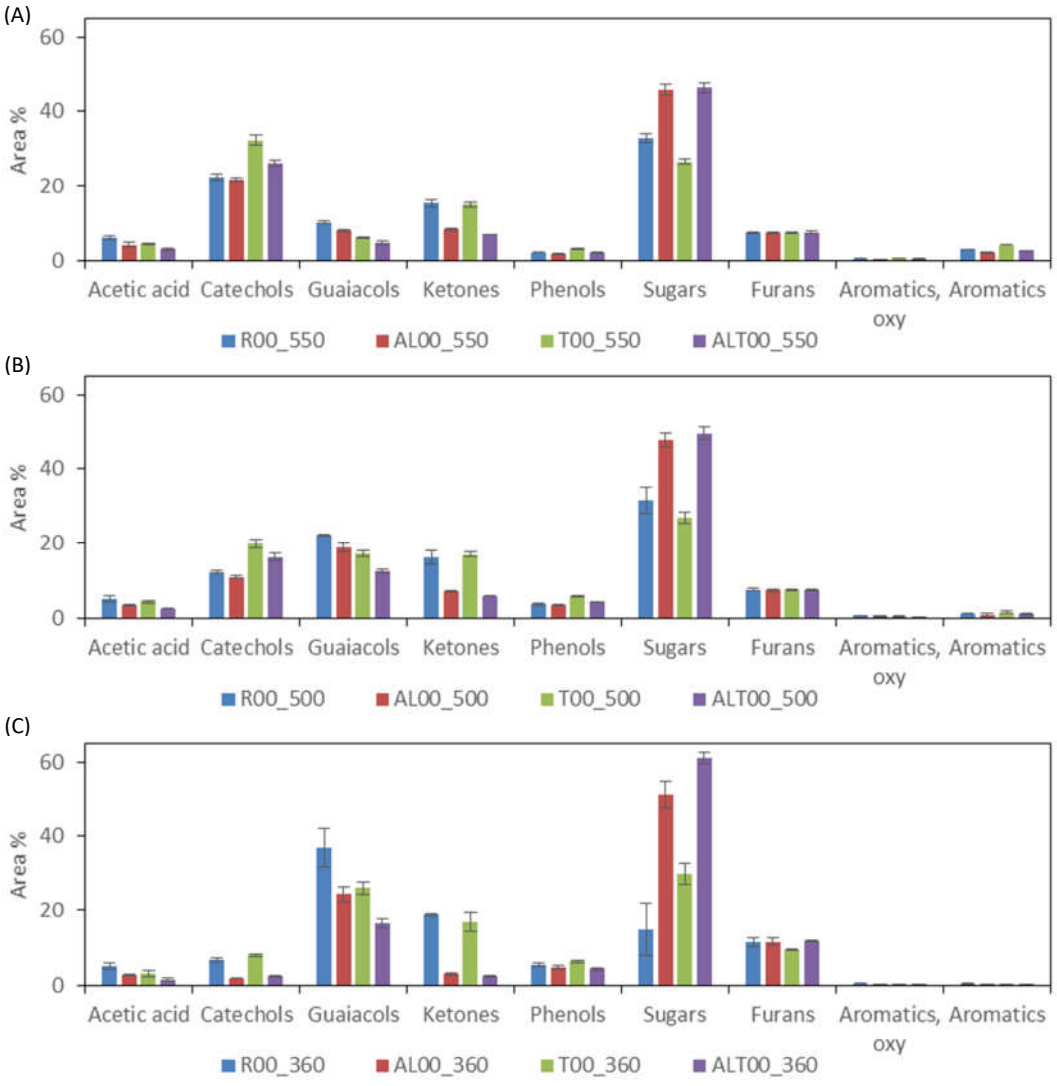

Figure 6A-1: The impacts of biomass pretreatments in non-catalytic pyrolysis, (A): 550 °C, (B): 500 °C, (C): 360 °C.

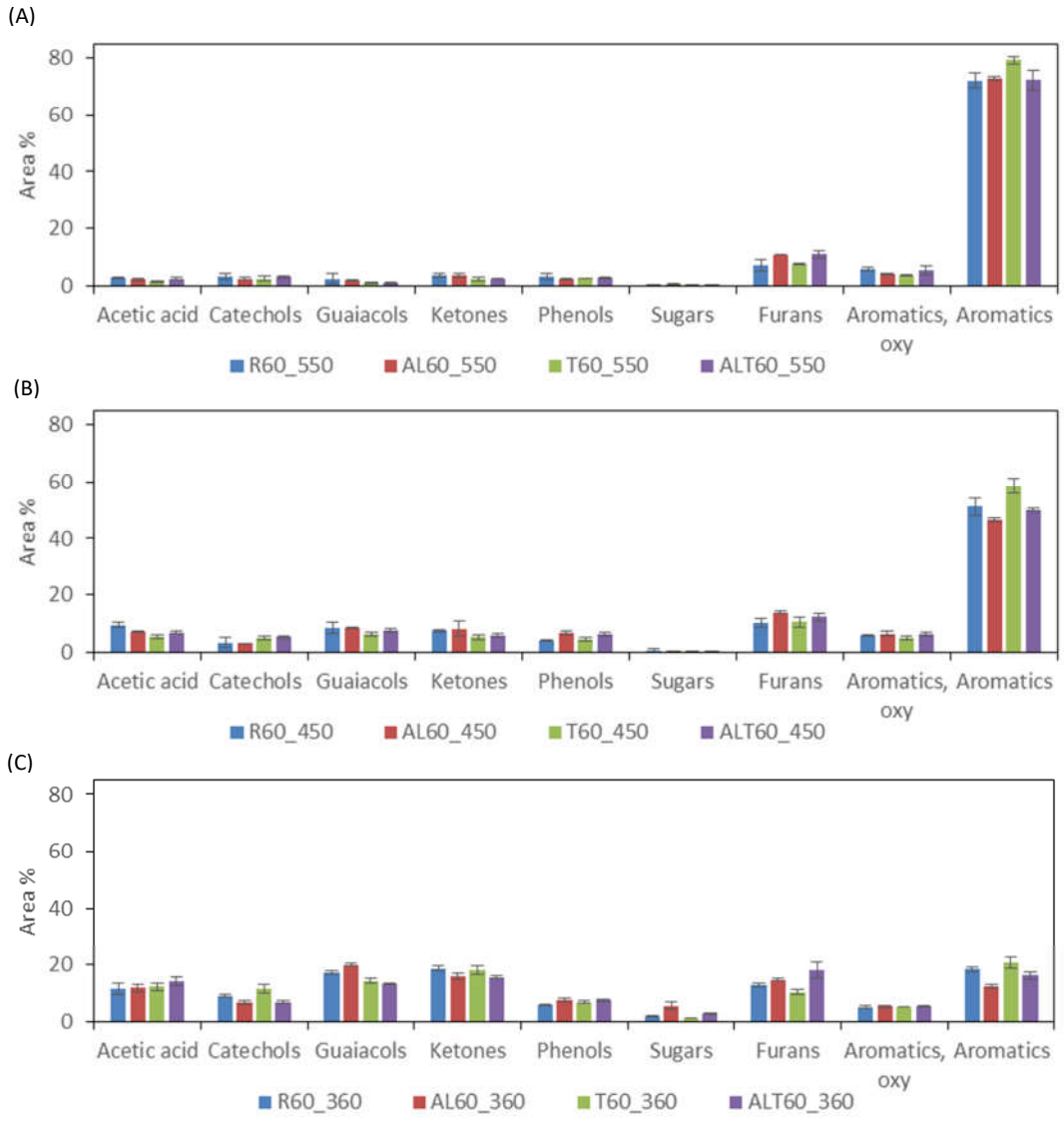

Figure 6A-2: The impacts of biomass pretreatments in catalytic pyrolysis, (A): 550 °C, (B): 450 °C, (C): 360 °C.

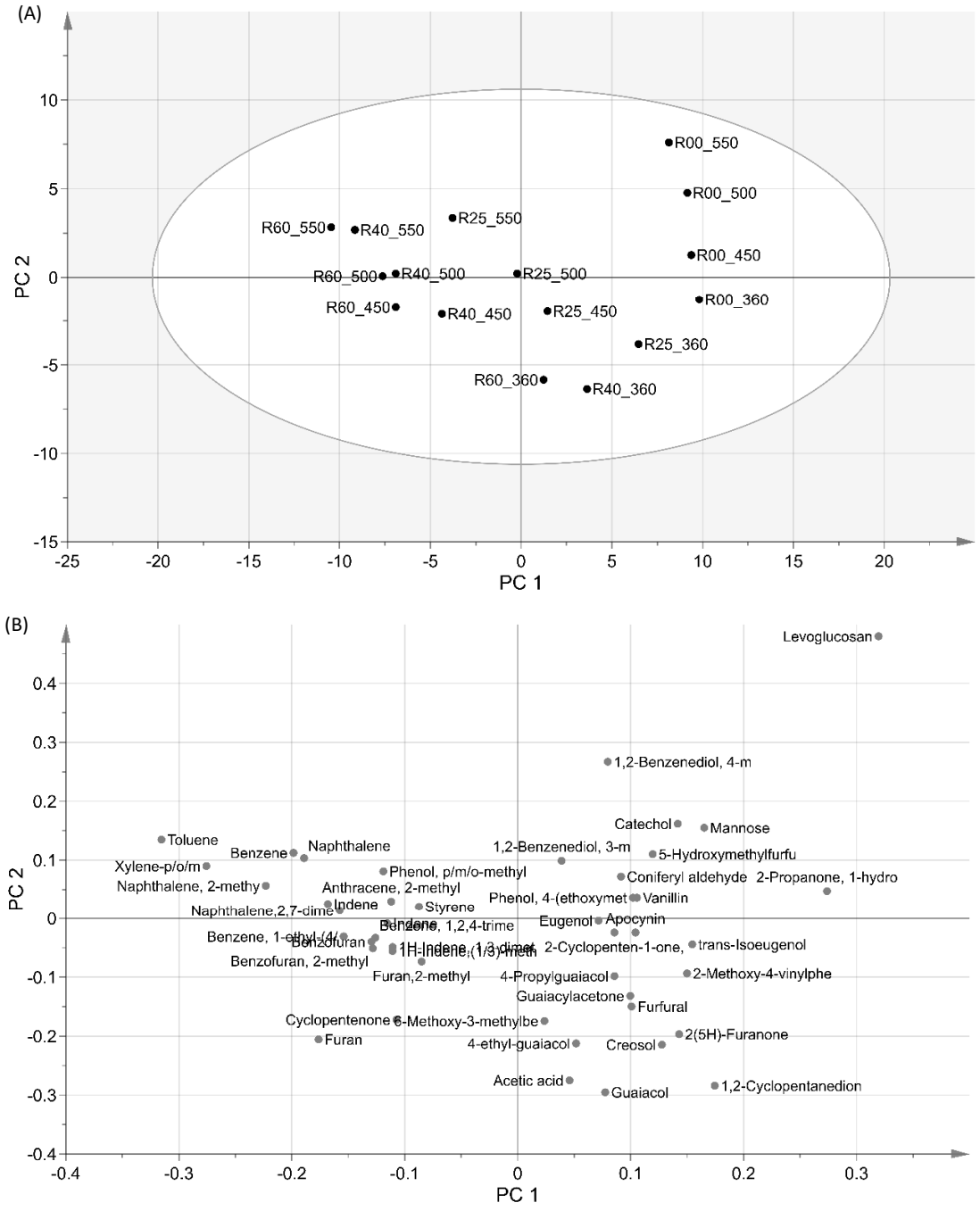

Figure 6A-3: Score (A) and loading (B) plots of PC1 and PC2 for the model in Rwood Py-GC/MS analysis at all temepratures and C/B ratios, PC1 explains 63 % of variance and PC2 17 %.

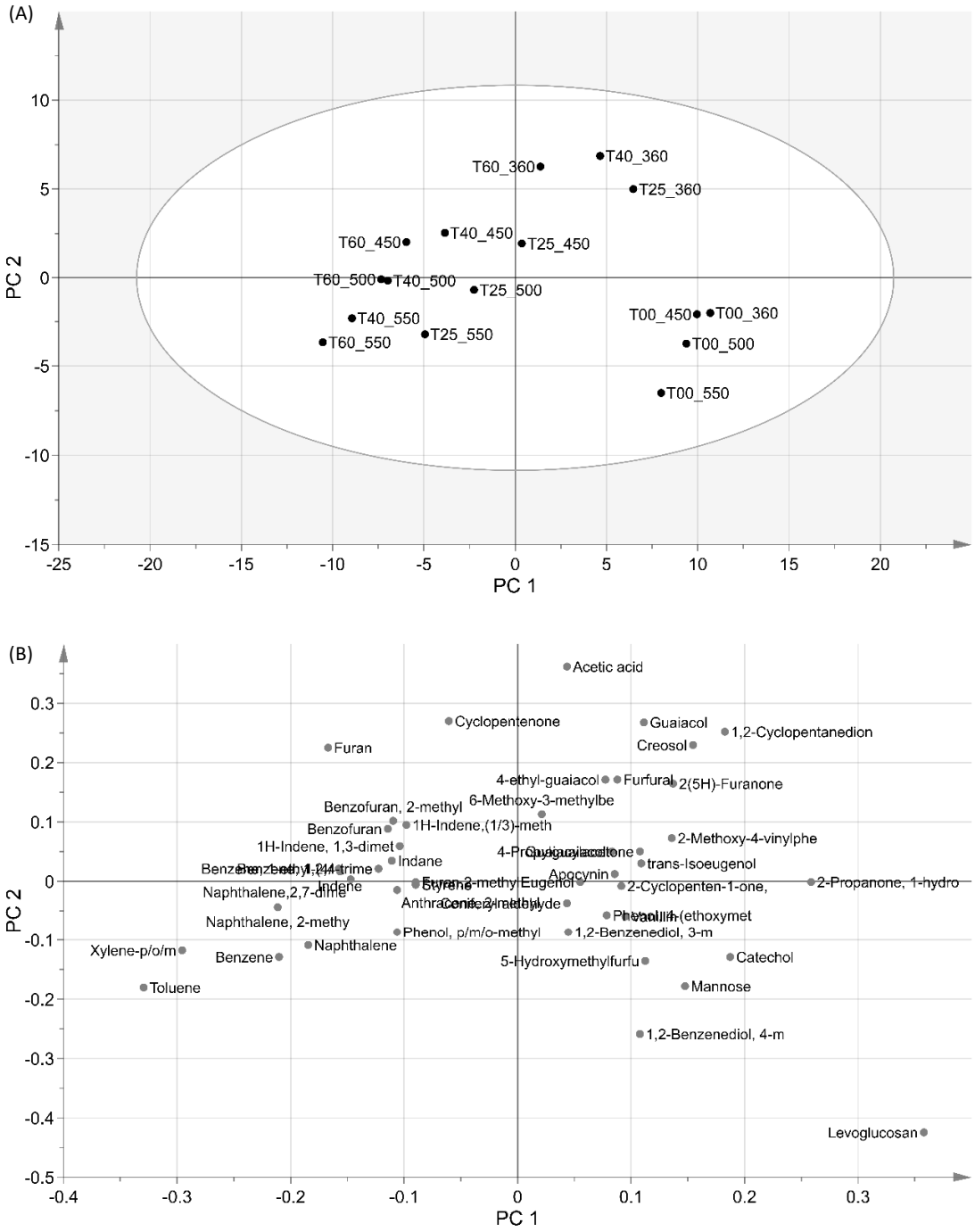

Figure 6A-4: Score (A) and loading (B) plots of PC1 and PC2 for the model in Twood Py-GC/MS analysis at all temepratures and C/B ratios, PC1 explains 65 % of variance and PC2 18 %.

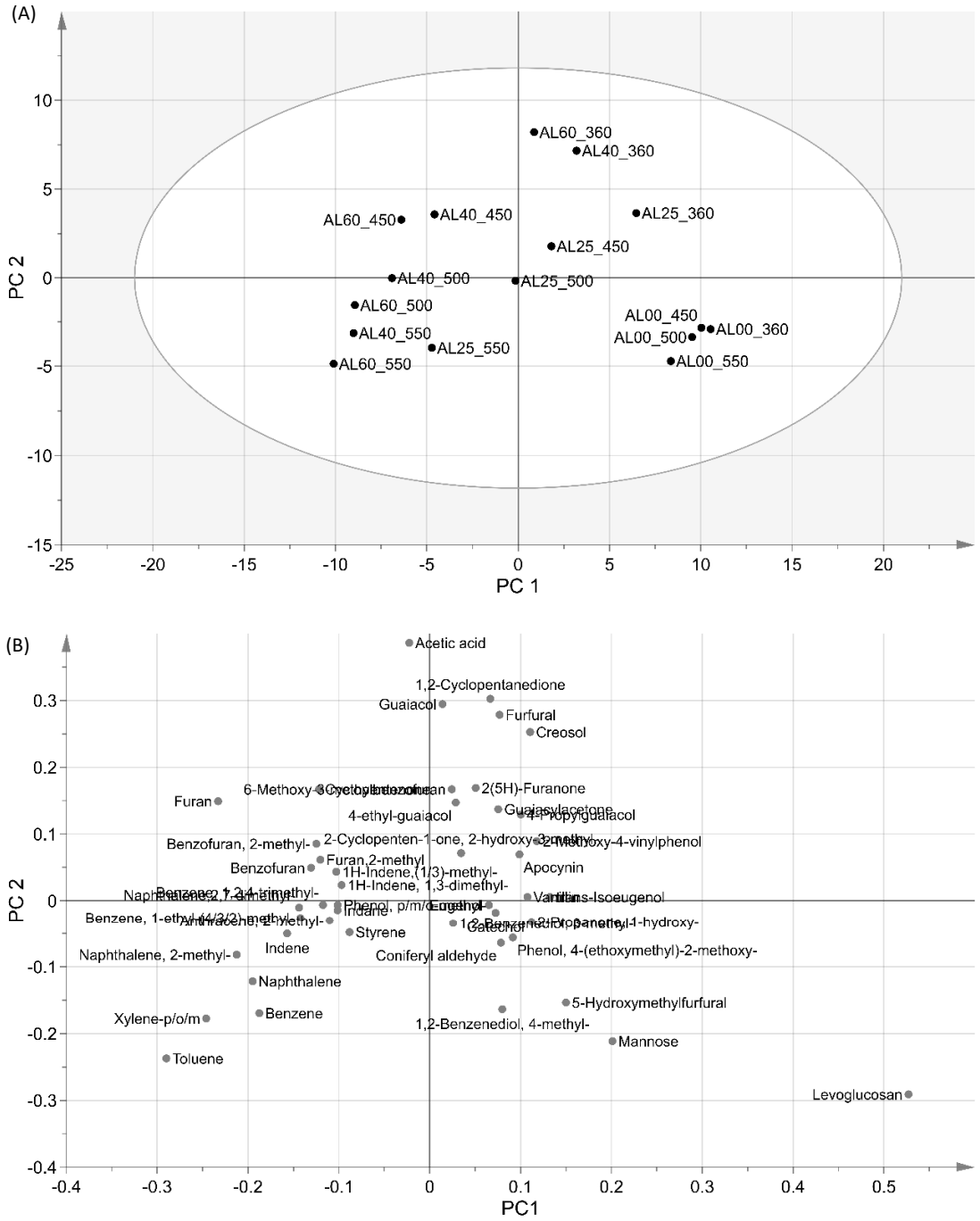

Figure 6A-5: Score (A) and loading (B) plots of PC1 and PC2 for the model in ALwood Py-GC/MS analysis at all temepratures and C/B ratios, PC1 explains 62 % of variance and PC2 20 %.